The Role of MicroRNAs in the Fibroblasts of Triple Negative and Basal-like Breast Cancer

Laura Mary Wastall

Submitted in accordance with the requirements for the degree of
Doctor of Philosophy

The University of Leeds
Faculty of Medicine & Health
School of Medicine
Leeds Institute of Biomedical and Clinical Sciences

April, 2017

The candidate confirms that the work submitted is her own and that appropriate credit has been given where reference has been made to the work of others.

Acknowledgements

I would like to acknowledge the patients whose tissues I have used in this study.

In addition I would like to thank the following people:

Supervisors: Dr Thomas Hughes, Professor Andrew Hanby and Dr Eldo Verghese

Collaborators: Dr James Thorne, Dr Mihaela Lorger, Dr Alastair Droop, Dr Ruth Darbyshire, Dr Claire Nash, Ms Caroline Strachan, Robyn Broad.

I would also like to thank Cancer Research UK for the funding for this project and the Breast Cancer Now Tissue Bank for making some materials available.

And last but not least, my family and friends whose support and encouragement has been essential for me to complete this work, in particular Andrew Wastall, Stephanie Gardner, Brian Gardner, Janet Wastall, Peter Wastall, Jane Robinson, Jennifer Chappell, Tamara Stewart, and Aidan Wastall for his patience and understanding.

“ The mammary gland is an organ that at once gives life to the young, but at the same time poses one of the greatest threats to the mother. ”

(Muschler and Streuli, 2010)

Abstract

Breast cancer is the second most common cancer worldwide and the fifth biggest cause of cancer-related deaths. Breast cancer subtype has a huge influence on tumour behaviour and prognosis. The basal-like subtype, which is typically – but not always – triple negative for receptor expression status limiting treatment options, represents one of the main subtypes with relatively poor prognosis. Breast cancer is a disease that comprises not only transformed luminal epithelial cells but also modified stroma, as a consequence of interactions between the cancer cells and the stroma. One of the most numerous cellular components of cancer stroma are fibroblasts. MicroRNA (miRNA) are short, single-stranded RNA molecules that modify protein expression through regulation of mRNA translation and/or mRNA stability. I have explored the expression and roles of miRNAs in the stromal fibroblast compartment of triple negative breast cancer, in particular of miR-21. I have used a variety of clinical samples and cell culture models to assess the potential clinical relevance of these levels and their potential functional effects.

I have found that miR-21 expression is significantly increased in stromal fibroblasts of triple negative breast cancer as compared to matched normal breast fibroblasts. However, miR-21 levels in the cancer associated fibroblasts did not significantly correlate with clinical outcomes. In tissue culture models, miR-21 was significantly up-regulated in breast fibroblasts by contact co-culture with epithelial cancer cells, suggesting that this interaction may be the cause of this increase in tumours. Using immortalised breast fibroblasts, I showed alteration of miR-21 levels did not significantly influence fibroblast migration or invasion. Nor did levels of miR-21 in these fibroblasts impact on the behaviour of breast epithelial cancer cells in a variety of co-culture settings. However, over-expression of miR-21 in primary breast cancer associated fibroblasts was associated with a small, but significant, increase in the migration of fibroblasts, and a small but significant decrease in the invasion of co-cultured tumour cells.

Overall, I conclude that miR-21 does not have a striking and consistent cancer-related role in the fibroblast compartment of triple negative breast cancers, however further work is required to assess potential roles in primary settings.

Table of Contents

List of Tables

List of Figures

List of Abbreviations

α-SMA	Alpha-Smooth Muscle Actin
ADAMTS1	A Disintegrin And Metalloproteinase with ThromboSpondin type 1 motif
AIB1	Amplified In Breast 1 also known as nuclear receptor co-activator 3
AP	Alkaline Phosphatase
AP-1	Activator Protein-1
ATCC	American Type Culture Collection
BSA	Bovine Serum Albumin
CAFs	Cancer Associated Fibroblasts
Cat no.	Catalogue number
CCR4	C-C chemokine receptor type 4
CD	Cluster of Differentiation
cDNA	complementary DeoxyriboNucleic Acid
CISH	Chromogenic *In Situ H*ybridisation
CK	CytoKeratin
Ct	Cycle threshold
CXCL12	C-X-C chemokine 12
CXCR4	C-X-C chemokine receptor type 4 also known as fusin and CD184
DCP	Decapping complex
DEPC	DiEthylPyroCarbonate
DGCR8	DiGeorge syndrome Critical Region 8

DIG	DIGoxigenin
DMEM	Dulbecco's Modified Eagle Medium
DMSO	DiMethyl SulfOxide
DNA	DeoxyriboNucleic Acid
DNase	DeoxyriboNuclease
Dr	Doctor
ECM	ExtraCellular Matrix
EDTA	EthyleneDiamineteTraacetic Acid
eIF	eukaryotic Initiation Factor
ER	oEstrogen Receptor
et al.	*et alia*
FACS	Fluorescence Activated Cell Sorting
FAP	Fibroblast Activation Protein
FBS	Foetal Bovine Serum
FFPE	Formalin Fixed Paraffin Embedded
FSP1	Fibroblast Specific Protein 1
GFP	Green Fluorescent Protein
GW182	Glycine-trytophan repeats family proteins
h	hour(s)
H&E	Haematoxylin and Eosin
HER2	Human Epidermal growth factor Receptor 2, also known as HER2/neu, CD430 and erbB-2
HEK-293	Human Embryonic Kidney-293
HGF	Hepatocyte Growth Factor
HIF-1α	Hypoxia-Inducible Factor 1-α
hTERT	human TElomerase Reverse Transcriptase

IDC-NST	Invasive Ductal Carcinoma of No Special Type
IHC	ImmunoHistoChemistry
IL	InterLeukin
ISH	*In Situ H*ybridization
KCl	Potassium Chloride
LB	Lysogeny Broth
LCM	Laser Capture Microdissection
LNA	Locked Nucleic Acid
LPC	Laser Pressure Catapulting
LTHT	Leeds Teaching Hospitals NHS Trust
m^7G	7-methylguanylate
MAPK/ERK	Mitogen-Activated Protein Kinase/Extracellular signal-Regulated Kinase
MCF-7	Michigan Cancer Foundation-7
min	minute(s)
miR	a specific microRNA
miRNA	microRNA
μl	microliter(s)
ml	millilitre(s)
μM	microMolar
mM	milliMolar
MMP	Matrix MetalloProteinase
mRNA	messenger RNA
MTT	3-(4,5-Dimethylthiazol-2-yl)-2,5-Diphenyltetrazolium Bromide)
NaCl	Sodium Chloride

NBT-BCIP	4-Nitro-Blue Tetrazolium and 5-Bromo-4-Chloro-3'-IndolylPhosphate
NF	Normal Fibroblast
NF-κB	Nuclear Factor Kappa-light-chain-enhancer of activated B cells
ng	nanogram(s)
nM	nanoMolar
NST	No Special Type
nt	nucleotides
PABP	Poly-A Binding Protein
PAN	Poly(A)-Nuclease
PBS	Phosphate-Buffered Saline
PD-1	Programmed cell Death protein 1
PD-L1	Programmed cell Death Ligand-1
PDCD4	ProgrammeD Cell Death protein 4
Pen-Strep	Penicillin-Streptomycin
poly-A	polyAdenylated
PR	Progesterone Receptor
Pre-miRNA	Precursor miRNA
Pri-miRNA	Primary miRNA
PTEN	Phosphatase and TENsin homolog
qPCR	quantitative Polymerase Chain Reaction
Ran-GTP	Ran Guanosine TriPhosphate
RCF	Relative Centrifugal Force
RHOB	Ras HOmolog gene family, member B
RISC	RNA Induced Silencing Complex

RNA	RiboNucleic Acid
RNase	RiboNuclease
rpm	revolutions per minute
RT	Reverse Transcription
SDF-1	Stromal cell-Derived Factor-1
SMR	Standardised Mortality Rate, number of deaths per hundred thousand population per year
snoRNA	small nucleolar RNA
snRNA	small nuclear RNA
SSC	Saline Sodium Citrate
TAMs	Tumour Associated Macrophages
TCF4	TransCription Factor 4
TG	ThapsiGargin
TGF-β	Transforming Growth Factor–β
TIMP3	Tissue Inhibitor of MetalloProteinases-3
TMA	Tissue MicroArray
TNBC	Triple Negative Breast Cancer
TPM1	TroPoMyosin alpha-1 chain
Tris-HCl	Tris-base HydroChloric acid
TSR	Tumour Stroma Ratio
U	Units
UK	United Kingdom
UTR	UnTranslated Region
VEGF-A	Vascular Endothelial Growth Factor A
WHO	World Health Organisation

Chapter 1
Introduction

1.1 Breast cancer

1.1.1 Epidemiology

Breast cancer is the most common cancer diagnosed in the UK and the second most common cancer worldwide, after lung cancer (ONS, 2014, WHO, 2016). It accounts for 31% of all cancer cases in women in the UK and 25% worldwide (CRUK, 2014, WCRFI, 2015). In the UK, approximately 1 in 8 women will develop breast cancer during their lifetimes (BCN, 2016). The incidence of female breast cancer in the UK has been increasing since the 1970s, from 73.8 per 100,000 in 1973 to 170.1 per 100,000 in 2013, although the rate of increase is levelling off (CRUK, 2014).

Breast cancer is the cause of approximately 11,000 deaths in women in the UK each year (11,400 in 2014) and 75 deaths in men (2014). Female breast cancer mortality rose in the 1970s and 1980s to a peak in 1986, with a standardised mortality rate (SMR, number of deaths per hundred thousand population per year) of 41.7, and has been declining steadily since then, to a SMR of 24 in 2012. This improvement is due in large part to changes in treatment, but also due to the introduction of mammographic breast cancer screening into the UK in 1988, which reached national coverage by the mid-1990s (Marmot, 2012). This decrease in SMR is reflected to some extent in the improvement in the lengths of time of survival after a breast cancer diagnosis, from 52% 5 year survival in the early 1970s to 86.6% in 2010-2011 (CRUK, 2014).

1.1.2 Subtypes

Breast cancer is a heterogeneous group of diseases with wide variation in morphology, clinical behaviour, response to treatment and outcome. This heterogeneity is partly reflected in World Health Organisation (WHO) classification into 22 different subtypes, several of these with multiple variants (Lakhani et al., 2012, Sinn and Kreipe, 2013). It is, however, notable that the most common subtype, invasive carcinoma of no special type (NST) makes up over 70% of all

breast cancers (Fulford et al., 2006, CRUK, 2014). The WHO classification is based primarily on microscopic morphological appearance. However, morphological characteristics alone are insufficient to sub-classify the majority NST grouping, which itself contains substantial heterogeneity in clinical behaviour.

Additional classification determined by immunohistochemistry (IHC) and/or *in situ* hybridisation (ISH) is now routinely carried out in clinical practice. Tumours are tested for expression of oestrogen receptor (ER), progesterone receptor (PR) and human epidermal growth factor receptor 2 (HER2), and are defined as either positive (+) or negative (-) using various clinical tests and cut offs (see below). The four major subtypes defined by morphology and receptor status are luminal A (generally ER+/PR+/HER2-), luminal B (generally ER+/PR+/HER2+ or ER+/PR+/HER2- and high grade or large tumour size or lymph node positivity or high proliferative activity), HER2 type (usually ER-/PR-/HER2+) and triple negative/basal-like (ER-/PR-/HER2-) (Metzger-Filho et al., 2013). The basal-like subgroup is often referred to as triple negative because of its receptor expression, although as discussed in section 1.1.3 this definition is too simplistic. The prevalences and further clinical information for these groups are summarised in Table 1-1.

With the advent of gene expression profiling and other profiling techniques, such as methylation profiling, there has been great advancement in attempts to classify breast cancer subtypes more accurately, reproducibly and with better predictive and prognostic information. This began with Perou *et al.* characterising histological subtypes based on gene expression profiles as well as potentially recognising other breast cancer subtypes, such as the normal-like subgroup (Perou et al., 2000). In 2009, a more concise set of 50 genes (PAM50) was identified with good prognostic performance and subtype classification (Parker et al., 2009). There have been further attempts to refine these, for example by placing greater emphasis on driver mutations, combining with methylation data or by integrating gene expression and copy number aberration data (Ali et al., 2014, List et al., 2014). The importance of the IHC classification system lies in its clinical relevance in determining therapeutic management for patients. Of particular relevance to my work is the fact that this classification separates out the triple negative group. Critically, there are no targeted drugs available for these patients and they have a worse prognosis than other

subtypes, which are treated with drugs targeting their expression of ER (Tamoxifen or aromatase inhibitors) or HER2 (Trastuzumab/Herceptin) (see Table 1-1).

Receptor expression subtype	Prevalence (approximate)	10 year relapse free survival (Arvold et al., 2011, Voduc et al., 2010)	Treatment options
Luminal A	30 - 70 %	87 - 95 %	• Surgery • Local radiotherapy • Selective oestrogen receptor modulator • Aromastase inhibitor • Cytotoxic chemotherapy
Luminal B	10 - 25 %	78 - 92 %	• Surgery • Local radiotherapy • Selective oestrogen receptor modulator • Aromatase inhibitor • Anti-HER2 receptor monoclonal antibody (if the tumour is HER2 positive) • Cytotoxic chemotherapy
HER2	5 - 15 %	73 - 88 %	• Surgery • Local radiotherapy • Anti-HER2 receptor monoclonal antibody • Cytotoxic chemotherapy
Triple negative	15 - 20 %	75 - 89 %	• Surgery • Local radiotherapy • Cytotoxic chemotherapy

Table 1-1 A summary of the prevalence, prognosis and treatment options for breast cancer subtypes

Basal-like and/or triple negative tumours are potentially of greater interest in terms of research because of their substantial clinical impact. They are more likely to occur in younger patients, are generally of larger size, higher grade, are more likely to have lymph node involvement at diagnosis and are biologically more aggressive (Partridge et al., 2016). There is variation within published studies as to whether tumours of special type which show basal characteristics, either morphology or IHC

markers, are included within the basal-like group (Gazinska et al., 2013, Leidy et al., 2014). This is important as the prognosis for special types can vary compared with basal-like invasive carcinoma NST, for example adenoid cystic and medullary carcinoma tend to have a better prognosis compared with stage matched invasive carcinoma NST whereas claudin-low subtype tends to do worse (Leidy et al., 2014). The triple negative subtype tends to relapse early, within 3-5 years, compared with other breast cancer subtypes, for example subtypes such as luminal A have a gradual increase in relapse rate and mortality as time passes, particularly after 10 years (Haque et al., 2012). Triple negative tumours are also more likely to show *BRCA1/2* inactivation, due to germline mutation and subsequent loss of heterozygosity, somatic mutation or promoter hypermethylation (Timms et al., 2014).

Interestingly, and potentially importantly in the context of my cell line based work, genomic studies of breast cancer cell lines have shown that their profiles also reflect the heterogeneity seen in primary breast tumours, suggesting that cell lines may reflect the subtype-specific behaviours seen clinically. Studies have also identified subgroups within the triple negative breast cancer cell lines based on gene expression profiling. The number of different groups identified and the name given to each group varies slightly from study to study. The profiles of these groups have been compared with breast tumour profiles and three main broad groups have been identified, a basal-like group, a mesenchymal/stem cell-like group and a luminal-like group (Neve et al., 2006, Lehmann et al., 2011).

1.1.3 Basal-like and triple negative subtypes

Within the NST group there is a recognised subset of tumours that co-express proteins normally expressed on the outer myoepthelial or basal layer of breast ducts. These proteins include the high-molecular weight cytokeratins CK5/6, CK14, CK17, epidermal growth factor receptor (EGFR), and smooth muscle markers such as smooth muscle actin and S100 protein (Fulford et al., 2006, Thike et al., 2010). There is no consensus definition or terminology for this subgroup, which contributes up to 15 % of all breast tumours (Fulford et al., 2006, Badve et al., 2011). The group is referred to as basaloid, basal-like, myoepithelial phenotype or the triple negative subtype (Jones et al., 2001, Nielsen et al., 2004, Rakha et al., 2008). Referring to this group as ‘triple negative subtype’ or using these terms synonymously is particularly

unhelpful as they are distinct groups. Although there is considerable overlap between these groups, not all basal-like breast cancers are ER-/PR-/HER2- and not all triple negative breast cancers show basal-like morphological features or have CK5/6, CK14 or CK17 positivity (Badve et al., 2011). For example, in studies where tumours have been grouped as basal-like by gene expression profiling, 14 - 46 % were ER positive (Sorlie et al., 2001, Calza et al., 2006, Nielsen et al., 2004). It is important to define the method and criteria by which breast cancer cases are subtyped to enable comparison between studies. It has been shown that age, grade and stage matched basal-like tumours have a worse prognosis following metastasis (Fulford et al., 2007). Basal-like tumours tend to be high grade and have specific identifying morphological features, including the presence of a central scar, tumour necrosis, spindle cells, squamous metaplasia, high mitotic count and high nuclear-cytoplasmic ratio (Fulford et al., 2006). Examples of these features are shown in Figure 1-1.

1.2 Breast tumour composition

1.2.1 Breast cancer cells

Breast cancer cells originally derive from luminal epithelial cells within the breast. The clinical classification of breast cancer is based primarily on the receptor expression and morphology of these cells and our understanding of breast cancer behaviour is based on the biology of these cells. However, breast cancer is a disease not only of transformed epithelial cells, but also as a consequence of their interaction with the stromal environment. Stroma is present in every breast cancer alongside the breast cancer cells and comprises of a number of different cellular components and extracellular matrix (see Figure 1-2).

1.2.2 Breast tumour stroma

The genetic alterations that arise in breast luminal epithelial cells during their progression to become cancer cells cause changes in epithelial cell phenotype and behaviour stimulating changes in surrounding cells and the extracellular matrix (ECM) (Ronnov-Jessen et al., 1996). Within a tumour, the fibroblasts, endothelial cells, inflammatory cells, other non-epithelial cells and ECM are collectively known as tumour stroma.

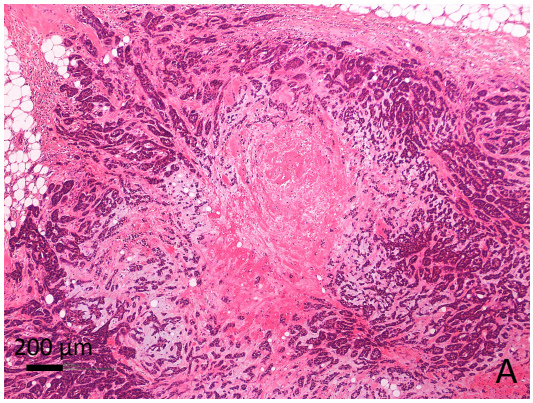

(A) Central scar within the tumour (low power)

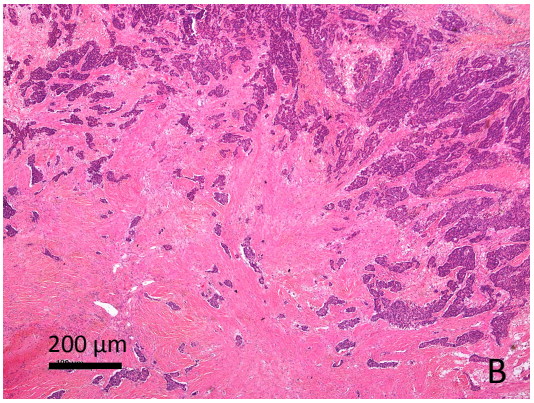

(B) Central scar within the tumour (high power)

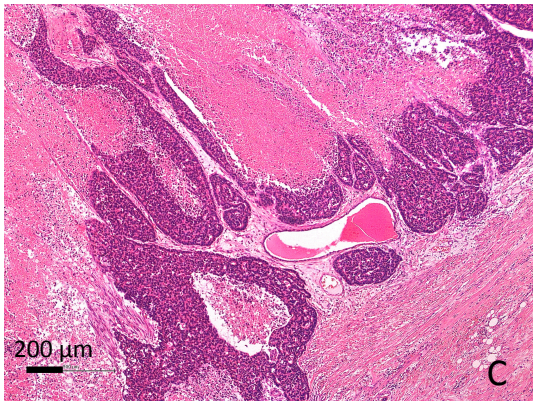

(C) Extensive tumour necrosis

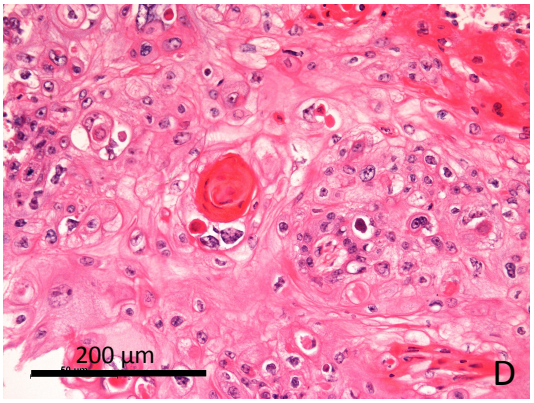

(D) Squamous metaplasia

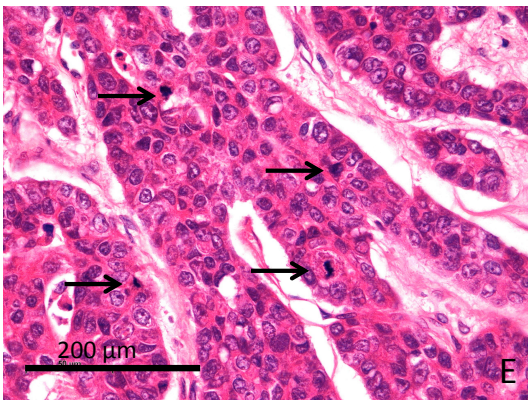

(E) Numerous mitoses within a single high power field

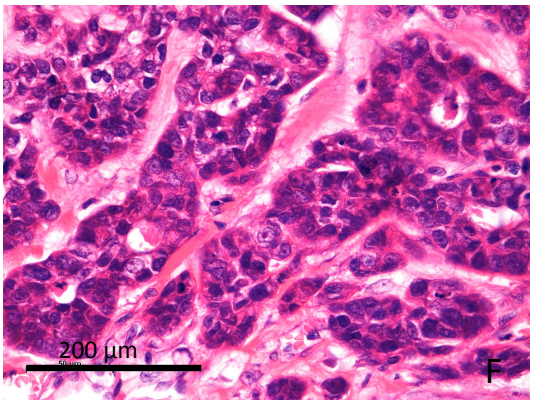

(F) High nuclear to cytoplasmic ratio

Figure 1-1 Representative histological features of basal-like breast tumours

Basal-like breast tumours were stained with haematoxylin and eosin (H&E) and images were selected to demonstrate specific features typical of the tumour type. A and B show a central scar within a tumour (A: low power; B: high power). C shows extensive tumour necrosis. D shows squamous metaplasia. E shows a high number of mitoses (arrows) within a single high power field. F shows high nuclear to cytoplasmic ratio (also nuclear pleomorphism and prominent nucleoli).

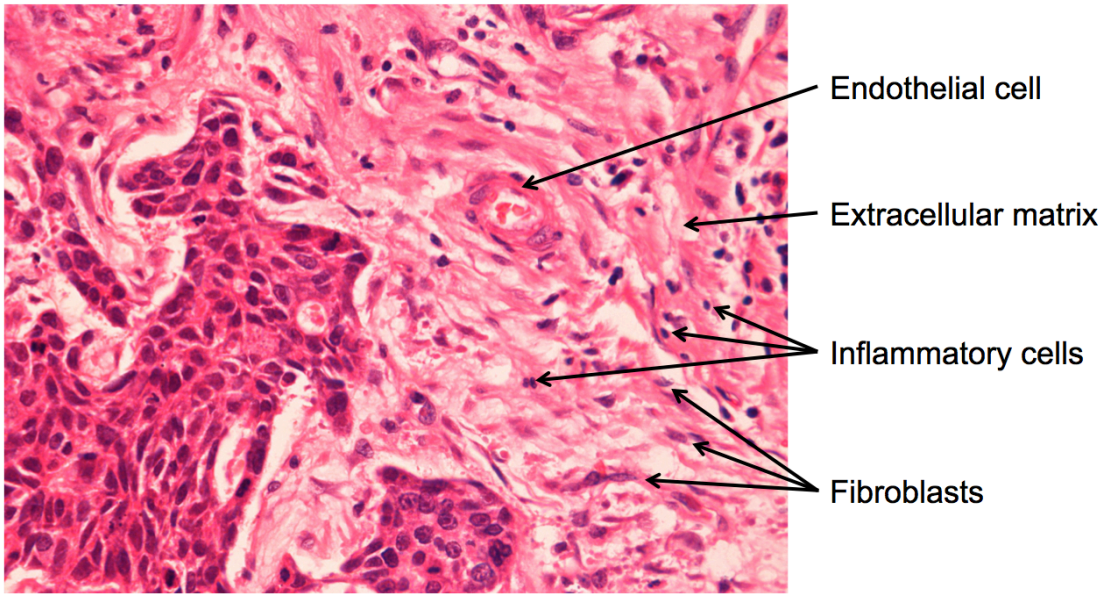

Figure 1-2 H&E image of breast cancer highlighting the different elements that make up tumour stroma

1.2.2.1 Extracellular matrix

In normal tissue the ECM provides a structural scaffold and contributes to the tensile strength of the tissue necessary to maintain tissue integrity. It includes the basement membrane, predominantly made up of collagen type IV, laminin, entactin and proteoglycans, loose intralobular stroma and more tightly packed interlobular stroma, predominantly composed of fibrillar collagens (types I and III), proteoglycans and glycoproteins (Lu et al., 2012). The ECM provides an adhesive surface for cells, provides cell survival signals via integrins, controls the mechanical forces cells are subject to and can regulate stability and bioavailability of growth factors and cytokines (Hynes, 2009, Oskarsson, 2013). It can interact directly with epithelial cells and influence the way they behave, for example without contact with laminin-1 epithelial cells fail to differentiate and produce milk under the hormonal influence of prolactin (Streuli et al., 1995, Oskarsson, 2013). The ECM is predominantly produced and maintained by fibroblasts, although some components of the basement membrane are made by myoepithelial cells (Chong et al., 2012, Gudjonsson et al., 2002). The basement membrane is obviously key to an important step in tumour development, progression from *in situ* to invasive disease – only once this layer has been breached can the cancer potentially spread beyond the breast and

result in death. This involves not only proteolysis, but also suppression of myoepithelial cell behaviour and alterations in tumour cell adhesion (Muschler and Streuli, 2010). Once the breast cancer becomes invasive there is increased crosslinking of the ECM and increased production of collagen and hyaluronic acid (Itano and Kimata, 2008, Provenzano et al., 2008, Levental et al., 2009). These biochemical and mechanical changes make the ECM stiffer. ECM molecules may also play a role in metastasis, establishing a premetastatic niche in non-mammary tissues (Psaila and Lyden, 2009).

1.2.2.2 Tumour vasculature

Development of a tumour vasculature is essential for tumours to grow beyond 500 μm (Brem et al., 1976). The tumour vasculature provides nutrients and oxygen to the tumour cells and removes waste products. Tumour vasculature is formed by co-opting existing blood vessels or through neoangiogenesis. It is not always easy to discern which process has lead to formation of the tumour vasculature within a given tumour as in either case the tumour vessels are abnormal, fragile and hypermaleable (Ziyad and Iruela-Arispe, 2011). Angiogenesis, the formation of new blood vessels from existing ones, is normally very tightly regulated, and is only activated in certain situations such as wound healing. Angiogenesis begins with activation of endothelial cells, which then release proteases that degrade the basement membrane. Endothelial cells and pericytes migrate into the surrounding matrix and proliferate, forming sprouts. These sprouts migrate towards the angiogenic stimulus along a chemotactic gradient using integrin adhesion molecules. Eventually the sprouts form a loop and develop a lumen to form a fully developed blood vessel connected to the original vessel they sprouted from (Flores-Perez et al., 2016). Co-opted blood vessels occur when the tumour expands and progressively takes over the local vasculature, changing the resident vessels physiology and morphology (Ziyad and Iruela-Arispe, 2011). The development of the tumour vasculature requires a proangiogenic environment established by tumour cells, cancer associated fibroblasts and resident inflammatory cells. Key molecules involved in the process of sprouting angiogenesis include hypoxia-inducible factor 1-α (HIF-1α), vascular endothelial growth factor A (VEGF-A), transforming growth factor–β (TGF-β), angiopoietins and plasminogen (Flores-Perez et al., 2016, Cesario et al., 2016, Gouri et al., 2016). VEGF stimulates endothelial proliferation and

migration, inhibits endothelial apoptosis, induces proteinases involved in ECM remodelling, increases vascular permeability and vasodilatation, and inhibits antigen-presenting dendritic cells.

1.2.2.3 Inflammatory cells

The immune system is thought to play a dual role in tumour development. Initially the immune system can suppress tumour growth by destroying cancer cells and/or inhibiting tumour outgrowth (Kaplan et al., 1998, Schreiber et al., 2011). It is only when the tumour has developed the ability to evade immune system recognition that the tumour can become established. Inflammatory cells may then play a role in supporting tumour growth, angiogenesis, invasion and metastasis (Ziyad and Iruela-Arispe, 2011). This section focuses on an established tumour where the tumour promoting influence of the immune system predominates. The inflammatory cells within a tumour are drawn from both the innate and adaptive arms of the immune system. Innate immune system cells including tumour associated macrophages (TAMs, mostly M2-type), neutrophils (N2-type) and mast cells promote tumour development by promoting angiogenesis, stimulating fibroblast proliferation and secreting factors involved with ECM-degradation and remodelling, the ECM changes can in turn promote metastatic spread (Pollard, 2009, Condeelis and Pollard, 2006, DeNardo et al., 2009, Nozawa et al., 2006, Coussens et al., 1999). The innate immune system cells can also produce factors that influence each other to convert to and maintain a tumour promoting phenotype, for example neutrophils produce IL-13 which may polarise TAMs to become M2-type (Neill et al., 2010, Nozawa et al., 2006, Shojaei et al., 2008, Egeblad et al., 2010). Tumour-infiltrating lymphocytes have been reported as positively associated with improved response to chemotherapy and survival in breast cancer (Denkert et al., 2010). However, cancers that show up-regulated programmed cell death ligand 1 (PD-L1) are able to inactivate lymphocytes within the tumour via interaction with programmed cell death protein 1 (PD-1) on the T-cell surface (Pardoll, 2012). The adaptive arm of the immune system can also contribute to tumour development as T_h2 T-helper cells produce cytokines that polarise TAMs to M2-type and T-regulatory cells directly suppress the anti-tumour activity of CD8+ cytotoxic T-cells (DeNardo et al., 2009, Yu et al., 2005). Increased infiltration with immune system cells, particularly

macrophages, is a poor prognostic sign in breast cancer (Leek et al., 1996, de Visser et al., 2006).

1.2.2.4 Fibroblasts

The most prominent change in breast stromal composition in response to neoplasia is an increase in the number of fibroblasts (Ronnov-Jessen et al., 1996, Orimo et al., 2005). They are the most common cell type in breast tumour stroma and are known as tumour associated or cancer associated fibroblasts (CAFs). CAFs proliferate more rapidly than normal fibroblasts and show greater activity and influence on surrounding cells. Other than location, there is no consensus way of defining or characterising CAFs and there is no specific marker that identifies all CAFs. Markers most frequently noted to be more highly expressed in CAFs compared with non-tumour fibroblasts include α-smooth muscle actin (α-SMA), vimentin, fibroblast specific protein 1 (FSP1) and fibroblast activation protein (FAP), although these markers are often shared with other cells including myofibroblasts, myoepithelial and mesenchymal stem cells and are not expressed by all CAFs (Huang et al., 2010, Kojima et al., 2010, Orimo et al., 2005, Liu et al., 2006, Sugimoto et al., 2006, Fearon, 2014). Markers with decreased expression in CAFs, compared with mammary fibroblasts not grown with breast cancer cells, include caveolin-1 and laminin (Mercier et al., 2008, Madar et al., 2013).

The precise origin of CAFs is not fully understood. Several studies have suggested that mammary normal fibroblasts (NFs) may develop into CAFs and have shown progressive increases in α-SMA expression in mammary fibroblasts with tumour development using an *in vivo* mouse model with human breast fibroblast and carcinoma lines (Kojima et al., 2010). Another study demonstrated epithelial-to-mesenchymal transition as a possible source of CAFs by stimulating a bladder cancer cell line with Fibroblast Growth Factor-1 (Billottet et al., 2008). An interesting study looking at male to female bone marrow stem cell transplants, identified cells with Y-chromosome (male cells) that also expressed α-SMA in subsequent tumours that developed in these (female) patients, suggesting that some CAFs may have derived from bone marrow cells (Worthley et al., 2009). Other possible sources of CAFs include endothelial cells that have undergone endothelial-to-mesenchymal transition following transforming growth factor-β (TGF-β)

stimulation (Zeisberg et al., 2007). In each of these studies the CAFs identified from a particular source account for some but not all of the CAFs within the tumour. This suggests that CAFs may be derived from a number of sources. It is not known whether characteristics of the person, factors within the tumour, or tumour type may determine from where the majority of CAFs derive in each tumour.

One molecule that may be involved in stimulation of the CAF phenotype is stromal cell-derived factor-1 (SDF-1, CXCL12), which increases CAF α-SMA expression. A second candidate is TGF-β, which is secreted by CAFs, stimulates α-SMA expression and CAF tumour-promoting chemokine secretion (Kojima et al., 2010, Kuzet and Gaggioli, 2016). Fibroblasts grown with breast cancer cells *in vivo* showed progressive increase in TGF-β expression in CAFs with time. In correlation with the increase in TGF-β expression Smad2/3, a TGF-β signal transducer, translocated to the nucleus suggesting activation of Smad2/3 signalling in CAFs. SDF-1 expression in CAFs also increased with time cultured with tumour cells as did expression of SDF-1 receptor CXCR4. This suggests that CAFs respond to signals that perpetuate the CAF phenotype via autocrine signalling loops, possibly explaining the finding that the CAF phenotype is maintained in *in vitro* culture without continuous interaction with tumour cells (Kojima et al., 2010, Orimo et al., 2005).

CAFs play a central role in the tumour stroma by interacting with many of the stromal elements. CAFs produce a wide variety of matrix components including collagen type I, tenascin C and fibronectin as well as matrix remodelling enzymes such as matrix metalloproteinase 1 (MMP1) and MMP3 (Augsten, 2014). CAFs produce cytokines and chemokines that interact with the immune system such as IL-6 and IL-8, which stimulate macrophages and induce chemotaxis in neutrophils respectively (Balkwill, 2004). They play a role in establishing tumour blood supply by producing pro-angiogenic factors such as vascular endothelial growth factor (VEGF) and SDF-1 that can recruit endothelial progenitor cells (Kalluri and Zeisberg, 2006, Kuzet and Gaggioli, 2016). Most important is the role CAFs play in promoting tumour growth, invasion and metastasis, partly through the previously mentioned interactions with other stromal elements, but also through direct interaction with tumour cells. These include secretion of SDF-1, which directly stimulates CXCR4 on tumour cells leading to increased tumour cell migration and

metastatic ability; hepatocyte growth factor (HGF) which stimulates increased epithelial-mesenchymal transition and cell motility; and ADAMTS1 (a disintegrin and metalloproteinase with thrombospondin type 1 motif) which stimulates breast cancer cell invasion *in vitro* (Orimo et al., 2005, Balkwill, 2004, Kuzet and Gaggioli, 2016, Tyan et al., 2012). As well as paracrine signalling, it is thought that CAFs may mediate some of their effect by direct cell-cell contact with tumour cells (Sadlonova et al., 2009). CAFs have been shown to play a direct role in facilitating tumour cell invasion by formation of a pathway of reduced resistance through the ECM by directed ECM remodelling (Gaggioli, 2008).

The tumour microenvironment and particularly CAFs play a dynamic role in tumour behaviour, highlighted by the response to chemotherapy. Following treatment with chemotherapy a dramatic increase in number of CAFs can be observed and targeting CAFs alongside tumour cells produced an enhanced response, reducing recruitment of tumour-promoting immune cells and inhibiting angiogenesis, in a colorectal cancer model (see section 1.2.2.3) (Li et al., 2016). CAFs can also mediate chemoresistance through secretion of prostaglandin E_2 and sphingosine-1-phosphate; via activation of the PI3K-Akt pathway and by ECM remodelling causing increased tension between fibres increasing interstitial pressure and diminishing drug delivery (Castells et al., 2012, Heldin et al., 2004, Sirica, 2011).

1.2.3 Tumour stroma ratio

The proportion of stroma within a tumour varies from one patient to another, with stroma being 20-90% of the tumour (Dvorak, 1986). The proportion of tumour that is stroma can be visually estimated using the tumour stroma ratio (TSR). The TSR has been shown to be of prognostic significance in a number of solid tumours, including colorectal cancer, oesophageal adenocarcinoma, non-small cell lung cancer, early cervical carcinoma and triple negative breast cancer; in all these examples, tumours that are more than 50% stroma are associated with worse prognosis and shorter relapse-free survival (Mesker et al., 2009, Courrech Staal et al., 2010, Wang et al., 2013, Liu et al., 2014a, de Kruijf et al., 2011, Dekker et al., 2013, Moorman et al., 2012). Within breast cancer the importance of TSR on patient prognosis varies according to subtype. The influence of TSR in ER+ breast cancer is less clear cut with one study indicating low TSR actually may actually confer better

survival, although other studies show different results (Downey et al., 2014, Dekker et al., 2013, de Kruijf et al., 2011). This variability may in part be due to the different ways TSR is estimated. It can be done by examining the whole tumour area and basing the TSR on a visual assessment of the area with the highest degree of stromal formation or by selecting a smaller tumour area and superimposing a grid with systematic random points and assessing each point individually. In triple negative breast cancer TSR is consistently identified as an independent prognostic factor, the 5 year disease free survival in stroma-poor tumours is over 80% whereas in stroma-rich tumours it is approximately 50% (Moorman et al., 2012, de Kruijf et al., 2011).

1.2.4 Stromal targeted therapies

Given the importance of the role of the stroma in patient prognosis it is not surprising that drugs targeting the stroma is a highly active area of research. The complex interactions between different elements that make up the stroma and the difficulty in differentiating tumour stroma from normal stroma have meant that successfully translating these drugs from experimental models to human trials has not always had the expected outcome. Of the drugs available these are at differing stages of development and show varying results.

One of the most controversial stromal targeted therapies is bevacizumab (Avastin). Bevacizumab is classified as an anti-angiogenic, an inhibitor of all isoforms of vascular endothelial growth factor A (VEGF-A). Bevacizumab has been shown to be of benefit and is licenced for use in metastatic colorectal cancer, non-small cell lung cancer, renal cell carcinoma and glioblastoma multiforme (Wagner et al., 2012). In phase III randomised, double-blind placebo controlled trials of metastatic breast cancer it has been shown to improve overall response rate and progression free survival, but not to have a significant effect on overall survival or quality of life for the patient (Miller et al., 2007, Robert et al., 2011, Miles et al., 2010, Wagner et al., 2012). It is currently licensed for use in metastatic breast cancer in the European Union, although it is no longer recommended by the National Institute for Health and Care Excellence (NICE) and approval in the USA has been withdrawn.

Other anti-angiogenic treatments include vandetanib, an inhibitor of the VEGF receptor, which is licensed for use in medullary thyroid cancer, and an antibody to

the angiogenic stimulator platelet-derived growth factor C, which inhibits growth of anti-VEGF resistant tumour cells in co-culture with CAFs but has not yet entered routine clinical use (Crawford et al., 2009).

There have been attempts to counteract the increased activity of MMPs using Matrix metalloproteinase inhibitors (MMPI), such as tanomastat, prinomastat and marimastat. These are anti-angiogenic, and inhibit migration of cells through their effects on ECM remodelling and may have a role in fibroblast differentiation. This group of drugs showed promising effects on breast cancer spread in animal models, with significant decrease in the number and size of metastatic deposits in a mouse model following resection of the primary tumour (Sledge et al., 1995). In patient trials the most promising results have been seen in the phase III clinical trial of marimastat in advanced gastric cancer that showed an increase in progression-free survival and overall survival compared with placebo (Bramhall et al., 2002). Phase III trials of the MMPI tanomastat have not been as promising, with trials halted early due to significant increase in disease progression and mortality in small cell lung cancer compared with placebo (Brown, 2000). In breast cancer development of marimastat has faltered due to serious musculoskeletal adverse effects in phase II trials and poor pharmacokinetics, with the drug falling below therapeutic levels between doses (Miller et al., 2002, Overall and Kleifeld, 2006). There is hope that third generation MMPI with improved specificity will have wider clinical use with fewer adverse affects (Cepeda et al., 2016). There has also been advancement in understanding that MMPs may have different roles depending on tumour stage and that treating early stage tumours is more likely to have the desired effect than later stage metastatic disease (Overall and Kleifeld, 2006).

Volociximab, another ECM targeting drug, inhibits angiogenesis by blocking the interaction between $\alpha_5\beta_1$ integrin and fibronectin. It has been shown to have a low toxicity profile in phase I and II clinical trials but unfortunately only limited effects in patients with ovarian or peritoneal cancer (Bell-McGuinn et al., 2011, Ricart et al., 2008).

1.2.4.1 Therapies targeting CAFs

Given the inter-connectedness of the tumour stroma and the central role CAFs play in co-ordinating between many different stromal parts, CAFs provide an ideal target

to influence many aspects of the tumour microenvironment. Treatments that target CAFs are an emerging area of investigation, however development has been limited by the lack of clarity concerning the origin of CAFs and the lack of a CAF-specific marker. Fibroblast activation protein (FAP) is a CAF marker that has shown some promise. Although it is expressed in wound healing myofibroblasts and weakly in normal fibroblasts, it is expressed at much higher levels in CAFs. FAP has been targeted in a number of different approaches: using a monoclonal antibody against FAP to stimulate an immune response to the tumour microenvironment; using a small molecule inhibitor of FAP activity (FAP is a protease); and harnessing the activity of FAP to convert a prodrug to its active form within the tumour, as detailed below.

Sibrotuzumab, a monoclonal antibody against FAP demonstrated a good safety profile in phase I trials of patients with colorectal and non-small cell lung cancer, although no objective tumour response was seen (Scott et al., 2003). One possible explanation for this is the effectiveness of the tumour microenvironment in switching the immune reaction to a tumour promoting response.

Talabostat (PT-100), an FAP inhibitor, has shown a modest effect *in vitro* and *in vivo* in models of colorectal and breast cancer where it slowed tumour growth (Huang et al., 2011). It showed a much greater effect in colorectal cancer models when combined with the chemotherapeutic oxaliplatin, with greatly reduced tumour growth and increased overall survival (Li et al., 2016). Oxaliplatin has been shown to stimulate accumulation of CAFs and an increase in CAF associated cytokines, which explained the increased response to combined treatment. Talabostat has shown good safety profiles, but no strong evidence of clinical effectiveness in phase II clinical trials in patients with non-small cell lung cancer (Eager et al., 2009).

Harnessing the activity of FAP as a way to target drugs specifically and exclusively to the tumour has been attempted. The naturally occurring plant toxin Thapsigargin (TG) is a potential candidate cytotoxic that can be targeted to FAP expressing cells. TG exerts its cytotoxic effects by causing a rise in intracellular calcium leading to apoptosis and therefore is effective against cells that are not actively dividing as well as those that are. When TG is bound to a FAP-specific peptide, this peptide prevents TG from being able to enter cells. When in contact with FAP expressing cells the

peptide with a FAP-specific cleavage site was cleaved and the active form of the TG toxin became available. This prodrug has shown promising results *in vitro* and *in vivo* using the breast cancer cell line MCF-7 and because of its specificity very low concentrations of the prodrug were effective (Brennen et al., 2012). One possible problem with this approach is the small but potentially important effect of soluble-FAP activity in human plasma (Lee et al., 2006).

1.3 MicroRNAs

MicroRNAs (miRNAs) are short, non-coding single-stranded RNA molecules of ~21-22 nucleotides (nt) that act as post-transcriptional regulators of protein expression. Over 1,800 precursor and 2,500 mature *Homo sapiens* miRNA sequences have been identified, predominantly by small RNA deep sequencing (MiRbase, 2016, Kozomara and Griffiths-Jones, 2014). MiRNAs have been shown to be involved with many biological processes including cell growth, differentiation, tissue morphogenesis and apoptosis (Kloosterman and Plasterk, 2006). The link between miRNAs and cancer was first made in 2002 in B cell chronic lymphocytic leukaemia where deletion or down-regulation of miR-15 and miR-16 was seen in 68% of cases (Calin et al., 2002).

1.3.1 MicroRNA production

The majority of miRNAs are encoded by their own independent transcription units located in regions between protein coding genes. Alternatively, there are also a large number located intronically that are transcribed with the host mRNA (Ambros et al., 2003, Lin et al., 2006, Barik, 2008, Frediani and Fabbri, 2016). In some cases several miRNAs are located within the same region, and can be transcribed as a single transcript that is subsequently cleaved to produce individual miRNAs. MiRNAs are transcribed by RNA polymerase II as primary transcripts of several kilobases in length and include both a 5' cap and a 3' poly-adenylated (poly-(A)) tail (Yin et al., 2015). Primary transcripts (pri-miRNAs), typically several kilobases in length, base-pair internally to form hair-pin loops containing the bases destined to form mature miRNAs. The heterodimer Drosha, an RNase III type endonuclease, and DGCR8 (DiGeorge syndrome critical region 8) recognise the hair-pin structures and cleave the pri-miRNA to a ~70 nt precursor miRNA (pre-miRNA) (Zeng, 2006,

Lee et al., 2003). Following export from the nucleus by exportin 5 and cofactor Ran-guanosine triphosphate (Ran-GTP), Dicer cleaves pre-miRNAs into molecules with ~20 nt double-stranded sections with 2 nt single-stranded overhangs at each end (Ketting et al., 2001, Svobodova et al., 2016, Kim et al., 2016). Argonaute proteins interact with these as part of the ribonucleoprotein RNA induced silencing complex (RISC). RISC selects and stabilises the mature miRNA allowing the double stranded miRNA sequence to unwind and separate to form a single stranded mature miRNA, with the complementary strand being discarded, see Figure 1-3 (Graves and Zeng, 2012).

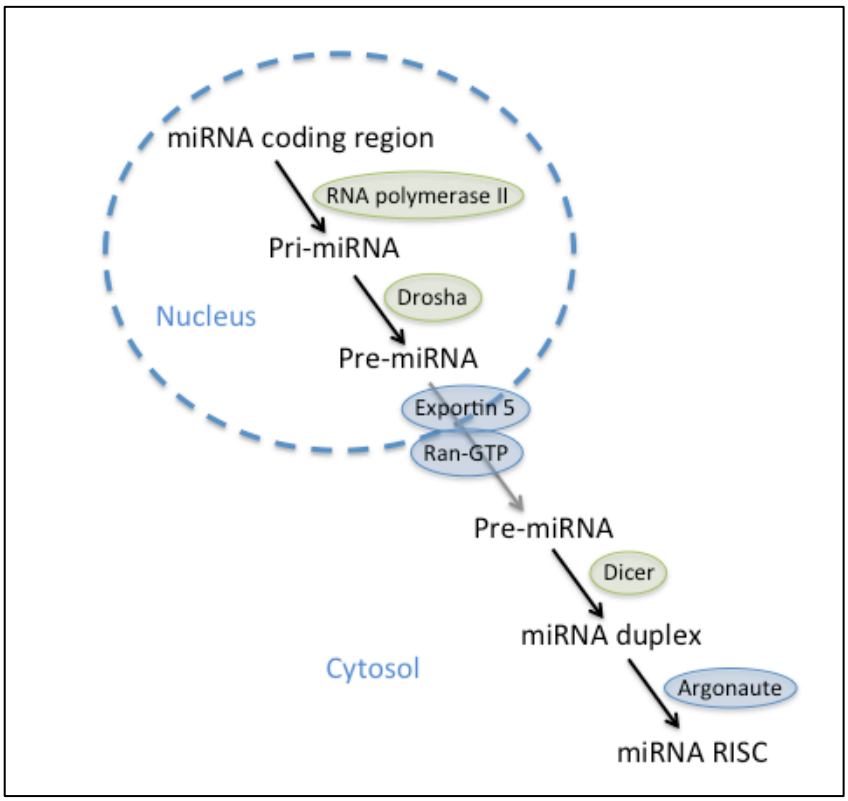

Figure 1-3 MiRNA biogenesis

The process of miRNA biogenesis begins with transcription followed by successive cleavage steps to produce the final mature miRNA strand in complex with RISC. The key enzymes involved in the process are highlighted in green.

1.3.2 The mechanism of action of microRNAs

There are thought to be two main mechanisms by which miRNAs functionally regulate protein expression. The first mechanism occurs when miRNAs bind to the

3’ untranslated region (UTR) of target mRNAs resulting in translational repression, and in some instances mRNA deadenylation and degradation (Filipowicz et al., 2008, Fabian and Sonenberg, 2012). This mechanism requires only imperfect complementarity (further detail regarding this binding is outlined below). The second mechanism occurs when the miRNA binds with perfect or near perfect complementarity within the open reading frame of the target mRNA resulting in cleavage and degradation of the target mRNA by the Argonaute component of RISC (Reis et al., 2015). This process is dominant mainly in plants, so I will therefore focus on the former mechanism.

Several studies have shown that miRNAs cause a decrease in their target mRNA levels and that when a miRNA pathway is inhibited or miRNA levels are experimentally increased or decreased target mRNA levels are inversely altered (Guo et al., 2010, Giraldez et al., 2006). However, many studies have also shown that mRNA degradation is not the only outcome and that miRNA silencing can occur without mRNA degradation and that reversal of repression can occur quickly when cellular conditions are altered, indicating that the intact mRNA can still be present (Yang et al., 2010, Bhattacharyya et al., 2006).

Functional repression of protein expression by miRNA complexes is thought to take place at the translation initiation stage. Translation of mRNAs proceeds from the 5’ to the 3’ end. Given that miRNAs bind to the 3’ UTR, circularisation of mRNAs must occur as part of translation initiation in these situations. The precise molecular interactions by which miRNA-RISC interferes with initiation is unclear. It has been shown that Argonaute and the glycine-tryptophan repeat family proteins, GW182, components of RISC are essential for miRNA mediated silencing as when either is depleted or their interaction is blocked miRNA mediated silencing is impaired (Fabian and Sonenberg, 2012, Behm-Ansmant et al., 2006, Schmitter et al., 2006, Eulalio et al., 2008). It has also been shown that artificially tethering Argonaute or GW182 to target mRNAs causes repression, suggesting that miRNAs determine which mRNAs are targeted but are not directly involved in silencing expression (Behm-Ansmant et al., 2006, Pillai et al., 2004).

Various studies have indicated interaction with a number of stages of initiation including the binding of eukaryotic translation initiation factors (eIFs) and ribosomal

recruitment. In particular, miRNA-RISC is thought to interfere with the binding of eIF4G, with eIF4G-eIF4E interaction and with eIF4E recognition of and binding to the 7-methylguanylate (m^7G) cap of the mRNA (Kiriakidou et al., 2007, Pillai et al., 2005, Fabian and Sonenberg, 2012). The presence of a m^7G cap has been shown to be required for translational repression, and a poly(A) tail - whilst not essential - confers greater sensitivity to miRNA activity. In HEK-293 cells, miRNA mediated translation repression was partially relieved by the addition of non-physiological length poly(A) tails over 0.8 kb in length (Wang et al., 2006, Filipowicz et al., 2008, Pillai et al., 2005, Humphreys et al., 2005, Walters et al., 2010). One candidate for this mechanism of action is poly(A) binding protein (PABP) that can interact with eIF4G to stimulate mRNA circularisation and translation. GW182 has been shown to interact with PABP and may inhibit this function (Huntzinger et al., 2010). It has been shown that there is decreased ribosomal 60S subunit recruitment in miRNA targeted mRNA, confirming that inhibition occurs at the initiation stage (Fabian and Sonenberg, 2012, Wang et al., 2008).

MiRNAs not only repress translation but can also cause mRNA decay, via the deadenylation-dependent pathway. It is suggested that even where degradation of mRNA occurs, translational repression may precede this event (Chen et al., 2009). MiRNA mediate mRNA degradation by targeting them to processing/GW-bodies, which are cytoplasmic sites of mRNA degradation (Liu et al., 2005). The CCR4-NOT deadenylation complex has been shown to be required for miRNA mediated mRNA decay. When CAF1 or NOT1 proteins, both of which form part of the CCR4-NOT complex, were depleted, mRNA degradation but not translation repression was inhibited (Behm-Ansmant et al., 2006). Chen *et al.* confirmed the requirement for CCR4-NOT and showed that its action can be assisted and hastened by PAN2-PAN3 mediated poly(A) shortening and is followed by DCP2 mediated decapping (Chen et al., 2009). PABP is also proposed to enhance miRNA mediated deadenylation by bringing miRNA-RISC recruited deadenylation machinery close to the poly(A) tail. PABP over-expression in HEK-293 cells led to partial derepression of miRNA mediated silencing in part through decreased deadenylation of target mRNAs, and depletion of PABP in a mouse system prevented miRNA-mediated deadenylation (Fabian et al., 2009, Walters et al., 2010). Exactly how these complexes interact with each other and the miRNA-RISC is currently not fully

understood. It is not known what determines whether an mRNA will follow the degradation or translation repression pathway.

1.3.3 MicroRNA binding

There is reasonably good understanding regarding the base paring interactions between miRNAs and mRNAs. The seed region, nucleotides 2-8 at the miRNAs 5' end, is the area where base pairing specificity is very important for the miRNA-mRNA interaction. It requires perfect or near perfect complementarity and contiguous binding to the mRNA for miRNA binding and functionality (Doench and Sharp, 2004, Brennecke et al., 2005, Lewis et al., 2005, Filipowicz et al., 2008). Within the miRNA binding site on the mRNA, an adenine in position 1 and an adenine or uracil in position 9 improves the inhibitory ability of the miRNA even if these residues do not base pair with the miRNA (Lewis et al., 2005, Nielsen et al., 2007). Reasonable complementarity towards the 3'end, particularly between residues 13-16, stabilises the interaction (Grimson et al., 2007). Although, mismatches and bulges can be tolerated in this region. This region becomes more influential when the seed region base pairing is suboptimal, see Figure 1-4.

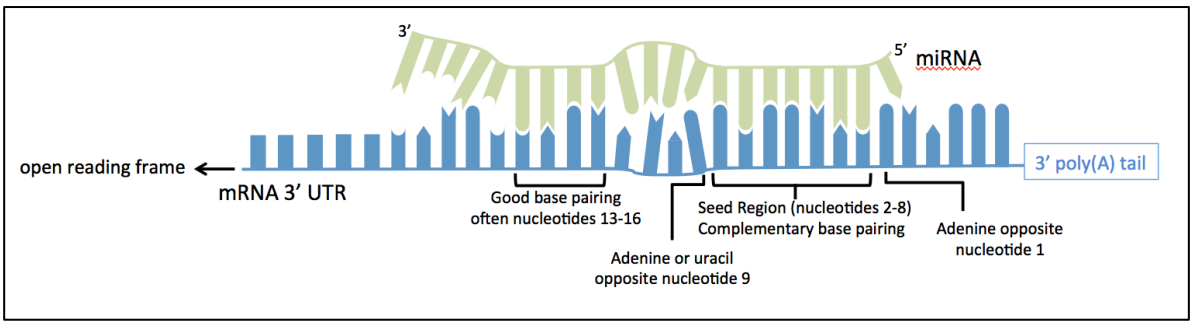

Figure 1-4 MiRNA binding

This diagram shows the important base pairing interactions for miRNA binding and targeting. The mRNA strand represented in blue and the miRNA in green, each base is represented by a coloured block.

The position of the miRNA binding site within the 3' UTR is also important. A site close to the termination codon or the poly(A) tail in long 3' UTRs improves inhibitory ability. MiRNA binding sites within the 3' UTR are often present in multiple copies. Multiple sites for the same or different miRNAs are generally

required for effective repression (Vella et al., 2004). Sites that are 10-40 nt apart tend to act co-operatively (Grimson et al., 2007). There is no evidence to suggest that the RISC has any miRNA or mRNA binding specificity.

Unfortunately, these binding criteria are sufficiently general that bioinformatic predictions frequently identify many hundreds or thousands of possible sites for any miRNA of interest; critically, often only a few of these turn out to be within mRNAs actually targeted by the miRNA. In addition, some experimentally characterised binding sites deviate substantially from these rules, even requiring a bulged nucleotide in the seed region (Vella et al., 2004). For these reasons experimental confirmation is essential to confirm mRNA targets.

1.3.4 MicroRNA nomenclature

MicroRNA (miRNA) naming conventions have changed over time as more is known about them. Currently the full name of a miRNA will include the species abbreviation e.g. hsa for *Homo sapiens*, miR to indicate that it is a mature miRNA sequence and the number assigned to that sequence, for example hsa-miR-101. A -3p or -5p suffix may be added if both arms of the hairpin precursor are processed into mature miRNA; this indicates which arm of the hairpin is being referred to, for example miR-17-5p and miR-17-3p are different mature sequences processed from opposite arms of the same hairpin loop. Sometimes a letter or number suffix may be added to the miRNA name to indicate different miRNA of the same family. A letter is added for miRNA mature sequences that have very similar mature products, e.g. hsa-miR-10a and hsa-miR-10b differ in only one base. A number is added to indicate identical mature miRNA that originate from distinct hairpin loci, e.g. hsa-miR-16-1 and has-miR-16-2 originate from chromosomes 13 and 3 respectively. Prior to this standardisation of miRNA naming an asterisk was sometimes used to indicate the minor miRNA product from a hairpin loop rather than -3p or -5p. A # was also previously used to indicate a precursor miRNA that gave rise to more than one mature miRNA, the ones labelled # were the less predominant of the product. The –as suffix indicating that the miRNA was transcribed from the DNA antisense strand is also no longer assigned to new miRNA that are identified, instead miRNA transcribed from opposite chromosomal strands are typically given different numbers (miRBase, 2011, Griffiths-Jones et al., 2006).

1.3.5 MicroRNAs as oncomiRs and tumour suppressors

The definition of the term oncomiR has evolved over time. Initially it was used to refer to miRNA that play an "oncogenic" role, more recently this term has been used more broadly to refer to a miRNA that is involved in a cancer, i.e. can function as an oncogene or a tumour supressor (Ma, 2016, Budd et al., 2015). To avoid confusion, I will avoid using the term oncomiR instead use the phrase oncogenic miRNA or tumour suppressor miRNA. MiRNAs act as oncogenes when their increased expression increases the likelihood or severity of cancer, presumably by targeting mRNA(s) coding for tumour suppressor protein(s); such as an anti-apoptotic factor, a protein involved with DNA repair, or a cell cycle inhibitor. One of the first miRNAs identified as having an oncogenic effect was miR-17. One mechanism through which miR-17 has its effect in lymphoma is via targeting the pro-apoptotic cell cycle transcription factor E2F1 (O'Donnell et al., 2005).

Conversely, a miRNA may act as a tumour suppressor by inhibiting translation of an oncoprotein. As mentioned in section 1.3, the first miRNAs found to be down-regulated in malignancy were miR-15 and miR-16. These miRNAs inhibit translation of BCL2, an important anti-apoptotic protein (Cimmino et al., 2005). Interestingly miR-17 in breast cancer has been indicated to have a tumour suppressive effect, decreasing breast cancer cell proliferation by inhibiting translation of the ERα co-activator AIB1 (Hossain et al., 2006). Identifying miRNAs that act as tumour suppressors and oncogenes, their target mRNAs, and the role the target proteins have in carcinogenesis, malignant transformation and metastasis is a key aim in furthering our understanding of cancer and could potentially lead to new and better targeted therapies.

1.3.5.1 Oncogenic and tumour suppressing miRNAs in CAFs

There have been a variety of studies looking at the expression and role of miRNAs in CAFs in a range of cancer types. I will focus on those studies that have looked at miRNAs in breast cancer CAFs – the vast majority of which are very recent. The majority of these studies identified miRNAs that were up-regulated or down-regulated in CAFs either by comparing primary CAFs and NFs isolated from fresh breast tissue or by measuring the levels of miRNAs in fibroblast conditioned medium. This identified a number of miRNAs with altered expression in CAFs,

including down-regulation of miR-320 and the miR-200 family and up-regulation of miR-9, miR-221/222, miR-378, miR-143 and miR-21 (Tang et al., 2016, Baroni et al., 2016, Donnarumma et al., 2017, Bronisz et al., 2011, Shah et al., 2015, Sansone et al., 2017). I have discussed the role of miR-21 in CAFs in a separate section (see section 1.4). Most miRNA identified have been investigated in one or two studies. The reason why different studies identified different miRNAs as up-regulated and down-regulated may be because they have looked at fibroblasts from different breast cancer subtype, although often this is not stated; in the initial analysis of a larger number of miRNA different miRNAs are included; or because the changes they observe are specific to the one or few fibroblasts they have analysed.

Following identification of miRNAs with altered expression the next step has generally been to confirm the functional role of the miRNA by increasing and decreasing expression of the miRNA(s) of interest in fibroblasts and assessing the impact this has on fibroblast behaviour and tumour cell behaviour in co-culture. The third avenue of investigation has been to identify targets for the miRNA by referring to published work and bioinformatics analysis, followed by confirmation of these targets using luciferase reporter assays of the targets mRNA 3'UTR. This has been done in very few breast cancer fibroblast studies. Further detail about each miRNA is outlined below.

The miR-200 family (miR-200a, miR-200b, miR-200c, miR-141 and miR-429) were down-regulated with a mean 2.5-fold change when comparing matched pairs of CAFs with NFs isolated from 20 breast cancer resection specimens. This was confirmed *in vitro* as when NFs were co-cultured with breast cancer cells they showed a significant decrease in miR-200 family expression after 30 days. MiR-200 family over-expression in CAFs decreased their migration and invasion. FLI1 and TCF-12 were confirmed as targets of the miR-200 family. These proteins are thought to be involved in ECM remodelling, which could explain the effect the miR-200 family has on migration and invasion of fibroblasts (Tang et al., 2016). MiR-200b has also been noted to be down-regulated in gastric cancer CAFs and to decrease CAF migration and invasion in this setting as well (Kurashige et al., 2015).

MiR-9 has been found to be increased in CAFs compared with NFs isolated from triple negative breast cancer patients, but not in other breast cancer subtypes. When

miR-9 was transfected into NFs it increased their migration and invasion and transfection of miR-9 inhibitor into CAFs decreased their migration and invasion. Fibroblasts transfected with miR-9 were found to secrete it into the cell culture medium, and conditioned medium from these fibroblasts increased migration, invasion and decreased E-cadherin expression in triple negative tumour cell lines. The mRNA targets of miR-9 were not explored in this study (Baroni et al., 2016).

MiR-143 and miR-378 were found to be present at higher levels in CAF exosome samples compared with NF exosomes isolated from breast biopsies. When T47D breast cancer cells were treated with the CAF exosomes they showed increased mammosphere formation and increased markers of stemness and epithelial to mesenchymal transition (EMT) (Donnarumma et al., 2017). These findings suggests that the influence of CAFs on tumour cell behaviour and protein expression may in part be mediated by miRNA secreted into exosomes that are then taken up by tumour cells.

PTEN has been frequently identified as down-regulated during the conversion of NFs to CAFs. In a breast cancer mouse model with PTEN-null fibroblasts, 9 miRNAs of the 400 profiled showed at least a 2-fold change and were conserved between mice and humans. MiR-320 was selected from these 9 for further investigation as it was previously reported as down-regulated in breast cancer. When miR-320 was re-expressed in PTEN-null fibroblasts in tissue culture conditioned medium from these fibroblasts lead to decreased tumour cell proliferation and migration. *In vivo* the mouse mammary tumours showed decreased tumour cell proliferation and decreased neoangiogenesis (Bronisz et al., 2011). MiR-320 has also been found to be down-regulated in CAFs in hepatocellular carcinoma. In hepatocellular carcinoma this decrease has been linked with increased tumour cell proliferation, migration and metastasis (Zhang et al., 2017b).

MiR-221/222 has been identified as secreted by breast CAFs into tissue culture medium. Conditioned medium from these cells has been shown to decrease ER expression in MCF-7 cells, and this repression was relieved when miR-221/222 was knocked down in CAFs (Shah et al., 2015). MiR-221 has also been found to be at increased levels in the serum of patients who developed metastases following hormone treatment for breast cancer (Sansone et al., 2017). If miR-221 plays a role

in decreasing ER expression in these patients, this would explain the increased chance of them becoming resistant to treatment.

1.4 MicroRNA-21 (miR-21)

1.4.1 MiR-21 expression

The gene for miR-21 is on chromosome 17q23.2, within an intron of the gene for the vacuole membrane protein TMEM49, although the miRNA gene has its own promoter region and can be transcribed independently of the host gene. The primary miR-21 transcript from its own promoter is ~3,500 nt long, while the mature miRNA is 21 nt (MiRbase, 2016). MiR-21 is an established oncogenic miRNA and has been found to be up-regulated in a wide range of cancers including breast, pancreas, lung, gastric, prostate, colon, head and neck, oesophageal, leukaemia, lymphoma, multiple myeloma, glioblastoma, osteosarcoma and spermatocytic seminoma (Buscaglia and Li, 2011). The role and specific targets of miR-21 in each of these malignancies may vary. In glioma, miR-21 expression correlated with grade and was highest in grade IV glioblastomas (Gabriely et al., 2008), whereas in multiple myeloma, expression of miR-21 in bone marrow mononuclear cells correlated with response to chemotherapy (Zhang et al., 2012a).

A key caveat to many studies in which tumoural expression of miR-21 has been examined is that expression was typically examined using whole tumour samples, containing tumour cells admixed with stromal cells and ECM (Song et al., 2010). In many cases, it has been assumed that over-expression of miR-21 occurred in the tumour cells, as opposed to in the stromal cells or even potentially as a result of changes in the relative proportions of different cell types. Studies looking at miR-21 cellular localisation within cancer tissues, typically using *in situ* hybridisation, are less common. These studies have shown that location of miR-21 expression varies between different cancer types. In cervical and melanocytic lesions and in glioma miR-21 expression was predominantly identified in tumour cells (Yao and Lin, 2012, Grignol et al., 2011, Dillhoff et al., 2008, Hermansen et al., 2013). Whereas in colorectal, prostate, gastric, oesophageal, non-small cell lung, and breast cancer, and diffuse large B cell lymphoma, miR-21 expression was been predominantly seen in the stromal compartment, specifically within CAFs (Lee et al., 2016, Bullock et al.,

2013, Kjaer-Frifeldt et al., 2012, Guan et al., 2016, Melbo-Jorgensen et al., 2014, Uozaki et al., 2014, Stenvold et al., 2014, Hug et al., 2015, Nielsen et al., 2014, Munch-Petersen et al., 2015, Nouraee et al., 2013). Interestingly, in cancer types where both tumour cell and stromal staining were present and analysed separately the stromal staining but not the tumour cell staining correlated with clinicopathological factors, such as disease free survival and lymph node status, suggesting that in these cancers it is the stromal miR-21 that has the greater influence on tumour behaviour (Guan et al., 2016, Hug et al., 2015, Stenvold et al., 2014, Kjaer-Frifeldt et al., 2012). In one colorectal cancer study miR-21 expression was quantified by qPCR using laser microdissected CAFs, which confirmed the results seen with *in situ* hybridisation that miR-21 expression was increased in CAFs compared with normal fibroblasts but not in epithelial cells (Bullock et al., 2013).

Studies concerning the location of miR-21 in breast cancer report a variety of findings that are not obviously compatible with each other. An initial study in breast cancer suggested that miR-21 was located in tumour cells (Gong et al., 2011). However, more recent studies together with improvements in *in situ* hybridisation staining have shown that miR-21 is predominantly located within CAFs. Between different studies there was variation in the staining of miR-21 seen in tumour cells with one reporting that only a few clusters of breast cancer cells occasionally stained positively whilst another found that in the occasional cases where tumour cells were positive this tended to be uniform (Nielsen et al., 2014, Rask et al., 2011).

1.4.2 Regulation of miR-21 expression

There is relatively little known about what influences the expression of miR-21 in breast cancer, and essentially nothing is known in the context of breast cancer fibroblasts. In terms of up-stream factors, a study by Huang *et al.* showed that increased HER2/neu receptor expression increased miR-21 expression within breast cancer cells and that stimulating these cells with a HER2 agonist further increased the level of miR-21. Using pathway inhibitors it was indicated that this was brought about via the mitogen-activated protein kinase/extracellular signal-regulated kinase (MAPK/ERK) pathway (Huang et al., 2009b). Another study has shown that in ER+ breast cancer cells, miR-21 levels are decreased following stimulation with oestradiol (Selcuklu et al., 2012). Different factors may stimulate miR-21 expression

in different breast cancer subtypes, and it is not known what stimulates miR-21 expression specifically in triple negative breast cancer.

In breast cancer cell lines, five transcription factors have been investigated as regulators of miR-21 expression. The activity of transcription factor ETS-1, activated by the MAPK/ERK pathway, correlated with miR-21 expression levels (Huang et al., 2009b). Genotoxic treatment has been shown to activate and recruit the transcription factor NF-κB to the miR-21 promoter region (Niu et al., 2012). TCF4, a down-stream effector of the Wnt signalling pathway, has been shown to bind to a promoter region upstream of miR-21 and Wnt signalling increased miR-21 expression and effects (Lan et al., 2012). Bone morphogenetic protein 6 negatively regulates miR-21 expression via decreased transcription of the δEF1 and AP-1 transcription factors which bind to the miR-21 promoter region (Du et al., 2009). Understanding the factors that regulate miR-21 expression could allow targeting and inhibition of its action as a potential therapeutic strategy.

1.4.3 Role of miR-21 in Cancer

Increased miR-21 expression in breast cancer has been positively correlated with increased cancer cell proliferation index (Ki-67), lymph node positivity, advanced breast cancer stage and poor prognosis, although most of these studies included all breast cancer subtypes combined and did not determine whether the miR-21 was in the tumour cells or the stroma (Yan et al., 2008, Huang et al., 2009a, Rask et al., 2011, Hug et al., 2015). In a more detailed and comprehensive study by MacKenzie *et al.* it was found that when looking at all breast cancer subtypes combined, increased miR-21 expression correlated with shorter disease free survival, but in luminal A subtype increased miR-21 in cancer cells was associated with disease recurrence whereas increased stromal miR-21 in triple negative breast cancer was associated with disease recurrence (MacKenzie et al., 2014).

Similar findings have been seen in other cancer types, including prostate, pancreatic and gastric cancers and glioma where increased miR-21 expression correlated with worse clinicopathological factors or worse patient outcomes (Guan et al., 2016, Morinaga et al., 2016, Melbo-Jorgensen et al., 2014, Uozaki et al., 2014, Stenvold et al., 2014, Hermansen et al., 2013, Dillhoff et al., 2008). Interestingly, in prostate and gastric cancer studies when location of miR-21 expression was analysed, it was

found that the stromal miR-21 expression correlated with worse outcomes, but tumour cell miR-21 expression did not, and in non-small cell lung cancer tumour cell miR-21 correlated with good prognosis but stromal miR-21 correlated with poor prognosis (Melbo-Jorgensen et al., 2014, Uozaki et al., 2014, Stenvold et al., 2014). These findings suggest that miR-21 may play different roles in tumour cells compared with stromal cells in cancer, and that in certain cancer types, including triple negative breast cancer, it is the stromal miR-21 that is important in influencing overall tumour behaviour.

1.4.4 MiR-21 targets

1.4.4.1 MiR-21 targets in breast cancer

A large number of miR-21 targets have been identified, with at least 30 validated to varying extents in a variety of different tumours. The targets that have been studied in breast cancer epithelial cells line are outlined here. Targets have been identified by looking at protein expression levels and sometimes mRNA levels that were negatively correlated with miR-21 expression and altered by experimental manipulation of miR-21 levels/activity. Potential miR-21 binding site or sites in the 3' UTR of these suspected target mRNAs have then been identified using bioinformatics. 3' UTRs were typically then cloned into luciferase mRNA reporters to confirm that the 3' UTR is targeted. In some studies a further validation was carried out by deleting or mutating the miR-21 binding site within the 3' UTR abrogating the miR-21-dependent luciferase down-regulation. Target mRNAs where this has been done include Jagged1 (Selcuklu et al., 2012), PDCD4 (Frankel et al., 2008, Lu et al., 2008), TPM1 (Zhu et al., 2007), RHOB (Connolly et al., 2010), PTEN (Meng et al., 2007, Li et al., 2012), and TIMP3 (Song et al., 2010). These proteins are involved in a diverse range of carcinogenic and malignant processes. Jagged1 is known as an intercellular ligand of Notch and has been implicated in angiogenesis. PDCD4 can stimulate an apoptotic pathway. TPM1 decreases anchorage independent growth (Zhu et al., 2007). RHOB increases cell adhesion and decreases cell migration (Connolly et al., 2010). PTEN causes cell cycle arrest, induces apoptosis, and reduces cell migration (Connolly et al., 2010), invasion and stem cell phenotypes (Weng et al., 1999, Li et al., 2012).

PTEN and TIMP3 are of particular interest when considering possible targets for miR-21 in CAFs. TIMP3 is an inhibitor of MMP3 (Song et al., 2010). Although research thus far has looked at miR-21 targeting of TIMP3 in epithelial cells, given that CAFs are known to be involved in regulating and remodelling the ECM, if miR-21 is up-regulated in CAFs the mRNA for TIMP3 could be a potential target. As discussed above PTEN has been shown to be a tumour suppressor in mammary fibroblasts, involved in suppressing several malignant processes in CAFs. Therefore miR-21 could be a mechanism by which PTEN expression is regulated in fibroblasts leading to an activated or myofibroblastic phenotype and behaviour.

As mentioned in section 1.2.2.4, TGF-β can simulate the CAF phenotype. MiR-21 is up-regulated within 2 hours of TGF-β stimulation and has been shown to be required for this pathway, suggesting that miR-21 is required for the CAF phenotype (Li et al., 2013).

1.4.4.2 MiR-21 targets in fibroblasts

A limited number of potential miR-21 targets have been identified in fibroblasts from various tissues. These may be of more relevance to breast CAFs than the targets described above that were identified in epithelial cells. In cardiac hypertrophy miR-21 expression in fibroblasts has been shown to target and down-regulate Spry1 expression leading to decreased inhibition of the MAPK/ERK pathway and decreased apoptosis. This resulted in increased fibroblast survival and increased cardiac fibrosis (Thum et al., 2008). The MAPK/ERK pathway has been suggested to increase miR-21 expression in breast cancer. It is possible a positive feedback loop is operating. In colorectal cancer, miR-21 has been found to be up-regulated in fibroblasts. Reversion-inducing cysteine-rich protein with Kazal motifs (RECK) has been investigated as one possible target. RECK is an inhibitor of MMPs and thereby decreases ECM remodelling. Bullock *et al*. showed increased MMP activity in cell culture when miR-21 was over expressed (Bullock et al., 2013). It is possible RECK is a target of miR-21 in breast CAFs as well as colorectal CAFs.

1.5 Hypothesis and aims

In this research project I have focused on basal-like and triple negative breast cancers and the role of fibroblast and fibroblast-epithelial interaction in tumour behaviour; looking specifically at the expression of miRNAs in fibroblasts and the function of miR-21 in these cells. My hypothesis is that miRNAs, and miR-21 in particular, in CAFs have key roles in the behaviour of triple negative, basal-like breast cancers.

The aims of this project were to:

1) identify miRNAs differentially expressed between NFs and CAFs in triple negative, basal-like breast cancers;
2) determine the functional role of a selected miRNA in CAFs;
3) determine the impact of a selected miRNAs in CAFs on the behaviour of epithelial cancer cells.

Chapter 2
Materials & Methods

2.1 Ethical approval

Ethical approval for use of the archival breast tissue and associated anonymised data from Leeds Teaching Hospitals NHS Trust (LTHT) was granted by Leeds (East) Research Ethics Committee to my supervisor Professor Andrew Hanby (reference 06/Q1206/180, see Appendix A). Fresh breast tissue samples, from which breast fibroblasts were extracted, were supplied by the Breast Cancer Now Breast Tissue Bank (Leeds), under approval from the Leeds (East) Research Ethics Committee (reference 09/H1306/108, see Appendix B) and were transferred to my research team under material transfer agreements.

All the work and methods outlined in this chapter were carried out by myself except where a colleague's contribution has been specifically stated.

2.2 Case selection

2.2.1 Selection of triple negative, basal-like subtype cases for laser capture microdissection

A suitable cohort of triple negative, basal-like breast cancer cases for laser capture microdissection (LCM) was identified, initially, by searching the Leeds Teaching Hospitals Trust histopathology database for breast resections from 01/01/2008 to 01/10/2012 that contained the word 'basal' in their histopathology report (Appendix C). This yielded 113 cases. Not all basal-like breast cancer cases will have been identified in the pathology report, as this subtype is not typically stated. However, as only a small cohort of cases was required this search strategy was adequate to identify sufficient number of cases. In addition, identifying cases in this way means that reports where basal-like subtype was mentioned were more likely to the have more of the classical morphological features of basal-like breast cancer. The pathology report, slides and blocks from the search results cases were reviewed to

identify suitable cases. During the review of each report, certain cases were excluded from the 'basal' search results. Cases were excluded if

i) basal was used in a context other than to refer to tumour subtype;

ii) the tumour was of a special subtype such as metaplastic, neuroendocrine or adenosquamous;

iii) the report was from a recurrence rather than a primary tumour;

iv) or the patient had been treated with chemotherapy prior to resection.

This excluded 27 cases, leaving 86 potential cases. Breast cancers of special subtype, such as metaplastic and neuroendocrine, are sometimes included in the basal-like group and sometimes excluded as they have different prognoses. In this cohort breast cancers of special type were excluded. This cohort was identified as those where basal was stated in the pathology report. These two factors meant that this cohort of cases may not be representative of all basal-like breast cancers. It was selected to be a more homogenous basal-like group and representative of the commonest type of basal-like breast cancer, invasive carcinoma of no special type with typical basal-like morphological features. Selecting a homogenous group meant that as the cohort size was small this increased the chance of identifying common changes within the group. Whereas if there was variation between the cases important alterations in CAFs may be missed if they occurred in only one subtype.

These cases were confirmed as triple negative and basal-like using immunohistochemistry for ER, PR, HER2, CK5 and CK14 and HER2 fluorescence *in situ* hybridization, if required. ER, PR and HER2 tests were carried out at the time of initial reporting. CK5 and CK14 had been done on many of these cases. Where it had not been done at the time of reporting, it was carried out by a specialist biomedical scientist and then reviewed by myself and a subspecialist breast histopathologist (supervisor, Prof Andrew Hanby). I reviewed and confirmed the results of all the immunohistochemistry tests, including those that had been done at the time of reporting.

The tissue availability for these cases was assessed by retrieving the slides and blocks from storage and reviewing the H&E stained sections. Suitable cases and blocks were those that had sufficient tumour stroma and had a block of non-tumour

breast tissue from at least 1 cm away from the tumour (see Figure 2-1). Tumour stroma was defined as non-tumour cell areas within the tumour, the invasive front of the tumour cells was used to delineate the edge of the tumour and fibroblasts from beyond this line were not microdissected. Areas of tumour stroma heavily admixed with necrotic material or inflammatory cells were avoided during microdissection. 1-2 tumour blocks and 1 normal tissue block were identified for each case. Normal tissue was defined as greater than 10 mm from the tumour as this is equivalent to or greater than clinically clear margins (Taghian et al., 2005).

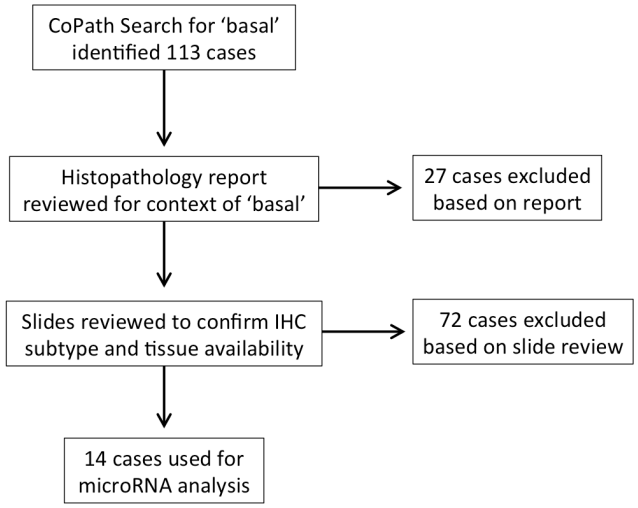

Figure 2-1 Flow diagram of cases selected for laser capture microdissection

This diagram outlines how many cases were excluded at each stage and how the final set of 14 cases was selected.

After these exclusions a total of 14 cases were selected. These tumours were all invasive ductal carcinoma of no special type (IDC-NST); triple negative, defined as ER Allred score 0/8, PR Allred score 0/8, HER2 copy number amplification negative; and expressed basal cytokeratins CK5 and CK14. Table 2-1 contains the details of the patient characteristics for this cohort of 14 cases.

Characteristic	Number of cases (%)
Age at diagnosis	62 years (34 - 81 years) mean (range)
Laterality	
Left	8 (57 %)
Right	6 (43 %)
Resection	
Wide local Excision	11 (79 %)
Mastectomy	3 (21 %)
Histological Grade	
I	0 (0 %)
II	1 (7 %)
III	13 (93 %)
Lymph nodes	
0	14 (100 %)
1-4	0 (0 %)
>4	0 (0 %)
Invasive tumour size	21.7 mm (7.3 mm) mean (standard deviation)

Table 2-1 Characteristics of the 14 breast patients, and their triple negative, basal-like breast cancers that were used for laser capture microdissection and qPCR miRNA expression analysis

2.2.2 Selection of triple negative breast cancer cases for tissue microarray construction

In order to construct a tissue microarray (TMA) of triple negative breast cancer cases, searches were carried out to identify as many invasive TNBC cases within the LTHT archive as possible. Cases were included from 01/01/2008 – 30/03/2013 (this end date was used to allow at least 3 years follow up for each case). Three different search strategies were combined to maximise the cohort:

1) a 'free text' search of computerised histopathology reports containing the words 'triple negative' in the clinical details;

2) triple negative cases selected from the results of a search for 'B5b' (the clinical code for invasive carcinoma in a biopsy) carried out by Catherine Turner (undergraduate medical student) for invasive breast cancer biopsy reports in 2011 with receptor status from each report recorded;

3) cases identified as triple negative by the multi-disciplinary team meeting co-ordinator, collected by Ms Caroline Strachan (MD student within my research group).

The case lists from these searches were reviewed to exclude duplicates, and a final list of cases was compiled.

2.3 Tissue microarray construction

To construct the tissue microarray (TMA), 1-3 tumour blocks from each case were selected and appropriate areas of tumour were manually marked on a haematoxylin and eosin (H&E) stained slide. When available archival H&E slides were marked, but when these were unavailable new sections were taken and stained with H&E. Slides were marked to identify areas of tumour mixed with stroma, avoiding acellular or poorly cellular areas such as those with large amounts of necrosis or sclerosis. An 18 x 15 or 16 grid was used. Non-breast tissue cores were inserted around the edge of the grid and through the grid as an off-centre orientation cross. Three 0.6 μm cores of tumour tissue were taken from each case and consecutively inserted into the recipient wax block. Recipient wax blocks were x-rayed prior to use to confirm they did not contain any air bubbles. If the depth of tissue in the donor block was thin, 2 cores were stacked on top of each other. A total of 3 blocks containing 150 cases (450 cores) were constructed.

2.4 Cutting sections

Sections were taken from paraffin blocks using a Leica RM2235 microtome at 5 or 10 μm. For subsequent laser microdissection (LCM), 3 or 4 sections of 10 μm thickness were taken from each paraffin block using a new, clean blade. The top few sections from each block were discarded, in case of RNA breakdown in the top layer. These were floated on a water bath of diethylpyrocarbonate (DEPC) (Sigma-

Aldrich, Cat no. D5758) treated and autoclaved water heated to 35 °C and lifted onto Membrane Slides NF 1.0 PEN (Carl Zeiss Ltd., Cat no. 415190-9081-000). Care was taken to ensure the sectioning environment was relatively free from RNases by cleaning all equipment with RNase Zap (Life Technologies, Cat no. AM9780) prior to use. Slides were dried overnight at 55 °C to fix the tissue to the membrane and then stored in RNase-free containers at -20 °C. At the same time a 5 μm section from each block was cut onto an uncoated glass slide (Thermo Scientific Superfrost™ Plus Microscope Slides, Cat no. 4951PLUS4) for staining with haematoxylin and eosin in order to act as a guide during LCM (LCM-guide). Sections of blocks for H&E staining, or sections of TMAs were cut in the same way as LCM-guide slides.

2.5 Staining with haematoxylin and eosin

All steps were carried out at room temperature. The LCM-guide sections, or sections of tumour blocks for mark-up for TMA manufacture, were stained using a standard H&E staining protocol and covered with a glass coverslip (Torres et al., 2013, Schmitz et al., 2010). In brief, sections were treated as follows: dewaxed in xylene 4 x 3 min, 100% ethanol 4 x 3 min, rehydrated in graded ethanols (75%, 50%, 25%) 3 x 3 min, washed in running tap water 2 min, stained with Mayer's Haematoxylin (Sigma Aldrich, Cat no. MHS1) 2 min, washed in running tap water until clear, washed in Scott's tap water substitute (Sigma-Aldrich, Cat no. S5134), washed in tap water 1 min, counterstained with eosin (Sigma Aldrich, Cat no. 230251) 2 min, washed in running tap water 1 min, dipped in 100% ethanol 15 s, washed in 100% ethanol 3 x 3 min, xylene 3 x 3 min and mounted with DPX (Sigma Aldrich, Cat no. 06522).

For sections on membrane slides destined for LCM, slides were cooled prior to staining to enhance tissue adherence and the dewaxing and staining steps were shortened to minimise RNA degradation. The dewaxing and staining steps were as follows: 60 s in xylene, 30 s in xylene, 60 s in 100% ethanol, 30 s in Mayer's Haematoxylin, 120 s in phosphate-buffered saline (PBS), 10 s in eosin, followed by rinses in 70% ethanol and 100% ethanol, and finally slides were allowed to air dry.

2.6 Laser capture microdissection

LCM was carried out on the Zeiss PALM Laser Capture Microdissection Microscope. Initially I reviewed the LCM-guide slides to identify areas of fibroblasts with very few admixed inflammatory cells, epithelial cells or necrosis. The equivalent area was then identified on membrane-mounted sections. These areas of fibroblasts were cut along the perimeter with the laser and fired into lids of AdhesiveCap 500 opaque PCR Tubes (Carl Zeiss Ltd., Cat no. 415190-9201-000) by laser pressure catapulting (LPC). The microscope settings used for LCM were cut energy 71, focus 65, LPC energy 100, focus 65 at 100x magnification. The area dissected from each case varied between 5.2 - 27.4 x 10^6 μm^2 depending on the density of fibroblasts.

2.7 RNA extraction

Total RNA was extracted from formalin fixed paraffin embedded (FFPE) fibroblast-enriched samples or from cell culture fibroblasts using the RecoverAll™ Total Nucleic Acid Isolation Kit for FFPE (Ambion®, Cat no. AM1975) or the mirVana™ miRNA Isolation Kit (Ambion™, Cat. No. AM1560), respectively, broadly following the manufacturer's protocols. Briefly, FFPE fibroblast samples were initially protease and DNA nuclease digested (proprietary enzymes) and then the RNA was purified using column-based glass fibre filters. The initial deparaffinisation step was omitted as this was carried out prior to staining and LCM. RNA was eluted from filters with 60 μl nuclease-free water. To increase yield, this eluate was passed through the filter three times (a further modification from the manufacturer's protocol). In the case of cell culture samples, briefly, following cell lysis the nucleic acid molecules were separated from proteins by acid-phenol:chloroform, a glass fibre column was then used to purify the RNA and the product was eluted with nuclease-free water (Ambion™, Cat no. AM9937). 242 – 571 ng RNA was extracted from FFPE fibroblast enriched samples, while 600 ng – 2 μg was typically extracted from tissue culture samples.

2.8 Reverse transcription of miRNA

Reverse transcription (RT) was carried using either the pre-designed Megaplex™ Primer Human Pools Sets v2.1 or v3.0 (Applied Biosystems™, Cat nos. 4399966 & 4444750) or individually selected TaqMan® microRNA RT primers (Applied Biosystems™, Cat no. 4427975) with the TaqMan® MicroRNA Reverse Transcription Kit (Applied Biosystems™, Cat no. 4366596) following the manufacturer's protocol. 120 ng of FFPE fibroblast enriched RNA was used for each primer pool, 240 ng from each sample in total. With tissue culture samples, where amounts of RNA were less restricted, typically 500 – 1,000 ng was used. The volumes of RNA for the different samples were standardised by evaporating the liquid in a Savant speed vac SC110 centrifuge and resuspending in 3 μl nuclease-free water. Briefly, 3 μl RNA was added to 100 mM deoxyribonucleotide triphosphates, MultiScribe Reverse Transcriptase, 10X RT buffer, nuclease-free water, RNase inhibitor, $MgCl_2$ and RT primer or megaplex primer pool with a final reaction volume of 7.5 μl. When using individual RT primers the thermal programme was 16 °C for 30 min, 42 °C for 30 min, 85 °C for 5 min and finally chilled at 4 °C. For the megaplex reactions, pulsed reverse transcription reaction conditions were used because they improve detection sensitivity without bias (Tang et al., 2006). Thermal cycling conditions were 16 °C for 2 min, 42 °C for 1 min, 50°C for 1 s, repeated for 40 cycles, then 85 °C for 5 min and finally cooled to 4 °C. Following reverse transcription samples were either used immediately for qPCR analysis or stored at -20 °C.

2.9 Preamplification of miRNAs

Pilot experiments showed that quantitative polymerase chain reaction (qPCR) sensitivity was problematic with levels of RNA as low as 100 ng. Therefore preamplification was used. The Applied Biosystems® TaqMan® PreAmp Primer Pools and Master Mix was chosen because this system allows amplification with relatively-little bias, giving extremely high correlations between relative levels of cDNA pre- and post-amplification (Mestdagh et al., 2008). The manufacturer's protocol was followed. Briefly, 2.5 μl of RT cDNA product was added to TaqMan®

PreAmp Master Mix (Applied Biosystems™, Cat no. 4391128), nuclease-free water and either Megaplex™ PreAmp Primers Human Pool A (Applied Biosystems™, Cat no. 4399233) or Pool B (Cat no. 444282). Thermal cycling conditions were 95 °C for 10 min, 22 °C for 2 min, 72 °C for 2 min, 12 cycles of 95 °C for 15 s followed by 60 °C for 4 min, 99.9 °C for 10 min and finally cooled to 4 °C. After thermal cycling 75 µl 0.1X Tris-EDTA was added to each sample and samples were stored at -20 °C.

2.10 Quantitative polymerase chain reaction (qPCR)

Quantitative polymerase chain reaction (qPCR) was carried out either in 384 well TaqMan Low Density Array (TLDA) cards (TaqMan® Array Human MicroRNA A+B Cards Set v2.0 and v3.0, Applied Biosystems™, Cat no. 4398965 & 4444913) or in 96 well plates with TaqMan® Small RNA qPCR primers (20X) (Applied Biosystems™, Cat no. 4427975). When using a TLDA card, following the manufacturer's protocol, 450 µl TaqMan® Universal PCR Master Mix, No AmpErase® UNG (Applied Biosystems™, Cat no. 4324018), 441 µl nuclease-free water and 9 µl preamplification product were mixed and dispensed into 8 reservoirs on each card. The reaction mixture was drawn into each well containing a specific primer by centrifugation and the card was sealed. The qPCR reaction was carried out and quantified by the 7900HT Fast Real-Time PCR System (Applied Biosystems™, Cat no. 4329001). With individual primer qPCR, scaled down volumes of the manufacturer's protocol were used. Briefly, within each well was 0.5 µl TaqMan® Small RNA qPCR primer, 5 µl TaqMan® Universal Master Mix II, 3.835 µl Nuclease-free water and 0.665 µl RT or preamp product were combined. The qPCR was run on the 7500 Real Time PCR System (Applied Biosystems™, Cat no. 4351105). The passive reference within the wells was ROX dye and the detector dye was FAM. A no template control was included for each primer on each plate. Reactions were carried out as technical triplicates. The thermal cycling conditions for both reactions were 50 °C for 2 min, 95 °C for 10 min, 40 cycles of 95 °C for 15 s followed by 60 °C for 60 s.

2.10.1 qPCR data analysis

Each qPCR well was reviewed for adequate passive reference signal. The amplification curves for each qPCR plate were reviewed and the cycle threshold (Ct) set in the linear exponential phase. Target Ct values were normalised by subtracting the geometric mean of the reference Ct values (ΔCt). Small nuclear RNA (snRNA) U6 and small nucleolar RNA RNU48 were used as references, as they are stably expressed at high levels across a range of human tissue types and cell lines and have been validated by other studies (Torres et al., 2013, Davoren et al., 2008). Relative expression levels were calculated using $2^{-\Delta Ct}$ (assuming 100% primer efficiency). With the low density qPCR array wells with Ct <40 were regarded as 'detected' and expression levels calculated.

For the TLDA qPCR normalised Ct values ($2^{-\Delta Ct}$) were loaded into 'R' for clustering analysis (R Core Team, 2016). Analyses were performed on pool A individually and pools A and B combined. The Euclidean distance between each pair of samples was computed, then agglomerative hierarchical clustering was performed on the distance matrix using complete linkage. This analysis was carried out by the bioinformatician Dr Alastair Droop (University of Leeds).

2.11 Chromogenic *in situ* hybridisation

5 μm sections were taken from whole tissue or TMA blocks (section 2.4). Sections for the work were cut by Sarah Perry, an experienced FFPE tissue sectioner. Chromogenic *in situ* hybridisation (CISH) was carried out using the miRCURY LNA™ microRNA Detection (FFPE) probes and ISH Optimization Kit 2 (Exiqon, Cat No. 90002) using the published manufacturer's recommended protocol with optimisation of the appropriate steps (Jorgensen et al., 2010). CISH involved hybridisation of locked nucleic acid (LNA) miRNA-complementary probes. LNA probes have increased thermal stability that increases the binding strength and specificity of the probe to the miRNA of interest. LNA probes were labelled at 3' and 5' ends with non-mammalian hapten, digoxigenin (DIG). DIG is recognised by a specific anti-DIG antibody conjugated directly to alkaline phosphatase (AP). AP converts substrate NBT-BCIP (4-nitro-blue tetrazolium and 5-bromo-4-chloro-3'-indolylphosphate) to form a dark blue precipitate.

To ensure the experimental setup was relatively RNase free, all solutions were made with DEPC-treated water and autoclaved; all glassware was heat treated for 8 hours at 180 °C prior to use and sterile and RNase free filter pipette tips were used. Cooled slides were deparaffinised by being washed in xylene for 3 x 5 min, dipped 20 times then washed for 5 min in 99.9% ethanol, dipped 10 times then washed for 5 min in 96 % and 70% ethanol and washed for 2 min in phosphate buffered saline (PBS). Proteinase-K digestion was carried out using 300 µl of 15 µg/ml proteinase-K reagent per slide for 10 min at 37 °C. Following demasking with proteinase-K, the slides were dehydrated in serial ethanols by being dipped 10 times then washed for 1 min in 70%, 96% and 100% ethanols. The hybridisation probe was denatured at 90 °C for 4 min. Hybridisation was carried out using 25 µl per slide at 53 °C for 1 hour. The concentration of probe (5 nM – 1 µM) was optimised for each probe individually. To ensure even coverage of probe over the whole tissue section and prevent evaporation of the probe, a coverslip was placed on top of the tissue and the edges sealed with Marabu-Fixogum Rubber Cement (Fred Aldous, Cat no. 010160032). After hybridisation, the fixogum and coverslips were removed, taking care not to disrupt tissue sections. The sections then went through stringency washes in serial saline sodium citrate (SSC) solutions at 53 °C to remove excess, non-specifically bound probe. SSC solutions were made up with UltraPure™ SSC, 20X stock (Invitrogen™, Cat no. 15557044). Wash steps were 5 min 5X SSC, 2 x 5 min 1X SSC, 3 x 5 min 0.2X SSC and finally in PBS at 20 °C. Slides were loaded onto a Shandon™ Sequenza™ (Thermo Scientific™, Cat no. 73-310-017) with PBS 0.1% Tween-20 (Sigma-Aldrich, Cat no. P9416). Endogenous AP activity was blocked using PBS with 0.1% Tween-20, 2% sheep serum (Sigma-Aldrich, Cat no. S3772) and 1% bovine serum albumin (BSA) (Sigma-Aldrich, Cat no. A8531) for 15 min. Anti-DIG antibody (Roche, 150 U in 200 µl, Cat no. 11093274910) at 1 in 800 dilution with dilutant PBS, 0.05% Tween-20, 1% sheep serum, 1% BSA was applied to slides for 1 h. After antibody binding, slides were washed with PBS 0.1% Tween-20 for 3 x 3 min. AP substrate was prepared fresh on the day of the experiment by dissolving 1 tablet NBT-BCIP (Roche, Cat no. 11697471001) in 10 ml Milli-Q water with 20 µl Levamisole (Sigma-Aldrich, Cat no. 31742-250MG) 100 mM stock. Slides were then incubated with AP substrate for 2 hours at 30 °C in the dark. To terminate the reaction, slides were washed with KTBT an aqueous solution of 50

mM Tris-HCl, 150 mM NaCl, 10 mM KCl for 2 x 5 min. The slides were then washed 2 x 1 min H_2O and the counter stain Nuclear Fast Red™ (Sigma-Aldrich, Cat no. N3020) was applied for 1 min. Slides were removed from the slide rack, washed in running tap water for up to 10 min, dehydrated in serial ethanols, dipped 10 times then washed for 1 min in 70%, 96% and 99.9% ethanol. Finally coverslips were mounted using Eukitt® quick-hardening mounting medium (Sigma-Aldrich, Cat no. 03989).

For each tissue block CISH was carried out with positive and negative controls, and with the miRNA probes of interest. The positive control was 5'-DIG labelled probe against U6 snRNA at 5 nM. The negative control was double-DIG labelled scrambled probe at the same concentration as the experimental probe. MiR-21 double-DIG labelled probe was used at 400 nM. CISH with probes 1 μM miR-30a and 800 nM miR-27b was also attempted.

2.11.1 CISH scoring

A scoring system was developed by myself and Dr Eldo Verghese (supervisor, and breast pathology consultant within LTHT). The scoring system developed is similar to the histoscore (H-score) in terms of the way it is calculated (Nenutil et al., 2005). The percentage of cells stained was assessed (0 – 100) and the intensity of the staining was assessed; (1) for weak, (2) for moderate and (3) for strong staining. The intensity score was multiplied by the percentage of the target cell type scoring at that intensity to give an overall H-score 0 – 300. Positive staining was often predominantly seen in CAFs located closest to tumour cells within the tumours. The tumour sections were therefore scored as staining in the whole population of CAFs, staining in CAFs $\leq$ 0.075 mm from a tumour cell, and CAFs > 0.075 mm from a tumour cell. An eye-piece graticule was used to determine distances of fibroblasts from tumour cells. Ten high power fields were scored on each whole tissue section.

50% of sections were scored twice, independently, by Dr Eldo Verghese and myself. The inter-observer correlation for this ordinal scoring system was calculated using the intraclass correlation coefficient rather than the kappa-statistic because the staining was scored using a 0 – 300 score rather than a few discrete groups.

Scoring of TMA cores was carried out in a similar way using the H-score, but rather than scoring 10 high power fields, the entire core was scored at high power. When

scoring the CAFs in TMA cores, the separation of CAFs into CAFs ≤ 0.075 mm and CAFs > 0.075 mm from tumour cells was not done, all CAFS were scored together because a large proportion of the tissue within a core is < 0.075mm from the edge of the core, and therefore may have been close to tumour cells outside the core, but could be miscategorised. Cores were deemed to be adequate if at least a quarter of the core tissue was present. If not all three cores were present on the slide or adequate following CISH staining data from cores that were present was included and used to calculate the mean CISH score.

2.11.2 Comparison of CISH scores with clinical and survival data

CISH TMA scores were correlated with clinicopathological parameters. The parameters correlated were patient age at diagnosis, tumour size, tumour grade, number of positive lymph nodes at initial resection or following axillary node clearance and Nottingham Prognostic Index. The clinicopathological parameters were correlated with miR-21 CISH score using Spearman's correlation as appropriate for ordinal data. It was not appropriate to carry out a multivariate analysis with these data as the means of each variable were not compared, the individual values for each case were correlated.

CISH TMA scores were correlated with disease free survival, disease specific survival and overall survival using Kaplan-Meier curves. For the calculation of clinical outcomes date of diagnosis was defined as the date the diagnostic core biopsy was taken. Disease free survival was defined as the time from the date of diagnosis to the date of first relapse either radiological, clinical or pathological, whichever was the earliest (outcome 1) or the time to the most recent clinical encounter if no relapse had occurred (outcome 0). Disease specific survival was defined as the time from the date of diagnosis to the date of death from breast cancer (outcome 1); or date of death from another cause or patient still alive at most recent clinical encounter (outcome 0). Overall survival was defined as the time from diagnosis to the date of death from any cause (outcome 1) or patient still alive at most recent clinical encounter (outcome 0). Lymph node status was defined as any number of lymph nodes positive or no metastasis to lymph nodes, micrometastasis and isolated tumour cells identified in lymph nodes were defined as negative, in line with clinical classification (Galimberti et al., 2013). There is variation in whether

lymph nodes are classified as positive or negative when micrometastasis (0.2-2 mm), are present. The classification of micrometastasis as negative lymph node is based on the standard practise in Leeds Teaching Hospitals Trust.

2.11.3 CISH and qPCR comparative analysis

The qPCR relative expression was correlated with CISH H-scores to determine how similar the results from these two different techniques were. The H-score is an ordinal scale and the qPCR relative expression is an interval scale therefore the Pearson correlation coefficient was used to compare these values.

2.12 Molecular cloning

2.12.1 Transformation and propagation

Competent *E. coli* (NEB® 5-α Competent *E. coli*, New England Biolabs® Inc., Cat no. E0554s) were transformed by thawing 50 µl on ice, adding 2-3 µl (<500 ng complete plasmid or <25 ng DNA ligation mix) DNA, giving a heat-shock at 42 °C for 45 s, then placing back on ice for 2 min. Propagation occurred by adding, initially, 250 µl SOC outgrowth medium (Biolabs, Cat no. B9020S) for 45 min at 37 °C in a shaking incubator at 300 rpm. This was then either poured onto an ampicillin agar plate or added to 500 ml LB-ampicillin medium and incubated overnight at 37 °C. LB ampicillin medium was made by adding 20 g LB-Broth (Sigma-Aldrich, Cat no. L3022) to 1 l distilled water, autoclaving and adding 500 µl ampicillin (Sigma-Aldrich, Cat no. A5354, 100 mg/ml stock solution). Single colonies grown on an agar plate were selected using a pipette tip and grown overnight in 2-3 ml LB ampicillin medium.

2.12.2 Plasmid purification

Plasmid was purified from bacteria using either the HiSpeed Plasmid Midi Kit (Qiagen, Cat no. 12643) or the QIAprep Spin Miniprep Kit (Qiagen, Cat no. 27106) following the manufacturer's protocol exactly.

2.12.3 Cloning pmirGLO-21 reporter plasmid

In order to prepare vector for inserting oligos containing a miR-21 target site, pmirGLO Dual-Luciferase miRNA Target Expression Vector (Promega, Cat no.

E1330, Figure 2-2), underwent restriction digestion using site specific restriction enzymes in appropriate buffers.

Features List and Map for the pmirGLO Vector

SV40 late poly(A) signal	106–327
SV40 early enhancer/promotor	426–844
hRluc-neo fusion protein coding region	889–2664
Synthetic polyadenylation signal	2728–2776
β-lactamase (Amp^r) coding region	3037–3897
*Col*E1-derived plasmid origin of replication	4052–4088
Human phosphoglycerate kinase promoter	5094–5609
luc2 reporter gene	5645–7297
Multiple cloning site (MCS, Figure 1)	7306–7350

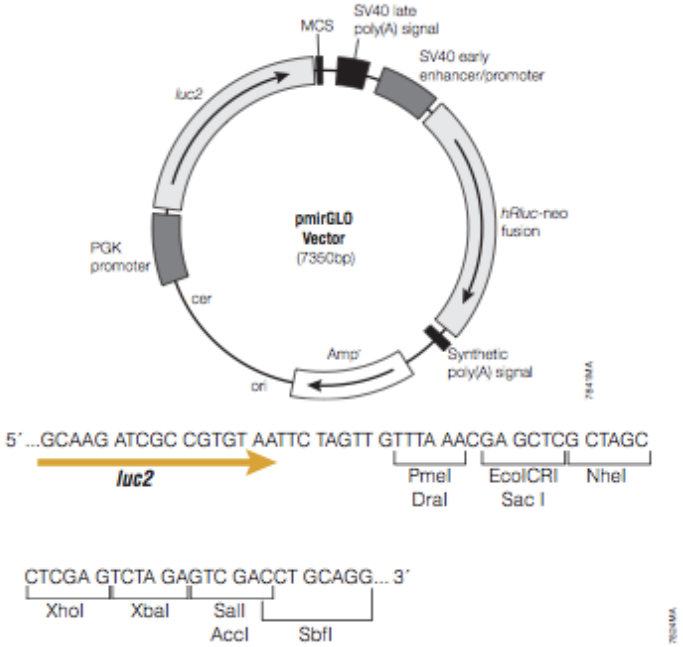

Figure 2-2 Plasmid map of pmirGLO plasmid

This map was provided by Promega who supplied the pmirGLO plasmid for cloning and insertion of the desired miRNA target site.

2.5 µg plasmid DNA was added to 2.5 µl Sac1 (New England BioLabs® Inc., Cat no. R0156S), 5 µl 10X NEbuffer 1 (New England BioLabs® Inc., Cat no. B7001S), 0.5 µl 100X Bovine Serum Albumin (BSA, New England BioLabs® Inc., Cat no. B9000S) and the total volume made up to 50 µl with DNase-RNase-free water and incubated at 37 °C for 4 hours. The product was purified using the QIAquick Purification Kit (Qiagen, Cat no. 28104) following the manufacturer's protocol

exactly, eluting in 50 µl DNase-RNase-free water. For the second restriction digestion 1.5 µg DNA was added to 1.5 µl Sal1 (New England BioLabs® Inc., R0138S), 5 µl 10X NEbuffer 3 (New England BioLabs® Inc., Cat no. B7003S), BSA and DNase-RNase-free water and incubated as described above. The digestion product was purified as described above using the QIAquick Purification Kit.

The oligonucleotides (see Appendix D) for insertion into the plasmid were annealed by being suspended in 46 µl annealing buffer (10 mM Tris-HCl, pH 7.5-8.0, 50 mM NaCl, 1mM EDTA), heated to 95 °C and allowed to cool slowly. A ratio of 1:1 for each oligonucleotide was used.

For the ligation reaction a ratio of 1:3 vector to insert was used. The vector and insert were combined with 1 µl T4 DNA Ligase Reaction Buffer (New England BioLabs® Inc., Cat no. B0202S), 1 µl T4 DNA Ligase (New England BioLabs® Inc., Cat no. M0202S) and made up to a final volume of 10 µl with DNase-RNase-free water and incubated overnight at 16 °C.

2.12.4 Sequencing

Sanger sequencing of plasmids was carried out using the BigDye Terminator v3.1 Cycle Sequencing Kit (Applied Biosystems, Cat no. 4337455). 1 µl Big Dye 3.1, 1 µl purified plasmid, 1 µl primer, 1.5 µl Big Dye buffer and 5.5 µl DNase-RNase-free water were mixed and thermal cycled 96 °C for 1 min, 25 cycles of 96 °C for 10 s, 50 °C for 5 s, 60 °C for 4 min, then held at 4 °C. After cycling, 5 µl 125 mM EDTA and 60 µl 100% ethanol were added to each sample and spun at 3060 x Relative Centrifugal Force (RCF) for 30 min at 22 °C. The plate was then inverted and spun at 8 x RCF for 1 min. 60 µl 70% ethanol was added to each sample and spun 805 x RCF for 15 min at 4 °C. The plate was then inverted again and spun at 8 x RCF for 1 min to remove supernatant and allowed to dry. The plate was then either frozen until needed or 10 µl Hi Di Formamide (Applied Biosystems™, Cat no. 4440753) added to each well and loaded onto the 3130xl Genetic Analyzer (Applied Biosystems™).

2.13 Tissue culture

2.13.1 Source of cell lines and basic culture conditions

The triple negative breast epithelial cancer cell line MDA-MB-231 was obtained from American Type Culture Collection (ATCC® HTB-26). A derivative stably expressing green fluorescent protein and firefly luciferase (MDA-MB-231-GFP-f.luc) was created by lentiviral transduction with appropriate vectors by Dr Mihaela Lorger (University of Leeds) as described previously (Lorger and Felding-Habermann, 2010). Fibroblast lines were created by immortalisation of fibroblasts extracted from primary breast cancer resections and reduction mammoplasties using a retrovirus allowing stable over-expression of hTERT as described previously (Verghese et al., 2011). NF-1 and NF-2 lines have been described previously (Verghese et al., 2013, Simpkins et al., 2012), while further lines were created specifically for this work as detailed in section 2.13.2. Specifically, CAF-1 cells were extracted from breast tumour tissue and immortalised, while CAF-2 cells were extracted from breast tumour tissue and cultured as primary (non-immortal) cells.

All cells were grown at 37 °C in 5% CO_2. Cells were grown in Dulbecco's Modified Eagle Medium, high glucose, GlutaMAX™ Supplement (DMEM, Gibco™, Cat no. 10566016) with 10% heat inactivated Foetal Bovine Serum (FBS, Sigma-Aldrich, Cat no. F7524-500ML) (complete medium), unless stated otherwise for specific protocols. To passage, cells were washed with PBS and detached from the flask using 1-4 ml Trypsin, (Gibco® 2.5 % (10X), Cat no. 15090-046) diluted with PBS to 1X at 37 °C for approximately 3-10 min. Trypsin was deactivated using complete medium. The cell suspension was centrifuged at 400 x RCF for 5 min and supernatant discarded. Cells were re-suspended in complete medium seeded into a new flask. Cells were passaged 1 in 2 – 1 in 5 every 2-5 days, to maintain growth in the exponential phase.

2.13.2 Fibroblast extraction

Human breast fibroblasts were extracted from fresh tissue in the form of breast cancer resections, sourced from the Leeds Breast Tissue Bank (see section 2.1 & Appendix B). 6-well plates were prepared in advance by coating with 1 ml of 50 μg/ml Collagen, Type 1 solution from rat tail (Sigma-Aldrich, Cat no. C3867-1VL)

diluted in 0.02 M acetic acid and subsequent incubation at 37 °C for minimum 1 hour to allow the collagen to set. Wells were rinsed thoroughly, at least 3 times, with PBS to ensure all the acid was removed. Plates were then either used immediately or stored at 4 °C for up to 1 week. Fresh tumour tissue, typically 7 x 7 x 2 mm in size, was chopped up using surgical blades on a petri dish, with a small amount of primary preparation medium added. Primary preparation medium was RPMI 1640 Medium (Gibco™, Cat no. 11875093) with 5% FBS. Excess fat was removed from tissue and the minced up tissue was added to a T25 flask. 5 ml primary preparation medium, 1 ml Collagenase from *Clostridium histolyticum* (Sigma-Aldrich, Cat no. C2674-100MG), 50 µl Amphotericin B (250 µg/ml, Gibco™, Cat no. 15290026) and 50 µl Penicillin-Streptomycin (Pen-Strep, 5 000 U/ml, Gibco™, Cat no. 15070-063) were added to the flask with the tissue. The flask was incubated overnight at 37 °C.

After digestion the tissue was filtered and washed. Larger pieces of tissue that did not pass through the cell strainer were returned to the original tube and both tubes topped up to 20 ml with PBS. At this step fibroblasts were predominantly in single cell suspension and passed through the cell strainer, whereas epithelial cells were retained. Cells were collected by centrifugation at 290 x RCF for 3 min and pellets were re-suspended in 15 ml PBS. The centrifuge spin and re-suspension in PBS was repeated 3 times. After the final spin pellets were re-suspended in 3-9 ml complete medium. PBS was removed from collagen-coated wells and the wells were seeded with either cell strainer filtrate or larger tissue pieces. 1-3 wells were seeded depending on the size of each pellet. 30 µl Pen-Strep and 30 µl Amphotericin B was added to each well. Although the wells containing the larger pieces of tissue were likely to contain a mixture of cells including fibroblasts and epithelial cells, fibroblasts only were selected for growth in this medium as primary epithelial cells typically require additional factors such as insulin and hydrocortisone.

2.13.3 Fibroblast immortalisation

Once primary fibroblasts were established and growing, frozen stocks were prepared and, separately, cells were immortalised. In order to produce viral particles to allow immortalisation, Phoenix-AMPHO cells (phoenix-A, ATCC® CRL-3213™) were used. These were grown to 60% confluence in a T25 flask. 8 µl Lipofectamine®

2000 (Invitrogen™, Cat no. 11668-019) was incubated at room temperature with 2-3 μg pBABE-puro-hTERT plasmid (siPORT XP-1, Applied Biosystems, Cat no. AM4507) in serum-free medium for 20 min to allow complexes to form. 4 ml complete medium was added to the complexes and the medium changed on the phoenix-A cells to complex containing medium. Phoenix-A cells were incubated overnight at 37 °C. The next day the medium was changed to fresh, complete medium. The following day, the first harvest of virus supernatant was collected and fresh medium added to the cells, the virus supernatant was filtered through a 0.45 μm filter and stored overnight at 4 °C. On the fourth day a second virus supernatant was harvested, filtered, pooled with the first virus supernatant and used immediately or frozen at -80 °C. This work to produce cell supernatant containing viral particles was carried out by a colleague, Dr Claire Nash (then part of the wider breast group in Leeds; now at McGill University, Montreal).

Primary fibroblasts were grown in a T25 flask to 60% confluence. The medium was removed and Polybrene 1 μg/ml (1,5-dimethyl-1,5-diazaundecamethylene polymethobromide, hexadimethrine bromide, Sigma-Aldrich, Cat no. 107689), serum-free DMEM and 1 ml virus supernatant added to the flask. After overnight incubation at 37 °C, the medium was changed to complete medium. Cells were selected for having incorporated the virus simply by continued culture, as fibroblasts without the virus would enter senescence after 6-8 passages.

2.13.4 Co-cultures

MDA-MB-231 tumour cells were co-cultured with fibroblasts (NF or CAF lines) in three different ways; contact co-culture, transwell co-culture and conditioned medium. In each case cells were grown in co-culture for up to 3 days. 3 days co-culture was selected because it enabled cells to be seeded at a density where there was some contact between cells but sufficient space for the cells to proliferate without becoming over-confluent within the time period.

2.13.4.1 Contact co-culture

In contact co-culture fibroblasts and tumour cells were seeded together in flasks or wells in direct contact with each other, allowing for cell-cell communication as well as paracrine communication to take place.

2.13.4.2 Transwell co-culture

In transwell co-culture assays 1 x 10^5 fibroblasts were seeded into each well of a 24-well plate. 1 x 10^4 MDA-MB-231 cells were seeded into a 1 μm pore size PET membrane 24-well cell culture insert (BD Falcon, Cat. No. 353104). This permeable support was then placed into the fibroblast well allowing exchange of soluble factors but not movement of cells between the two compartments.

2.13.4.3 Conditioned media co-culture

In conditioned medium co-culture experiments, fibroblast cells were cultured with conditioned medium taken from separate MDA-MB-231 cultures, or – as a control – taken from parallel fibroblast cultures. Fibroblasts were seeded at 1 x 10^5 cells per well in a 24-well plate. Half the medium in each experimental well was replaced with medium from parallel MDA-MB-231 or fibroblast cultures. In an effort to reduce any influence of depletion of growth factors etc. within the media due to cell metabolism, the medium for conditioning was replaced every day, it was incubated with the cells for 24 h to become conditioned before being transferred to the experimental wells.

2.13.5 Fluorescence activated cell sorting

Fibroblasts and MDA-MB-231-GFP-f.luc cells were grown in contact co-culture, see section 2.13.4.1, and then separated by fluorescence activated cell sorting (FACS) based on GFP fluorescence (B530 FITC Green Fluorescent Protein detector) and side scatter, with the non-fluorescent cells (the fibroblasts) being collected. Typically 1 x 10^6 NF-1 or CAF-1 were seeded with 3-5 x 10^5 MDA-MB-231-GFP-f.luc into T75 or T150 flasks to achieve tumour cell : fibroblast ratios of 1:1 – 3:1 depending on comparative cell division rates. After 3 days growth, cells were suspended and washed three times in PBS, filtered (Falcon™, Cat no. 352340) and transferred to a polypropylene FACS tube (Falcon™, Cat no. 352063). A comparison sample of fibroblast cells mixed with tumour cells immediately prior to FACS was used. A purity of at least 96 % GFP-negative cells was achieved from the FACS cells collected. Typically 1- 4 x 10^5 cells were collected from FACS.

2.13.6 Transfection of cell lines

Cells were transfected with synthetic miRNAs and with DNA plasmids. A synthetic pre-miRNA mimic and a miRNA inhibitor were used to transiently, fast forward or reverse transfect cells. Briefly, miRNA mimics (Ambion, Cat no. 4464066) or mimic control (Ambion, Cat no. 4464058) or miRNA inhibitors (Ambion, Cat no. 4464084) or inhibitor control (Ambion, Cat no. 4464076) formed complexes with Hiperfect transfection reagent (Qiagen, Cat no. 301705) in serum-free DMEM at room temperature for 10 min. Cells were suspended in serum-free DMEM, as described for passaging in section 2.13.1. Cells were filtered, diluted to the appropriate concentration mixed with complexes and seeded into wells. The volume of transfection reagent used varied depending on the size of the well and was following the manufacturers recommendations, 24-well plate 3 μl per well, 96-well plate 0.5 μl per well. Following manufacturer's recommendation the concentration of transfected miRNA was optimised. Initially, transfection with 10 nM, 25 nM and 50 nM miRNA mimic were carried out. 10 nM was found to be sufficient to significantly increase miRNA levels within the cells, quantified by qPCR. It is well documented that concentration for miRNA inhibitor needs to be several fold higher than for miRNA mimic to produce a significant decrease in functional miRNA levels. Therefore 50 nM miRNA inhibitor was tested and found to significantly decrease miRNA functional levels. Transfection complexes were removed after 12-18 hours and complete medium added to each well.

Forward transfection with plasmid DNA was carried out by seeding cells and growing them for 24 hours in a 24-well plate. Transfection complexes were formed by incubating a ratio of 0.5 μg plasmid to 1 μl Lipofectamine® 2000 Reagent (Invitrogen, Cat no. 52887) in Opti-MEM™ medium (Gibco™, Cat no. 11058021) for 20 min at room temperature. The complexes were added to the fibroblast wells and incubated at 37 °C. After 6 h the medium was changed to complete medium.

2.13.7 MTT assays

In preparation, on the day prior to the experiment, MTT (3-(4,5-Dimethylthiazol-2-yl)-2,5-Diphenyltetrazolium Bromide) (Sigma-Aldrich, Cat no. M2128-1G) was made into a 5 mg/ml stock solution with PBS and stored in the dark at 4 °C. Fibroblasts (NF-1, NF-2, CAF-1 and CAF-2) were seeded at a density of 1-3 x 10^4

cells per well into a 24-well plate and allowed to grow for up to 5 days. On the day measurement of number of viable cells was taken, 50 µl MTT stock solution was mixed with 200 µl complete medium and added to each well of a 24-well plate. Plates were incubated at 37 °C, wrapped in foil for 3 hours to allow the reaction to take place. After 3 hours the MTT solution was removed and the formazan dye dissolved in propan-1-ol. The plate was gently shaken for 15 minutes to allow the dye to dissolve. The solution was then transferred to a 96-well plate and the optical density was measured at 570 nm using a plate reader (Opsys, Dynex Technologies or Berthold Mithras LB 940).

Optical density readings were normalised to the readings taken on the first day for each miRNA complex transfected, i.e. control readings from days 2-4 were normalised to day 1 control and miR-21 mimic readings from days 2-4 were normalised to miR-21 mimic reading on day 1. Initially MTT assays were carried out over 3 days, as small non-significant changes in measurements were noted on day 3 the assay was extended to 4 days to see if this trend in differential growth rate continued or increased. The mean reading for the three independent wells for each transfected miRNA within an experiment were compared using Student's t-tests. The means from each of three independent repeat experiments were combined and a Student's t-test carried out on the combined data.

2.13.8 Luciferase assays

Luciferase activity within cells was measured using the Dual-Luciferase® Reporter Assay System (Promega, Cat No. E1910). All solutions were made up to 1X concentration with 18 MΩ water filtered through a 0.45 µm filter to remove particulate matter and then further diluted 1:2 with filtered water. Cells were washed twice with PBS and lysed with passive lysis buffer for 15 min rocking gently at room temperature. The lysate was then either stored at -20 °C or transferred to a white 96-well plate for reading. Luciferase assay readings were taken on the Berthold Mithras LB940 Multimode Microplate Reader. The automated plate reader added 20 µl luciferase assay reagent, shook the plate for 2 s, waited for 2 s, then read the luminescence for 5 s, this measured the firefly luciferase activity. If a single luciferase assay was being done, this was the only reading that was taken from each well. If a dual-luciferase assay was being done 20 µl Stop&GLO was then added to

the well and the same settings used, shake 2 s, delay 2 s, read 5 s, this measured the *Renilla* luciferase activity. Two or three repeats were carried out with each fibroblast culture in contact co-culture with MDA-MB-231 luciferase expressing cells. The number of repeats with each fibroblast culture is indicated in the respective results figure.

2.13.9 Scratch wound assays

Scratch wound assays were used to measure migration and invasion. The formation of the wound was the same in both, but the setting up of the plate before and after differed. This assay was carried out with fibroblasts (NF-1, NF-2, CAF-1 and CAF-2) on their own and in contact co-culture with MDA-MB-231-GFP-f.luc, as described in section 2.13.4.1. 5-10 x 10^3 fibroblasts per well were seeded into a 96-well plate, with 5 x 10^3 MDA-MB-231-GFP-f.luc cells per well if required, to be just confluent at the time of scratching. In the migration scratch wound assay a wound was made in the wells using the Essen® 96-well WoundMaker™. This is a tool with 96 pins spaced at the same distance as the wells. The WoundMaker™ slides the pins along the surface of the centre of each well, removing the cells in a uniform line across the middle of each well to form the appearance of a wound or scratch in a confluent monolayer of cells. The wells were washed twice with media to remove any debris within the wound and the plate was loaded onto the IncuCyte® Zoom Live-Cell Analysis System (Essen Bioscience). The Incucyte was programmed to scan each well at 10x magnification, every hour for 48-72 hours. Cell migration was measured using relative wound density and % GFP confluence metrics. Relative wound density was used as the wound can take up to 48 hours to close, this metric assesses the density of cells within the wound taking into account the background cell density to remove the influence of cell division within the wound in increasing wound confluence.

For the invasion assay wells were coated with 50 µl 300 µg/ml Collagen, Type 1 solution from rat tail, (Sigma-Aldrich, Cat no. C3867-1VL) prior to seeding. Before wounding the wells a chilled reagent plate was setup. The reagent plate contained a column of wells containing 200 µl chilled 5x Neutralisation solution and a column of wells containing 150 µl collagen type I solution 3.75 mg/ml for each pair of experimental columns. 5x Neutralisation solution was made by mixing 1 ml 7.5%

$NaHCO_3$ (Sigma-Aldrich, Cat No. 401676-2.5KG-D), 1 ml FCS and 2 ml serum-free DMEM. The reagent plate was kept cool using the 96F CoolBox® Microplate System (BioCision, Cat No. BCS-147) together with the CoolSink® XT 96F (BioCision, Cat No. BCS-536). A scratch was made horizontally across the centre of each well using the WoundMaker™ as described above. The experimental wells were washed twice with complete medium and placed on a second CoolSink® XT 96F within a 96F CoolBox® for 5 min to chill. During this time 37.5 µl chilled 5x Neutralisation solution was transferred into the collagen type I containing wells to neutralise the acid within the wells. After 5 min the medium was removed from the experimental wells. 50 µl neutralised collagen type I was then quickly added to the wounded experimental wells, taking care not to allow bubbles to form in the collagen. Both plates were kept chilled and chilled pipette tips were used to prevent the collagen type I setting before it was added to the experimental wells. If any bubbles formed they were removed by blowing ethanol vapour across the surface of the collagen. The experimental plate was then transferred to a 37 °C incubator onto a pre-warmed CoolSink® for 30 min to allow the collagen to set. After 30 min 100 µl complete medium was added to each well. Again any bubbles were removed using ethanol vapour. The plate was then loaded into the Incucyte. The plate was left for 10 min for the temperature to equilibrate and to allow condensation to clear from the plate before incucyte scanning.

The Incuctye software was programmed to recognise cells and the wound. From these measurements it calculated the density of cells in the wound compared with the density of cells in the wound in the first scanned image. It also compared the density of cells in the wound with the density of cells outside of the wound to take into account increase in cell density within the wound due to cell proliferation rather cell migration from outside the wound. The calculation of relative wound density was made using the equation below.

$$\text{Relative wound density (\%)}$$

$$= 100 \text{ x } \frac{(\text{density of wound region at time } t - \text{density of wound region at time 0})}{(\text{density of cell region at time } t - \text{density of cell region at time 0})}$$

Two or three repeats were carried out with each fibroblast culture in contact co-culture with MDA-MB-231 GFP expressing cells. The number of repeats with each fibroblast culture is indicated in the respective results figure.

2.13.10 Chemotherapy resistance assay

2 x 10^4 cells per well of a 96-well plate were seeded in contact co-culture, as described in section 2.13.4.1. This assay was carried out with fibroblasts NF-1, NF-2, CAF-1 and CAF-2 in contact co-culture with MDA-MB-231-GFP-f.luc. Epirubicin was added to the wells for 24 hours and then changed to fresh complete medium. Epirubicin was made up into high dose and low dose working concentrations of 79 μM and 1 μM, respectively. Epirubicin stock was dissolved in Dimethyl Sulfoxide (DMSO, Sigma-Aldrich, Cat No. 472301-100ML). DMSO without epirubicin was added to control wells. 48 h following treatment with epirubicin cell viability of MDA-MB-231-GFP-f.luc cells was measured using the luciferase assay as described in section 2.13.7. Data were normalised by dividing by luciferase activity in untreated (DMSO only) control wells. Two or three repeats were carried out with each fibroblast culture in contact co-culture with MDA-MB-231 luciferase expressing cells. The number of repeats with each fibroblast culture is indicated in the respective results figure.

Chapter 3
Differential expression of microRNAs between normal breast fibroblasts and breast cancer associated fibroblasts

3.1 Abstract

Stromal fibroblasts modify behaviour of epithelial breast cancer cells. My aim in this chapter was to identify microRNAs (miRNA) that are differentially expressed between normal breast fibroblasts and cancer associated fibroblasts (CAFs) of triple negative, basal-like breast cancers, with a view to understanding better CAF biology and therefore the potential molecular mechanisms by which CAFs influence cancer cells.

First, samples of matched pairs of normal fibroblasts (NFs) and CAFs were prepared by laser microdissection from four triple negative, basal-like breast cancer cases. MiRNA expression profiles were determined using qPCR arrays. 48 miRNAs were found to be consistently differentially expressed between NFs and CAFs in these cases. Next, samples of matched NFs and CAFs were prepared from a further ten triple negative, basal-like breast cancers, and expression of selected miRNAs, miR-21, miR-27b and miR-30a-3p, was examined. Differential expression of miR-21, miR-27b and miR-30a-3p was confirmed in this larger cohort ($p = 0.0006$, $p = 0.0295$ and $p < 0.05$ respectively). In order to validate my laser microdissection and qPCR methodology, expression was also examined using chromogenic *in situ* hybridisation in the same 14 cases. This confirmed the finding that miR-21 expression is increased in CAFs, but miR-27b and miR-30a-3p expression was not successfully validated. Finally, expression of miR-21 was examined in an independent cohort of 150 triple negative breast cancer cases, using chromogenic *in situ* hybridisation on a tissue microarray supported by extensive clinical and pathological data. In support of my other findings, miR-21 expression was typically stromal rather than within epithelial cells. However, significant correlations between expression and clinical outcomes, including survival, were not evident.

In view of the well-established role of miR-21 as an oncogenic miRNA, I concluded that the function of miR-21 within the fibroblast compartment of breast cancer was worthy of further study (chapters 4 and 5).

3.2 Introduction

CAFs play key roles in co-ordination between tumour cells and many of the other elements within the cancer stroma. CAFs produce a wide variety of matrix components, which in turn play a role in bioavailability of growth factors as well as tensile strength of the tumour. They produce a range of signalling molecules, including cytokines that influence the behaviour of inflammatory cells and pro-angiogenic factors (Augsten, 2014, Kalluri and Zeisberg, 2006). CAFs, most importantly, interact with the tumour cells and can increase tumour cell migration, metastatic ability and resistance to chemotherapy (see section 1.2.2.4) (Augsten, 2014, Kuzet and Gaggioli, 2016).

The proportion of stroma in triple negative breast cancers is thought to have an influence on the risk of breast cancer recurrences (de Kruijf et al., 2011, Moorman et al., 2012). It is not known exactly which elements of the stroma have the biggest influence, but it is probable that various stromal components are necessary for this effect. It is therefore likely that CAFs contribute to this worsening of prognosis.

The importance of the role of miRNAs in regulation of gene expression has become increasingly recognised (Bhattacharyya et al., 2006, Guo et al., 2010). Being able to influence gene expression means that miRNAs can affect the functions and activity of the cell, they can therefore influence which growth factors and other signalling molecules CAFs express as well as the levels of different extracellular matrix components they produce.

In this chapter I address the first of my project aims, to identify miRNAs that are differentially expressed between NFs and CAFs in triple negative, basal-like breast cancer (see section 1.5). I hope to identify miRNA that may affect gene expression in CAFs and ultimately influence the behaviour of tumour cells through CAF-epithelial cell interaction.

3.3 Results

3.3.1 Array profiling of microRNA expression in matched NFs and CAFs

My aim was to identify differentially expressed miRNAs between 4 matched pairs of NFs and CAFs. To do this, first, I carried out laser capture microdissection

(LCM) to prepare matched samples highly enriched for NFs and CAFs from 4 cases. CAFs were taken from stroma next to carcinoma cells and NFs from benign breast tissue at least 10 mm away from tumour in the same individual patients. Images are shown in Figure 3-1 to demonstrate typical tissue regions selected as NFs and CAFs.

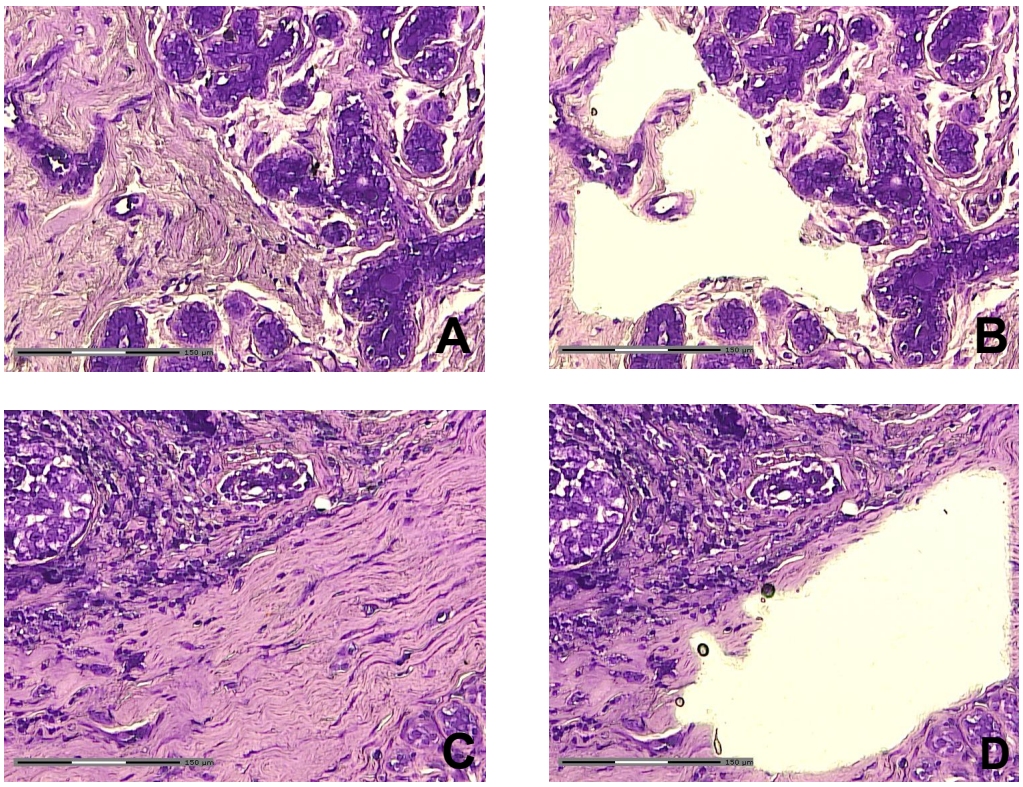

Figure 3-1 Representative images demonstrating LCM of fibroblasts

Archival tissue blocks containing normal breast tissue (A) and tumour tissue (C) from triple negative, basal-like breast cancer resections were identified. Blocks were sectioned and stained with haematoxylin and eosin, before regions of fibroblasts were identified and isolated using laser capture microdissection (B and D).

Expression levels of 671 miRNAs, along with the reference RNAs snRNA U6 and snoRNA RNU48, were quantified using low density qPCR arrays. Of the 671 miRNA analysed, 291 were not detected in any of the 8 samples and 110 were detected in all of the samples.

There is no consensus in the literature for exactly which reference(s) should be used for miRNA normalisation (Pan et al., 2016, Shidfar et al., 2016, Chen et al., 2016a).

Each miRNA was normalised to the geometric-mean of the references snRNA U6 and snoRNA RNU48 (Davoren et al., 2008, Torres et al., 2013), as these were expressed at suitable levels in all 8 samples (i.e. within a range that was not hugely different from many of the miRNAs to be tested: Ct-values 18-27), and this pairing could realistically be used in future follow up studies of individual miRNAs, where – for example – array median normalisation would not be possible.

For my first analysis, I used unsupervised agglomerative hierarchical clustering to look at the similarity in overall expression of the different miRNA across the 8 samples (4 NFs and 4 CAFs). The dendrograms representing these relationships are shown in Figure 3-2. This analysis was carried out by bioinformatician Alastair Droop.

This analysis initially revealed that the miRNA expression in NFs and CAFs from cases 1 and 3 clustered in their matched pairs, showing that their expression patterns were more similar to each other than other samples. By contrast, the other cases did not cluster in their matched pairs, showing that these paired normal and cancer samples were relatively divergent. However, when this analysis was limited to a subset of the miRNAs contained on only one of the two array cards and which is focused on the more highly expressed miRNAs (Figure 3-2B), all 4 cases clustered in their pairs. This demonstrated that the second array card may introduce noise to this analysis, as it contains a high proportion of miRNAs detected close to the limit of detection. It also demonstrated that matched NFs and CAFs are relatively similar to each other, more so than to other unrelated NFs or CAFs.

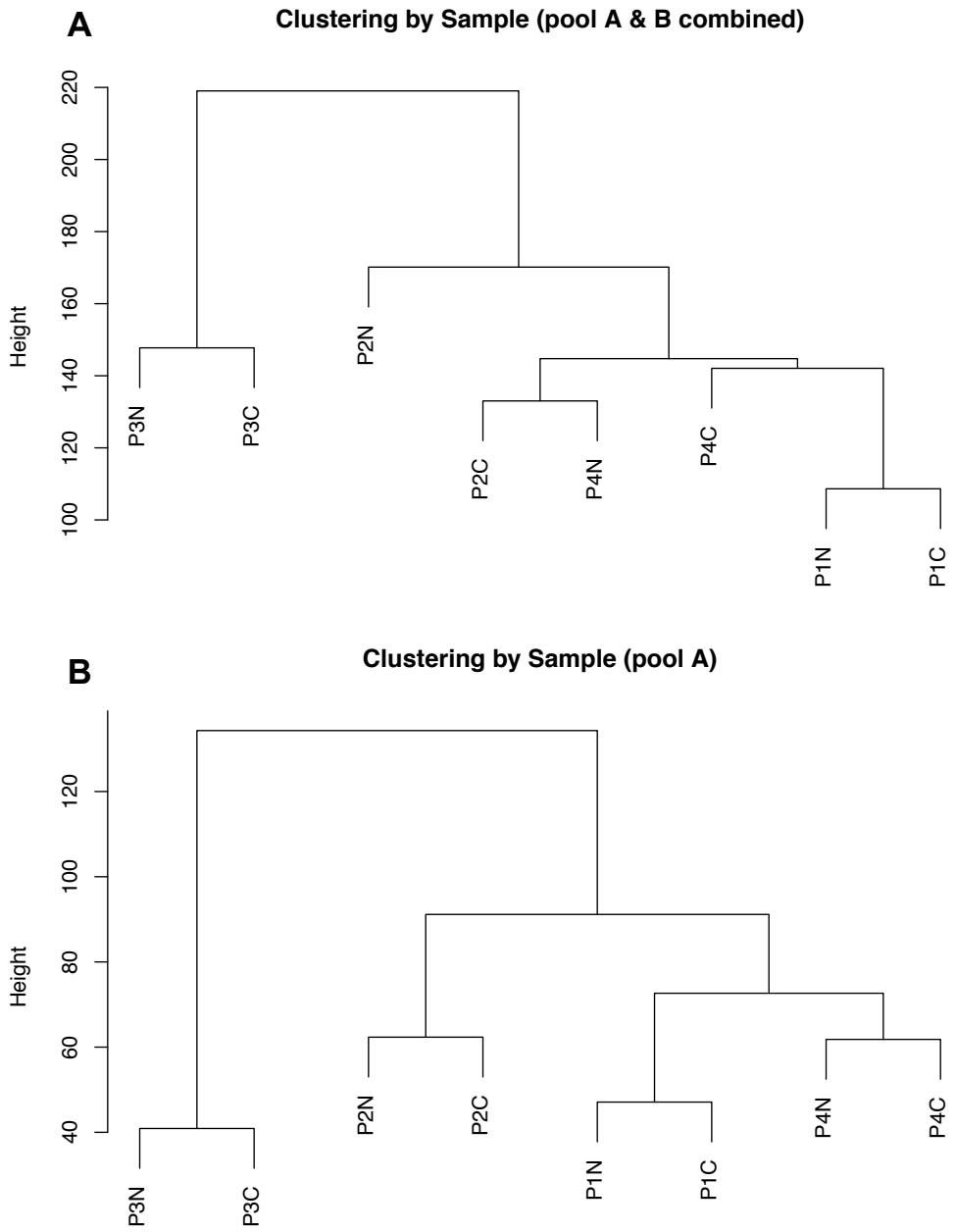

Figure 3-2 Dendrograms showing clustering of NF and CAF samples based on miRNA expression

Matched NF and CAF samples were isolated from 4 triple negative, basal-like breast cancer cases. Total RNA was extracted and miRNA expression quantified using array qPCR, normalised to the geometric mean of U6 and RNU48 expression. (A) Unsupervised agglomerative hierarchical clustering based on miRNA expression of the 380 miRNAs detected in at least one fibroblast sample. (B) Unsupervised agglomerative hierarchical clustering based on miRNA expression of a subset of these miRNAs, 178 in total, which were selected by the array suppliers as the more highly expressed and studied miRNAs ("pool A" only). P number refers to the case number, while N and C identify NF and CAF samples, respectively.

Next, I examined the differential expression of individual miRNAs between CAFs and NFs. I defined up-regulation or down-regulation in CAFs as >1.001 or <0.999 fold change compared with the matched NF samples, respectively. MiRNAs were also defined as up-regulated or down-regulated if detected in one sample of a matched pair but not the other, although for these it was not possible to calculate a fold difference. Table 3-1 shows the total number of miRNAs potentially up-regulated and down-regulated for each cancer case, with a minimum number of 87 (case 4, down-regulated) and a maximum number of 187 (case 4, up-regulated). Figure 3-3 shows the number of miRNAs with over-lapping up-regulation or down-regulation across the 4 cases. It should be noted that these assessments include all the array data, inclusive of some miRNAs that were expressed at very low levels (Cts >35) in both the matched CAF and NF samples, and some miRNAs with some evidence of non-logarithmic amplification profiles; therefore some data are potentially unreliable. I have filtered data using some quality metrics in later assessments.

Case	Number of miRNAs up-regulated	Number of miRNAs down-regulated
1	91	183
2	166	99
3	112	165
4	187	87

Table 3-1 Number of miRNA up-regulated and down-regulated in each case

MiRNA expression profiles in 4 matched pairs of NFs and CAFs were determined. The table shows the number of miRNAs up-regulated and down-regulated in CAFs compared with matched NFs.

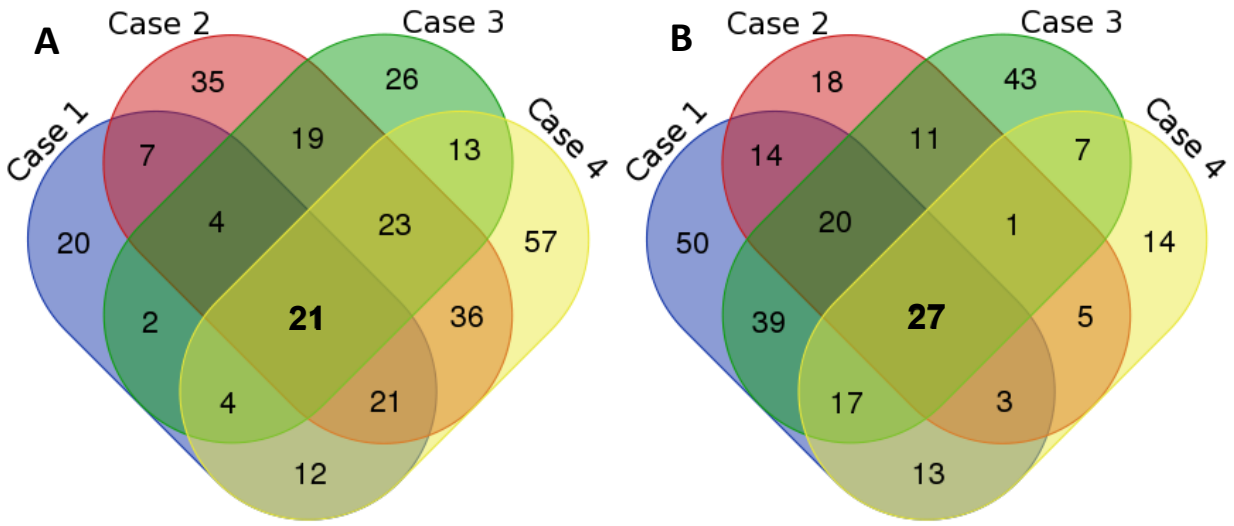

Figure 3-3 Venn diagrams showing numbers of miRNAs up-regulated (A) and down-regulated (B) in CAFs compared to matched NFs in 4 cases of triple negative, basal-like breast cancer, and showing overlaps between the cases.

MiRNA expression profiles in 4 matched pairs of NFs and CAFs were determined. Figure 3-3 shows the numbers of miRNAs that were up-regulated (A) and down-regulated (B) in CAFs compared with matched NFs. The central figure in bold highlights the number of miRNAs consistently up-regulated or down-regulated in all 4 cases.

21 miRNAs were consistently more highly expressed in CAFs compared with matched NFs and 27 miRNAs were consistently down-regulated in CAFs compared with matched NFs (Figure 3-3). These miRNAs are listed in Table 3-2 and Table 3-3, respectively. To enhance the reliability of the data I manually reviewed the amplification curves and Ct values for each miRNA. In some cases amplification curves did not have smooth sigmoidal shapes, indicative of reliable amplification, but more jagged shapes that may suggest technical problems (see Appendix E). Cases where Ct >35 in a matched fibroblast pair were also identified. Cases with high Ct values and/or irregular amplification curves were deemed to be potentially unreliable, this is indicated by the presence of asterisks in tables 3-2 and 3-3.

MicroRNA	Mean fold change	Minimum fold change	Maximum fold change	Detected in 8 fibroblast samples	
miR-213	∞*	∞	∞	No	(4 samples)
miR-200b#	23.50*	23.5	137.8	No	(5 samples)
miR-21	6.92	2.08	11.98	Yes	
miR-27b	2.46	2.06	2.86	No	(6 samples)
miR-223#	2.03	1.92	2.14	No	(6 samples)
miR-296	4.33	1.50	10.97	Yes	
miR-21#	21.32	1.42	39.70	Yes	
miR-708	2.26	1.38	2.93	Yes	
miR-193b	4.43	1.37	11.52	Yes	
miR-19a	1.91	1.35	2.79	Yes	
miR-125a-5p	5.09	1.34	11.27	Yes	
miR-425#	1.25	1.13	1.37	No	(6 samples)
miR-99b	1.25	1.10	1.33	No	(7 samples)
miR-574-3p	2.70	1.05	5.61	Yes	
miR-127	7.12	1.05	10.90	Yes	
miR-214	3.09	1.04	5.82	Yes	
miR-222	2.30	1.04	2.84	Yes	
miR-142-3p	2.77	1.03	6.00	Yes	
miR-886-3p	2.35	1.02	5.67	Yes	
miR-342-3p	4.02	1.02	10.97	Yes	
miR-193b#	2.22	1.01	3.42	No	(6 samples)

Table 3-2 MiRNAs with higher expression in CAFs as compared to matched NFs

Table 3-2 lists miRNAs expressed at higher levels in CAFs compared with NFs in all 4 pilot cases, with the largest minimum fold change at the top. It shows the mean fold change across the 4 cases, the minimum fold change and if the miRNA was detected in all CAF and NF samples. When not present in all 8 samples the mean was calculated from cases where it was present in both NF and CAF samples.

* indicates values that were not reliable because the amplification curves were not smooth, sigmoidal shaped or the Ct >35. The # on some miRNAs indicates precursor miRNAs that give rise to more than one mature miRNA, the ones labelled # are the less predominant of the two (see section 1.3.4).

miR-213 was detected in CAFs, but undetectable in the 4 NF samples. It was therefore not possible to calculate a fold change in expression level for this miRNA, this is indicated by ∞.

MicroRNA	Mean fold change	Minimum fold change	Maximum fold change	Detected in 8 fibroblast samples	
miR-760	175800726*	69129	308993233	No	(7 samples)
miR-581	6.97*	6.97	6.97	No	(5 samples)
miR-335#	4.41*	4.13	4.68	No	(6 samples)
miR-30a-3p	4.21	3.21	5.65	Yes	
miR-645	3.24	3.14	4.92	Yes	
miR-573	15.52*	2.17	52.97	Yes	
miR-335	2.49	1.93	3.05	No	(6 samples)
miR-942	6.12	1.78	17.40	Yes	
miR-378	31612682*	1.74	126450719	Yes	
miR-126#	6.20	1.68	15.85	Yes	
miR-630	5.95*	1.67	10.76	No	(7 samples)
miR-99a#	2.79	1.63	3.90	No	(7 samples)
miR-632	2.08	1.61	2.84	Yes	
miR-139-5p	12.22	1.59	32.00	No	(7 samples)
miR-218	6.65	1.57	11.48	Yes	
miR-let-7c	3.82	1.58	7.91	Yes	
miR-30e-3p	3.76	1.50	5.68	Yes	
miR-451	12.01625*	1.45	15.78	Yes	
miR-205	5.29	1.45	12.45	No	(7 samples)
miR-381	224498*	1.44	717192	Yes	
miR-140	2.06	1.42	3.87	Yes	
miR-29c	3.23	1.42	6.15	Yes	
miR-195	3.85	1.41	7.90	Yes	
miR-126	7.53	1.39	15.68	Yes	
miR-549	4.74	1.26	14.31	Yes	
miR-638	1.91	1.15	3.03	No	(7 samples)
miR-188-5p	2.20	1.05	3.06	Yes	

Table 3-3 MiRNAs with lower expression in CAFs as compared to matched NFs

Table 3-3 lists miRNAs expressed at lower levels in CAFs compared with NFs in the 4 pilot cases, with the largest minimum fold change at the top. It shows the mean fold change across the 4 cases, the minimum fold change and if the miRNA was detected in all CAF and NF samples. When not present in all 8 samples the mean was calculated from cases where it was present in both NF and CAF samples.

* indicates values that were not reliable because the amplification curves were not smooth, sigmoidal shaped or the Ct >35. The # on some miRNAs indicates precursor miRNAs that give rise to more than one mature miRNA, the ones labelled # are the less predominant of the two (see section 1.3.4).

A total of 38 miRNAs with consistent up- or down-regulation passed quality control screening with respect to amplification dynamics and level of expression that could be reliably detected, and were therefore potentially worthy of further study. A further screening mechanism was required to identify miRNAs to prioritise in further work. I selected for further validation miR-21, miR-27b and miR-30a-3p because they had a minimum fold change >2 in all 4 cases and they had the highest mean fold changes.

MicroRNA	Mean fold change	Minimum fold change	Maximum fold change	Detected in 8 fibroblast samples
miR-760	175800726*	69129	3089935233	No (7 samples)
miR-581	6.97*	6.97	6.97	No (5 samples)
miR-335#	4.41*	4.13	4.68	No (6 samples)
miR-30a-3p	4.21	3.21	5.65	Yes
miR-645	3.24	3.14	4.92	Yes
miR-573	15.52*	2.17	52.97	Yes
miR-335	2.49	1.93	3.05	

3.3.2 MiR-21 and miR-27b are significantly up-regulated and miR-30a-3p is significantly down-regulated in CAFs

My next aim was to confirm that selected candidate miRNAs from the screen above, namely miR-21, miR-27b and miR-30a-3p were indeed deregulated in fibroblasts from triple negative, basal-like breast cancers. First, I carried out a repeat analysis of the RNA extracted from the cases used for the array screen, since the screen was performed as only one technical replicate for each biological sample, presenting a risk of technical errors. Individual qPCRs (as opposed to array cards) were performed for miR-21, miR-27b and miR-30a-3p (normalisers snRNA U6 and snoRNA RNU48) using technical triplicates and relative expression was determined (Figure 3-4). All three miRNAs demonstrated similar results to those from the array screen.

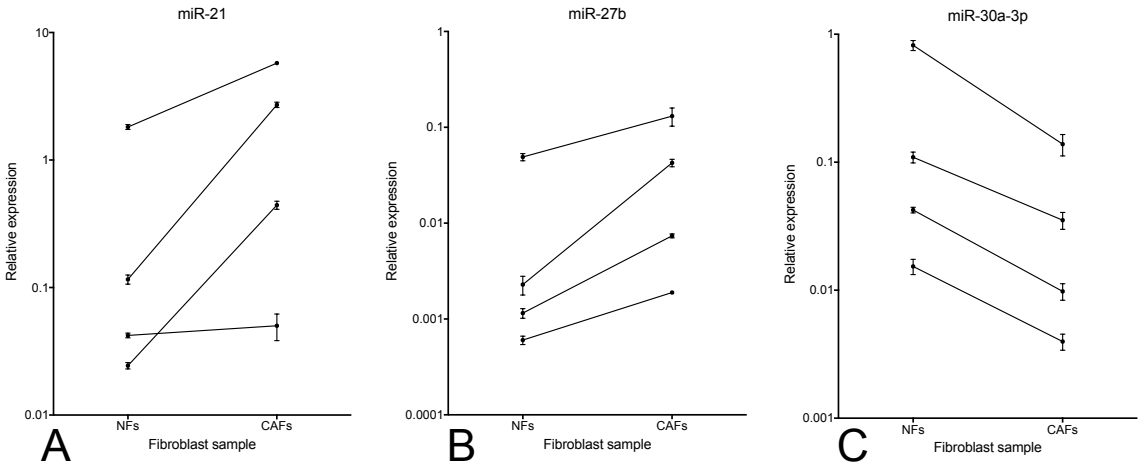

Figure 3-4 MiR-21, -27b and -30a-3p were differentially expressed between NFs and CAFs in 4 cases of triple negative, basal-like breast cancer

Matched samples of normal breast fibroblasts (NFs) and cancer associated fibroblasts (CAFs) were prepared from 4 triple negative, basal-like breast cancer patients. Relative expression of miR-21 (A), miR-27b (B) and miR-30a-3p (C) was determined (normalised to U6 and RNU48) by qPCR. Each circle represents the expression level for one fibroblast sample. The lines between the NF and CAF circles identify the matched sample for each case. The error bars represent the standard deviation of the technical triplicate repeats.

Next, I isolated matched NFs and CAFs from a further ten cases of triple negative, basal-like breast cancer using LCM. Relative expression of miR-21, miR-27b and miR-30a-3p was determined for these ten cases, and the data were combined with the data from the original 4 screening cases (Figure 3-5).

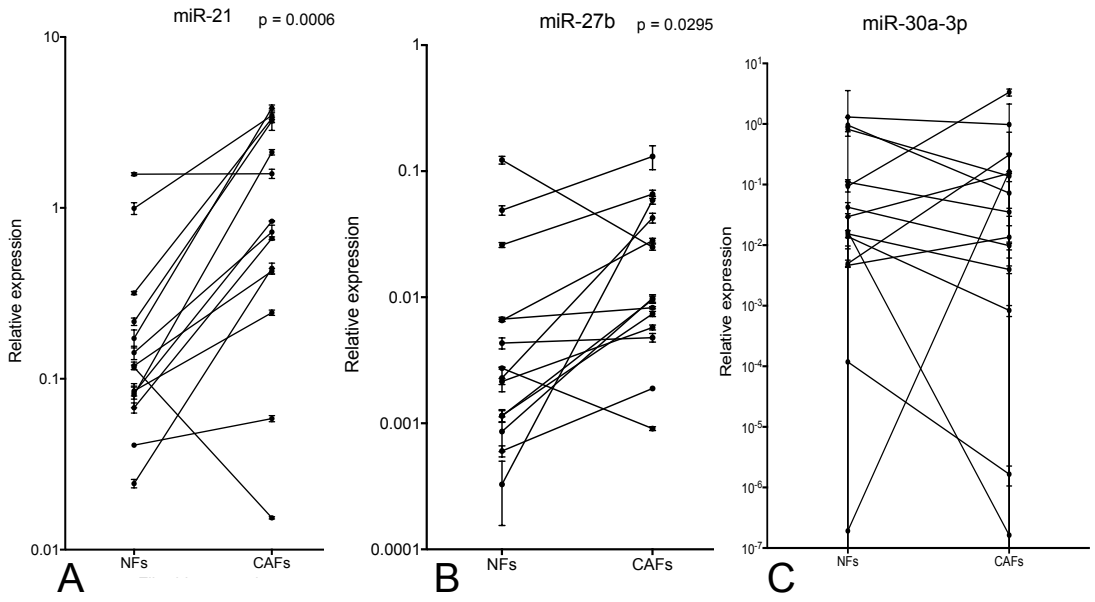

Figure 3-5 MiR-21 and miR-27b are significantly differentially expressed between NFs and CAFs in 14 triple negative, basal-like breast cancers

Matched samples of normal breast fibroblasts (NFs) and cancer associated fibroblasts (CAFs) were prepared from 14 triple negative, basal-like breast cancer patients. Relative expression of miR-21 (A), miR-27b (B) and miR-30a-3p (C) was determined (normalised to U6 and RNU48) by qPCR. Each circle represents the expression level for one of the samples. The lines between the NF and CAF circles identify the matched sample for each case. The error bars represent the standard deviation of the technical triplicate repeats. The Wilcoxon matched pairs signed rank test was used to assess the significance of any differential expression, as shown.

Expression of miR-21 and miR-27b was higher in CAFs compared with NFs in 12 of the 14 cases, whereas for miR-30a-3p the technical variability for each data-point was so high that conclusions could not easily be drawn. The significance of these differential expressions was assessed using Wilcoxon matched pairs signed-rank test (after a Shapiro-Wilk test had demonstrated that the data were not normally distributed; Appendix F). MiR-21 and miR-27b were significantly up-regulated in CAFs ($p = 0.006$ and $p = 0.0295$ respectively), while miR-30a-3p demonstrated no significant difference ($p = 0.9515$).

I reviewed the amplification curves for miR-30a-3p to try to determine reasons for technical variability within these samples. The amplification curves for miR-30a-3p have a shallower slope in the exponential phase (see Appendix G). One explanation for this could be the presence of a PCR inhibitor (Schrader et al., 2012). To attempt

to overcome this issue, samples were diluted by a range of factors up to 1000-fold, potentially reducing the influence of any PCR inhibitors, at the cost of reducing assay sensitivity. Results of qPCR with 1000-fold diluted samples, and excluding cases with continued poor amplification and high technical variability, are shown in Figure 3-6; miR-30a-3p was significantly down-regulated in CAFs in the cohort of 10 remaining cases. This optimisation work was carried out by a colleague, Dr Ruth Darbyshire (Academic FY2 visiting scientist).

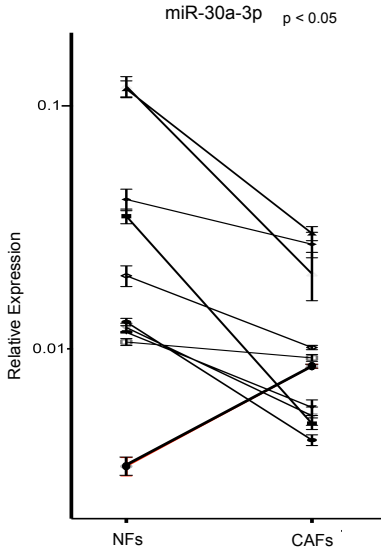

Figure 3-6 MiR-30a-3p is significantly down-regulated in CAFs as compared to matched NFs

Matched samples of normal breast fibroblasts (NFs) and cancer associated fibroblasts (CAFs) were prepared from 14 triple negative, basal-like breast cancer patients. Relative expression of miR-30a-3p was determined (normalised to U6 and RNU48) by qPCR. Data from 10 cases that passed assessments of qPCR data quality are shown. Each circle represents the expression level for one fibroblast sample. The lines between the NF and CAF circles identify the matched sample for each case. The error bars represent the standard deviation of the technical triplicate repeats.

3.4 Deregulation of miR-21 within fibroblasts, but not other miRNAs, was confirmed by *in situ* hybridisation

3.4.1 MiR-21 in situ hybridisation showed staining predominantly in CAFs

My next aim was to confirm my PCR-based findings using an alternative assay, while in addition examining whether expression of my miRNAs of interest was limited to the fibroblast component, or was also present within epithelial cells. In order to do this, I used chromogenic *in situ* hybridisation (CISH) to visualise expression of miR-21, miR-27b and miR-30a-3p on blocks representing the same 14 triple negative, basal-like breast cancer cases used above. Positive expression was labelled with a blue precipitate, while tissue was counterstained red (with the dye nuclear fast red). Examples of the staining with the positive control (U6) and with the probe for miR-21 can be seen in figure 3-7.

CISH staining for U6 (used as a positive control to demonstrate successful CISH) showed clear nuclear positivity in both benign and tumour tissue as expected (Figure 3-7A). Staining with a negative control probe of scrambled miR-21 sequence was generally negative, although one case stained positively in benign and tumour tissue in inflammatory cells, endothelial cells, tumour cells and fibroblasts, this case was excluded from further analysis.

CISH with the probe for miR-21 gave clear, specific positive and negative staining predominantly in the cytoplasm of CAFs, and little staining elsewhere. Positive staining intensity varied from weak to strong (see Figure 3-7D-F). In one case positive staining was seen in normal fibroblasts, in this case the staining was much stronger in the CAFs than in the NFs, in all other cases the NFs were negative. In one case staining was seen in tumour cells as well as in CAFs (see Figure 3-8A). It was noted that in several cases the CAFs closest to tumour cells stained more strongly than those further away (see Figure 3-8B and C), whereas in other cases all the CAFs stained with similar intensities.

The CISH staining for miR-27b and miR-30a-3p was not successful, no positive staining was seen. Probe concentration was increased from 400 nM up to 1.5 μm, until non-specific staining was seen.

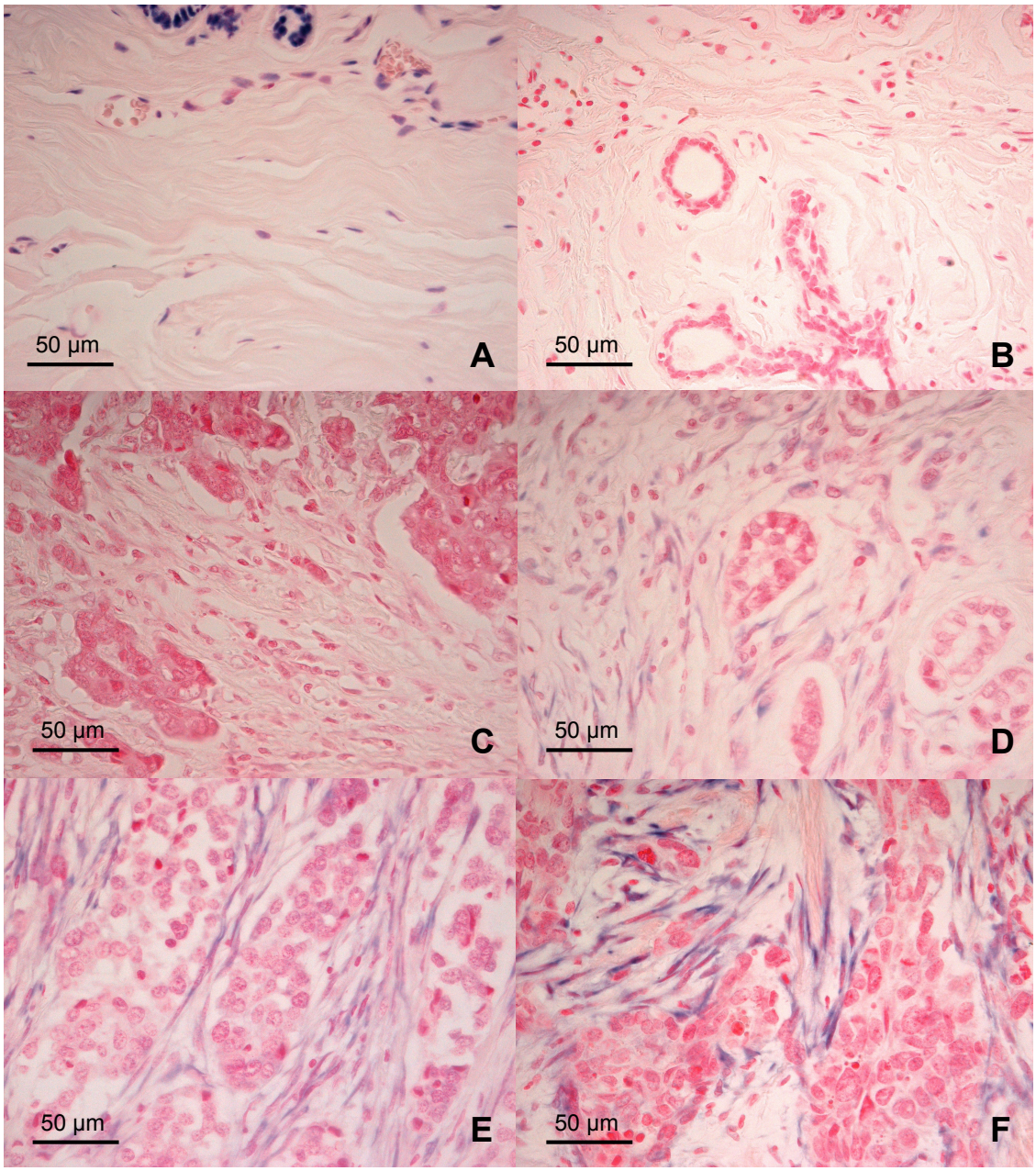

Figure 3-7 Representative images of chromogenic *in situ* hybridisation (CISH) staining of breast tissue for the snRNA U6 (positive control) and miR-21

Breast FFPE sections stained with CISH. CISH positive staining is blue, with a red counterstain. Part A was stained for snRNA U6 (positive control). Parts B-F were stained for miR-21 and show examples of no staining (B and C), weak staining (D), moderate staining (E) and strong staining (F). Parts A and B are sections of benign breast tissue, parts C-F are invasive tumour.

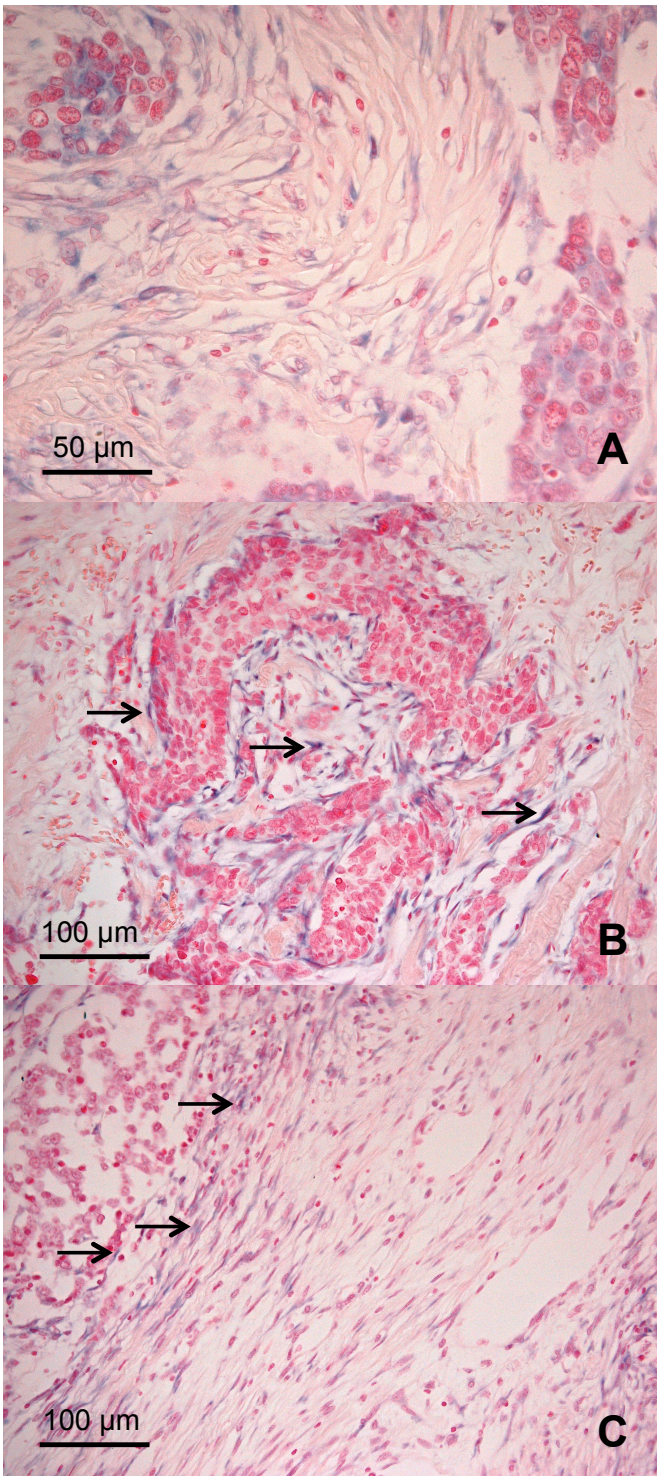

Figure 3-8 Representative images of CISH staining of breast tissue for miR-21 demonstrating specific features of the staining patterns

Invasive breast cancer FFPE sections were stained with CISH of miR-21 (blue) and counterstained red. (A) In one case, epithelial staining was seen. (B and C) In some cases, CAFs close to tumour cells arrows (→) were stained more strongly than CAFs further away.

MiR-21 expression in fibroblasts was quantified as a histoscore combining assessment of the proportion of cells stained, and their intensity (weak, moderate or strong, see section 2.11.1 for more details). The distribution of staining in CAFs was assessed by quantifying CAFs ≤ 75 μm from tumour cells and CAFs > 75 μm from tumour cells separately. The distance 75 μm was chosen based on a visual assessment of the CISH staining pattern, it was after this distance that the staining intensity decreased dramatically in cases where CAFs closer to tumour stained more intensely. Scoring was performed by myself, and additionally and independently by Dr Eldo Verghese (supervisor, and a histopathology consultant) for 50% of cases. Scores from the two independent scorers correlated closely (correlation coefficient absolute agreement 0.974; Appendix H) thereby validating the reproducibility of this scoring method.

One of the initial aims in carrying out CISH was to confirm the findings from my initial LCM and qPCR approach (Figures 3-5). I therefore compared expression levels determined by qPCR to CISH scores, using CISH scores for all fibroblasts or for either those closest to (≤75 μm) or further from tumour cells (>75 μm). All three comparisons were significantly positively correlated (r of at least 0.57; p of at least 0.0037; Figure 3-9) demonstrating that my LCM procedure was successful in enriching for fibroblasts, and that assessment of relative miR-21 levels using CISH was possible. I also examined the correlation between the scores for the two CAF populations (close to tumour cells and further away). Surprisingly, these were not significantly correlated with each other, although this could be due in part to the small sample size (Appendix I).

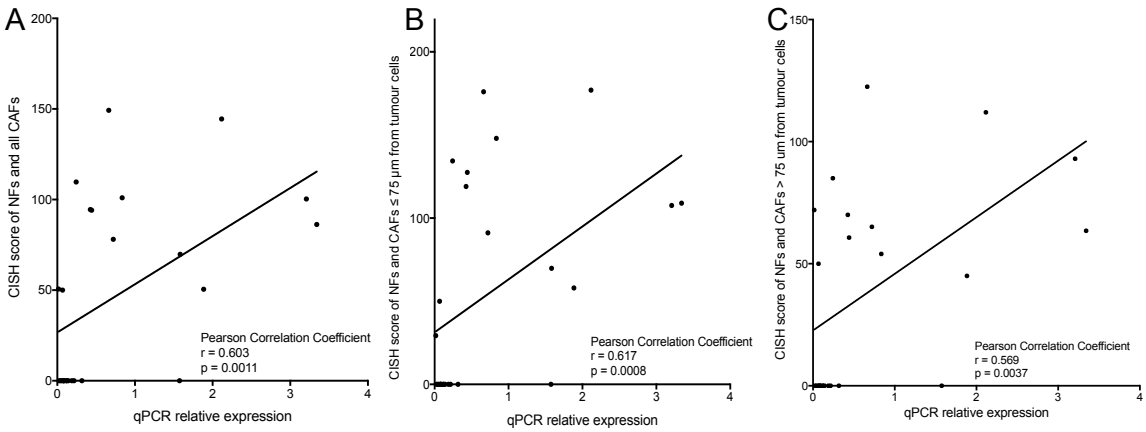

Figure 3-9 Assessments of miR-21 expression in NFs and CAFs by CISH H-score and by LCM / qPCR significantly correlate

Relative expression of miR-21 in NFs and CAFs was quantified, after LCM of the cells, by qPCR. Expression of miR-21 was also assessed using CISH in the same tissues and was quantified manually as H-scores of specific fibroblast populations as described. Correlations between the two assessments were examined using scatter plots and Pearson correlation coefficients. (A) CISH scores for staining in all fibroblasts. (B) CISH scores for NFs closest to epithelial cells and CAFs closest to tumour cells (≤75 μm). (C) CISH scores for NFs further from epithelial cells and CAFs further from tumour cells (> 75 μm). Each circle represents one sample of either NFs or CAFs. Linear regression has been plotted based on the data points and the Pearson correlation calculated.

3.5 Tissue microarray CISH

Based on my finding that miR-21 is relatively highly expressed in CAFs using a relatively small cohort of 14 patients, I was interested to assess whether this finding was generally applicable to a larger cohort, and potentially whether expression correlated with specific clinical or pathological features. Therefore, I constructed a tissue microarray (TMA), containing triplicate cores of cancer tissue from 150 triple negative breast cancer cases and supported by extensive clinical and pathological information (Table 3-4). The previous 14 cases were not included in the TMA to avoid repeating CISH staining and scoring on these cases and duplicating the data. MiR-21 expression was visualised using CISH and scored as previously, with final scores for each case being taken as the mean score from the cores available for that case. The mean score, rather than the highest score, was chosen to include in the analysis to be more representative of the entire CAF population rather than a small subset of intensely staining CAFs. CAFs as a whole population were scored, rather than separate assessments of those close to or further from tumour cells. This was because: (i) previous results above suggested separate analyses did not add value; (ii) within TMA cores much of the tissue is within 75 μm of the core edge and therefore could be incorrectly classified as not near tumour cells when tumour cells were in fact immediately next to the core in the donor tissue; and (iii) examples of both close and far fibroblasts were frequently not present in the limited core tissue available. Some cores were lost from slides during staining, an expected and documented occurrence in TMA-based research (Parsons, 2009), and in some cores tissue became very disrupted and scoring was not possible; therefore, it was not possible to score every case. 70% (105/150 cases) were scored. As with the previous sections, positive staining was predominantly seen in CAFs, with tumour cells rarely staining (only 2 cases, 1.3 %). Staining intensity varied from negative to strong.

Characteristic	Number of cases (%)
Age at diagnosis	61 years (32 - 93 years) mean (range)
Histological Grade	
I	3 (2 %)
II	20 (13 %)
III	124 (83 %)
Not assessable	3 (2 %)
Lymph nodes	
0	95 (63 %)
1-4	33 (22 %)
>4	19 (13 %)
None taken	3 (2 %)

Table 3-4 Summary of clinicopathological features of the triple negative breast cancer cases included in tissue microarray

To confirm that TMAs were a reliable way to assess miR-21 staining I correlated the CISH scores between different cores from the same cases, to see if they were similar to each other. A strong positive correlation between scores in different cores would suggest that miR-21 expression was sufficiently homogenous throughout the tissue for valid assessment in TMAs. Correlation analysis between scores for cores 1 and 2 (random designations in the TMA plan) for each case where both scores were available gave a strong positive correlation (Spearman's rank correlation coefficient = 0.75; $p < 0.0001$). Correlation between cores 1 and 3 and 2 and 3 also showed strong positive correlation (Spearman's correlation cores 1 and 3 $r = 0.5879$; $p < 0.0001$ and Spearman's correlation cores 2 and 3 $r = 0.7413$; $p < 0.0001$). The whole tissue section CISH carried out in section 3.4.1 showed reasonable homogeneity across the section. Both the core correlation and the whole section staining suggest that TMA are a suitable format for this analysis.

The CISH H-scores for the TMA were 0 – 220. To show the distribution of TMA CISH H-scores a cumulative frequency distribution has been plotted (Figure 3-10).

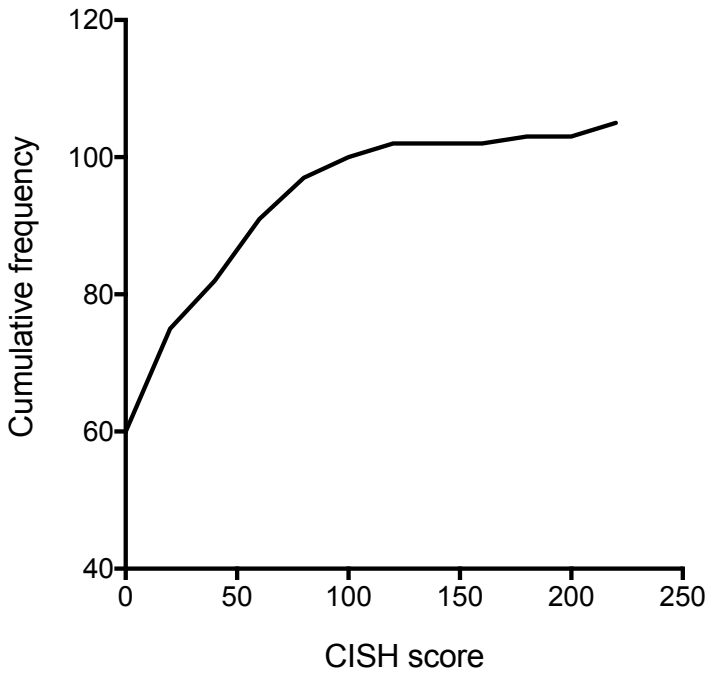

Figure 3-10 Cumulative frequency distribution of TMA CISH H-scores

105 TMA cases were successfully stained with CISH miR-21 probe. The CISH staining intensity and percentage was quantified using a H-score. This shows the cumulative frequency of the TMA CISH H-scores.

The relevance of miR-21 expression within the fibroblast compartment to clinical or pathological factors was tested by assessing correlations between miR-21 expression (defined as mean CISH score for each case) and age at diagnosis, tumour size, grade, number of positive nodes and Nottingham Prognostic Index using Spearman's rank correlation coefficients (Table 3-5). Tumour grade showed a weak, but significant (ignoring multiple testing) positive correlation with miR-21 expression in CAFs, but other factors did not correlate.

Clinicopathological Parameter	Spearman's correlation coefficient	P value
Age at diagnosis	0.06038	0.5406
Tumour size	-0.02563	0.7972
Tumour grade	0.2318	0.0191
Number of positive lymph nodes at diagnosis	0.1215	0.219
Nottingham Prognostic Index	0.1412	0.1569

Table 3-5 Tumour grade significantly correlates with miR-21 expression in CAFs

MiR-21 expression in CAFs was quantified in a cohort of triple negative breast cancers using CISH and H-scores. Spearman's correlation coefficients were used to assess correlations between clinicopathological features and miR-21 expression.

The relevance of miR-21 to cancer outcome was also tested by assessing the impact of expression on disease free survival, disease specific survival and overall survival using Kaplan Meier analyses (Figure 3-12). Expression was dichotomised into low/negative and high using cut offs determined by modified receiver operating characteristic curves, separately for each clinical outcome (Figure 3-11). For disease free survival, the cut off was CISH score >60, for disease specific survival this was CISH score >145, and for overall survival this was CISH score > 20. MiR-21 staining intensity did not significantly correlate with clinical outcome in these analyses. Some alternative cut offs could also be suggested from the receiver operating characteristic curves (Appendix J-1); these were also used for further Kaplan Meier analyses (Appendix J-2), however it remained the case that miR-21 expression in fibroblasts did not correlate significantly with clinical outcome.

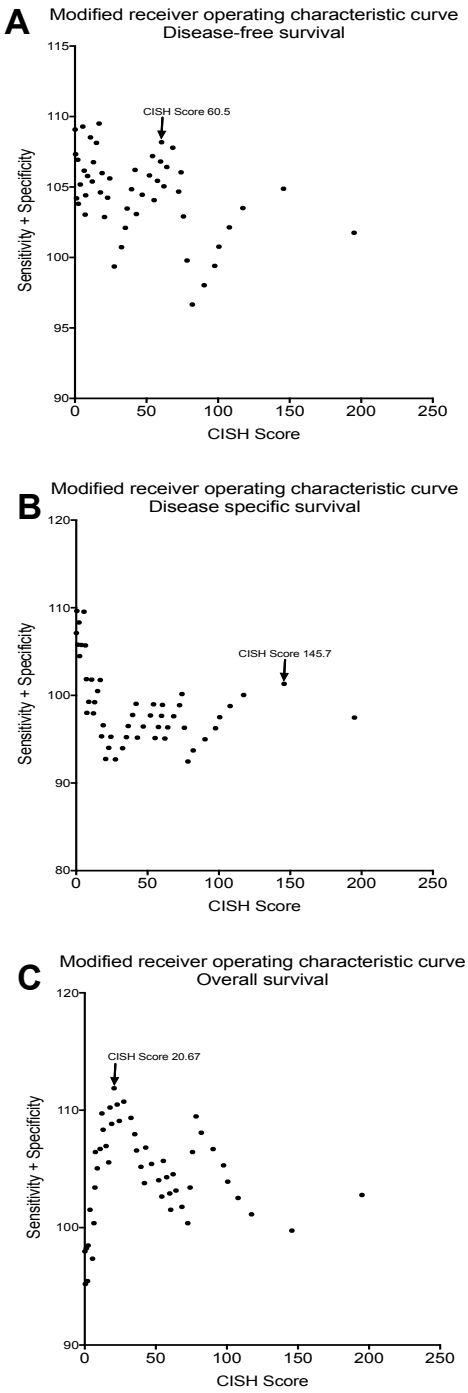

Figure 3-11 Modified receiver operating characteristic curves used to determine the optimal cut off point for CISH score low vs. CISH score high

CISH score was correlated with the clinical outcomes disease free survival, disease specific survival and overall survival. The data was dichotomised at each CISH score within the range and the sensitivity and specificity calculated. Each circle represents the CISH cut-off score plotted against the sum of sensitivity and specificity for each clinical outcome, disease free survival (A), disease specific survival (B) and overall survival (C). The optimal CISH cut-off score was determined from the peak of each curve.

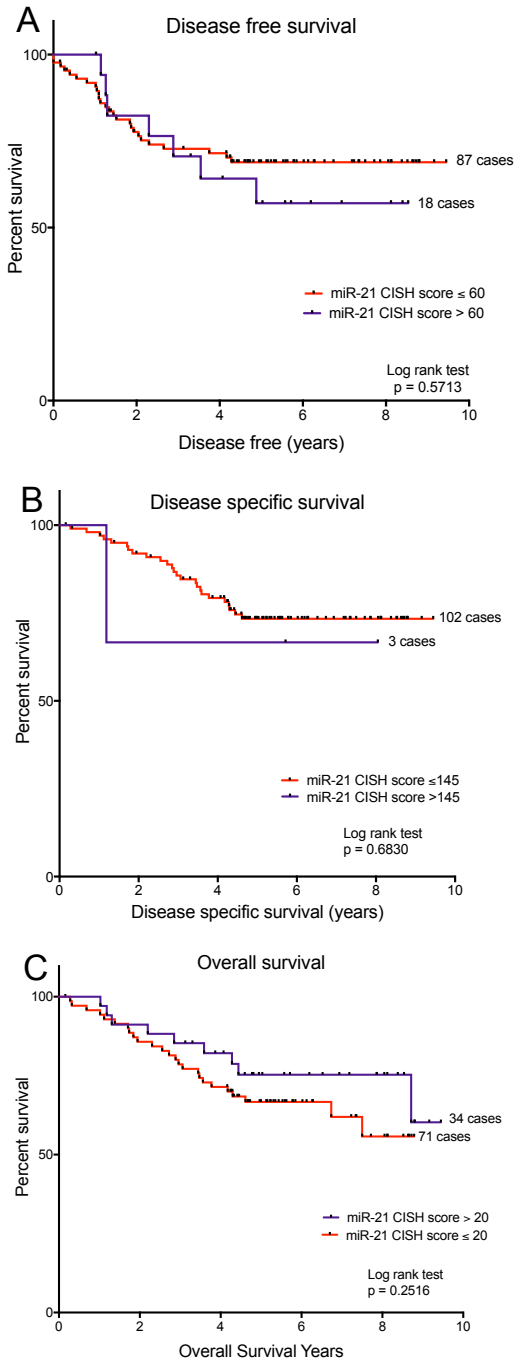

Figure 3-12 Clinical outcomes do not significantly correlate with miR-21 expression in CAFs

MiR-21 expression in CAFs was determined in a cohort of triple negative breast cancers using CISH and H-scores. Cases were dichotomised into low and high expression groups based on cut-offs defined by receiver operating characteristic curve analyses (Figure 3-11) as shown. Kaplan Meier analyses for the clinical outcomes disease free survival (A), disease specific survival (B) and overall survival (C) were carried out on these groups. Red lines represent low/negative expression while purple lines represent high expression. The small black squares represent the point at which a subject was censored.

3.6 Discussion

3.6.1 Choice of miRNAs for further study

The array analysis I performed allowed identification of 21 miRNAs that were up-regulated in CAFs compared with matched NFs and 27 miRNAs that were down-regulated in CAFs in the 4 pilot cases (Figure 3-3). It was not possible to investigate fully the functional role of each of these miRNA, therefore I wanted to determine which of these miRNA were more likely to be biologically important rather from those occurring by chance. To do this the fold-change of up-regulation or down-regulation was analysed. I looked at both the mean fold change and the minimum fold change to determine which miRNA were altered the most in CAFs and to confirm that this wasn't the result of a large change in one case and relatively modest changes in the other cases (Tables 3-2 and 3-3). This is based on the assumption that a larger change and a change that is consistent across more cases is more likely to be biologically significant. This approach has been taken in a number of studies, including those looking at miRNAs in nipple discharge and serum samples of breast cancer patients (Zhang et al., 2015, Zhang et al., 2017a, Wang et al., 2009). However, it is possible that very minor changes in specific miRNA may also be important to the cells.

MiRNA expression profiling in breast cancer has been carried out on a variety of breast cancer samples including whole tumour samples, patient serum and nipple discharge samples, however isolating a specific part of the tumour, the CAFs, and profiling them separately from the rest of the tumour provides a rare insight into the biological changes within CAFs (Tanic et al., 2015, Zhang et al., 2012a, Shin et al., 2015). MiR-21 was not identified as significantly increased in nipple discharge or whole tumour samples, and was identified as decreased in the serum of triple negative breast cancer patients compared with non-triple negative breast cancer patients. This highlights the difference in results that can be obtained when looking at one specific component or cell-type within a tumour and when using matched benign breast tissue from the same patient for comparison.

Using the mean and minimum fold-change in miRNA expression miR-21, miR-27b and miR-30a-3p were selected for further validation (see Tables 3-2 and 3-3). This was done by carrying out a triplicate single-primer PCR on these four cases and a

further 10 matched pairs of NFs and CAFs. The single-primer PCR confirmed the findings that miR-21 and miR-27b are significantly up-regulated in CAFs and that miR-30a-3p is significantly down-regulated in CAFs (Figures 3-5 and 3-6). Figure 3-5 parts A and B also showed that 2 of the 14 cases did not follow the general pattern, that miR-21 and miR-27b expression were not up-regulated in 2 patient samples. These were the same patient samples for both miRNA. The samples and clinical outcomes were reviewed. There was no difference in the amount of RNA or the quality of the RNA extracted from these samples and there was no significant difference in clinical parameters or outcomes for the patients from which these samples were taken, including tumour morphology, size, grade, lymph node status, disease free survival or overall survival. As the patient samples that did not follow the overall pattern, i.e. an increase in miRNA levels in CAFs for miR-21 and miR-27b, were the same for both miRNA this suggests that in these cases the conversion of normal fibroblasts to CAFs may have harnessed different biochemical pathways compared with the other 12 cases. As there is little known about the mechanisms involved in the conversions of cells into CAFs it is not possible to identify the exact differences between these two pathways, however my work does suggest that whichever pathway is followed this does not alter patient outcomes, although with such low numbers firm conclusions cannot be drawn.

The finding that miR-21 qPCR expression is increased in CAFs is similar to the results published by Bullock *et al.* in colorectal cancer. They carried out LCM of colorectal cancer stroma and qPCR of 10 cases and found that miR-21 expression was on average 4-fold higher in tumour stroma than in normal stroma (Bullock et al., 2013), I observed a average 2-fold increase in CAFs compared with NFs.

My results showed that miR-27b was significantly up-regulated in CAFs compared with matched NFs (Figure 3-5). No other study has looked at miR-27b qPCR expression exclusively in fibroblasts, however there are a number of studies that have looked at miR-27b expression in whole tumour samples and breast cancer cell lines using qPCR. These showed mixed results, depending on whether cell lines or patient samples were used and which breast cancer subtype was selected. MiR-27b expression has been found to be decreased in luminal breast cancer whole tumour samples, to show no significant change in expression levels in breast adenoid cystic carcinoma compared with normal breast tissue and to be increased in triple negative

breast cancer cell lines compared with a non-invasive breast cell line (Takahashi et al., 2015, Wang et al., 2009, Kiss et al., 2015). In triple negative breast cancer miR-27b expression has also been found to be correlated with worse disease free survival, but has not been compared with levels in normal breast tissue (Liu et al., 2015, Shen et al., 2014). These findings together with my work suggested that increased miR-27b may be of importance specifically in the triple negative breast cancer subtype.

MiR-30a-3p was significantly down-regulated in CAFs as compared to matched NFs (Figure 3-6). This finding is supported by a study that also identified miR-30a-3p down-regulation when looking at whole tumour samples compared with matched normal tissue in fresh tissue of 8 breast cancers using a miRNA microarray (Yan et al., 2008). MiR-30a-3p down-regulation has been associated with early recurrence, and levels are to be generally lower in ER negative breast cancers (Perez-Rivas et al., 2014). However, this study looking at breast cancer recurrence did not separate breast cancers by subtype and given that a proportion of basal-like breast cancers are known to relapse early, some of the miRNA changes they observed may be identifying subtype specific changes rather than an independent early recurrence signature. Therefore the clinical significance of my and others' findings on miR-30a-3p down-regulation remains largely unclear.

3.6.2 ISH for miRNAs – technical challenges, but cell-type specific conclusions

The CISH staining for miR-27b and miR-30a-3p was not successful, with no positive staining seen. Probe concentration was increased from 400 nM up to 1.5 μm, until non-specific staining was seen. One possible explanation for the lack of specific staining is that the expression of these miRNA was below the level of detection by CISH. MiR-21 was generally expressed at higher levels in CAFs, (a mean relative expression value of 1.50), whereas the relative expression of miR-27b and miR-30a-3p were 0.03 and 0.38 respectively. These values are 4 – 50 fold lower than the expression of miR-21. It could be possible therefore that there is not enough miR-27b or miR-30a-3p present to bind to the probe to produce visible positive blue staining. In a study looking at detection of herpes virus in FFPE and frozen tissue qPCR was found to be more sensitive than ISH or conventional PCR (Crockford et

al., 2008), supporting the idea that CISH sensitivity may be limiting. MiR-27b CISH has been successfully carried out in the epithelial keratinocyte layer of oral biopsies (Zhang et al., 2012b), although the relative expression of miR-27b in oral keratinocytes compared with triple negative, basal-like breast cancer tissue is not known. CISH of miR-30a-3p has not been published.

CISH has been successfully carried out in breast tissue for only a small number of miRNAs; 13 in total, including miR-21 (Quesne et al., 2012, Jang et al., 2014, Minemura et al., 2015, Cao et al., 2016, Song et al., 2016a, Song et al., 2015, Hanna et al., 2012). Breast tissue itself is not thought to present particular technical challenges when carrying out CISH compared with other cancer tissues types. However, it is more technically challenging to carry out CISH on FFPE tissue than frozen tissue or cell lines because formalin fixation and the presence of paraffin can mask the miRNA target and cause cross-linking reducing the sensitivity of the technique (Warford, 2016). This reduced sensitivity in FFPE tissue could explain why miR-27b and miR-30a-3p CISH did not work in my breast tissue samples, whereas miR-21 which is at higher expression levels in these cases was above the detectable range.

The miR-21 CISH staining showed a variety of staining patterns, with normal fibroblasts largely staining negatively, except in one case, and CAFs in all cases staining positively. The staining pattern in CAFs varied with similar staining throughout the CAF population in some cases, and heterogeneous staining in others (both strong and weak staining in different populations of CAFs). Where there was variable staining, the CAFs closest to tumour cells stained more strongly and those further from islands of tumour cells stained more weakly (Figure 3-8). This is similar to results seen by Nielsen *et al.* and Hug *et al.* (Hug et al., 2015, Nielsen et al., 2014). In a study looking at 26 specimens, 16 malignant and 10 benign, Hug *et al.* noted "miR-21-positive spindle-like cells were found to surround tumour cell islands", a similar description to what was seen in our cases. However, in contrast to our findings, they noted that miR-21 was detected in epithelial cell cytoplasm in most high-grade specimens, whereas we saw tumour cell staining in only one case, however they did not comment on the subtype of these cases, and it may be that these were not triple negative, basal-like cases and that therefore differences in staining in the tumour cells may not be unexpected (Hug et al., 2015). Qi *et al.*

identified positive tumour cell cytoplasm staining in 15 out of 17 invasive ductal carcinomas, although again, the receptor status of these cases was not mentioned (Qi et al., 2009). It is known that the staining patterns are different in different subtypes, for example in a study looking at miR-21 CISH staining in HER2 positive breast cancer Nielsen *et al.* saw staining either only in the stroma (36 %) or in the stroma and the tumour cells (64 %) (Nielsen et al., 2014). This reinforces the importance of being specific about which breast cancer subtype is being referred to, and taking it into account, particularly when carrying out studies with small numbers of cases.

The expression of miR-21 in CAFs as quantified by CISH intensity and percentage of positive cells correlated well with the qPCR relative expression assessments. This is important not only in the context of my work in confirming the qPCR findings, but also in that it validates *semi-quantitative* assessment of CISH staining and therefore provides greater validity to studies that correlate CISH staining with clinical and patient outcome data. A more quantitative alternative to CISH staining is radio-isotope labelled ISH. The ISH signal can then be measured in a more automated, quantitative way using phosphorimage analysis. One major disadvantage of this method is that it can be less sensitive because the signal is not amplified at the alkaline phosphatase substrate conversion step and may therefore not be appropriate for miRNA detection (Chotteau-Lelievre et al., 2006).

The importance of using CISH to assess cell type location of miRNA and therefore how to investigate and interpret miRNA roles in tumour biology was highlighted by recent findings on the expression of miR-143 and miR-145 in colorectal cancer. When measuring levels in whole tumour samples miR-143 and miR-145 were found to be down-regulated in colon cancer and up-regulation was thought to inhibit tumourigenesis. However, when ISH was used to determine their cellular localisation they were found to be expressed in myofibroblasts and mesenchymal derived smooth muscle cells and shown to be involved in repair processes following epithelial cell injury (Chivukula et al., 2014, Kent et al., 2014). Their roles as a tumour suppressor were not supported by work assessing roles in the appropriate cell types.

3.6.3 Comparing LCM-qPCR and CISH expression: does each technique validate the other?

I tried to assess the accuracy and reliability of using semi-quantitative scoring of CISH signal intensity and percentage by comparing the results with those obtained from qPCR relative expression. Figure 3-9 shows the comparison between qPCR relative expression and CISH scores. Pearson correlation was chosen to compare these data as qPCR relative expression is an interval variable and this was consistent with the linear regression plotted. However, as the number of cases was low (13 in total) and as the scatter plots in Figure 3-9 do not show a clear linear relationship it was difficult to determine if linear regression was appropriate. Spearman correlation looks for a monotonic but not a linear relationship, this may have been more appropriate with low case numbers.

There are a few studies that have tried to compare qPCR with ISH. In one of these studies detection of human papilloma virus DNA in human cervical cancer biopsies by RT-PCR and CISH was compared (Biesaga et al., 2012). This is very different to the comparison I carried out, both in the initial questions and setting that was used and the type of analysis consequently undertaken. This study was for potential use in a clinical setting comparing detection of viral DNA under both systems, therefore relative abundance was not relevant in this case, merely whether the viral DNA was classified as present or absent. The sensitivity, specificity, positive predictive values and negative predictive values were therefore compared, rather than the relative expression levels measured by both systems. In similarity to my work the RT-PCR was regarded as the gold-standard for measuring nucleic acid sequence and CISH was compared to it. This study also found that CISH was not as sensitive as qPCR, which is consistent with my finding that miR-21 was detectable by CISH but miR-27b and miR-30a-3p were not. A second relevant study looked at HER2 amplification detection in gastric carcinoma, again to assess potential clinical detection methodologies, and compared IHC with 3 different FISH methods and qPCR. (Stanek et al., 2014). This study found that quantification by qPCR, FISH and IHC was comparable in intestinal-type gastric carcinoma but not in diffuse-type gastric carcinoma. This agrees to some extent with my finding that ISH and qPCR quantification correlate with each other. However, it also suggests that this cannot be assumed for every cancer type, and of particular interest, it suggests that ISH can be

the more sensitive technique in circumstances where the cell-type of interest is not the majority cell-type within the tissue.

The finding that miR-21 CISH score correlated well qPCR expression is useful both in the context of my work and in validating the work of others. It meant that I could look at miR-21 expression in CAFs in a much larger number of cases and compare this with clinicopathological parameters and with patient outcomes. This confirmed the validity of the experimental approach of using miR-21 CISH staining to determine cellular expression and comparing this with clinical outcomes in breast cancer (Nielsen et al., 2014, Qi et al., 2009).

3.6.4 MiR-21: the most promising miRNA of interest in the fibroblast compartment

MiR-21 showed the most significant up-regulation in CAFs by both qPCR and CISH. I also found that tumour grade showed a small but significant correlation with miR-21 CISH score ($p = 0.0191$, Table 3-5). Disease free survival showed a small, non-significant decrease with stronger miR-21 staining. It is possible that the sample size of 150 cases was underpowered to detect any true, relatively small, difference in survival in this analysis. Based on the assumption of 30 % core loss and 25 % of cases staining strongly, as seen in this sample, the sample size would need to be above 725 cases to detect a significant difference in disease free survival, if it exists. In a study of 901 breast cancer cases MacKenzie *et al.* found that stromal miR-21 in triple negative breast cancers, but not other subtypes, correlated with disease recurrence, which also suggests my TMA work may have been underpowered for this analysis (MacKenzie et al., 2014). Stromal miR-21 expression has been correlated with worse clinical outcomes in gastric cancer, prostate cancer and non-small cell lung cancer (Melbo-Jorgensen et al., 2014, Uozaki et al., 2014, Stenvold et al., 2014). In colorectal cancer, miR-21 in fibroblasts has been shown to increase tumour cell invasion and decrease tumour cell chemotherapy sensitivity in tissue culture (Bullock et al., 2013). My findings together with other published work suggests that miR-21 may play an oncogenic role in some cancer types including triple negative breast cancer. However, no work has been done to investigate the functional role of miR-21 within triple negative breast cancer. I therefore concluded

this is an important area for further investigation. It is worth pointing out that when I committed to the choice of miR-21 for further study, in 2013, the vast majority of the literature that now suggests stromal miR-21 is potentially important in cancer had yet to be published. Therefore, this choice was at the time based on my data and data showing potential importance of miR-21 in cancer overall, as opposed to published work on stromal roles.

Chapter 4

Investigation of the role of microRNA-21 in breast fibroblasts

4.1 Abstract

Expression of miR-21 is increased in cancer associated fibroblasts compared with adjacent non-tumour fibroblasts in a number of different tumours, including colorectal cancer, oesophageal squamous cell carcinoma, prostate cancer, gastric cancer and, from my own work in chapter 3, triple negative breast cancers. The functional importance of this over-expression for either breast fibroblast behaviour, or for the behaviour of breast cancers, remains unclear. My aim was to explore the effect miR-21 has on the behaviour of breast fibroblasts, by increasing the levels of miR-21 within these cells and assessing any changes in various cancer-related behaviours – namely growth, migratory and invasive abilities.

Four breast fibroblast cultures were used: two representative of normal breast fibroblasts, and two representative of breast cancer associated fibroblasts. I found that increasing miR-21 had no significant effect on fibroblast growth or invasion in any of these cell types. Concerning migration, over-expression of miR-21 increased migration in one culture of cancer associated fibroblasts, CAF-2, but not the other fibroblast lines. I concluded that miR-21 does not have a striking or consistent cell autonomous role in breast fibroblasts with respect to the cancer-related behaviours I have tested.

4.2 Introduction

MiR-21 is known to be significantly up-regulated in breast cancer compared with normal tissue adjacent to tumour and samples from non-cancer patients (Yan et al., 2008, Song et al., 2016b, Iorio et al., 2005). However, the vast majority of these studies have analysed whole tumour samples or, in some cases, serum. My work described in chapter 3 has shown that in fact miR-21 is significantly up-regulated in the fibroblast compartment of triple negative, basal-like breast cancers, and also that expression within epithelial breast cancer cells is relatively low compared to the CAFs.

A considerable amount of work has been done looking at the effects of miR-21 in breast cancer (epithelial) cell lines. This has shown that transfection with miR-21 mimics significantly increased growth, migration and invasion in MCF-7 (luminal A) and MDA-MB-231 (triple negative) cell lines using MTT, scratch wound and transwell assays, respectively, and that using miR-21 inhibitors significantly decreased growth, migration and invasion in these cell lines (Kuang and Nie, 2016, Yan et al., 2011, Zhang et al., 2016). However, since the expression of miR-21 is predominantly in CAFs rather than in epithelial cancer cells in human triple negative, basal-like breast cancers (chapter 3), therefore the relevance of these findings to the behaviour of human cancers are uncertain. In this chapter I have attempted to examine the role of miR-21 in breast fibroblasts with respect to the cancer-related behaviours of growth, migration and invasion.

4.3 Results

4.3.1 Establishing a model system for investigation of effects on miR-21 in breast fibroblasts

My first aim was to establish a cell culture model system to use in future experiments. In several studies, fibroblasts from organs other than the origin of the cancer being studied have been used to investigate potential roles of cancer fibroblasts. For example, foetal lung fibroblasts were used in a colorectal cancer study, gingival fibroblasts were used when studying oesophageal cancer, and human skin and mouse embryo fibroblasts were used in breast cancer studies (Bullock et

al., 2013, Nouraee et al., 2013, Porretti et al., 2014, Paquette et al., 2011). I used human breast fibroblast cultures as I felt that these would be most appropriate and relevant to my work. There is no single way to define cancer associated fibroblasts; I have therefore based my definition on the sample and location from which cells were extracted. I chose to use, in the main, immortalised fibroblasts as these were experimentally most convenient in terms of allowing consistent experimental approaches over a long period of time, and previous work published in the group successfully manipulated miRNA expression in these cells (Verghese et al., 2013). I used two fibroblast lines extracted from normal breast tissue (designated NF-1 and NF-2) and a single immortalised fibroblast line extracted from a triple negative breast cancer (designated CAF-1). I also used a primary triple negative breast cancer associated fibroblast culture (designated CAF-2). I chose to use both normal fibroblasts and cancer associated fibroblasts as it has been reported that the different behaviours associated with this distinction can be maintained in immortalised cultures (Calvo et al., 2013).

First I assessed the baseline levels of miR-21 expression in these four cell types using qPCR (Figure 4.1)

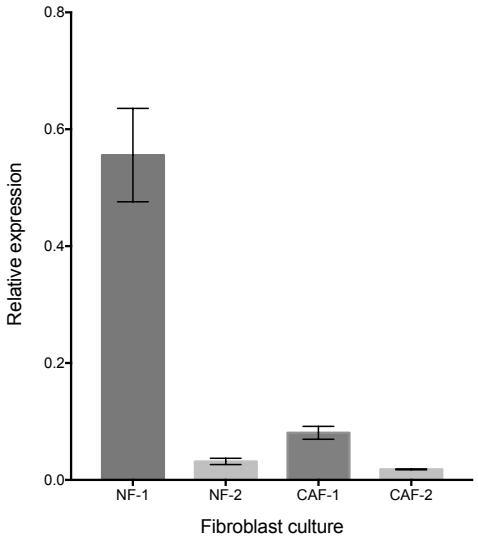

Figure 4-1 MiR-21 levels vary between different fibroblast cultures

Relative expression levels of miR-21 were determined using qPCR (normalised to the geometric mean of U6 and RNU48) in each of four different fibroblasts cultures (2 representative of normal fibroblasts, NF, and 2 representative of cancer associated fibroblasts, CAF). Data points represent the means of technical triplicates, while error bars represent standard deviations.

Expression level of miR-21 varied across the different fibroblast cultures by 30 fold, with NF-1 having the highest constitutive expression and CAF-2 having the lowest.

This finding may at first appear slightly surprising, as in chapter 3 I have shown that miR-21 is up-regulated in CAFs. However, in this new analysis, each fibroblast culture, whether NFs or CAFs, has been extracted from a separate individual, while my previous finding was based on comparison of paired NFs and CAFs from the same patient. In the previous work, I observed a wide degree of variation in the miR-21 expression levels in the NFs and CAFs (Figure 3-5 qPCR relative expression = 0.015 – 4.00), with up-regulation in CAFs being specific to individuals, rather than having levels in all CAFs above all NFs. The variation in levels in Figure 4-1 (qPCR relative expression = 0.018 – 0.56) is within the range of the previous expression levels and is therefore compatible with my previous findings and I proceeded to use all four fibroblast cultures for functional experiments.

Next, I aimed to establish whether transient transfections were able to increase levels of miR-21 in the fibroblast cultures. I transfected the NF-1 and CAF-1 lines

with either miR-21 mimic or control (scrambled miRNA) and then measured the miR-21 levels over 4 days using qPCR (Figure 4-2).

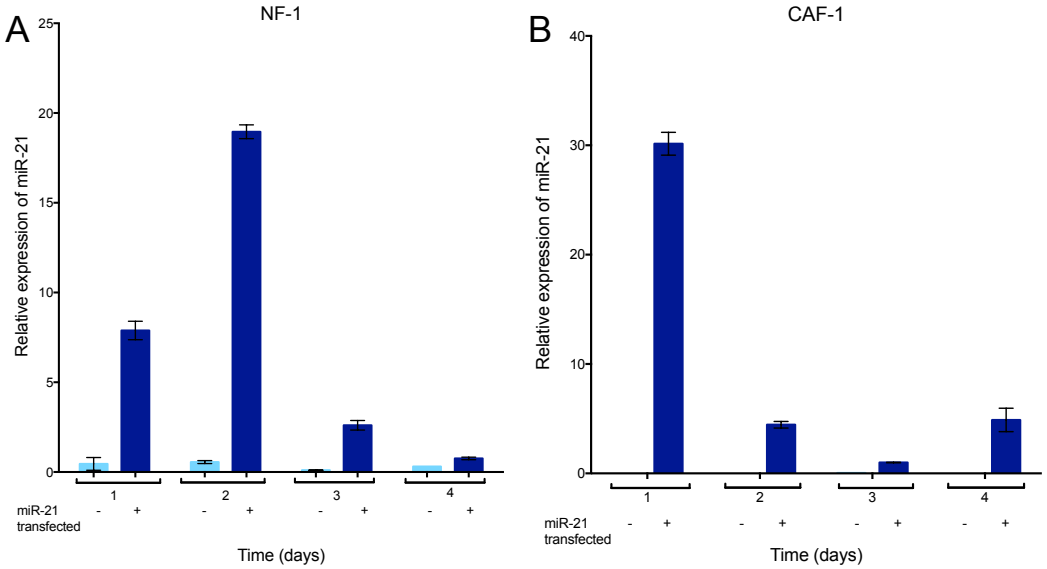

Figure 4-2 Transfection of immortalised breast fibroblasts with miR-21 mimics successfully increases miR-21 levels in fibroblasts for up to 4 days

Fibroblasts were transiently transfected with either miR-21 mimic (dark blue bars) or control scrambled miRNA (light blue bars). RNA was extracted from fibroblasts following transfection for 4 consecutive days and measured using qPCR. Data points represent the means of technical triplicates and errors bars represent standard deviations. Part A is NF-1 and part B is CAF-1.

Figure 4-2 demonstrates that transfection with miR-21 mimic increased levels of miR-21 in fibroblasts by up to >1000 fold (CAF-1). Over-expression was greatest 1 or 2 days after transfection, but still remained substantial and significant after 4 days.

4.3.2 Increasing miR-21 has no effect on fibroblast growth

My next aim was to assess the impact of miR-21 over-expression in breast fibroblasts on cancer-related behaviours, starting with cell growth. Fibroblast cultures (NF-1, NF-2, CAF-1 and CAF-2 primary) were transfected as above with miR-21 mimic or control, and cell number was assessed every day from 1 to 4 days after transfection using MTT assays. Experiments were performed as three independent biological replicates and are analysed both in combination, and individually (Figures 4-3 and 4-4).

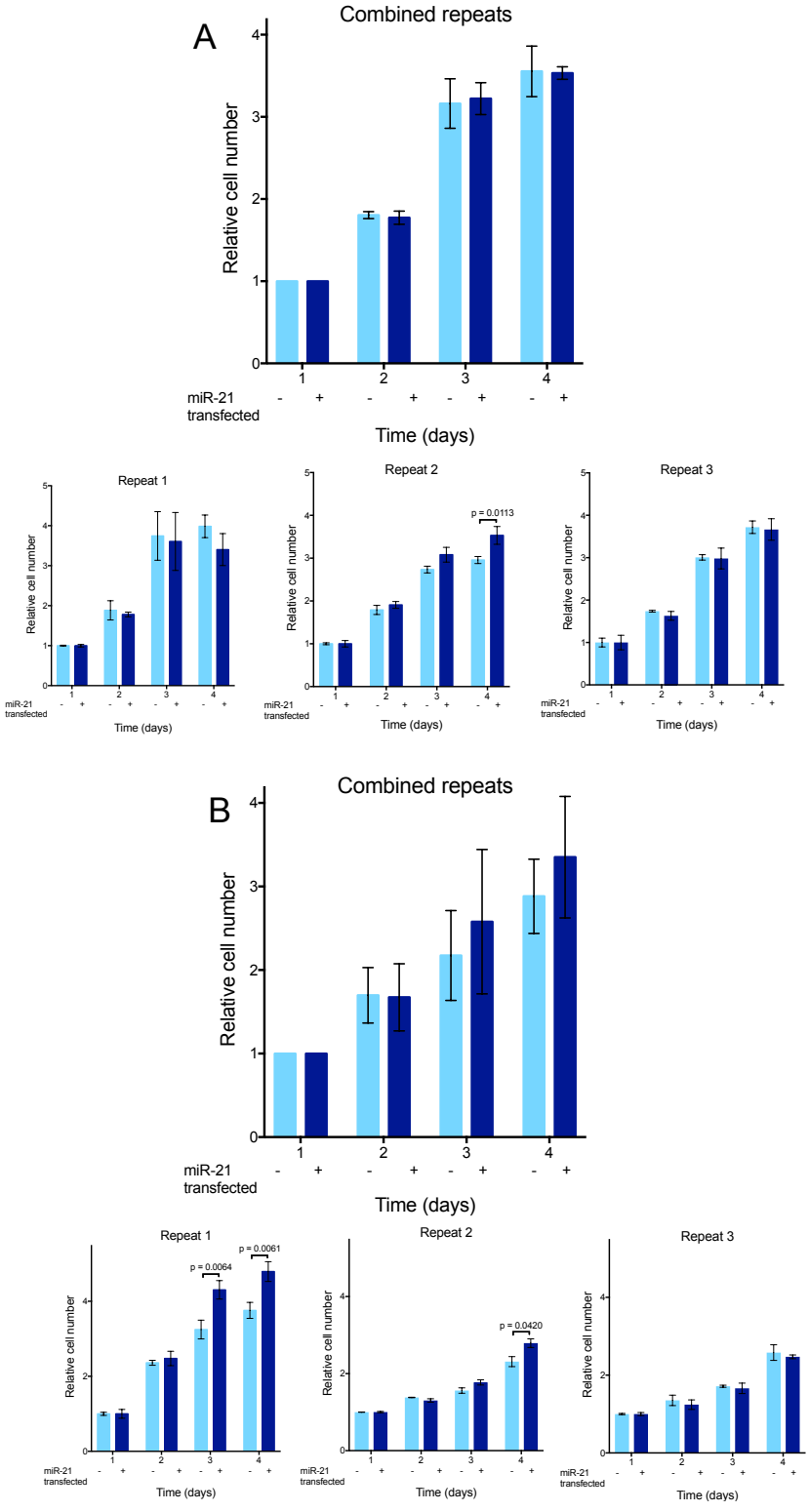

Figure 4-3 MiR-21 does not affect growth in normal breast fibroblasts

NF-1 (A) and NF-2 (B) were transfected with miR-21 mimic (dark blue) or control (light blue) and MTT assays were used to monitor growth over the subsequent 4 days (1-4). Data represent cell density relative to day 1 and are displayed as the mean (+/- SEM) of 3 independent experiments (top panel), with each separate experiment shown below (means +/- SD).

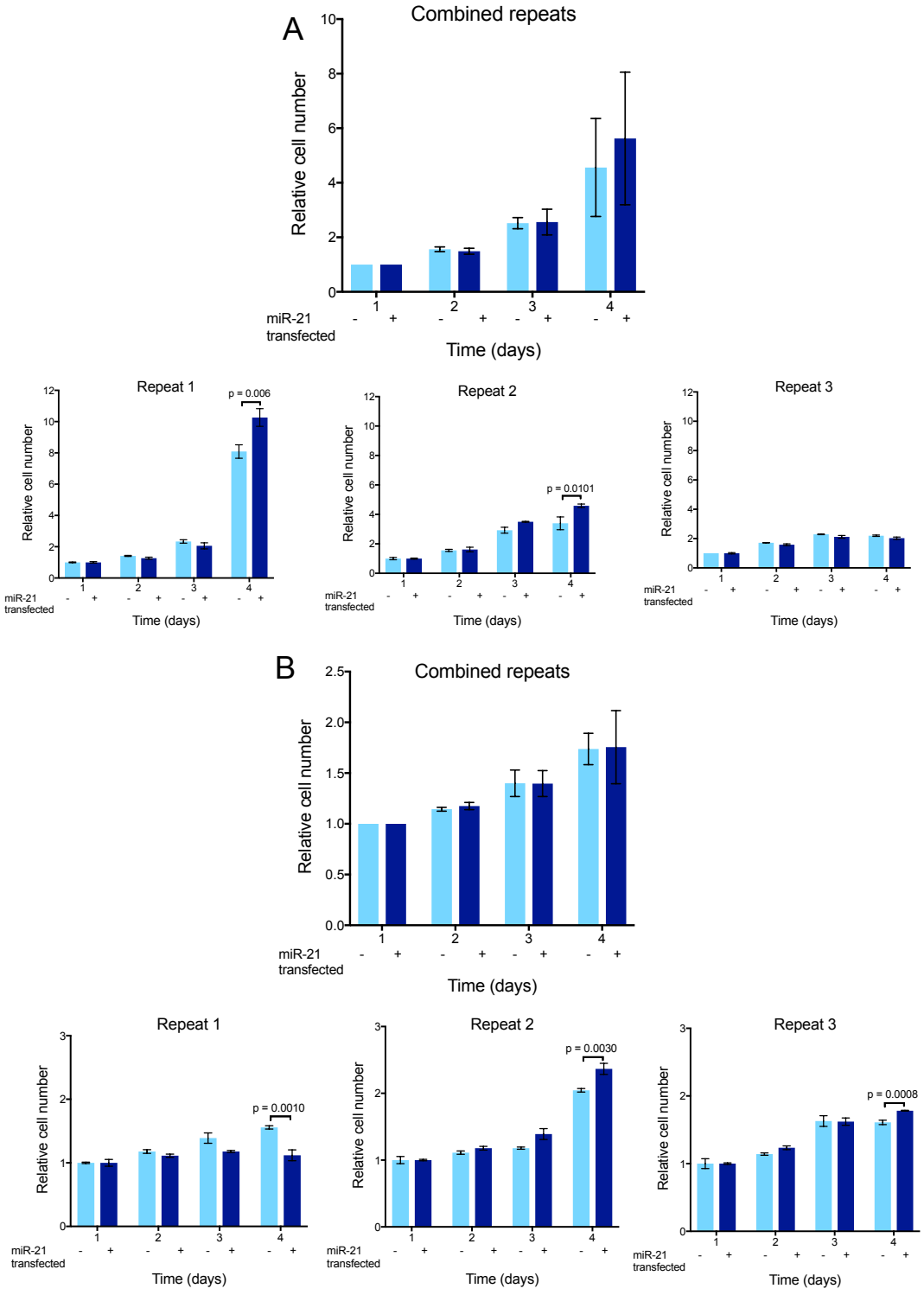

Figure 4-4 MiR-21 does not affect growth in breast cancer associated fibroblasts

CAF-1 (A) and CAF-2 (B) were transfected with miR-21 mimic (dark blue) or control (light blue) and MTT assays were used to monitor growth over the subsequent 4 days (1-4). Data represent cell density relative to day 1 and are displayed as the mean (+/- SEM) of 3 independent experiments (top panel), with each separate experiment shown below (means +/- SD).

Increasing levels of miR-21 in fibroblasts did not significantly alter cell numbers in any of the 4 fibroblast cultures. Some individual repeat experiments appeared to show changes between miR-21 mimic and control, mainly, but not exclusively, of miR-21 inducing enhanced growth (NF-1 repeat 2, NF-2 repeat 2, CAF-1 repeat 1, CAF-2 repeat 3). However, these results were not reproducible or significant when analysed in the context of the combined data.

4.3.3 Increased levels of miR-21 increases migration in CAF-2

My next aim was to investigate the influence of miR-21 on migration of breast fibroblasts. Fibroblasts were transfected as before with miR-21 mimic or control, and migration was assessed using scratch wound assays. Migration was assessed using live cell imaging, taking images each hour, and was quantified as relative wound density. Experiments were performed as three independent biological replicates and were analysed in combination (Figures 4-5 and 4-6). In order to combine replicates that sometimes had rather different kinetics of wound closure, migration throughout the whole closure period was quantified as the area under the curve for relative wound density vs. time and is displayed as miR-21 mimic transfected relative to control transfected (Salomon et al., 2013, Salomon et al., 2014).

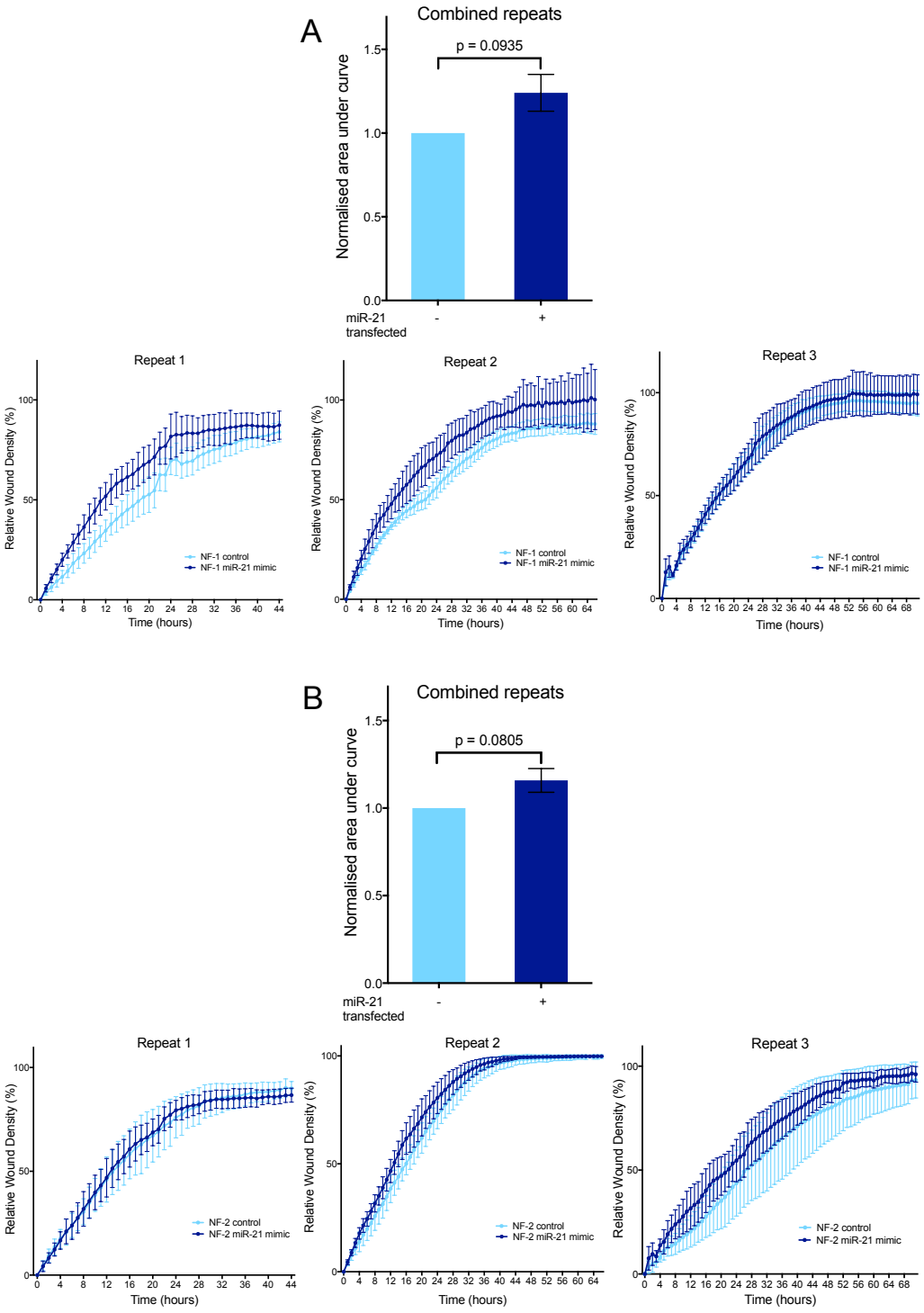

Figure 4-5 Over-expression of miR-21 does not affect migration in normal breast fibroblasts

NF-1 (A) and NF-2 (B) were transfected with miR-21 mimic (dark blue) or control (light blue), following this a scratch wound closure assay was used to measure migration. Data are displayed as the relative mean of the area under the curve of wound density vs. time (+/- SEM) of 3 independent experiments (top panel), with each separate wound density vs. time plot from individual experiments shown below (means of 6 wells +/- SD).

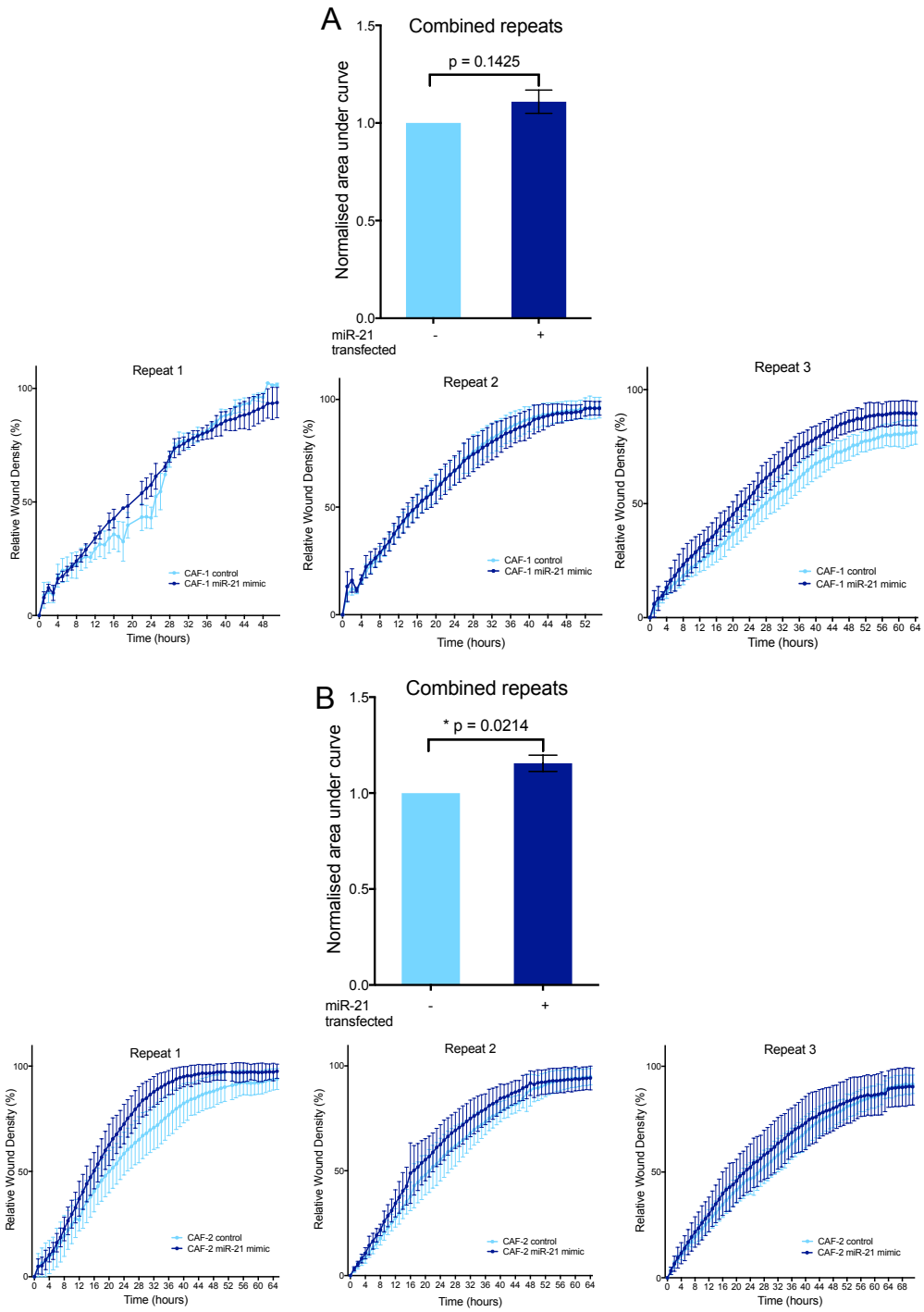

Figure 4-6 Over-expression of miR-21 significantly increases migration in CAF-2

CAF-1 and CAF-2 were transfected with miR-21 mimic (dark blue) or control (light blue), following this a scratch wound closure assay was used to measure migration. Data are displayed as the mean of the area under the curve (+/- SEM) o 3 independent experiments (top panel), with each separate experiment shown below (means of 6 wells +/- SD). Part A shows the data from CAF-1 and part B from CAF-2. * indicates significant difference in wound closure rate.

For normal fibroblasts, miR-21 over-expression had no statistically significant influence on migration ($p = 0.0935$ and $p = 0.0805$). However, with CAFs, migration significantly increased when miR-21 levels were increased in CAF-2 ($p = 0.0214$), but not in CAF-1 ($p = 0.1425$).

4.3.4 Increased miR-21 levels does not significantly affect invasion in breast normal or cancer associated fibroblasts

My next aim was to investigate the influence of miR-21 on fibroblast invasion. As previously, fibroblasts were transfected with miR-21 mimic or control, and invasion was assessed using scratch wound assays through collagen type I. Invasion was assessed using live cell imaging and was quantified as relative wound density, as before. Three independent biological replicates were performed and, as previously (section 4.3.3), these have been analysed in combination as the area under the curve for relative wound density vs. time and is displayed as miR-21 mimic relative to control transfected (Figure 4-7 and 4-8).

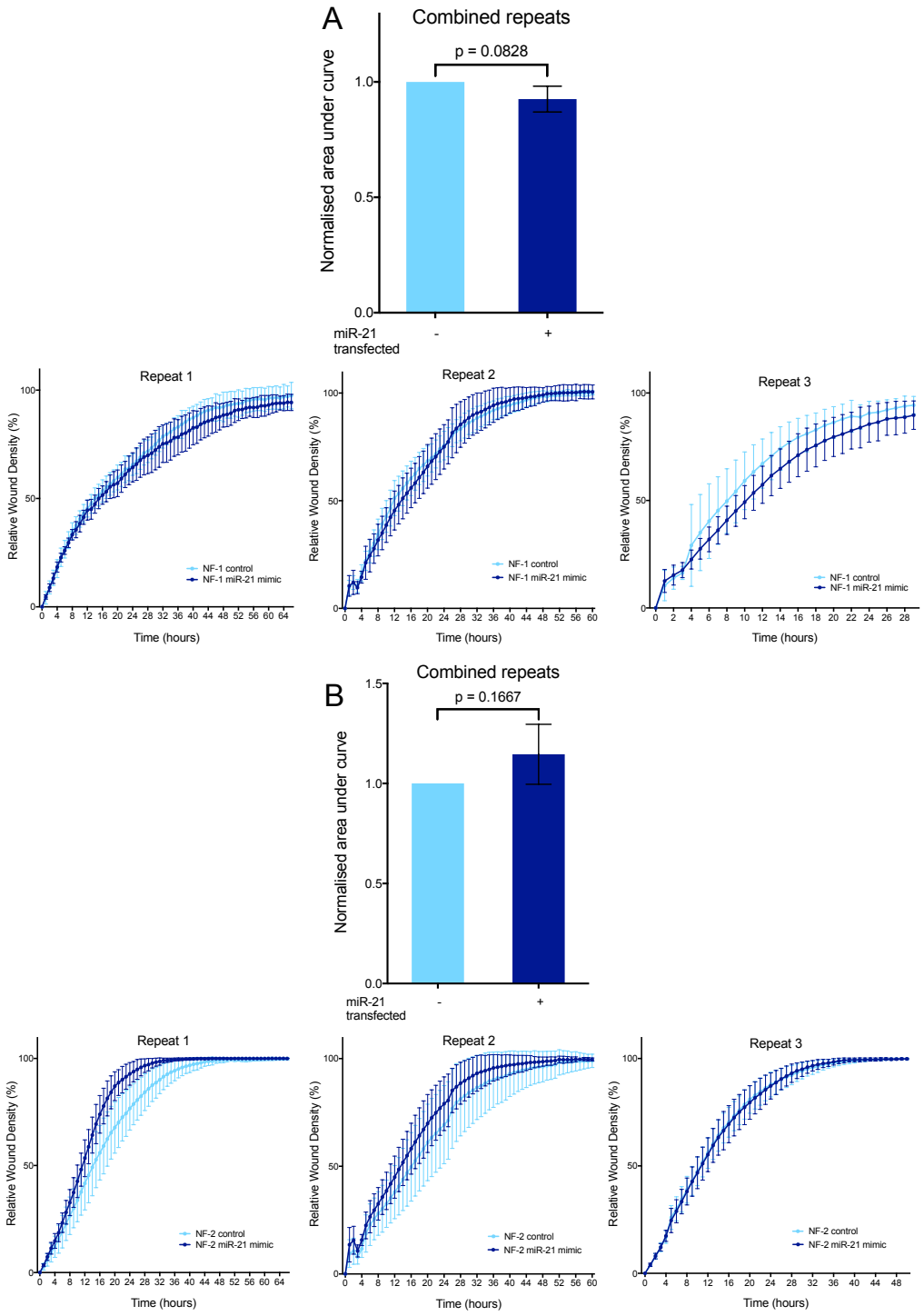

Figure 4-7 Over-expression of miR-21 does not affect invasion in normal breast fibroblasts

NF-1 (A) and NF-2 (B) were transfected with miR-21 mimic (dark blue) or control (light blue), and then invasion into collagen type I was assessed using scratch would closure assays. Data are displayed as the relative mean of the area under the curve of wound density vs. time plots (+/- SEM) of 3 independent experiments (top panel), with each separate wound density vs. time plot from individual experiments shown below (means of 6 wells +/- SD).

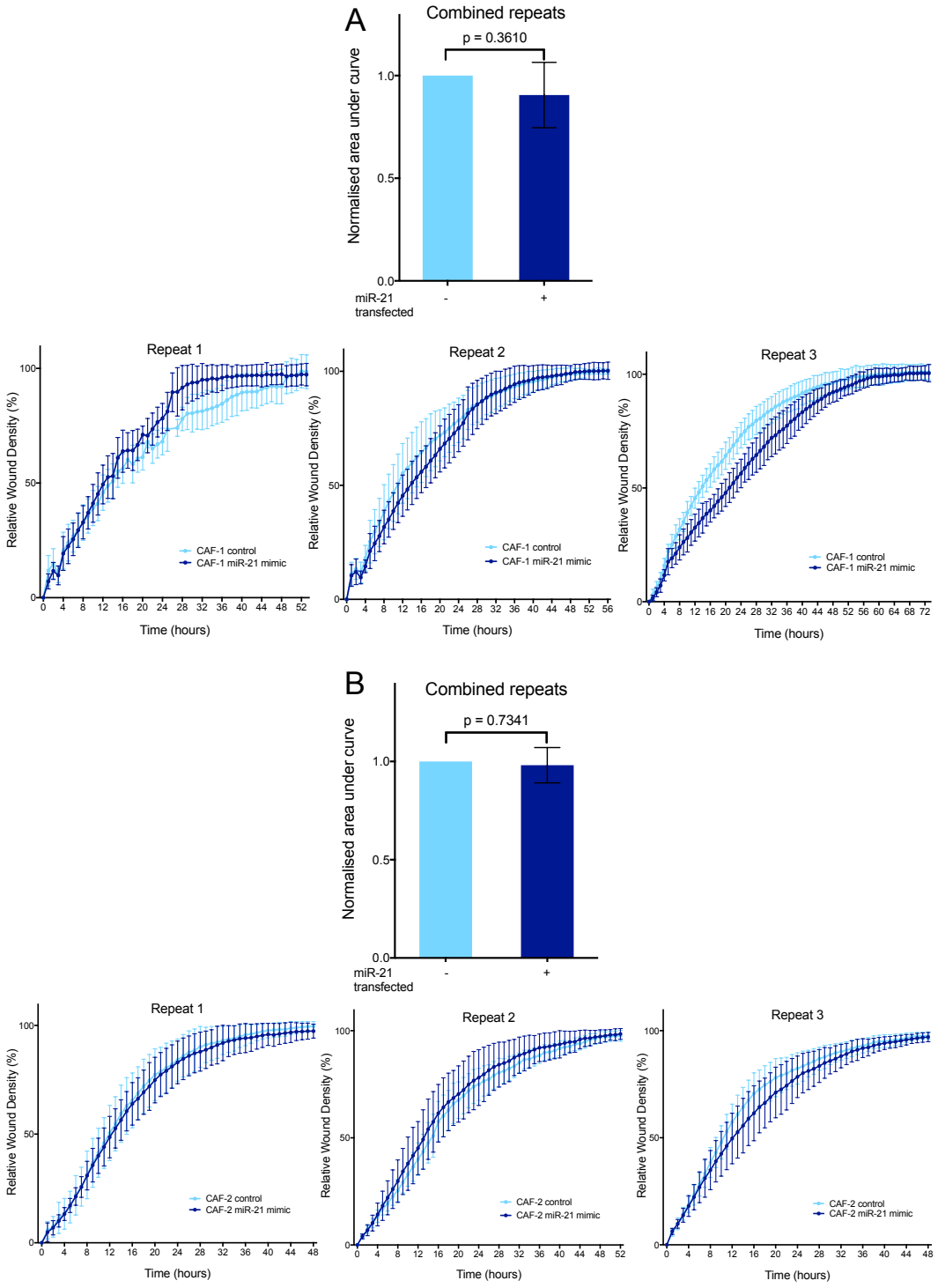

Figure 4-8 Over-expression of miR-21 does not affect invasion in breast cancer associated fibroblasts

CAF-1 (A) and CAF-2 (B) were transfected with miR-21 mimic (dark blue) or control (light blue), and then invasion into collagen type I was assessed using scratch would closure assays. Data are displayed as the relative mean of the area under the curve of wound density vs. time plots (+/- SEM) of 3 independent experiments (top panel), with each separate wound density vs. time plot from individual experiments shown below (means of 6 wells +/- SD).

Increasing levels of miR-21 in fibroblasts did not significantly alter the ability of fibroblasts to invade through collagen type I for any of the 4 fibroblast cultures (NF-1, NF-2, CAF-1 and CAF-2) (Figures 4-7 and 4-8).

4.4 Discussion

4.4.1 The effect of miR-21 on fibroblast growth

Increasing levels of miR-21 in fibroblasts did not significantly alter cell proliferation over 4 days in any of the 4 fibroblast cultures. Some individual replicate experiments did show significant changes between miR-21 mimic and control (for example, in Figures 4-3 part B and 4-4 respectively 2 or 3 of the repeats showed statistically significant differences on day 4) however these results were not significant when analysed in the context of the combined data. It is possible that combining these data in this way has led to a type II statistical error of incorrectly rejecting the alternative hypothesis of a true effect, however, any differences appear to be at best small and inconsistent. The more important questions may be not whether these effects are statistically significant, but whether they are biologically relevant, which I believe is potentially unlikely due to their small and inconsistent nature

MiR-21 over-expression had no significant effect on fibroblast growth in either normal fibroblasts or cancer associated fibroblasts. There has been very little work in breast fibroblasts or cancer associated fibroblasts from other tumours that has looked at the influence of miR-21 over-expression on fibroblast behaviour in this way. One study, that has some similarities, used primary stromal cells extracted from phyllodes breast tumours. This study found that transfection with miR-21 mimic increased growth of stromal cells (Gong et al., 2014). Other studies have looked at the effect on growth of altering expression of miR-21 in fibroblast-like synovial cells from rats; pulmonary fibrosis fibroblasts from mice; and primary human keloid fibroblasts. These studies showed varying results. In rat fibroblast-like synovial cells, constitutive down-regulation of miR-21 by lentiviral transduction lead to a significant decrease in growth rate. A similar result was seen with mouse pulmonary fibrosis fibroblasts where transient transfection with miR-21 mimics significantly increased cell proliferation, whereas the opposite was seen with human

keloid fibroblasts where transient transfection with miR-21 mimics significantly decreased growth (Chen et al., 2016b, Liu et al., 2014b, Liu and Qian, 2015). This confirms that fibroblasts from different species, different locations and different tumours display different characteristics when their miR-21 levels are altered and that fibroblasts should not be regarded as one homogenous group. It also highlights the importance of investigating the role of miR-21 in the specific fibroblasts of interest, not relying on results from other settings.

4.4.2 The effect of miR-21 on fibroblast migration

My work has shown that migration significantly increased when miR-21 levels were increased in CAF-2 cells ($p = 0.0214$; Figure 4-6). However, in the other fibroblast cultures (NF-1, NF-2 and CAF-1) there was no significant effect, although numerically migration was marginally increased (Figures 4-5 and 4-6; $p = 0.0935$, $p = 0.0805$, $p = 0.1425$, respectively). This lack of a consistent influence across the different fibroblasts could be due to a number of key influences. (i) CAF-2 cells were the only primary cells included in the analysis – it is possible primary cells behave differently in response to transfection with miR-21 than immortalised fibroblast lines. (ii) All the fibroblasts were extracted from different individuals – it is possible differences in response simply reflect biological differences between individuals. (iii) CAF-2 had the lowest endogenous miR-21 levels (Figure 4-1) – it is possible that this would make them the most sensitive to miR-21 over-expression, as endogenous miR-21 levels may be less likely to be saturated.

Other studies have looked at the effect of miR-21 on fibroblast migration in phyllodes stromal cells, prostate fibroblasts and skin fibroblasts. Transfection of miR-21 mimics into primary phyllodes stromal cells significantly increased transwell migration compared with cells transfected with controls (Gong et al., 2014). Similarly, normal prostate fibroblasts (WPMY-1) showed a significant increase in transwell migration when transfected with miR-21 mimics (Sanchez et al., 2016). Finally, in human skin fibroblasts, cells transfected with miR-21 mimics reportedly showed increased migration in a scratch wound assays, although the published data contained no quantification or statistical analyses of the size or significance of this increase, and therefore this report may not be robust (Madhyastha et al., 2012). Overall these studies seem to point to a consistent picture

of miR-21 increasing cell migration in fibroblasts. This finding was partly backed up by my work, as this difference was also seen in CAF-2, but not completely as the other fibroblast cultures did not show this increase, although there was a trend towards this.

4.4.3 The effect of miR-21 on fibroblast invasion

In my work I found that increasing levels of miR-21 in normal breast fibroblasts and in breast cancer associated fibroblasts made no difference to their invasive ability and there was no suggestion of a trend in the results (Figs. 4-7 and 4-8). This is in contrast to the effect miR-21 has on fibroblast migration where it was significantly increased migration in CAF-2. There are very few other studies looking at the effect of miR-21 levels specifically on fibroblast invasion. The only related study looked at the effect of miR-21 on the stromal cells in benign and malignant breast phyllodes tumour. This found that transient transfection to over-express miR-21 significantly increased the invasive ability of stromal cells from both benign and malignant phyllodes tumours (Gong et al., 2014). This result is not wholly unexpected as it is the stromal cells in phyllodes tumour that have genetically altered, and have increased independent proliferative ability and in malignant phyllodes developed invasive ability, becoming tumour cells. Whereas in breast carcinoma it is the epithelial cells that undergo genetic changes. Therefore this study may be more comparable to the studies looking at the effect of miR-21 on tumour cell invasion, where it is known that transfection of miR-21 into epithelial and connective tissue tumour cells increases their invasive ability (Silva and Aboussekhra, 2016, Han et al., 2016, Yang et al., 2017), rather than comparable to the work I have done.

4.4.4 Conclusions

I have shown that over-expression of miR-21 in breast fibroblasts has no consistent effect on fibroblast growth, migration or invasion, although one CAF culture did demonstrate enhanced migration. This is in contrast to a number of published studies where miR-21 has been shown to influence these activities significantly, although in every case a different tissue type has been used to supply the fibroblasts – something that may highlight tissue-specific differences in fibroblast biology.

Chapter 5
The influence of miRNA-21 levels in fibroblasts on the behaviour of breast tumour cells

5.1 Abstract

Expression of miR-21 is increased in cancer associated fibroblasts of triple negative, basal-like breast cancers as compared to normal breast fibroblasts. My aim was to test the functional relevance of this increase with respect to the behaviour of epithelial breast cancer cells. A series of co-culture experiments were performed, culturing breast fibroblasts, either normal fibroblasts (NF-1 or NF-2) or cancer associated fibroblasts (CAF-1 or CAF-2), with epithelial breast cancer cells (MDA-MB-231) with or without transfections to manipulate miR-21 expression levels. Expression levels were assessed using qPCR and a luciferase reporter and epithelial cell behaviour was assessed in proliferation, migration, invasion and chemotherapy resistance assays.

Increasing or decreasing levels of miR-21 in any of the 4 fibroblast cultures did not significantly alter epithelial cancer cell growth, migration or resistance to chemotherapy in a co-culture setting. I found that decreasing miR-21 significantly increased the invasion of tumour cells when in co-culture with the cancer associated fibroblast culture, CAF-2, but not with any of the other fibroblast lines. These findings do not provide compelling evidence of a substantial role of miR-21 in fibroblasts in affecting the behaviour of cancer cells, however, more work in other primary CAF cultures and potentially other breast cancer cell lines is needed to confirm this.

5.2 Introduction

MiR-21 is significantly up-regulated in breast cancer compared with adjacent normal tissue or non-cancer breast tissue (Yan et al., 2008, Song et al., 2016b, Iorio et al., 2005). My work, described in chapter 3, has shown that in fact miR-21 is significantly up-regulated in the fibroblast compartment of triple negative, basal-like breast cancers, and also that expression within epithelial breast cancer cells is relatively low compared to the CAFs, suggesting that the cancer-related role of miR-21 may be in this compartment.

Functional work has been carried out in breast epithelial cancer cells to test for potential roles of miR-21. This has shown that transfection with miR-21 mimic significantly increased growth in MCF-7 (luminal A) and MDA-MB-231 (triple negative) cell lines and that using miR-21 inhibitors significantly decreased growth. Migration and invasion were also significantly increased in MCF-7 and MDA-MB-231 cell lines when transfected with miR-21 mimics, and decreased by miR-21 inhibitors (Kuang and Nie, 2016, Yan et al., 2011, Zhang et al., 2016). However, as miR-21 expression is predominantly in CAFs rather than in tumour cells, at least in triple negative, basal-like breast cancers, the relevance of these findings to actual cancer biology is uncertain.

I have already described work in which I assessed whether miR-21 levels influence breast fibroblast behaviour, with respect to growth, migration and invasion (chapter 4). Next, I wanted to develop a co-culture tissue culture model that would enable me to determine what effects over-expression of miR-21 in CAFs has on the behaviour of triple negative breast cancer cells. I wanted to use this model to investigate the cancer-related behaviours of growth, migration, invasion and resistance to chemotherapy in the tumour cells when levels of miR-21 were altered in fibroblasts.

A key fact to note is that many of the changes associated with the conversion of NFs to become CAFs are known to be induced directly by the presence of the epithelial cancer cells, for example by factors secreted by tumour cells, such as TGF-β (Calon et al., 2014, Casey et al., 2008). There is some evidence that up-regulation of miR-21 is one of these changes induced directly by epithelial cancer cells, as this has been seen in colorectal cancer and pancreatic adenocarcinoma (Ali et al., 2015, Bullock et al., 2013). Also, TGF-β has been shown to increase miR-21 levels in skin

fibroblasts (Li et al., 2013, Kuninty et al., 2016b). It was important for me to assess whether up-regulation of endogenous miR-21 in fibroblasts would occur in my co-culture system of breast fibroblasts with breast epithelial cancer cells, in order to understand the regulation of fibroblast endogenous miR-21 levels, and therefore how to manipulate experimentally miR-21 levels by transfection. This has not previously been studied in the context of breast cells.

5.3 Results

5.3.1 Co-culture of fibroblasts with MDA-MB-231 cells

My first aim was to investigate whether epithelial breast cancer cells directly influenced miR-21 expression in fibroblasts in order to understand better the endogenous miR-21 levels in fibroblasts and therefore to be able to experimentally manipulate them appropriately and more effectively with transfections. I used the well-established triple negative breast cancer cell line, MDA-MB-231, as a representative epithelial cancer cell line for these experiments.

5.3.1.1 MDA-MB-231 cells induced up-regulation of miR-21 in breast fibroblasts in direct co-culture

My initial experimental design was to compare expression of miR-21 in a mono-culture of fibroblasts, with expression of miR-21 within the fibroblast compartment of a fibroblast-epithelial co-culture. In order to be able to isolate the fibroblasts from the co-culture, I used MDA-MB-231 cells that over-expressed GFP and therefore the cell types could be separated using fluorescence activated cell sorting (FACS). As the cell sorting process could potentially also influence expression levels, it was important that the mono-culture fibroblasts also underwent sorting. Therefore the mono-culture fibroblasts were mixed, on ice, with GFP-positive MDA-MB-231 cells and sorted immediately prior to RNA extraction, thereby undergoing treatment as similar as possible to the co-cultured cells. I used 2 fibroblast lines - a NF and a CAF line (NF-1 and CAF-1) to see if the influence of tumour cells on fibroblast miR-21 levels varied with fibroblast line and potentially whether the source of the fibroblasts, benign breast tissue compared with breast cancer tissue, made a difference to how the fibroblasts responded in co-culture.

Fibroblasts were cultured for 3 days either alone (mono-culture), or with GFP-tagged MDA-MB-231 at an initial ratio of 1:1, and then both cultures underwent FACS as described above to isolate fibroblasts, based on lack of GFP expression. MiR-21 levels were assessed by qPCR (Figure 5-1).

Contact co-culture with MDA-MB-231 significantly increased the levels of miR-21 in both fibroblast lines by up to 4-fold (Figure 5-1). As an aside, experiments were carried out using transfer of epithelial conditioned medium or physically separate co-culture in transwells to examine further the mechanisms of the influence of MDA-MB-231 cells on NF-1 and CAF-1 miR-21 levels. These showed no significant up-regulation of miR-21 in the fibroblasts, suggesting that direct cell-to-cell contact between epithelial and fibroblast cells may be required, although there was some variability between individual repeats making robust conclusions difficult (Appendix K).

The fact that contact co-culture of fibroblasts NF-1 or CAF-1 with MDA-MB-231 significantly increased miR-21 levels in these fibroblasts, has key implications for design of experiments to test functional roles of miR-21 in fibroblasts with respect to epithelial behaviour in co-cultures. In this context, the influence of fibroblasts transfected with miR-21 mimics compared to control transfections may be particularly problematic, as miR-21 would in fact be up-regulated to some extent in both samples because of induction of endogenous expression by epithelial cells, albeit substantially more in the mimic transfected sample. I concluded that use of miRNA inhibitors may be more appropriate, allowing comparison of the influence of co-culture enhanced endogenous levels (inhibitor control transfected) with reduced levels (inhibitor transfected), and that this approach would be prioritised in some cases.

At the end of this (section 5.4) I return to the observation that direct co-culture with MDA-MB-231 cells induced changes in miRNA expression in fibroblasts and analyse whether these extend beyond miR-21, however at this stage the focus remained on miR-21.

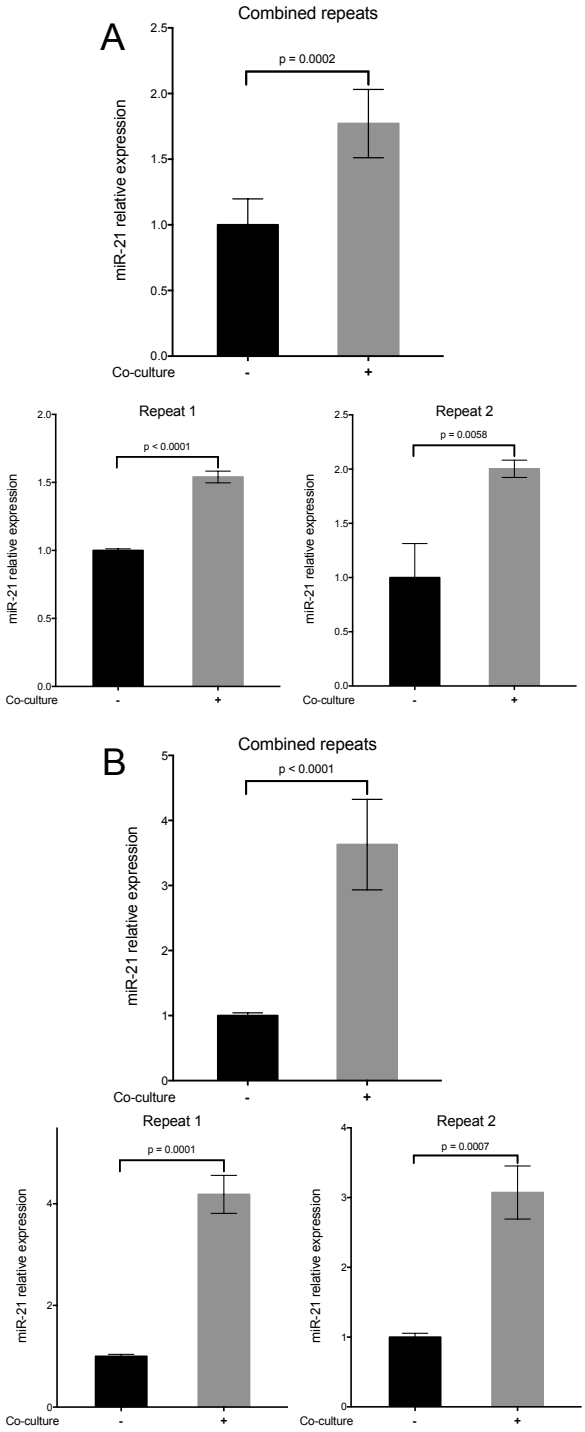

Figure 5-1 Co-culture with tumour cells increases miR-21 in NF-1 and CAF-1

Fibroblasts (NF-1 and CAF-1) were either co-cultured for 3 days with GFP-positive MDA-MB-231 cells or were mixed immediately prior to FACS. The mixed cell populations were separated by FACS on the basis of GFP expression, and miR-21 levels measured in fibroblasts by qPCR. Data are displayed as the mean (+/- SEM) of two independent experiments (top panel), with each separate experiment shown below (means +/- SD of technical triplicates; bottom panel). Part A shows the data from NF-1 and part B from CAF-1.

5.3.2 Establishing a model system for investigating the effects of miR-21 in fibroblasts on the behaviour of epithelial tumour cells

I confirmed previously (Figure 4-2) that transfection of breast fibroblasts with miR-21 mimics successfully increased miR-21 levels, using qPCR. To decrease levels of miR-21 in fibroblasts, I transfected them with miR-21 inhibitors. MiRNA inhibitors are complementary strands of RNA that binds to their target miRNAs, preventing them from having functional effects within the cells. It was not appropriate to confirm by qPCR that miR-21 inhibitor transfection had successfully inhibited miR-21, because the inhibitors do not necessarily decrease the absolute levels of their targets within the cell, only the functional level. I therefore cloned a miR-21 reporter plasmid to assess miR-21 activity, and to confirm that the miR-21 inhibitor transfection was effective. The miR-21 reporter plasmid contained a firefly luciferase expression cassette with an exactly complementary miR-21 binding site in its 3'UTR, and a *Renilla* luciferase expression cassette for plasmid transfection efficiency normalisation. Fibroblasts were transfected with miR-21 inhibitor or inhibitor control, or miR-21 mimic or mimic control. On the following day fibroblasts were transfected with miR-21 reporter plasmid, and on the following day dual luciferase assays were performed (Figure 5-2).

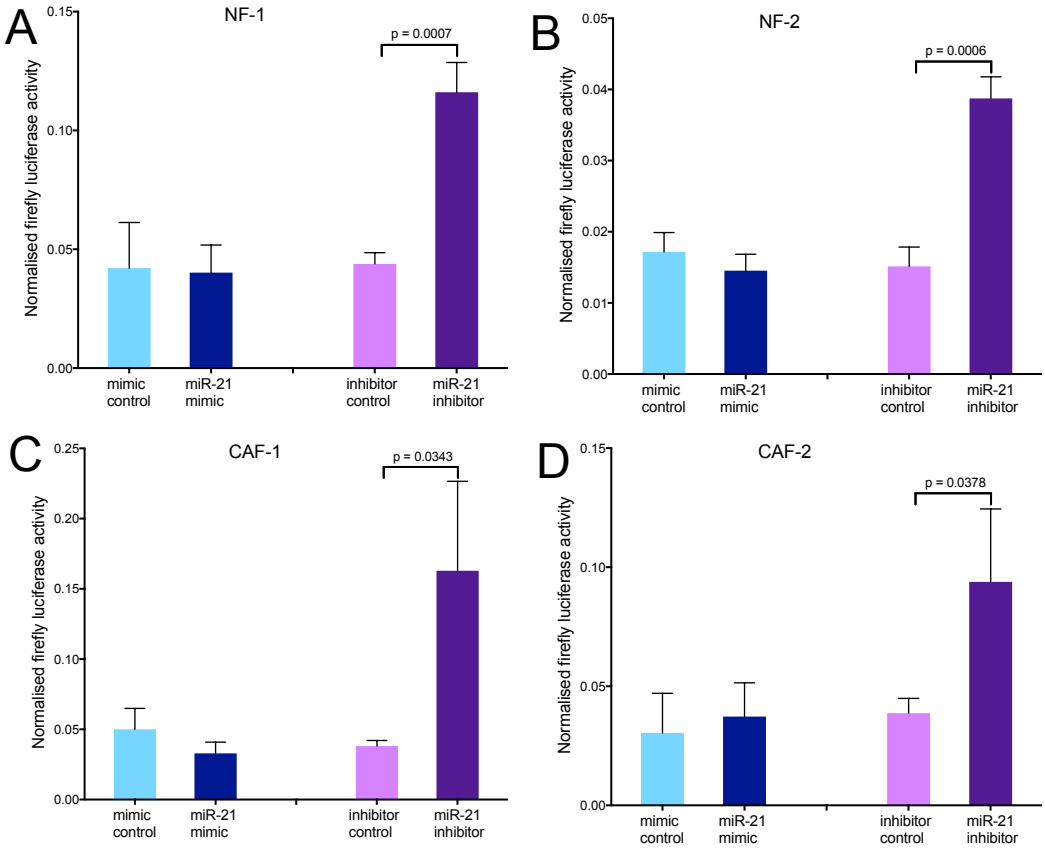

Figure 5-2 MiR-21-inhibitor decreases miR-21 activity in fibroblasts

Fibroblasts were transfected with miR-21 mimic or miR-21-inhibitor or the appropriate control. They were then transfected with miR-21 reporter plasmid containing a perfect miR-21 binding site in the firefly luciferase 3'UTR. On the following day firefly luciferase and *Renilla* luciferase were measured. Firefly activity measurements were normalised to *Renilla* activity. Data represent means (+/- SD) of three independent wells. Part A shows data for NF-1, part B NF-2, part C CAF-1 and part D CAF-2. Significance values derive from Student's t-tests.

I concluded that miR-21 inhibitors had successfully inhibited miR-21 activity in all four fibroblast lines, as demonstrated by de-repression of miR-21 reporter expression by up to 4-fold. Concerning and surprising was the fact that the miR-21 mimic apparently caused no functional repression of this reporter (despite the fact that I have previously shown mimics to allow successful and substantial miR-21 over-expression; Figure 4-2). One interpretation of this result is that it is possible a perfect miR-21 binding site is not representative of the influence of miR-21 over-expression. MiRNA binding sites are usually only poorly complementary and miRNA-target binding is comparatively weak. In this case, the reporter's perfect

binding site would compete for miR-21 binding very effectively, therefore it may be that the reporter is fully inhibited even in the absence of miR-21 over-expression, meaning that additional repression by miR-21 mimic cannot be detected. This hypothesis may also imply that the functional influence detected from the miR-21 inhibitor under-represents its true functional impact. The more effective demonstration of the functional influence of the miR-21 inhibitor, as opposed to the mimic, provided a further reason for prioritising inhibitor studies in some cases, addition to the reason given already in section 5.3.1.1.

5.3.3 Altering levels of miR-21 in fibroblasts does not affect growth of tumour cells

In investigating the effects of altering miR-21 levels in fibroblasts, my first aim was to examine the influence on epithelial tumour cell growth. Co-cultures of fibroblasts and epithelial cancer cells were to be used, but I wanted to test any changes in epithelial tumour cell growth only, therefore I used MDA-MB-231 transduced to express firefly luciferase, and used luciferase activity as a way of assessing tumour cell number within the co-culture.

To investigate the effect that altering the levels of miR-21 in fibroblasts has on the growth of MDA-MD-231 tumour cells, first fibroblasts (four different breast fibroblast cultures: NF-1, NF-2, CAF-1 or CAF-2) were transfected with miR-21 mimic, miR-21 inhibitor or appropriate control. Following transfection MDA-MB-231-luciferase-expressing cells were seeded into the same wells. After 1, 2 and 3 days co-culture MDA-MB-231 growth was quantified by measuring luciferase activity (Figures 5-3 to 5-6).

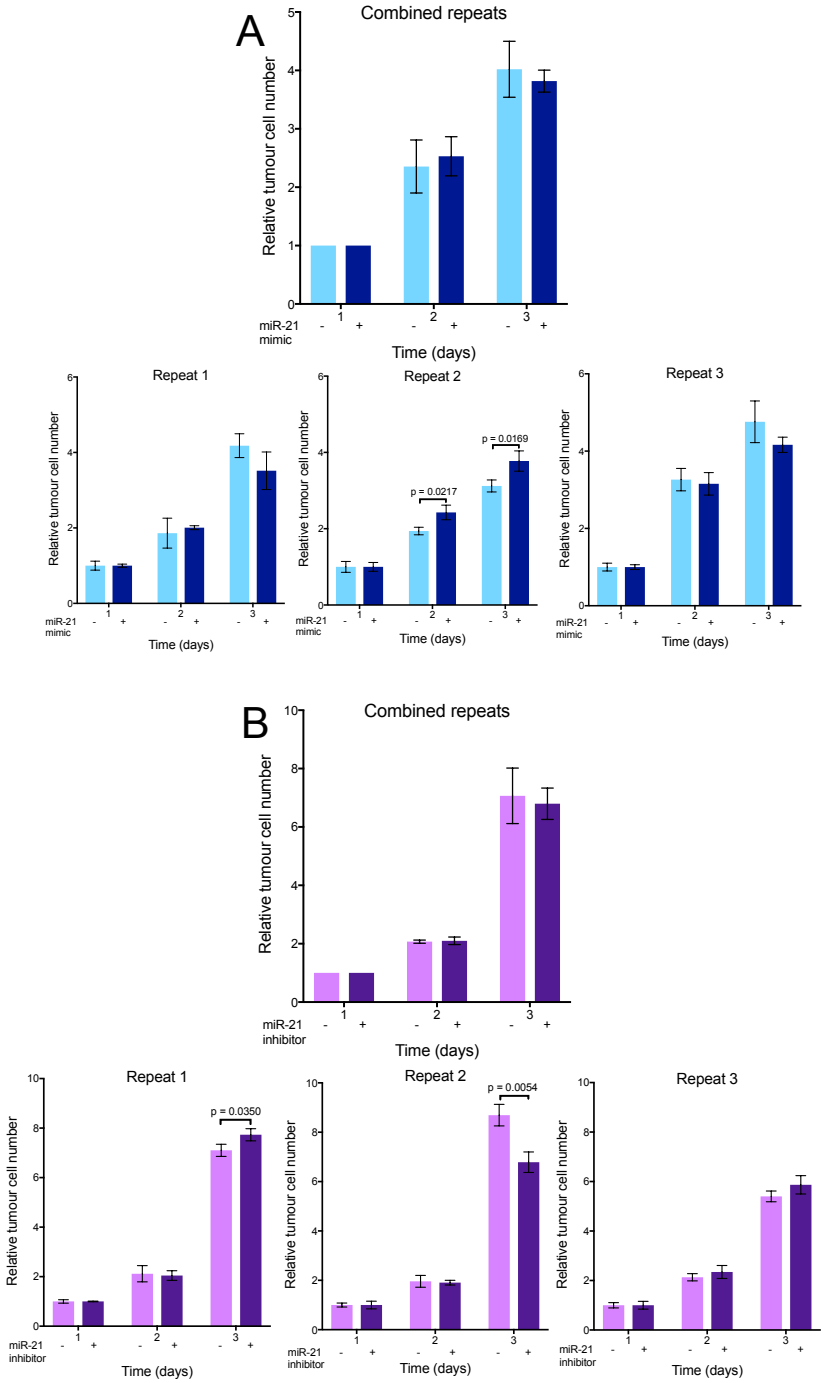

Figure 5-3 Increasing or decreasing miR-21 levels in NF-1 does not affect growth of MDA-MB-231 in contact co-culture

NF-1 cells were transfected with either miR-21 mimic (dark blue) or miR-21 inhibitor (purple) or the respective control (light blue and pink respectively). MDA-MB-231-luciferase-expressing cells were seeded into the same wells. Luciferase activity was measure after 1-3 days. Data are displayed as the mean (+/- SEM) of 3 independent experiments (top panel), with each separate experiment shown below (means +/- SD). Part A shows the data from NF-1 transfected with miR-21 mimic and part B from NF-1 transfected with miR-21 inhibitor.

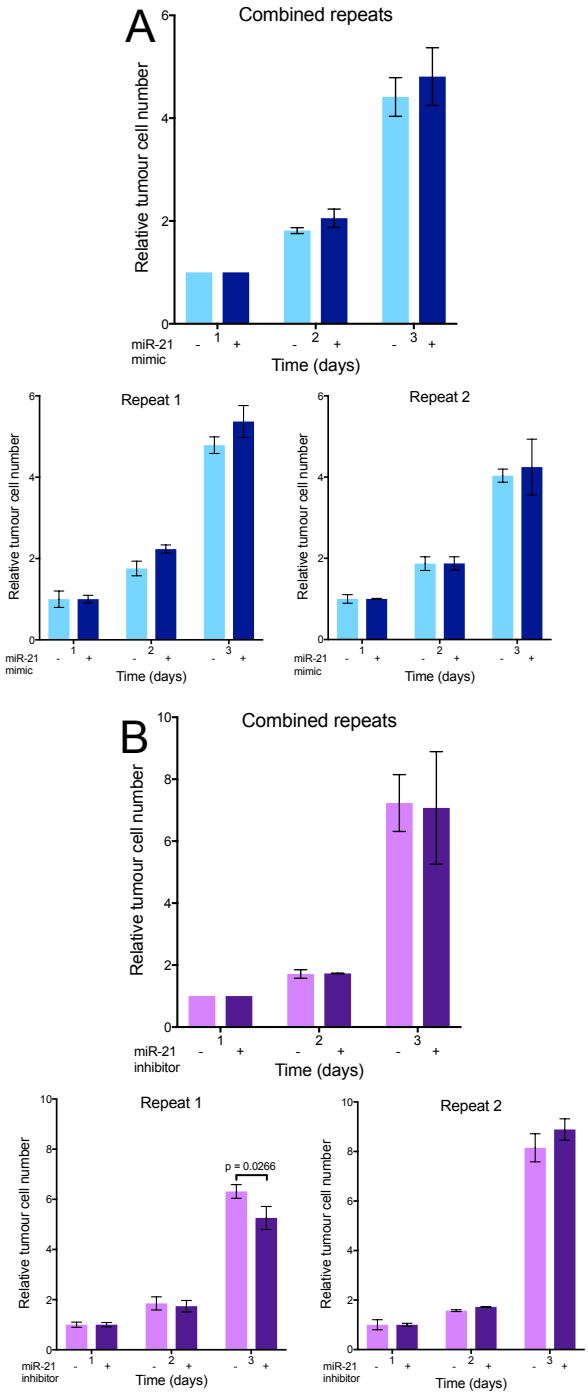

Figure 5-4 Increasing or decreasing miR-21 levels in NF-2 does not affect growth of MDA-MB-231 in contact co-culture

NF-2 cells were transfected with either miR-21 mimic (dark blue) or miR-21 inhibitor (purple) or the respective control (light blue and pink respectively). MDA-MB-231-luciferase-expressing cells were seeded into the same wells. Luciferase activity was measure after 1-3 days. Data are displayed as the mean (+/- SEM) of 2 independent experiments (top panel), with each separate experiment shown below (means +/- SD). Part A shows the data from NF-2 transfected with miR-21 mimic and part B from NF-2 transfected with miR-21 inhibitor.

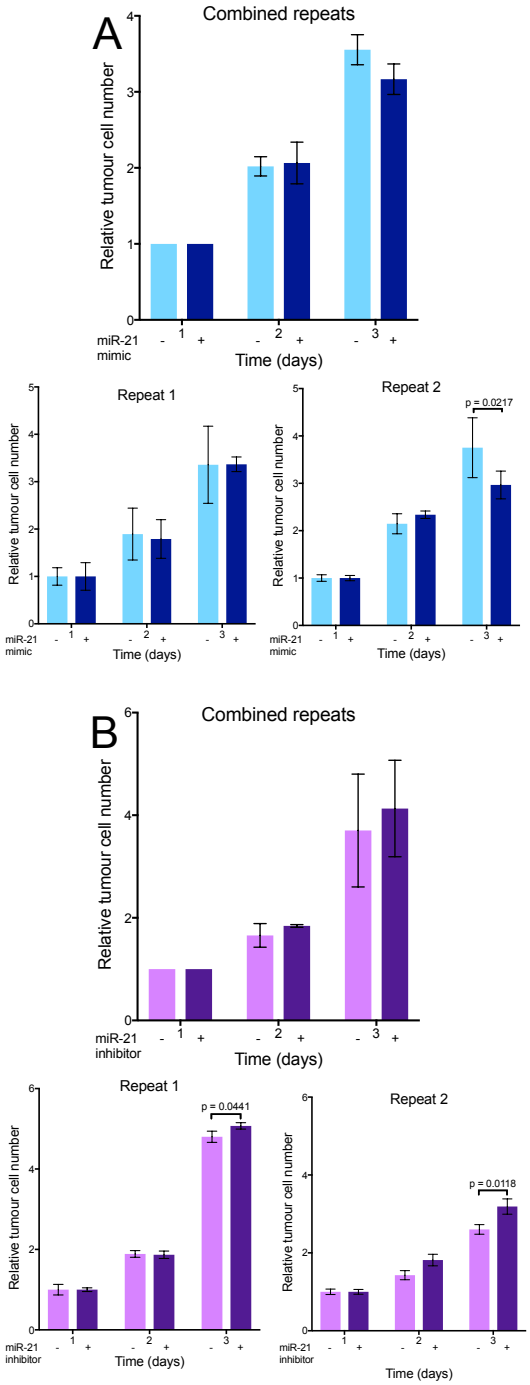

Figure 5-5 Increasing or decreasing miR-21 levels in CAF-1 does not affect growth of MDA-MB-231 in contact co-culture

CAF-1 cells were transfected with either miR-21 mimic (dark blue) or miR-21 inhibitor (purple) or the respective control (light blue and pink respectively). MDA-MB-231-luciferase-expressing cells were seeded into the same wells. Luciferase activity was measure after 1-3 days. Data are displayed as the mean (+/- SEM) of 2 independent experiments (top panel), with each separate experiment shown below (means +/- SD). Part A shows the data from CAF-1 transfected with miR-21 mimic and part B from CAF-1 transfected with miR-21 inhibitor.

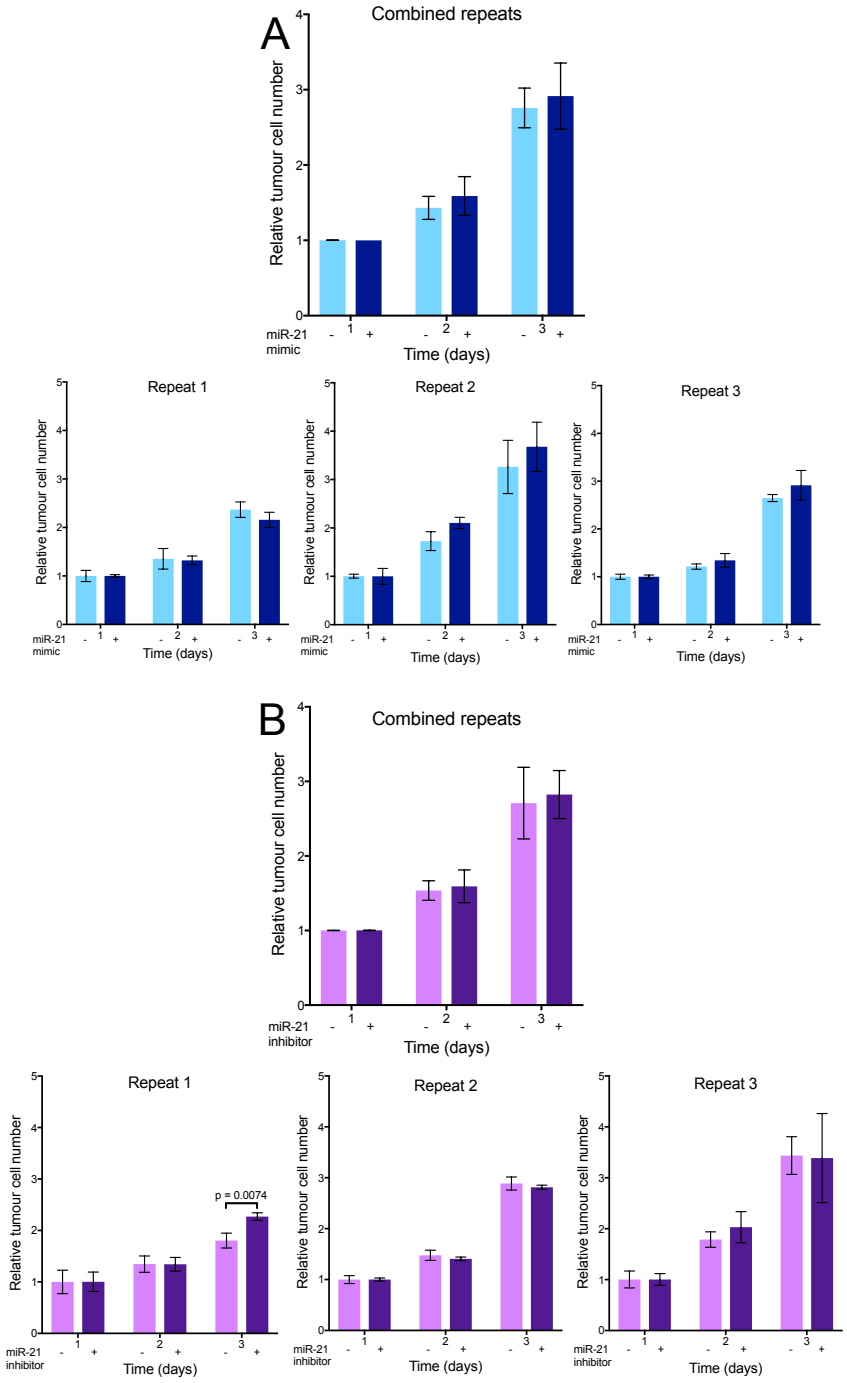

Figure 5-6 Increasing or decreasing miR-21 levels in CAF-2 does not affect growth of MDA-MB-231 in contact co-culture

CAF-2 cells were transfected with either miR-21 mimic (dark blue) or miR-21 inhibitor (purple) or the respective control (light blue and pink respectively). MDA-MB-231-luciferase-expressing cells were seeded into the same wells. Luciferase activity was measure after 1-3 days. Data are displayed as the mean (+/- SEM) of 3 independent experiments (top panel), with each separate experiment shown below (means +/- SD). Part A shows the data from CAF-2 transfected with miR-21 mimic and part B from CAF-2 transfected with miR-21 inhibitor

Increasing or decreasing levels of miR-21 in fibroblasts, by using miR-21 mimics or inhibitors, did not significantly alter tumour cell growth with any of the 4 fibroblast cultures, (NF-1, NF-2, CAF-1, CAF-2). Some individual repeat experiments appeared to show changes in growth on day 3, mainly, but not exclusively, of lower miR-21 levels inducing enhanced growth (e.g. Figure 5-5B and Figure 5-6B repeat 1). However, these results were not significant when analysed in the context of the combined data.

5.3.4 Altering levels of miR-21 in fibroblasts does not affect migration of tumour cells

My next aim was to look at the effect of altering levels of miR-21 in fibroblasts on migration of epithelial tumour cells. To do this I transfected fibroblasts with either miR-21 mimic, miR-21 inhibitor or appropriate control. I then seeded MDA-MB-231 cells into the same wells. On the following day, after allowing time for cells to settle and adhere, a scratch was made in the cell layer and the time for the cells to migrate into these "wounds" was measured hourly using a live cell imaging system. To differentiate between migration of epithelial cells and fibroblasts, epithelial cells labelled with GFP were used and the migration of GFP-fluorescent cells into the wound was measured. Data are shown hourly for each individual experimental repeat, and repeats were combined by calculating the relative areas under the migration vs. time curves (Figures 5-7 to 5-10) (Salomon et al., 2013, Salomon et al., 2014).

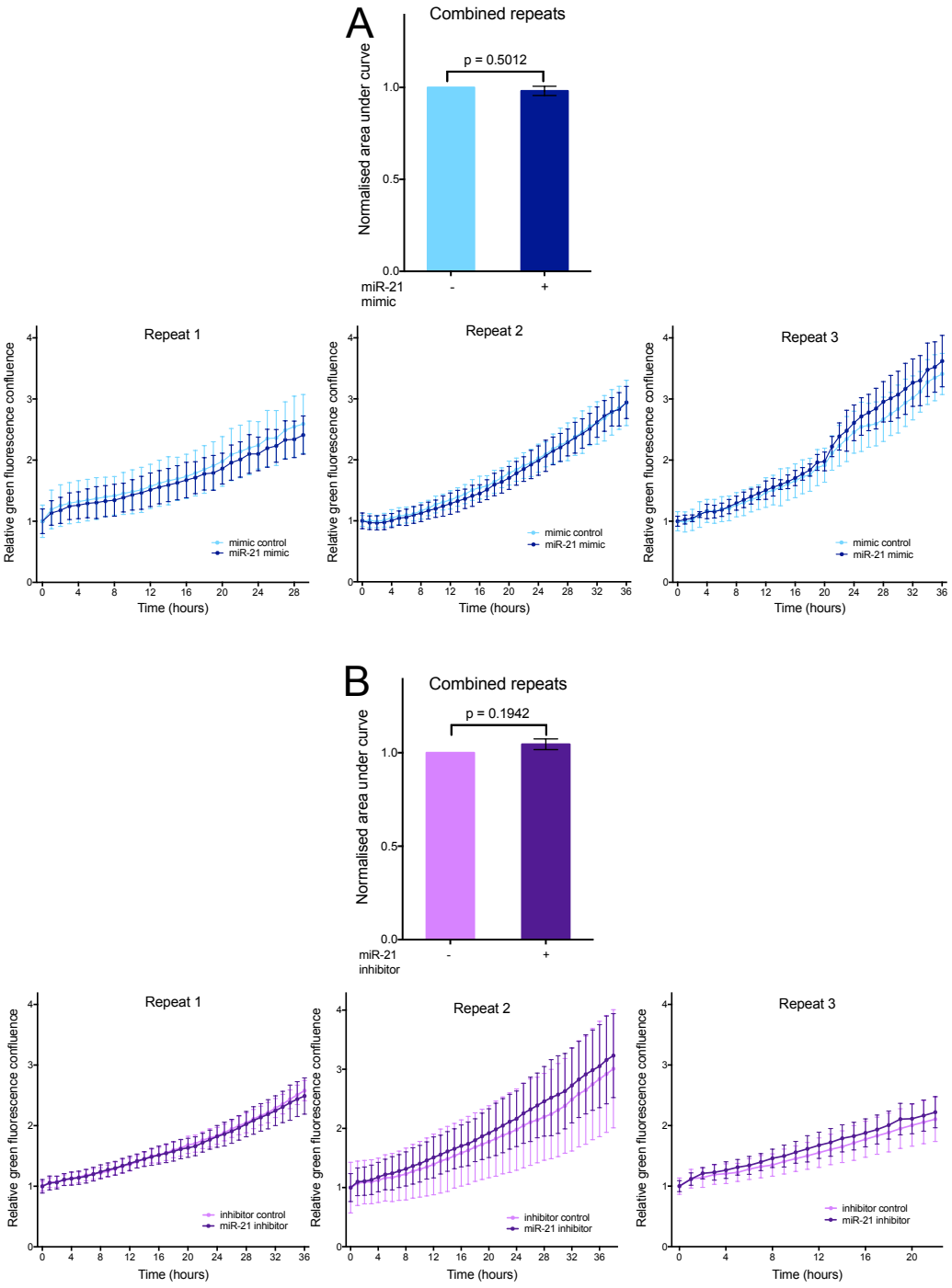

Figure 5-7 Increasing or decreasing miR-21 levels in NF-1 does not affect migration of MDA-MB-231 in contact co-culture

NF-1 cells were transfected with either miR-21 mimic (dark blue) or miR-21 inhibitor (purple) or the respective control (light blue and pink respectively). MDA-MB-231-GFP cells were seeded into the same wells. Following this a scratch wound closure assay was used to measure migration. Data are displayed as the mean of the area under the curve (+/- SEM) of 3 independent experiments (top panel), with each separate experiment shown below (mean of 6 wells +/- SD). Part A shows the data from NF-1 transfected with miR-21 mimic and part B from NF-1 transfected with miR-21 inhibitor.

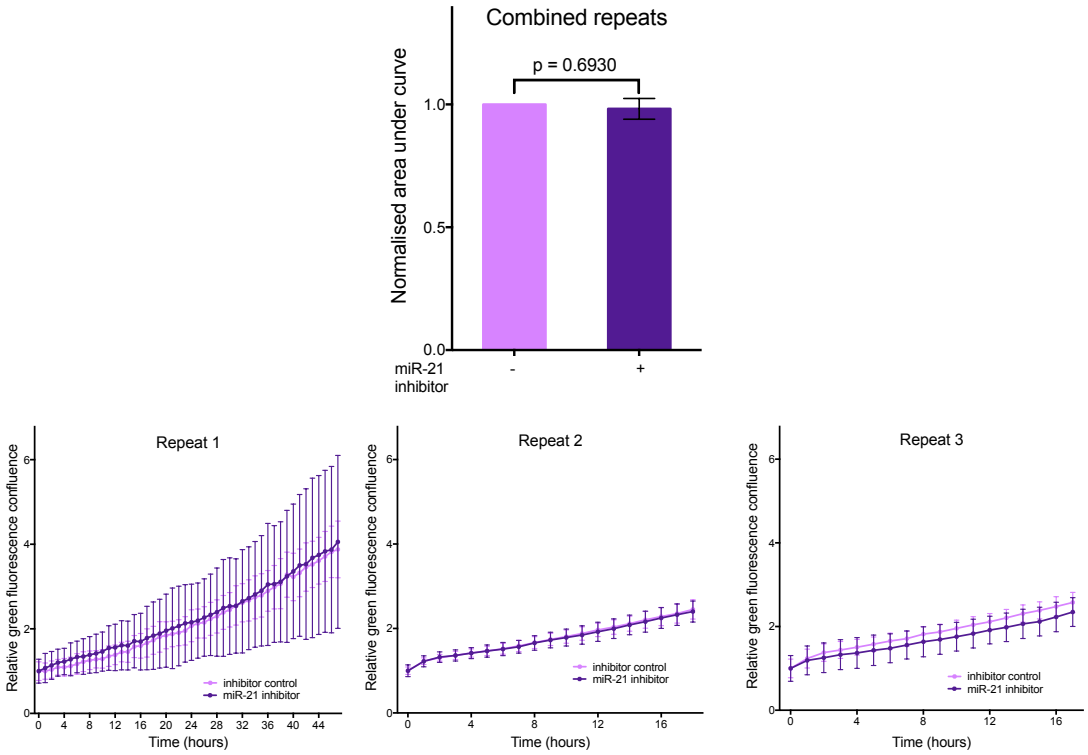

Figure 5-8 Decreasing miR-21 levels in NF-2 does not affect migration of MDA-MB-231 in contact co-culture

NF-2 cells were transfected with miR-21 inhibitor (purple) or inhibitor control (pink). MDA-MB-231-GFP cells were seeded into the same wells. Following this a scratch wound closure assay was used to measure migration. Inhibitor assessments were prioritised for the reasons stated in sections 5.3.1.1 and 5.3.2. Data are displayed as the mean of the area under the curve (+/- SEM) of 3 independent experiments (top panel), with each separate experiment shown below (mean of 6 wells +/- SD).

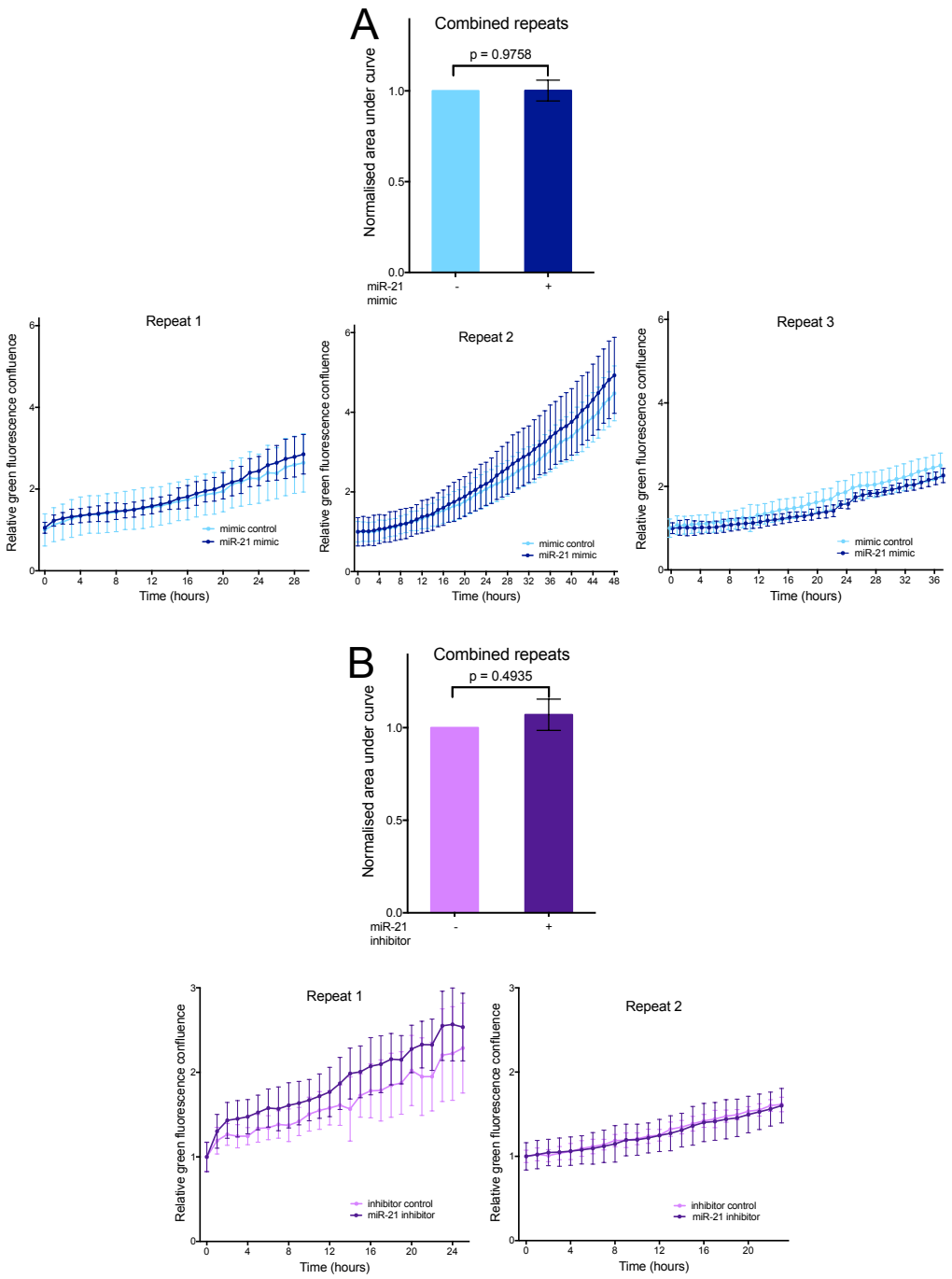

Figure 5-9 Increasing or decreasing miR-21 levels in CAF-1 does not affect migration of MDA-MB-231 in contact co-culture

CAF-1 cells were transfected with either miR-21 mimic (dark blue) or miR-21 inhibitor (purple) or the respective control (light blue and pink respectively). MDA-MB-231-GFP cells were seeded into the same wells. Following this a scratch wound closure assay was used to measure migration. Data are displayed as the mean of the area under the curve (+/- SEM) of 2 or 3 independent experiments (top panel), with each separate experiment shown below (mean of 6 wells +/- SD). Part A shows the data from CAF-1 transfected with miR-21 mimic and part B from CAF-1 transfected with miR-21 inhibitor.

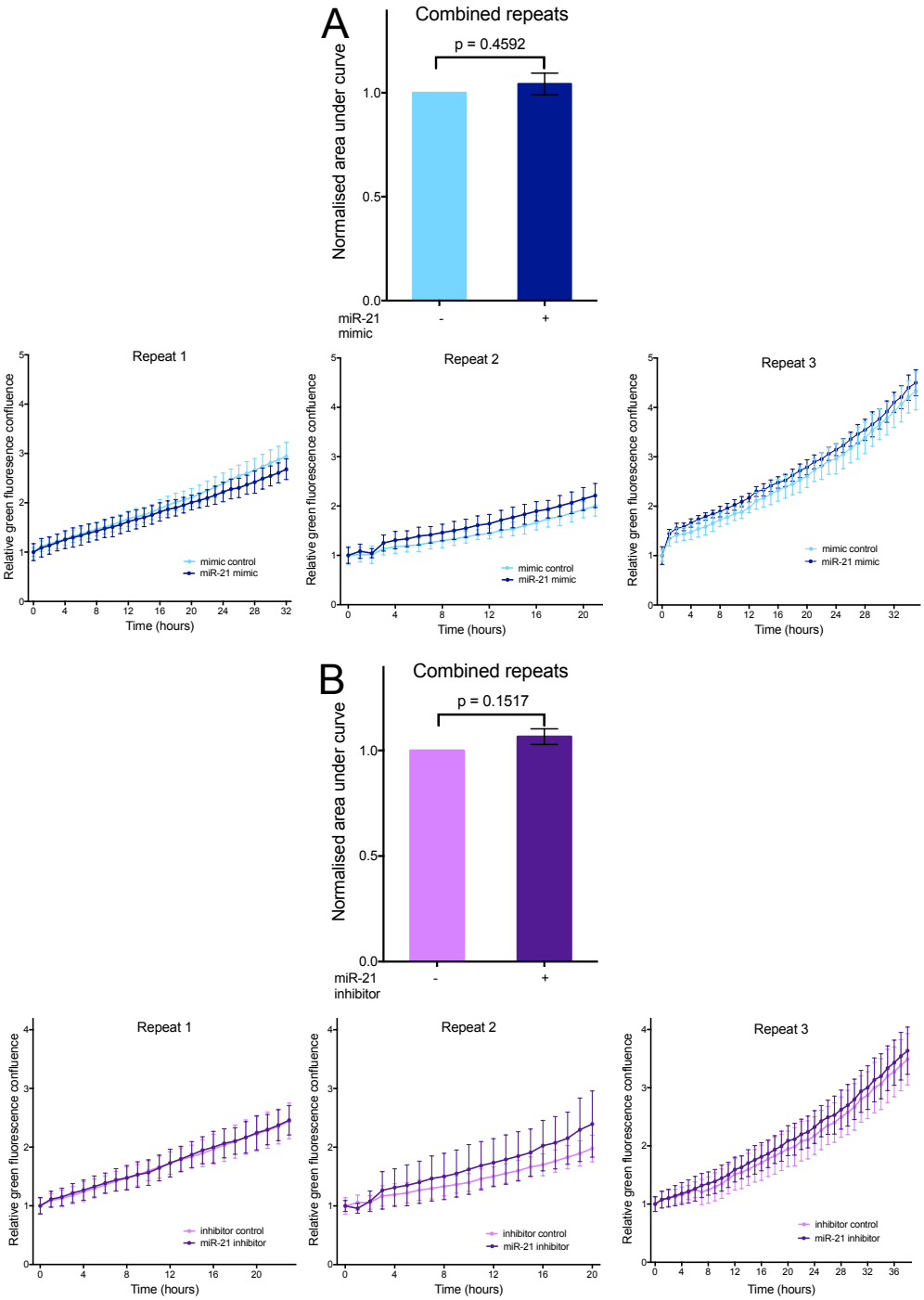

Figure 5-10 Increasing or decreasing miR-21 levels in CAF-2 does not affect migration of MDA-MB-231 in contact co-culture

CAF-2 cells were transfected with either miR-21 mimic (dark blue) or miR-21 inhibitor (purple) or the respective control (light blue and pink respectively). MDA-MB-231-GFP cells were seeded into the same wells. Following this a scratch wound closure assay was used to measure migration. Data are displayed as the mean of the area under the curve (+/- SEM) of 3 independent experiments (top panel), with each separate experiment shown below (mean of 6 wells +/- SD). Part A shows the data from CAF-2 transfected with miR-21 mimic and part B from CAF-2 transfected with miR-21 inhibitor.

Increasing or decreasing the levels of miR-21 in fibroblasts did not significantly alter the speed of migration of MDA-MB-231 tumour cells in a contact co-culture setting (Figures 5-7 to 5-10).

5.3.5 Lower levels of miR-21 in CAF-2 fibroblasts, but not in other breast fibroblast lines, increases invasion of MDA-MB-231 tumour cells

My third aim was to look at the effect of altering levels of miR-21 in fibroblasts on the invasion of epithelial tumour cells. Fibroblasts were transfected with either miR-21 mimic, miR-21 inhibitor or their respective control and were seeded onto a layer of collagen type 1. MDA-MB-231 cells (GFP labelled) were seeded into the same wells the following day. After cells had adhered, a scratch was made in the cell layer and a second layer of collagen type I was added to the wells to cover the cells and to provide a barrier for invasion. The time for the cells to migrate into the "wound" was measured hourly using live cell imaging. As with the migration scratch wound assay, to differentiate between the invasion of epithelial cells and fibroblasts, the invasion of GFP-fluorescent epithelial cells into the wound was measured. Data are shown hourly for each individual experimental repeat, and repeats were combined by calculating the relative areas under the invasion vs. time curves (Figures 5-11 to 5-14) (Salomon et al., 2013, Salomon et al., 2014).

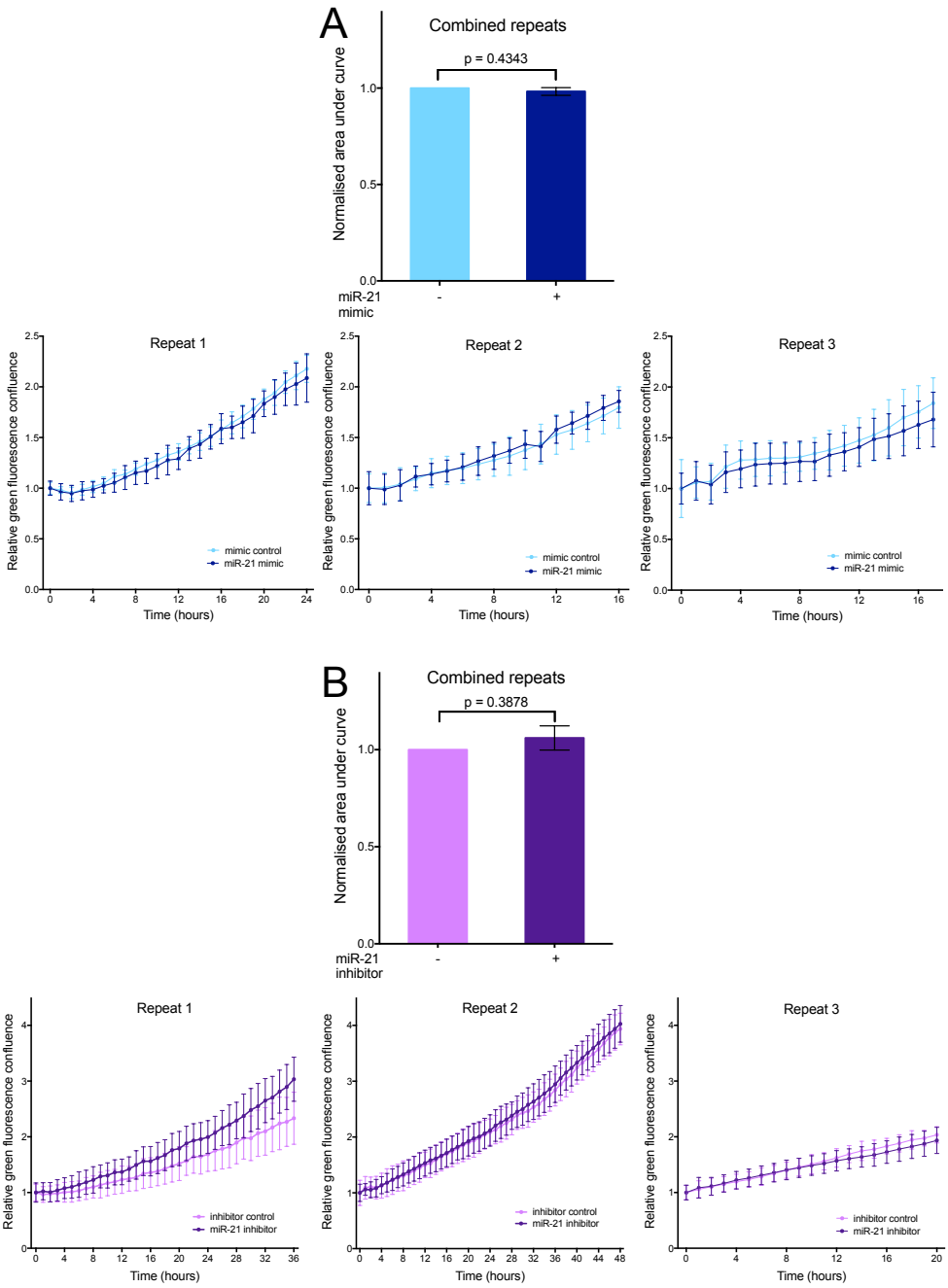

Figure 5-11 Increasing or decreasing miR-21 levels in NF-1 does not affect invasion of MDA-MB-231 in contact co-culture

Wells were coated with collagen type I. NF-1 cells were transfected with either miR-21 mimic (dark blue) or miR-21 inhibitor (purple) or the respective control (light blue and pink respectively). MDA-MB-231-GFP cells were seeded into the same wells. Following this, a scratch was made across the culture and a second layer of collagen type I was added. Invasion of epithelial cells into the collagen filled scratch was quantified as GFP density. Data are displayed as the mean of the area under the curve (+/- SEM) of 3 independent experiments (top panel), with each separate experiment shown below (mean of 6 wells +/- SD). Part A shows the data from NF-1 transfected with miR-21 mimic and part B from NF-1 transfected with miR-21 inhibitor.

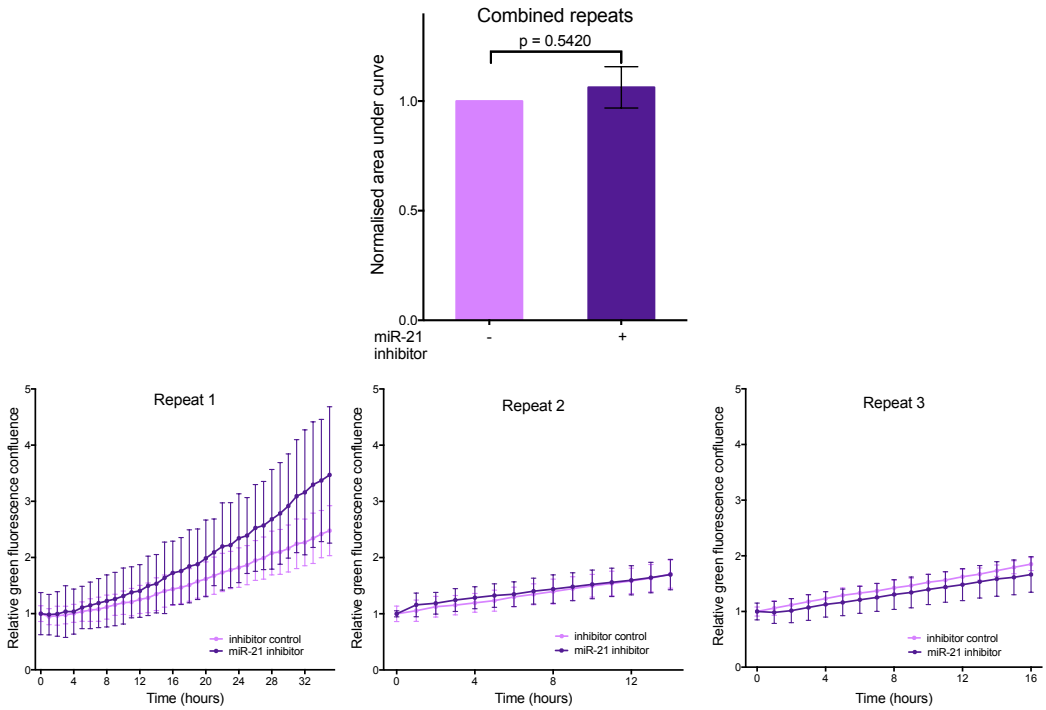

Figure 5-12 Decreasing miR-21 levels in NF-2 does not affect invasion of MDA-MB-231 in contact co-culture

Wells were coated with collagen type I. NF-2 cells were transfected with miR-21 inhibitor (purple) or inhibitor control (pink). MDA-MB-231-GFP cells were seeded into the same wells. Following this, a scratch was made across the culture and a second layer of collagen type I was added. Invasion of epithelial cells into the collagen filled scratch was quantified as GFP density. Data are displayed as the mean of the area under the curve (+/- SEM) of 3 independent experiments (top panel), with each separate experiment shown below (mean of 6 wells +/- SD).

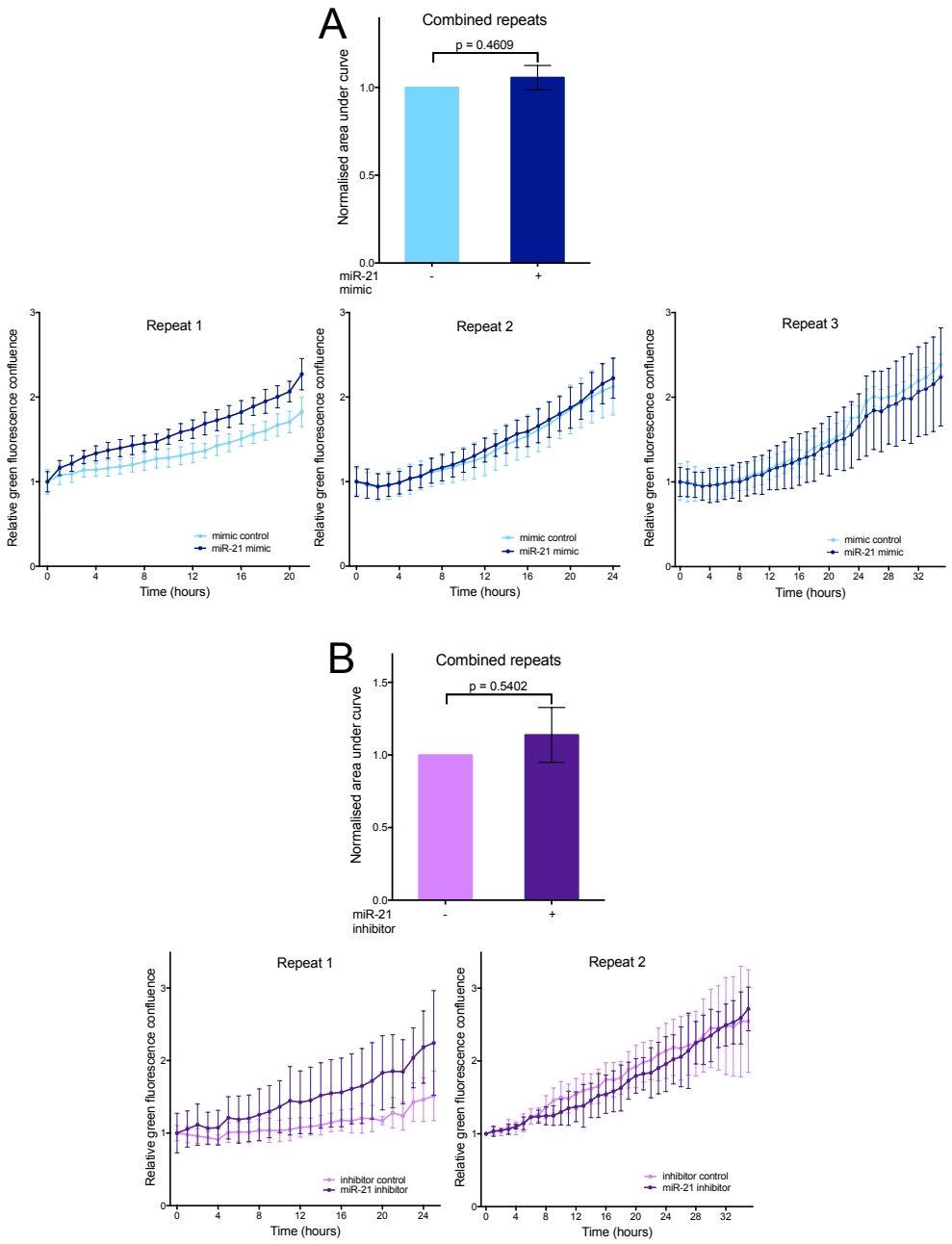

Figure 5-13 Increasing or decreasing miR-21 levels in CAF-1 does not affect invasion of MDA-MB-231 in contact co-culture

Wells were coated with collagen type I. CAF-1 cells were transfected with either miR-21 mimic (dark blue) or miR-21 inhibitor (purple) or the respective control (light blue and pink respectively). MDA-MB-231-GFP cells were seeded into the same wells. Following this, a scratch was made across the culture and a second layer of collagen type I was added. Invasion of epithelial cells into the collagen filled scratch was quantified as GFP density. Data are displayed as the mean of the area under the curve (+/- SEM) of 2 or 3 independent experiments (top panel), with each separate experiment shown below (mean of 6 wells +/- SD). Part A shows the data from CAF-1 transfected with miR-21 mimic and part B from CAF-1 transfected with miR-21 inhibitor.

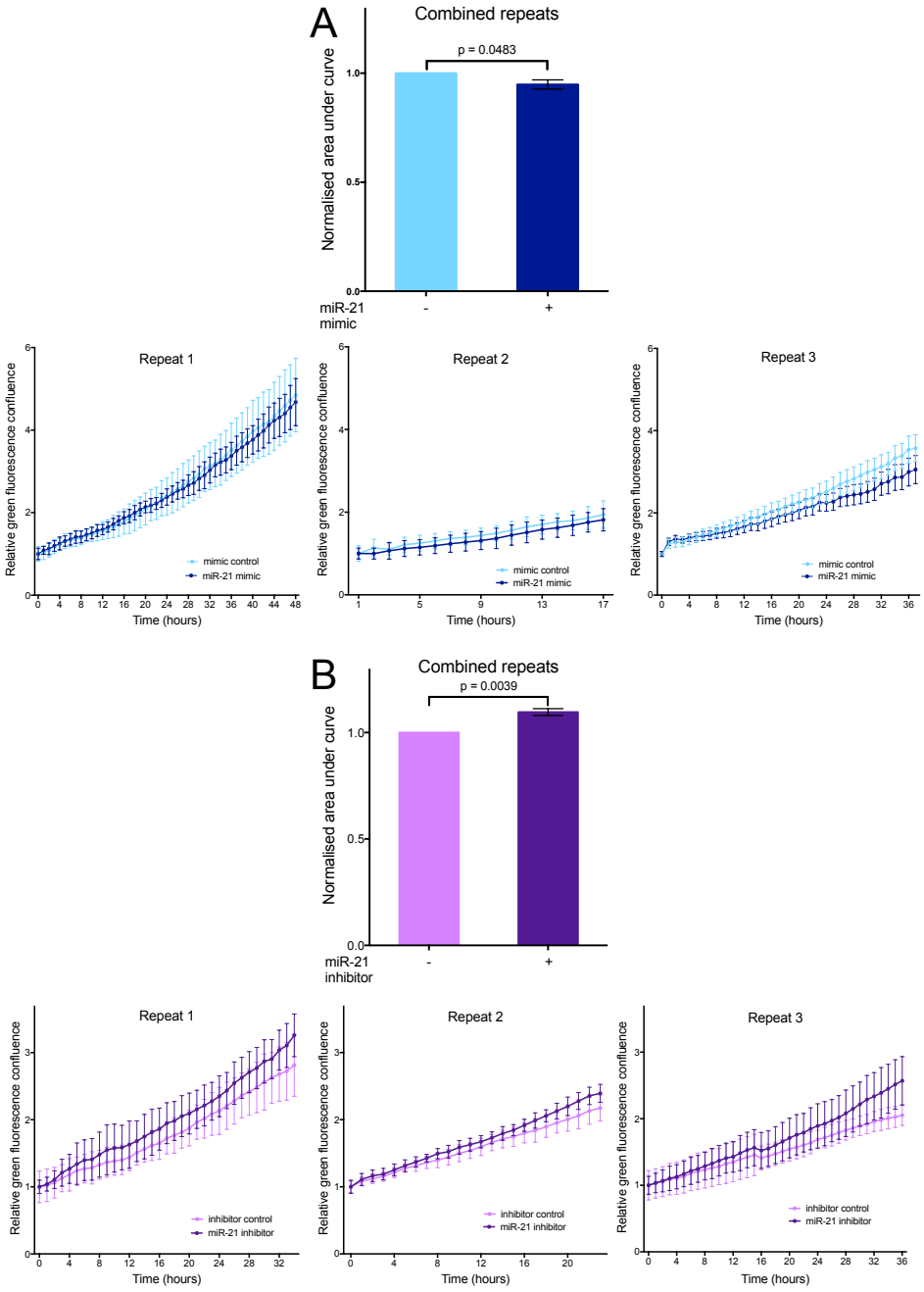

Figure 5-14 CAF-2 with lower levels of miR-21 significantly decreases invasion of MDA-MB-231 cells in contact co-culture

Wells were coated with collagen type I. CAF-2 cells were transfected with either miR-21 mimic (dark blue) or miR-21 inhibitor (purple) or the respective control (light blue and pink respectively). MDA-MB-231-GFP cells were seeded into the same wells. Following this, a scratch was made across the culture and a second layer of collagen type I was added. Invasion of epithelial cells into the collagen filled scratch was quantified as GFP density. Data are displayed as the mean of the area under the curve (+/- SEM) of 3 independent experiments (top panel), with each separate experiment shown below (mean of 6 wells +/- SD). Part A shows the data from CAF-2 transfected with miR-21 mimic and part B from CAF-2 transfected with miR-21 inhibitor.

Changing levels of miR-21 in fibroblast cultures NF-1, NF-2 and CAF-1, with either miR-21 mimic or miR-21 inhibitor, made no significant difference to the speed of MDA-MB-231 cell invasion within co-cultures (Figure 5-11 to 5-13). Whereas, when miR-21 levels were increased in CAF-2 fibroblasts with miR-21 mimic (Figure 5-14A) the invasion of MDA-MB-231 cells was significantly decreased ($p = 0.0483$), and when miR-21 levels were decreased in CAF-2 using a miR-21 inhibitor (Figure 5-14B) the invasion of MDA-MB-231 cells significantly increased ($p = 0.0039$). Both parts of Figure 5-14 suggest that when miR-21 levels are lower in CAF-2 fibroblasts the invasion of MDA-MB-231 cells is increased.

5.3.6 Altering levels of miR-21 in fibroblasts does not affect chemotherapy resistance in tumour cells

Next, my aim was to determine if increasing or decreasing levels of miR-21 in fibroblasts changed the sensitivity of tumour cells to a standard chemotherapy agent used in breast cancer treatment, the anthracycline, epirubcin. To do this I first transfected fibroblasts with either miR-21 mimic, miR-21 inhibitor or their respective control. I then seeded MDA-MB-231 (luciferase positive) cells into the same wells as the fibroblasts. On the following day epirubicin was added to the wells at low or high dose (1 μM or 79 μM) or the cells were treated with vehicle control. Cell survival exclusively in the MDA-MB-231 cells was measured by using luciferase activity as a proxy measure of viable MDA-MB-231 cell number (as previously in section 5.3.3). Data were normalised to the vehicle only control and are shown in Figures 5-15 to 5-18.

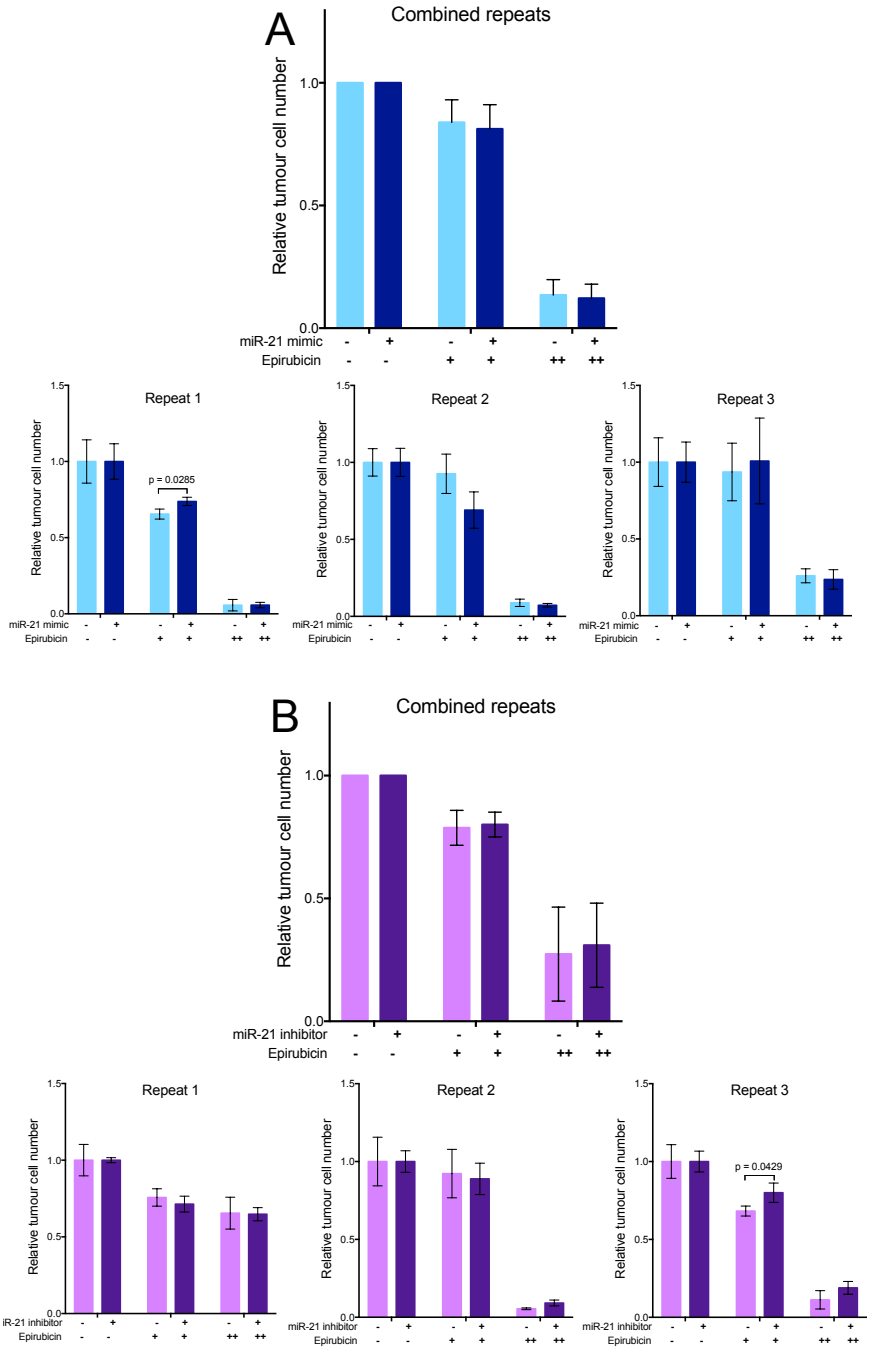

Figure 5-15 Increasing or decreasing miR-21 levels in NF-1 does not alter MDA-MB-231 survival/proliferation following epirubicin treatment

NF-1 cells were transfected with either miR-21 mimic (A, dark blue) or miR-21 inhibitor (B, purple) or the respective control (light blue and pink respectively). MDA-MB-231-luciferase-expressing cells were seeded into the same wells and then treated with epirubicin at a relatively low dose (1 μM) or a relatively high dose (79 μM). Luciferase activity was used to determine MDA-MB-231 cell number thereby measuring survival/proliferation. Data are displayed as means (+/- SEM) of 3 independent experiments (top panel), with each separate experiment shown below (means +/- SD).

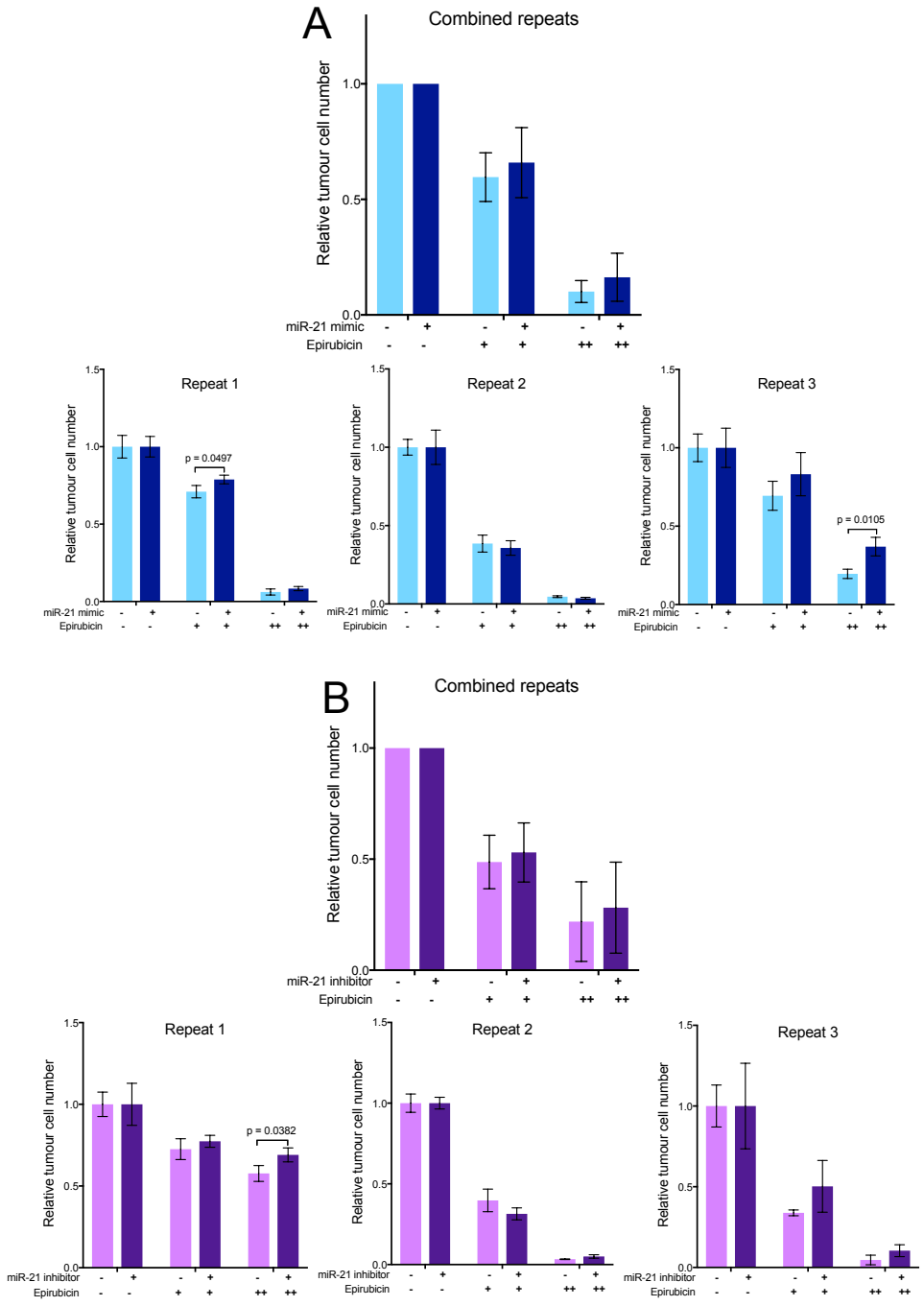

Figure 5-16 Increasing or decreasing miR-21 levels in NF-2 does not alter MDA-MB-231 survival/proliferation following epirubicin treatment

NF-2 cells were transfected with either miR-21 mimic (A, dark blue) or miR-21 inhibitor (B, purple) or the respective control (light blue and pink respectively). MDA-MB-231-luciferase-expressing cells were seeded into the same wells and then treated with epirubicin at a relatively low dose (1 μM) or a relatively high dose (79 μM). Luciferase activity was used to determine MDA-MB-231 cell number thereby measuring survival/proliferation. Data are displayed as means (+/- SEM) of 3 independent experiments (top panel), with each separate experiment shown below (means +/- SD).

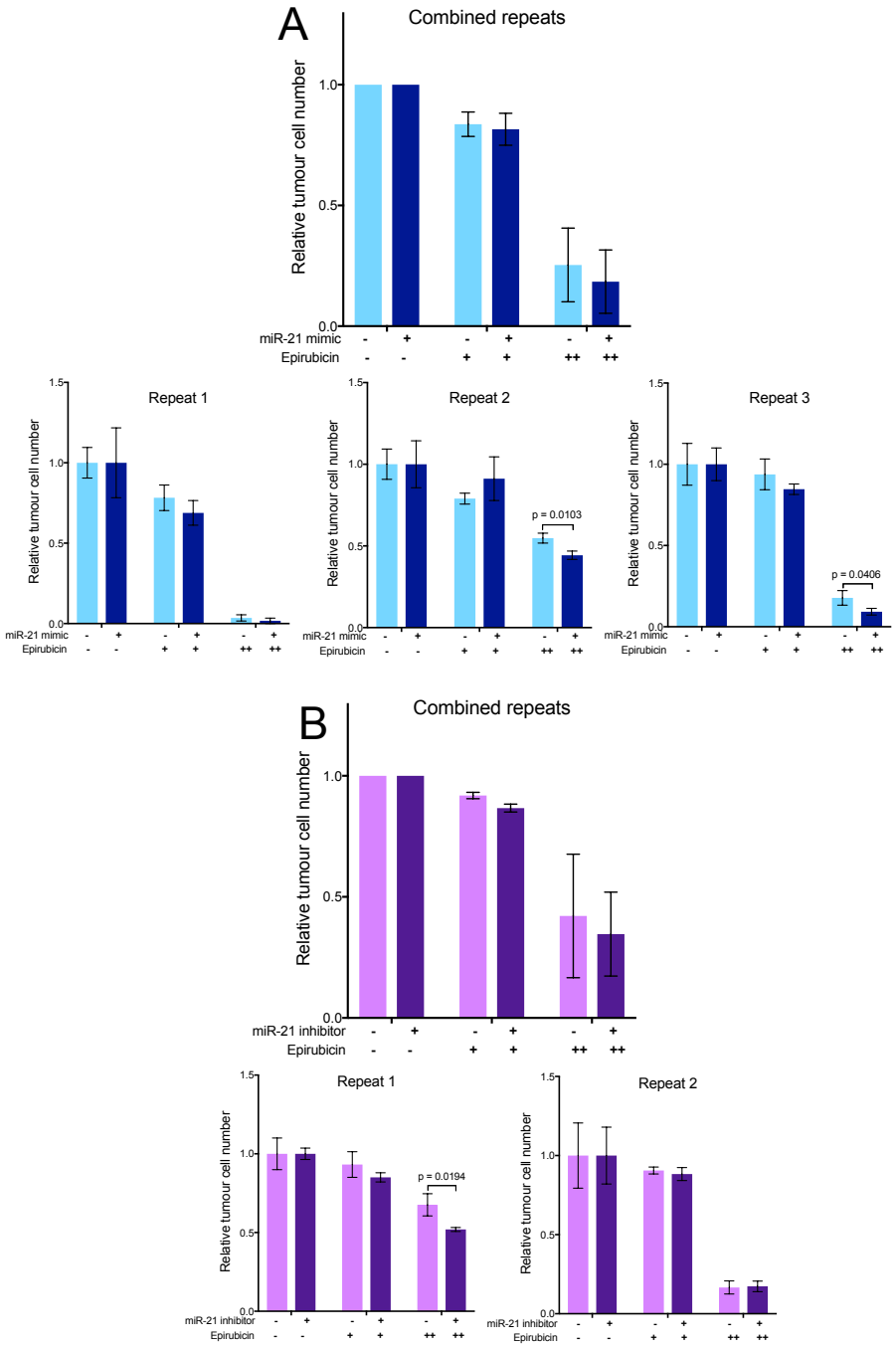

Figure 5-17 Increasing or decreasing miR-21 levels in CAF-1 does not alter MDA-MB-231 survival/proliferation following epirubicin treatment

CAF-1 cells were transfected with either miR-21 mimic (A, dark blue) or miR-21 inhibitor (B, purple) or the respective control (light blue and pink respectively). MDA-MB-231-luciferase-expressing cells were seeded into the same wells and then treated with epirubicin at a relatively low dose (1 μM) or a relatively high dose (79 μM). Luciferase activity was used to determine MDA-MB-231 cell number thereby measuring survival/proliferation. Data are displayed as means (+/- SEM) of 2 or 3 independent experiments (top panel), with each separate experiment shown below (means +/- SD).

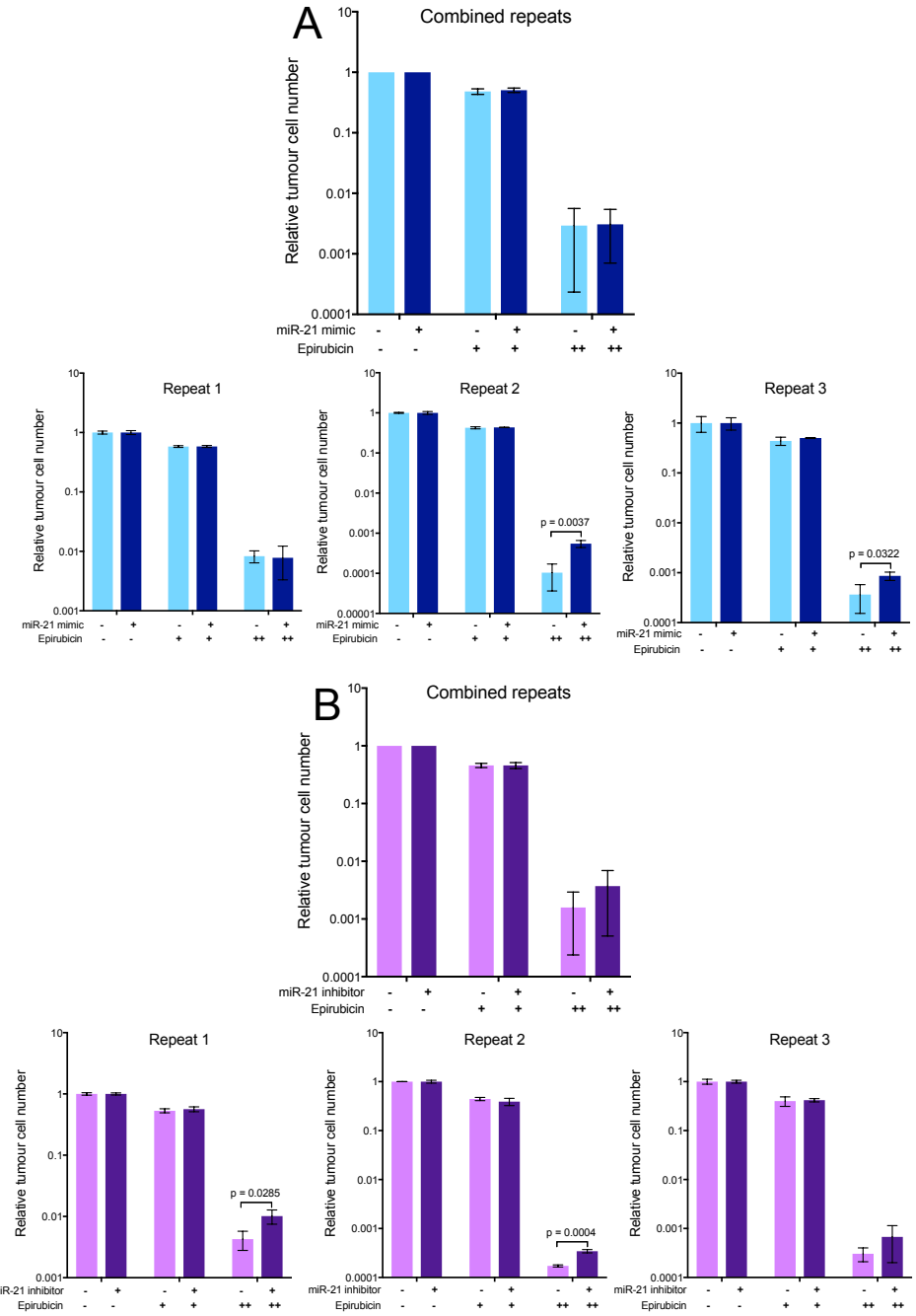

Figure 5-18 Increasing or decreasing miR-21 levels in CAF-2 does not alter MDA-MB-231 survival/proliferation following epirubicin treatment

CAF-2 cells were transfected with either miR-21 mimic (A, dark blue) or miR-21 inhibitor (B, purple) or the respective control (light blue and pink respectively). MDA-MB-231-luciferase-expressing cells were seeded into the same wells and then treated with epirubicin at a relatively low dose (1 μM) or a relatively high dose (79 μM). Luciferase activity was used to determine MDA-MB-231 cell number thereby measuring survival/proliferation. Data are displayed as means (+/- SEM) of 3 independent experiments (top panel), with each separate experiment shown below (means +/- SD).

Increased or decreased miR-21 levels in any of the four fibroblast cultures, NF-1, NF-2, CAF-1 and CAF-2, did not significantly alter the survival/proliferation of MDA-MB-231 cells in response to epirubcin treatment. As previously, some individual repeats did show some differences (e.g. repeats 2 and 3 with CAF-1 transfected with miR-21 mimic; Figure 5-17A), however, the combined assessments indicated there to be no significant differences.

5.4 MDA-MB-231 cells induce changes in expression of multiple miRNAs in co-cultured fibroblasts

I now return to the observation that miR-21 was induced in fibroblasts by co-culture with MDA-MB-231 cells (section 5.3.1.1 and Figure 5-1). My aim now was to determine whether co-culture induces changes in expression of other miRNAs in the fibroblasts, and whether these changes reflect the differences in miRNA levels in the matched normal versus CAF comparison made using LCM FFPE fibroblasts samples in chapter 3.

In the same way as in section 5.3.1.1 the CAF-1 fibroblast culture was grown in mono-culture or in contact co-culture with GFP-labelled MDA-MB-231 cells for 3 days. Cells then underwent fluorescence sorting to isolate the non-fluorescent fibroblasts (note – as before, the fibroblast mono-cultures were mixed, on ice, with GFP-labelled MDA-MB-231 cells immediately before fluorescence sorting, to control for any changes induced by the sorting process itself). MiRNA expression profiling was then carried out using Taqman low density qPCR arrays.

MiRNAs showing differential expression induced by the presence of the MDA-MB-231 cells were identified, and the numbers and identities of these were compared with the miRNAs identified as differentially expressed between NFs and CAFs from 4 clinical cases, previously (section 3.3.1).

The numbers of miRNAs up-regulated or down-regulated in the tissue culture model compared with those from the four clinical cases are shown in Figure 5-19, while Table 5-1 shows the identities of the miRNAs that show consistent deregulation between these two systems. I concluded that the majority (15/21) of the miRNAs

consistently up-regulated in CAFs from clinical breast cancers were recapitulated in the tissue culture system, while a minority of the miRNAs that were down-regulated (1/27) were recapitulated. The up-regulated miRNAs identified by array analysis included miR-21, as expected and in accordance with my previous analysis of this miRNA alone (Figure 5-1).

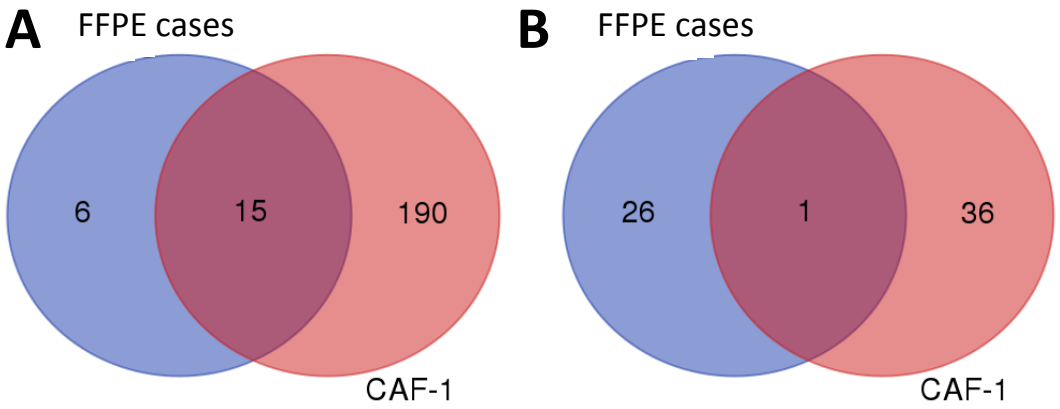

Figure 5-19 Number of miRNAs up- or down-regulated in CAF-1 cells by co-culture with MDA-MB-231 cells compared with those up- or down-regulated in CAFs from 4 clinical breast cancer cases

CAF-1 fibroblasts were grown in mono-culture or co-culture with MDA-MB-231 cancer cells. MiRNA expression was profiled in the CAF-1 cells in these cultures by qPCR arrays. MiRNAs consistently differentially expressed between matched NFs and CAFs from four cases of breast cancer were also identified by qPCR array profiling (section 3.3). These Venn diagrams show the numbers of miRNAs up-regulated (A) or down-regulated (B) in these experiments with the over-lap representing miRNAs consistently deregulated in tissue culture and clinical cases.

	Mean fold change in FFPE cases	Fold change in CAF-1
miR-127	7.12	7.59
miR-21	6.92	3.77
miR-125a-5p	5.09	1.87
miR-193b	4.43	3.76
miR-296	4.33	7.38
miR-342-3p	4.02	3.72
miR-214	3.09	3.82
miR-142-3p	2.77	∞ (not detected in mono-culture CAF-1)
miR-574-3p	2.7	1.87
miR-27b	2.46	3.79
miR-886-3p	2.35	3.74
miR-222	2.30	3.75
miR-708	2.26	3.79
miR-19a	1.91	3.77
miR-99b	1.25	7.20
miR-139-5p	0.25	0.94

Table 5-1 List of miRNA up- or down-regulated in CAFs as identified in clinical cases and in a co-culture model *in vitro*

This table lists the miRNAs from the intersects of the Venn diagrams in Figure 5-19.

5.5 Discussion

5.5.1 Co-culture of fibroblasts with MDA-MB-231 cells

My work showed that when fibroblasts and epithelial tumour cells were in contact co-culture miR-21 levels were significantly increased in fibroblasts. The effect of co-culture on *in vitro* miR-21 expression in fibroblasts in breast cancer has not previously been looked at. In a study of oesophageal cancer, using transwell and conditioned medium co-cultures, they found that when a squamous cell carcinoma line (KYSE-30) was co-cultured in transwells with gingival fibroblasts miR-21 levels in fibroblasts significantly increased, whereas this increase was not seen with conditioned medium. When Nouraee *et al.* carried out a similar experiment with an oesophageal adenocarcinoma cell line (FLO-1) a small non-significant increase in fibroblast miR-21 levels was seen in a transwell co-culture, but not with conditioned medium co-culture (Nouraee et al., 2013). This also suggests the idea that miR-21 up-regulation in co-culture is different in different cancer subtypes.

5.5.2 Manipulation of miR-21 levels in fibroblasts in co-cultures

A luciferase reporter was used to demonstrate that miR-21 inhibitor decreased functional levels of miR-21 within transfected fibroblasts. However, surprisingly, the luciferase reporter failed to detect functional over-expression of miR-21 after transfection with miR-21 mimics despite the fact that the transfection was evidently successful (Figure 4-2), suggesting that with this reporter the endogenous levels of miR-21 already fully repressed reporter expression (section 5.3.2 Figure 5-2).

Effective transfection with miR-21 mimic and miR-21 inhibitor is typically confirmed by qPCR in published work, and studies have shown significant increases in miR-21 levels using qPCR after transfection with miR-21 mimics and significant decreases in miR-21 levels by qPCR after transfection with miR-21 inhibitors (Xu et al., 2015, Liu et al., 2014b). However, it has been shown that levels of miRNAs detectable by qPCR are not necessarily the same as the actual intracellular levels or – perhaps most importantly - as functional levels within the cells (Thomson et al., 2013). The transfected miRNA mimic has to become bound to Argonaute proteins and then become incorporated into a RISC complex to become functional. Use of a

miRNA luciferase reporter or measurement of miRNA level following Argonaute immunoprecipitation are better ways to measure functional miRNA levels within cells. A luciferase reporter was used to confirm alteration of functional levels of miR-21 following transfection with miR-21 mimic in primary rat cardiac fibroblasts, it showed an almost 50% decrease in luciferase activity following transfection with miR-21 mimic (Thum et al., 2008). This differs from my findings and could be because the endogenous levels of miR-21 within these fibroblasts was different or because the miR-21 binding site within the 3'UTR also influences its functional activity. Some miR-21 binding sites may be very sensitive and show repression at low miR-21 levels, whereas other miR-21 binding sites, possibly those that are less complementary, may need higher levels of miR-21 for significant repression to occur. Confirmation of miR-21 inhibitor transfection leading to decreased levels of functional miR-21 within fibroblasts using a luciferase assay has not been published previously.

5.5.3 MiR-21 in fibroblasts and tumour cell growth

I found that increasing or decreasing the levels of miR-21 in fibroblasts did not significantly alter the growth of co-cultured breast cancer epithelial cells (Figures 5-3 to 5-6). Previous data have shown that increased miR-21 expression in breast cancers, quantified by qPCR of RNA extracted from whole tumour tissues, or higher miR-21 expression in CAFs, as assessed by *in situ* hybridisation, positively correlated with tumour cell Ki67 proliferation index (Rask et al., 2011, Huang et al., 2009a). However this does not necessarily imply a causal link between the miR-21 fibroblast level and tumour cell proliferation, and my work suggests that there is not a causal link. It should also be noted that these breast cancer studies were looking at all breast cancer subtypes in one study (Huang et al., 2009a), and luminal A breast cancer subtype in the other (Rask et al., 2011), whereas I have focused on triple negative breast cancers, so it is possible there are subtype specific differences with respect to miR-21 function. In contrast to my work, a study of colorectal cancer found that increasing the level of miR-21 in fibroblasts lead to significant increases in tumour cell growth (Bullock et al., 2013). Again, this conflict could be because miR-21 in fibroblasts has a different role in different cancer types.

5.5.4 MiR-21 and tumour cell migration

I have found that increasing or decreasing the levels of miR-21 in normal fibroblasts or cancer associated fibroblasts did not alter migration of co-cultured tumour cells (Figures 5-7 to 5-10). Specifically looking at the effect of miR-21 levels in fibroblasts on the migration of tumour cells has not been carried out in many other studies. One similar study used breast normal fibroblast conditioned medium and CAF conditioned medium to influence the behaviour of breast cancer cells. This study found that when miR-21 mimic was transfected into normal fibroblasts the migration of tumour cells increased, and conversely when a small molecule inhibitor of miR-21 was added to CAFs, the migration of tumour cells decreased in scratch wound assays (Ren et al., 2016). However, there was no quantification of the magnitude of this change, and no statistical analyses carried out to confirm that these changes were significant, therefore potentially this result should be interpreted with caution. These results differ from my findings in both result and experimental approach. The main difference in experimental design is that Ren *et al.* used conditioned medium transfer, whereas I used contact co-culture. When the small molecule inhibitor is added to fibroblasts it is not known if all the inhibitor is taken up into cells or if some could be carried across in the conditioned medium and act directly on the tumour cells. It is also not known whether it has any non-specific effects other than inhibiting the action of miR-21. These could explain the differences seen between their findings and mine.

One other related study was carried out using an oesophageal squamous cell carcinoma cell line (KYSE-30) and human gingival fibroblasts (HGF-1) (Nouraee et al., 2013). Nouraee *et al.* found that inhibition of miR-21 in fibroblasts caused no significant difference in the migration of tumour cells, in accordance with my findings.

5.5.5 MiR-21 and tumour cell invasion

I found that when miR-21 levels were increased in CAF-2 fibroblasts the invasion of tumour cells decreased, and when miR-21 levels were decreased by miR-21

inhibitor the speed of invasion of tumour cells increased (Figure 5-14). A suggestion of a similar trend was seen with NF-1, NF-2 and CAF-1, as miR-21 inhibitor in fibroblasts lead to a small increase in tumour cell invasion although this increase was not significant (Figures 5-11 to 5-13). These finding suggest that different fibroblasts may behave in different ways. There are two possible reasons for this. One is that CAF-2 are a primary fibroblast culture, while the other lines have been immortalised. It may be that during the immortalisation process other changes occur that make the fibroblasts respond less sensitively or differently to miR-21 inhibitor transfection. The second possible reason is that because each of these fibroblast cultures is isolated from a different individual they may each respond in a different way to changes in manipulation of the miR-21 levels in their fibroblasts because their tumours and tumour fibroblasts were fundamentally different in the first place.

My findings are different to those seen in other published work. Several different studies have shown that when miR-21 levels were increased in normal fibroblasts, the speed of invasion increased in associated cancer cells. This has been seen in several different adenocarcinomas, including colorectal cancer and pancreatic adenocarcinoma and even breast cancer cells (Bullock et al., 2013, Kadera et al., 2013, Ren et al., 2016). The converse has also been demonstrated, that when miR-21 levels were decreased in CAFs using either a small molecule inhibitor of miR-21 or miR-21 complementary inhibitor, invasion of breast cancer cells and pancreatic adenocarcinoma cells decreased (Ren et al., 2016, Kadera et al., 2013). In contrast to these, Nouraee *et al.* noted no significant change in the invasion of oesophageal squamous carcinoma cells when miR-21 inhibitor was transfected into fibroblasts (Nouraee et al., 2013). This suggests that miR-21 in fibroblasts may have different effects in different tumour types and subtypes.

5.5.6 MiR-21 and chemotherapy resistance

In my work I showed that increasing or decreasing levels of miR-21 in both normal fibroblasts and CAFs made no difference to epirubicin sensitivity of co-cultured cancer epithelial cells (Figures 5-15 to 5-18).

There is no other published work directly comparable to my findings with this assay in the context of breast cancer, although some related work has been published in

other cancer types. In colorectal cancer, the effect of increasing miR-21 levels in CAFs on the response of cancer cells to oxaliplatin has been measured. This showed that increased miR-21 in CAFs significantly decreased the cytotoxic effect of oxaliplatin (Bullock et al., 2013). This difference could be because it is a different cancer type or because, although oxaliplatin and anthracyclines are both cytotoxic, DNA-damaging chemotherapies, they may work in different ways as the mechanism of action of anthracyclines is not completely understood (Rabbani et al., 2005, Alcindor and Beauger, 2011). A study looking at pancreatic ductal adenocarcinoma miR-21 expression and response to chemotherapy found that high levels of miR-21 in CAFs correlated with decreased overall survival in multivariate analysis in patients that were treated with 5-fluorouracil, but miR-21 levels in CAFs did not correlate with survival following treatment with gemcitabine; this highlights that miR-21 may affect response to some chemotherapeutics but not others (Donahue et al., 2014). A further example looking at yet another therapeutic agent is that stromal miR-21 expression in breast cancer was not found to correlate with response to trastuzumab in HER2 positive breast tumours (Nielsen et al., 2014), however as this differs in cancer subtype and therapeutic agent it is difficult to relate this finding to my conclusions.

5.5.7 Comparisons between miRNAs altered in matched NFs and CAFs from clinical samples, and in the tissue culture setting

My work identified 15 miRNAs that were up-regulated and 1 miRNA that was down-regulated in CAFs compared with NFs in FFPE samples and also in co-culture compared with mono-culture growth conditions. The up-regulated miRNAs were miR-21, miR-125a-3p, miR-193b, miR-296, miR-214, miR-222, miR-127, miR-708, miR-19a, miR-142-3p, miR-574-3p, miR-342-3p, miR-886-3p, miR-27b and miR-99b. The down-regulated miRNA was miR-139-5p. The methodology of comparing differences in the clinical cell types (NFs vs. CAFs) and those de-regulated in tissue culture when fibroblasts were co-cultured with an appropriate epithelial line, may provide a useful way of identifying the most robustly deregulated – and therefore potentially most important – miRNAs (Nouraee et al., 2013). As discussed in section 1.4, miR-21 is known to up-regulated in several cancer types, including breast

cancer (Yan et al., 2008, Huang et al., 2009a, Rask et al., 2011, Hug et al., 2015). Below, I will briefly discuss data concerning expression and relevance of the other miRNAs in cancer fibroblasts.

For most of these miRNAs very little is known about their expression or function in CAFs in any cancer type. In a study looking at miRNA expression in primary breast CAFs compared with matched primary NFs, in contrast to my findings, this found miR-342 was down-regulated in CAFs (Zhao et al., 2012). However, the breast cancer subtype of the 6 patient samples used in this study were not stated and therefore breast cancer subtype specific difference may explain this conflict. MiR-214 has been found to be down-regulated in primary ovarian CAFs compared with normal omental fibroblasts from the same patients, but up-regulated in pancreatic stellate cells (myofibroblast-like cells) compared with adjacent normal tissue (Mitra et al., 2012, Kuninty et al., 2016a). In pancreatic stellate cells, miR-214 has also been suggested to play a role in TGF-β stimulation of stellate cells and activation of a tumour enhancing phenotype (Kuninty et al., 2016a). This suggests that miR-214 may show different alteration and regulation depending on the tumour type. I identified miR-214 as up-regulated in CAFs, and it is an interesting prospect that it may be involved in TGF-β stimulation and the CAF phenotype in breast CAFs as well. Conditioned medium from MDA-MB-231 cells has been shown to increase miR-214 expression in osteoclasts (Liu et al., 2017), suggesting that factors secreted by this specific cancer cell type may induce expression of this miRNA in a range of other cells, as demonstrated by my findings that miR-214 was increased in co-cultured fibroblasts.

Some findings concerning miRNAs found in serum or plasma of breast cancer patients may be of relevance. MiR-127 has been found to be increased and miR-139 decreased in the serum of breast cancer patients compared with people with no or benign breast disease (Lu et al., 2017, Dai et al., 2017). While miR-19a has been found to be increased in the serum of breast cancer patients with high grade disease compared with low grade (Sochor et al., 2014) – a key point being that triple negative breast cancers are more commonly high grade. These observations are compatible with my findings for these miRNAs as these changes are in the same direction as I find in CAFs, although this relies on the assumption that CAFs and/or

NFs secrete miRNAs into the circulation at meaningful levels – something that is not known.

Chapter 6
Discussion of results

In this chapter, I discuss some themes that cut across the different results chapters within the thesis. I also attempt to summarise how my work impacts overall on the understanding of the importance of miR-21 in cancer.

6.1 The up-regulation of miR-21 in fibroblasts is dependent on proximity to tumour cells

In situ hybridisation using probes targeted against miR-21 demonstrated that the strongest miR-21 expression often occurred in the fibroblasts closest to the tumour cells (sections 3.3.1 and 3.4). Furthermore, in a tissue culture model using breast fibroblasts and epithelial breast cancer cells I found that contact co-culture lead to a significant increase in the levels of miR-21 in the fibroblasts, although transwell co-culture and epithelial-conditioned medium transfer did not (section 5.3.1.1 and Appendix K). These findings both suggest that close proximity between tumour cells and fibroblasts is important in the increase in miR-21 levels seen in fibroblasts within a tumour. The finding that miR-21 is mainly over-expressed in the cytoplasm of stromal cells adjacent to malignant cells has previously been noted in breast cancer and oesophageal cancer (Nouraee et al., 2013, Hug et al., 2015). The reason for this increase being most prominent in fibroblasts closest to tumour cells could be because direct contact between tumour cells and fibroblasts is important in increasing miR-21 levels in fibroblasts or because the factor that stimulates the increase only diffuses a short distance at appropriate (i.e. functionally relevant) concentrations.

It is not known whether the increased fibroblast miR-21 levels occurred because the fibroblasts themselves transcribed more miR-21, or because miR-21 was transcribed within the epithelial cells (or even another cell type within the tumour), exported by these cells, possibly within exosomes, and then taken-up by fibroblasts. MiR-21 has been detected in the conditioned medium of numerous cancer cell lines, and if cancer cells *in vitro* secrete miR-21 this suggests it is possible that they secrete miR-

21 *in vivo* into the tumour microenvironment (Nouraee et al., 2013, Munagala et al., 2016). Indeed, within our own laboratory, a different worker (Samir Jana, visiting PhD student) has detected miR-21 within exosomes secreted by MDA-MB-231 cells, the triple negative breast epithelial cells used in my work (unpublished). In colorectal cancer, miR-21 has been identified as released by monocytes as well as by tumour cells (Patel and Gooderham, 2015). Some exosomes are known to be relatively stable and able to diffuse and travel some distance, as they are detected in the blood stream (Munagala et al., 2016). However, it is not known if all miRNA are transferred into exosomes, and whether all exosomes are stable over longer distances and time periods. Indeed some exosomes are thought to become bound to the extracellular matrix rather than freely diffusing through it (Huleihel et al., 2016). My own data make it clear that if the epithelial cancer cells are a source of the miR-21 that is detected in the fibroblasts, then miR-21 export from the epithelial cells must be very rapid and efficient since expression is not detected within the epithelial cells themselves, at least by *in situ* hybridisation.

6.2 The role of miR-21 in migration and invasion of CAF-2 fibroblasts and epithelial tumour cells

In comparing the results from sections 4.3.3, 4.3.4, 5.3.4 and 5.3.5, my work showed that increased levels/activity of miR-21 in CAF-2 fibroblasts:

(i) significantly increased migration of CAF-2 cells;
(ii) did not significantly affect invasion of CAF-2 cells;
(iii) did not significantly affect migration of epithelial tumour cells in the context of co-culture; and,
(iv) significantly *decreased* invasion of epithelial tumour cells in co-cultures.

These findings present two surprising results. Firstly, that miR-21 did not have the same influence in the matched migration and invasion assays, as both are scratch wound closure assays and activity in them requires some similar cell behaviours. Secondly, that increased miR-21 was associated with *increased* activity in one assay in fibroblast mono-cultures, but *decreased* activity of the tumour cells in the co-culture (albeit migration for one observation and invasion for the other).

Although extending lamellipodia and filopodia (actin-rich membrane protrusions) and re-organising the internal cytoskeleton to facilitate cell movement may involve the same proteins in both assays, a cell moving through collagen type I may require additional collagen digestion enzymes and possibly different cell tethering and adhesion proteins compared with a cell migrating across the surface of a plastic well through culture medium (Jacquemet et al., 2015, Machesky, 2008). This could explain the difference in the migration and invasion results.

It remains challenging to explain how increased CAF-2 migration relates to decreased epithelial tumour cell invasion. It has been demonstrated that carcinoma cells often invade collectively, rather than individually. It has also been demonstrated that carcinoma cells may follow behind stromal fibroblasts as they remodel the ECM (Gaggioli et al., 2007). Although increased miR-21 does not make the CAF-2 cells invade more slowly, it may alter their protein expression such that it alters the way they remodel the collagen type I as they invade. This could then impact on the invasion of the epithelial tumour cells, decreasing their rate of invasion.

This leads on to the question, which result is more clinically relevant? Movement through collagen type I is more similar to the situation within a tumour as normal breast ECM, into which tumour cells invade, is predominantly composed of collagen type I (Kauppila et al., 1998). Whereas migration through fluid could be thought of as more similar to cells moving through lymphatic or vascular channels, possibly tethered to the endothelial membrane as they search for sites to extravasate and establish a metastasis. Both assays are models used to try to identify factors relevant to the behaviour of CAFs within a human tumour and both may have relevance to specific circumstances. A key follow up would be to assess any such findings using *in vivo* studies, and by observation and manipulation of human breast cancers.

6.3 MiRNA co-operation

One area that has not been explored in my work is the idea that miR-21 alone may not have a large measurable impact on fibroblast behaviour or on the influence of fibroblasts on tumour cells, but that miR-21 may act in co-operation with other miRNAs. In section 3.3.1 I identified 21 miRNAs that were consistently up-

regulated and 27 miRNAs that were consistently down-regulated in CAFs compared with NFs in clinical samples. In section 5.4 the miRNA changes in CAFs were further explored using a tissue culture model, which identified 15 miRNAs that were up-regulated in both settings and 1 miRNA that was down-regulated. It may be that changes in the levels of more than one miRNA are required to see substantial changes in fibroblast behaviour and their influence on tumour cells. This has been seen in other cancer types, for example in ovarian cancer miR-31 down-regulation, and miR-214 and miR-155 up-regulation in fibroblasts were required to increase tumour growth (Mitra et al., 2012). It has also been suggested that miR-21 up-regulation in combination with down-regulation of miR-206 and let-7a could be important in regulating angiogenesis in ER positive breast cancer, and it has also been shown that miR-21 in combination with miR-155 has a cumulative effect on the expression of genes involved with breast cancer metastasis in ER positive breast cancer cell lines (Isanejad et al., 2016, Nikiforova et al., 2016). MiRNAs that may work co-operatively with miR-21 in the fibroblasts of triple negative breast cancer have yet to be investigated, and it would be possible to attempt to transfect cells with selections of mimics and inhibitors for multiple miRNAs. The potential complexity of manipulating up to 16 different miRNAs (based on the number of consistently deregulated miRNAs from my data) is – of course – huge.

6.4 Breast cancer cell line selection

In the co-culture work, sections 5.3 and 5.4, I used the cell line MDA-MB-231 as a line that is representative of triple negative human breast cancer cells. However, triple negative cancers are a broad subtype containing considerable heterogeneity, as identified by RNA expression analysis, DNA sequencing and hierarchical clustering (Mayer et al., 2014). MDA-MB-231 is a metastatic cell line extracted from a pleural effusion (Cailleau et al., 1978). It was classified as basal-like subtype by IHC, but further sub-classified as basal B and claudin-low (Neve et al., 2006, Parker et al., 2009, Perou et al., 2000, Subik et al., 2010, Prat et al., 2010). Claudin-low breast cancers show low or absent luminal differentiation markers and enrichment for epithelial-to-mesenchymal transition markers, immune response genes and cancer stem-cell/tumour initiating cell markers in gene expression studies. They generally have triple negative receptor expression and clinically, as a group, they show an

intermediate response to chemotherapy, between luminal and basal-like breast cancers (Prat et al., 2010). The basal A and basal B classification was used to describe the clustering into two major subdivisions seen within basal-like breast cancer cell lines. Basal A cell lines have transcriptional profiles more closely matched to breast tumour basal-like expression, whereas basal B lines have expression profiles with more stem-cell like features and may reflect clinical triple negative non-basal tumours (Neve et al., 2006, Kao et al., 2009). Interestingly, MDA-MB-231 has also been classified as mesenchymal stem-like based on gene expression profiling (Lehmann et al., 2011). Other triple negative, basal-like human breast cancer cell lines such as MDA-MB-468 and HC1599 have been classified as non-claudin-low, basal A subtype. The initial observations of miRNA alterations and CAFs were made in basal-like breast cancers, section 3.3.1, without making any assessment of claudin-low status. It would be interesting to assess potential differences between these classifications with respect to miRNAs, by expanding my initial patient cohort to power analyses of these subtypes and also assessing if co-culture with different basal-like cell lines produce different results. It is, of course, possible that miR-21 within fibroblasts may have more dramatic effects on other epithelial lines.

In section 5.3.5 I found that increased miR-21 levels in CAF-2 fibroblasts lead to decreased invasion of tumour cells. Mesenchymal-like and non-mesenchymal-like tumour cells are thought to invade the ECM using different mechanisms. Mesenchymal-like tumour cells, such as MDA-MB-231, have been found to re-align ECM fibrillar collagen to create microtracks along which cells can migrate, whereas invading tumour cells that retain epithelial markers are thought to follow fibroblasts tracks into the ECM (Gaggioli et al., 2007, Wolf et al., 2007). One might predict that non-mesenchymal tumour cell lines, such as MDA-MB-468, may have therefore responded differently to co-culture with CAF-2 fibroblasts, perhaps being stimulated to migrate faster literally following the enhancement of fibroblast migration stimulated by miR-21 (section 4.3.3). It is difficult to predict whether the results would be the same for the co-culture invasion assay, i.e. decreased invasion with increased CAF-2 miR-21 levels, or different because of the different way the tumour cells invade.

6.5 In conclusion: is miR-21 important in CAFs or not?

In my work I have shown significant up-regulation of miR-21 in triple negative breast cancer CAFs using qPCR and ISH (sections 3.3.1, 3.3.2 and 3.4.1). I have identified that increasing miR-21 in CAF-2 increased migration of fibroblasts and decreased invasion of tumour cells, by significant but small amount and made no difference to the migration or invasion of fibroblasts or tumour cells with the other fibroblast cultures (sections 4.3.3-4 and 5.3.4-5). It also made no difference to the proliferation of fibroblasts or tumour cells and no difference to the chemosensitivity of tumour cells (sections 4.3.2, 5.3.3 and 5.3.6). One possible explanation for this lack of a large impact on the behaviour of fibroblasts or tumour cells could be that miR-21 does not act in isolation, but in co-operation with other miRNAs. This has been discussed in section 6.3. Another explanation is that although miR-21 is transcribed in CAFs it has its most noticeable and important effects in other cell types. MiR-21 has been identified as being secreted in exosomes from the fibroblasts of oesophageal cancer and pancreatic adenocarcinoma (Nouraee et al., 2016, Nouraee et al., 2013, Takikawa et al., 2017). It could be that miR-21 is predominantly made and stored in fibroblasts but has its functional effects in tumour cells, as it has been found that increasing miR-21 levels in a variety of epithelial breast cancer cell lines increased epithelial to mesenchymal transition, induced gemcitabine resistance and increased tumour cell proliferation and invasion (Wu et al., 2016, Kuang and Nie, 2016, Yan et al., 2016). It may be that a signal or stimulus is needed for fibroblasts to release exosomal miR-21 or that the time it takes for fibroblasts to process miR-21 into exosomes, secrete them into the medium, for them to be taken up into tumour cells and then have their functional effects in tumour cells is longer than the 24 hours they were co-cultured together in the assays used to look at migration, invasion and chemotherapy resistance. For example, in one study fibroblasts and serous ovarian cancer cells were co-cultured together for 7 days to induce miRNA changes in CAFs and CAF-like changes in the behaviour of fibroblasts and, more importantly, to assess the influence of the fibroblasts on tumour cell behaviour (Mitra et al., 2012). It could be interesting to investigate whether and which miRNA are secreted by looking at fibroblast exosomes specifically from contact co-culture medium and analyse their miRNA content after a number of time periods. In summary, my data do not provide substantial evidence

of a compelling role for miR-21 in CAFs in controlling breast cancer biology overall, but there are so many different experimental approaches that could have been taken, that it is currently not possible for me to rule this potential role out.

6.6 MiR-21 as a potential biomarker or target in breast cancer

MiR-21 has been proposed as a possible diagnostic marker, prognostic marker and as a potential therapeutic target in breast cancer. It has been detected at increased levels in the serum of triple negative breast cancer patients and in breast cancer patients in general when compared with healthy controls or patients with benign breast disease (Han et al., 2017, Yang et al., 2016, Motawi et al., 2016, Hannafon et al., 2016). My findings support the idea of using miR-21 as a potential diagnostic marker as I also found that miR-21 levels were increased in triple negative breast cancer tissues (section 3.3.2), although I have not analysed circulating levels. However, when analysing miR-21 expression as a predictor of clinical and prognostic outcomes, I found no significant correlation (section 3.5). My findings do not support those suggesting that miR-21 may be a useful prognostic indicator of improved breast cancer survival or lymph node metastasis (Yang et al., 2016, Chang et al., 2016). It is useful when trying to identify new prognostic indicators to have an understanding of their biological role within the tumour, to be able to understand the advantages and limitations of a new clinical marker. My work has not identified a role for miR-21 in triple negative breast cancer that would support or explain its use as a prognostic marker.

MiR-21 has also been proposed as a potential therapeutic target in breast cancer (Rui et al., 2017, Ren et al., 2016). My findings show that miR-21 in fibroblasts does not affect the response of tumour cells to chemotherapy and does not alter the behaviour of tumour cells to a large enough extent likely to be of clinical use. My findings do not support the idea that miR-21 could be a potential new therapeutic target in triple negative breast cancer.

6.7 Critical review and future work

In reviewing the work I have done for my PhD and included in this thesis there are some aspects I would change if I had more time or alter given the overview of the work I have now. These are outlined in this final section.

During the analysis of the TMA CISH H-scores I treated this data as a continuous, ratio variable. In other published work, sometimes CISH scores are grouped and treated as an ordinal variable (Uozaki et al., 2014). Transforming the data in this way would then mean different statistical tests are more appropriate to use. For example instead of using the Spearman's correlation in Table 3-5 I would use the Kruskal-Wallis test for tumour grade and lymph node positivity.

The TMA did not include the 14 original cases that had had CISH carried out on them already because I did not want to duplicate the data. However, if they had been included this would have been a good way to confirm that H-scores from the TMA were the same or very similar to H-scores from whole tissue sections, further confirming the reliability TMAs as a method of analysing a larger number of cases. In the analysis and discussion of the TMA CISH work (Figure 3-12 and section 3.6.4) I determined that a larger sample size, over 700 cases in total, may be required to confirm whether disease free survival is significantly correlated with miR-21 ISH staining. I would like to obtain a TMA of further triple negative breast cancer cases to confirm and clarify this result.

The miR-21 CISH staining suggested that miR-21 was present at detectable levels in the CAFs but not in the tumour cells (Figure 3-7). I looked at the miR-21 levels in the fibroblasts cultures using qPCR and compared these with the levels detected in the FFPE fibroblast samples (section 4.3.1). There was no qPCR measurement of the miR-21 levels in the tumour cell line I used (MDA-MB-231). Measuring the level of miR-21 in the tumour cell line may provide further background to the interpretation of the contact co-culture miR-21 fibroblast levels (Figure 5-1) and subsequent contact co-culture functional experiments (Figure 5-3 to 5-18).

My work has shown that when the primary CAF culture (CAF-2) had increased levels of miR-21 migration of these fibroblasts significantly increased and invasion of MDA-MB-231 tumour cells in co-culture with them significantly decreased

(Figures 4-6 and 5-14). It is not known whether this finding was specific to these CAFs only or may be seen in other primary CAF cultures, as the other fibroblasts used were not primary but immortalised fibroblast lines. It would be interesting to carry out migration and invasion assays with other triple negative primary CAF cultures to see if these would behave in a similar way and therefore if these results are more widely and generally applicable.

The co-culture work was carried out with triple negative breast cancer cell line MDA-MB-231. As discussed in section 6.4 this cell line has also been classified as basal B and claudin-low. It was beyond the scope of this project but it would be interesting to see if the same results, e.g. a decrease in invasion of tumour cells occurred with a different triple negative breast cancer cell line, for example a basal A non-claudin-low subtype such as MDA-MB-468.

If there was unlimited time and resources available further work that could be carried out based on some of the results presented previously would include investigation of other miRNAs identified as potentially of interest, for example those listed in Table 5-1. As discussed in section 6.3 the role of miRNAs working in co-operation has not been explored, carrying functional assays following transfection with several miRNA mimics and inhibitors could also potentially lead to some very interesting findings.

List of References

ALCINDOR, T. & BEAUGER, N. 2011. Oxaliplatin: a review in the era of molecularly targeted therapy. *Curr Oncol,* 18**,** 18-25.

ALI, H. R., RUEDA, O. M., CHIN, S. F., CURTIS, C., DUNNING, M. J., APARICIO, S. A. & CALDAS, C. 2014. Genome-driven integrated classification of breast cancer validated in over 7,500 samples. *Genome Biol,* 15**,** 431.

ALI, S., SURESH, R., BANERJEE, S., BAO, B., XU, Z., WILSON, J., PHILIP, P. A., APTE, M. & SARKAR, F. H. 2015. Contribution of microRNAs in understanding the pancreatic tumor microenvironment involving cancer associated stellate and fibroblast cells. *Am J Cancer Res,* 5**,** 1251-64.

AMBROS, V., LEE, R. C., LAVANWAY, A., WILLIAMS, P. T. & JEWELL, D. 2003. MicroRNAs and other tiny endogenous RNAs in C. elegans. *Curr Biol,* 13**,** 807-18.

ARVOLD, N. D., TAGHIAN, A. G., NIEMIERKO, A., ABI RAAD, R. F., SREEDHARA, M., NGUYEN, P. L., BELLON, J. R., WONG, J. S., SMITH, B. L. & HARRIS, J. R. 2011. Age, breast cancer subtype approximation, and local recurrence after breast-conserving therapy. *J Clin Oncol,* 29**,** 3885-91.

AUGSTEN, M. 2014. Cancer-associated fibroblasts as another polarized cell type of the tumor microenvironment. *Front Oncol,* 4**,** 62.

BADVE, S., DABBS, D. J., SCHNITT, S. J., BAEHNER, F. L., DECKER, T., EUSEBI, V., FOX, S. B., ICHIHARA, S., JACQUEMIER, J., LAKHANI, S. R., PALACIOS, J., RAKHA, E. A., RICHARDSON, A. L., SCHMITT, F. C., TAN, P. H., TSE, G. M., WEIGELT, B., ELLIS, I. O. & REIS-FILHO, J. S. 2011. Basal-like and triple-negative breast cancers: a critical review with an emphasis on the implications for pathologists and oncologists. *Mod Pathol,* 24**,** 157-67.

BALKWILL, F. 2004. Cancer and the chemokine network. *Nat Rev Cancer,* 4**,** 540-50.

BARIK, S. 2008. An intronic microRNA silences genes that are functionally antagonistic to its host gene. *Nucleic Acids Res,* 36**,** 5232-41.

BARONI, S., ROMERO-CORDOBA, S., PLANTAMURA, I., DUGO, M., D'IPPOLITO, E., CATALDO, A., COSENTINO, G., ANGELONI, V., ROSSINI, A., DAIDONE, M. G. & IORIO, M. V. 2016. Exosome-mediated delivery of miR-9 induces cancer-associated fibroblast-like properties in human breast fibroblasts. *Cell Death Dis,* 7**,** e2312.

BCN 2016. Breast Cancer Now

http://www.breastcancercampaign.org/about-breast-cancer/breast-cancer-statistics.

BEHM-ANSMANT, I., REHWINKEL, J., DOERKS, T., STARK, A., BORK, P. & IZAURRALDE, E. 2006. mRNA degradation by miRNAs and GW182 requires both CCR4:NOT deadenylase and DCP1:DCP2 decapping complexes. *Genes Dev,* 20**,** 1885-98.

BELL-MCGUINN, K. M., MATTHEWS, C. M., HO, S. N., BARVE, M., GILBERT, L., PENSON, R. T., LENGYEL, E., PALAPARTHY, R., GILDER, K., VASSOS, A., MCAULIFFE, W., WEYMER, S., BARTON, J. & SCHILDER, R. J. 2011. A

phase II, single-arm study of the anti-alpha5beta1 integrin antibody volociximab as monotherapy in patients with platinum-resistant advanced epithelial ovarian or primary peritoneal cancer. *Gynecol Oncol,* 121**,** 273-9.

BHATTACHARYYA, S. N., HABERMACHER, R., MARTINE, U., CLOSS, E. I. & FILIPOWICZ, W. 2006. Relief of microRNA-mediated translational repression in human cells subjected to stress. *Cell,* 125**,** 1111-24.

BIESAGA, B., SZOSTEK, S., KLIMEK, M., JAKUBOWICZ, J. & WYSOCKA, J. 2012. Comparison of the sensitivity and specificity of real-time PCR and in situ hybridization in HPV16 and 18 detection in archival cervical cancer specimens. *Folia Histochem Cytobiol,* 50**,** 239-47.

BILLOTTET, C., TUEFFERD, M., GENTIEN, D., RAPINAT, A., THIERY, J. P., BROET, P. & JOUANNEAU, J. 2008. Modulation of several waves of gene expression during FGF-1 induced epithelial-mesenchymal transition of carcinoma cells. *J Cell Biochem,* 104**,** 826-39.

BRAMHALL, S. R., HALLISSEY, M. T., WHITING, J., SCHOLEFIELD, J., TIERNEY, G., STUART, R. C., HAWKINS, R. E., MCCULLOCH, P., MAUGHAN, T., BROWN, P. D., BAILLET, M. & FIELDING, J. W. 2002. Marimastat as maintenance therapy for patients with advanced gastric cancer: a randomised trial. *Br J Cancer,* 86**,** 1864-70.

BREM, S., BREM, H., FOLKMAN, J., FINKELSTEIN, D. & PATZ, A. 1976. Prolonged tumor dormancy by prevention of neovascularization in the vitreous. *Cancer Res,* 36**,** 2807-12.

BRENNECKE, J., STARK, A., RUSSELL, R. B. & COHEN, S. M. 2005. Principles of microRNA-target recognition. *PLoS Biol,* 3**,** e85.

BRENNEN, W. N., ROSEN, D. M., WANG, H., ISAACS, J. T. & DENMEADE, S. R. 2012. Targeting carcinoma-associated fibroblasts within the tumor stroma with a fibroblast activation protein-activated prodrug. *J Natl Cancer Inst,* 104**,** 1320-34.

BRONISZ, A., GODLEWSKI, J., WALLACE, J. A., MERCHANT, A. S., NOWICKI, M. O., MATHSYARAJA, H., SRINIVASAN, R., TRIMBOLI, A. J., MARTIN, C. K., LI, F., YU, L., FERNANDEZ, S. A., PECOT, T., ROSOL, T. J., CORY, S., HALLETT, M., PARK, M., PIPER, M. G., MARSH, C. B., YEE, L. D., JIMENEZ, R. E., NUOVO, G., LAWLER, S. E., CHIOCCA, E. A., LEONE, G. & OSTROWSKI, M. C. 2011. Reprogramming of the tumour microenvironment by stromal PTEN-regulated miR-320. *Nat Cell Biol,* 14**,** 159-67.

BROWN, P. D. 2000. Ongoing trials with matrix metalloproteinase inhibitors. *Expert Opin Investig Drugs,* 9**,** 2167-77.

BUDD, W. T., SEASHOLS-WILLIAMS, S. J., CLARK, G. C., WEAVER, D., CALVERT, V., PETRICOIN, E., DRAGOESCU, E. A., O'HANLON, K. & ZEHNER, Z. E. 2015. Dual Action of miR-125b As a Tumor Suppressor and OncomiR-22 Promotes Prostate Cancer Tumorigenesis. *PLoS One,* 10**,** e0142373.

BULLOCK, M. D., PICKARD, K. M., NIELSEN, B. S., SAYAN, A. E., JENEI, V., MELLONE, M., MITTER, R., PRIMROSE, J. N., THOMAS, G. J., PACKHAM, G. K. & MIRNEZAMI, A. H. 2013. Pleiotropic actions of miR-21 highlight the critical role of deregulated stromal microRNAs during colorectal cancer progression. *Cell Death Dis,* 4**,** e684.

BUSCAGLIA, L. E. & LI, Y. 2011. Apoptosis and the target genes of microRNA-21. *Chin J Cancer,* 30**,** 371-80.

CAILLEAU, R., OLIVE, M. & CRUCIGER, Q. V. 1978. Long-term human breast carcinoma cell lines of metastatic origin: preliminary characterization. *In Vitro,* 14**,** 911-5.

CALIN, G. A., DUMITRU, C. D., SHIMIZU, M., BICHI, R., ZUPO, S., NOCH, E., ALDLER, H., RATTAN, S., KEATING, M., RAI, K., RASSENTI, L., KIPPS, T., NEGRINI, M., BULLRICH, F. & CROCE, C. M. 2002. Frequent deletions and down-regulation of micro- RNA genes miR15 and miR16 at 13q14 in chronic lymphocytic leukemia. *Proc Natl Acad Sci U S A,* 99**,** 15524-9.

CALON, A., TAURIELLO, D. V. & BATLLE, E. 2014. TGF-beta in CAF-mediated tumor growth and metastasis. *Semin Cancer Biol,* 25**,** 15-22.

CALVO, F., EGE, N., GRANDE-GARCIA, A., HOOPER, S., JENKINS, R. P., CHAUDHRY, S. I., HARRINGTON, K., WILLIAMSON, P., MOEENDARBARY, E., CHARRAS, G. & SAHAI, E. 2013. Mechanotransduction and YAP-dependent matrix remodelling is required for the generation and maintenance of cancer-associated fibroblasts. *Nat Cell Biol,* 15**,** 637-46.

CALZA, S., HALL, P., AUER, G., BJOHLE, J., KLAAR, S., KRONENWETT, U., LIU, E. T., MILLER, L., PLONER, A., SMEDS, J., BERGH, J. & PAWITAN, Y. 2006. Intrinsic molecular signature of breast cancer in a population-based cohort of 412 patients. *Breast Cancer Res,* 8**,** R34.

CAO, Z. G., HUANG, Y. N., YAO, L., LIU, Y. R., HU, X., HOU, Y. F. & SHAO, Z. M. 2016. Positive expression of miR-361-5p indicates better prognosis for breast cancer patients. *J Thorac Dis,* 8**,** 1772-9.

CASEY, T. M., ENEMAN, J., CROCKER, A., WHITE, J., TESSITORE, J., STANLEY, M., HARLOW, S., BUNN, J. Y., WEAVER, D., MUSS, H. & PLAUT, K. 2008. Cancer associated fibroblasts stimulated by transforming growth factor beta1 (TGF-beta 1) increase invasion rate of tumor cells: a population study. *Breast Cancer Res Treat,* 110**,** 39-49.

CASTELLS, M., THIBAULT, B., DELORD, J. P. & COUDERC, B. 2012. Implication of tumor microenvironment in chemoresistance: tumor-associated stromal cells protect tumor cells from cell death. *Int J Mol Sci,* 13**,** 9545-71.

CEPEDA, M. A., PELLING, J. J., EVERED, C. L., WILLIAMS, K. C., FREEDMAN, Z., STAN, I., WILLSON, J. A., LEONG, H. S. & DAMJANOVSKI, S. 2016. Less is more: low expression of MT1-MMP is optimal to promote migration and tumourigenesis of breast cancer cells. *Mol Cancer,* 15**,** 65.

CESARIO, J. M., BRITO, R. B., MALTA, C. S., SILVA, C. S., MATOS, Y. S., KUNZ, T. C., URBANO, J. J., OLIVEIRA, L. V., DALBONI, M. A. & DELLE, H. 2016. A simple method to induce hypoxia-induced vascular endothelial growth factor-A (VEGF-A) expression in T24 human bladder cancer cells. *In Vitro Cell Dev Biol Anim*.

CHANG, J. T., WANG, F., CHAPIN, W. & HUANG, R. S. 2016. Identification of MicroRNAs as Breast Cancer Prognosis Markers through the Cancer Genome Atlas. *PLoS One,* 11**,** e0168284.

CHEN, C. Y., ZHENG, D., XIA, Z. & SHYU, A. B. 2009. Ago-TNRC6 triggers microRNA-mediated decay by promoting two deadenylation steps. *Nat Struct Mol Biol,* 16**,** 1160-6.

CHEN, X., LU, P., WANG, D. D., YANG, S. J., WU, Y., SHEN, H. Y., ZHONG, S. L., ZHAO, J. H. & TANG, J. H. 2016a. The role of miRNAs in drug resistance and prognosis of breast cancer formalin-fixed paraffin-embedded tissues. *Gene*.

CHEN, Y., XIAN, P. F., YANG, L. & WANG, S. X. 2016b. MicroRNA-21 Promotes Proliferation of Fibroblast-Like Synoviocytes through Mediation of NF-kappaB Nuclear Translocation in a Rat Model of Collagen-Induced Rheumatoid Arthritis. *Biomed Res Int,* 2016**,** 9279078.

CHIVUKULA, R. R., SHI, G., ACHARYA, A., MILLS, E. W., ZEITELS, L. R., ANANDAM, J. L., ABDELNABY, A. A., BALCH, G. C., MANSOUR, J. C., YOPP, A. C., MAITRA, A. & MENDELL, J. T. 2014. An essential mesenchymal function for miR-143/145 in intestinal epithelial regeneration. *Cell,* 157**,** 1104-16.

CHONG, H. C., TAN, C. K., HUANG, R. L. & TAN, N. S. 2012. Matricellular proteins: a sticky affair with cancers. *J Oncol,* 2012**,** 351089.

CHOTTEAU-LELIEVRE, A., DOLLE, P. & GOFFLOT, F. 2006. Expression analysis of murine genes using in situ hybridization with radioactive and nonradioactively labeled RNA probes. *Methods Mol Biol,* 326**,** 61-87.

CIMMINO, A., CALIN, G. A., FABBRI, M., IORIO, M. V., FERRACIN, M., SHIMIZU, M., WOJCIK, S. E., AQEILAN, R. I., ZUPO, S., DONO, M., RASSENTI, L., ALDER, H., VOLINIA, S., LIU, C. G., KIPPS, T. J., NEGRINI, M. & CROCE, C. M. 2005. miR-15 and miR-16 induce apoptosis by targeting BCL2. *Proc Natl Acad Sci U S A,* 102**,** 13944-9.

CONDEELIS, J. & POLLARD, J. W. 2006. Macrophages: obligate partners for tumor cell migration, invasion, and metastasis. *Cell,* 124**,** 263-6.

CONNOLLY, E. C., VAN DOORSLAER, K., ROGLER, L. E. & ROGLER, C. E. 2010. Overexpression of miR-21 promotes an in vitro metastatic phenotype by targeting the tumor suppressor RHOB. *Mol Cancer Res,* 8**,** 691-700.

COURRECH STAAL, E. F., WOUTERS, M. W., VAN SANDICK, J. W., TAKKENBERG, M. M., SMIT, V. T., JUNGGEBURT, J. M., SPITZER-NAAYKENS, J. M., KARSTEN, T., HARTGRINK, H. H., MESKER, W. E. & TOLLENAAR, R. A. 2010. The stromal part of adenocarcinomas of the oesophagus: does it conceal targets for therapy? *Eur J Cancer,* 46**,** 720-8.

COUSSENS, L. M., RAYMOND, W. W., BERGERS, G., LAIG-WEBSTER, M., BEHRENDTSEN, O., WERB, Z., CAUGHEY, G. H. & HANAHAN, D. 1999. Inflammatory mast cells up-regulate angiogenesis during squamous epithelial carcinogenesis. *Genes Dev,* 13**,** 1382-97.

CRAWFORD, Y., KASMAN, I., YU, L., ZHONG, C., WU, X., MODRUSAN, Z., KAMINKER, J. & FERRARA, N. 2009. PDGF-C mediates the angiogenic and tumorigenic properties of fibroblasts associated with tumors refractory to anti-VEGF treatment. *Cancer Cell,* 15**,** 21-34.

CROCKFORD, M., JONES, J. B., MCCOLL, K. & WHITTINGTON, R. J. 2008. Comparison of three molecular methods for the detection of pilchard herpesvirus in archived paraffin-embedded tissue and frozen tissue. *Dis Aquat Organ,* 82**,** 37-44.

CRUK 2014. Cancer Research UK

http://www.cancerresearchuk.org/cancer-info/cancerstats/types/breast/.

DAI, H., GALLAGHER, D., SCHMITT, S., PESSETTO, Z. Y., FAN, F., GODWIN, A. K. & TAWFIK, O. 2017. Role of miR-139 as a surrogate marker for tumor aggression in breast cancer. *Hum Pathol,* 61**,** 68-77.

DAVOREN, P. A., MCNEILL, R. E., LOWERY, A. J., KERIN, M. J. & MILLER, N. 2008. Identification of suitable endogenous control genes for microRNA gene expression analysis in human breast cancer. *BMC Mol Biol,* 9**,** 76.

DE KRUIJF, E. M., VAN NES, J. G., VAN DE VELDE, C. J., PUTTER, H., SMIT, V. T., LIEFERS, G. J., KUPPEN, P. J., TOLLENAAR, R. A. & MESKER, W. E. 2011. Tumor-stroma ratio in the primary tumor is a prognostic factor in early breast cancer patients, especially in triple-negative carcinoma patients. *Breast Cancer Res Treat,* 125**,** 687-96.

DE VISSER, K. E., EICHTEN, A. & COUSSENS, L. M. 2006. Paradoxical roles of the immune system during cancer development. *Nat Rev Cancer,* 6**,** 24-37.

DEKKER, T. J., VAN DE VELDE, C. J., VAN PELT, G. W., KROEP, J. R., JULIEN, J. P., SMIT, V. T., TOLLENAAR, R. A. & MESKER, W. E. 2013. Prognostic significance of the tumor-stroma ratio: validation study in node-negative premenopausal breast cancer patients from the EORTC perioperative chemotherapy (POP) trial (10854). *Breast Cancer Res Treat,* 139**,** 371-9.

DENARDO, D. G., BARRETO, J. B., ANDREU, P., VASQUEZ, L., TAWFIK, D., KOLHATKAR, N. & COUSSENS, L. M. 2009. CD4(+) T cells regulate pulmonary metastasis of mammary carcinomas by enhancing protumor properties of macrophages. *Cancer Cell,* 16**,** 91-102.

DENKERT, C., LOIBL, S., NOSKE, A., ROLLER, M., MULLER, B. M., KOMOR, M., BUDCZIES, J., DARB-ESFAHANI, S., KRONENWETT, R., HANUSCH, C., VON TORNE, C., WEICHERT, W., ENGELS, K., SOLBACH, C., SCHRADER, I., DIETEL, M. & VON MINCKWITZ, G. 2010. Tumor-associated lymphocytes as an independent predictor of response to neoadjuvant chemotherapy in breast cancer. *J Clin Oncol,* 28**,** 105-13.

DILLHOFF, M., LIU, J., FRANKEL, W., CROCE, C. & BLOOMSTON, M. 2008. MicroRNA-21 is overexpressed in pancreatic cancer and a potential predictor of survival. *J Gastrointest Surg,* 12**,** 2171-6.

DOENCH, J. G. & SHARP, P. A. 2004. Specificity of microRNA target selection in translational repression. *Genes Dev,* 18**,** 504-11.

DONAHUE, T. R., NGUYEN, A. H., MOUGHAN, J., LI, L., TATISHCHEV, S., TOSTE, P. & FARRELL, J. J. 2014. Stromal microRNA-21 levels predict response to 5-fluorouracil in patients with pancreatic cancer. *J Surg Oncol,* 110**,** 952-9.

DONNARUMMA, E., FIORE, D., NAPPA, M., ROSCIGNO, G., ADAMO, A., IABONI, M., RUSSO, V., AFFINITO, A., PUOTI, I., QUINTAVALLE, C., RIENZO, A., PISCUOGLIO, S., THOMAS, R. & CONDORELLI, G. 2017. Cancer-associated fibroblasts release exosomal microRNAs that dictate an aggressive phenotype in breast cancer. *Oncotarget*.

DOWNEY, C. L., SIMPKINS, S. A., WHITE, J., HOLLIDAY, D. L., JONES, J. L., JORDAN, L. B., KULKA, J., POLLOCK, S., RAJAN, S. S., THYGESEN, H. H., HANBY, A. M. & SPEIRS, V. 2014. The prognostic significance of tumour-stroma ratio in oestrogen receptor-positive breast cancer. *Br J Cancer,* 110**,** 1744-7.

DU, J., YANG, S., AN, D., HU, F., YUAN, W., ZHAI, C. & ZHU, T. 2009. BMP-6 inhibits microRNA-21 expression in breast cancer through repressing deltaEF1 and AP-1. *Cell Res,* 19**,** 487-96.

DVORAK, H. F. 1986. Tumors: wounds that do not heal. Similarities between tumor stroma generation and wound healing. *N Engl J Med,* 315**,** 1650-9.

EAGER, R. M., CUNNINGHAM, C. C., SENZER, N., RICHARDS, D. A., RAJU, R. N., JONES, B., UPRICHARD, M. & NEMUNAITIS, J. 2009. Phase II trial of talabostat and docetaxel in advanced non-small cell lung cancer. *Clin Oncol (R Coll Radiol),* 21**,** 464-72.

EGEBLAD, M., NAKASONE, E. S. & WERB, Z. 2010. Tumors as organs: complex tissues that interface with the entire organism. *Dev Cell,* 18**,** 884-901.

EULALIO, A., HUNTZINGER, E. & IZAURRALDE, E. 2008. GW182 interaction with Argonaute is essential for miRNA-mediated translational repression and mRNA decay. *Nat Struct Mol Biol,* 15**,** 346-53.

FABIAN, M. R., MATHONNET, G., SUNDERMEIER, T., MATHYS, H., ZIPPRICH, J. T., SVITKIN, Y. V., RIVAS, F., JINEK, M., WOHLSCHLEGEL, J., DOUDNA, J. A., CHEN, C. Y., SHYU, A. B., YATES, J. R., 3RD, HANNON, G. J., FILIPOWICZ, W., DUCHAINE, T. F. & SONENBERG, N. 2009. Mammalian miRNA RISC recruits CAF1 and PABP to affect PABP-dependent deadenylation. *Mol Cell,* 35**,** 868-80.

FABIAN, M. R. & SONENBERG, N. 2012. The mechanics of miRNA-mediated gene silencing: a look under the hood of miRISC. *Nat Struct Mol Biol,* 19**,** 586-93.

FEARON, D. T. 2014. The carcinoma-associated fibroblast expressing fibroblast activation protein and escape from immune surveillance. *Cancer Immunol Res,* 2**,** 187-93.

FILIPOWICZ, W., BHATTACHARYYA, S. N. & SONENBERG, N. 2008. Mechanisms of post-transcriptional regulation by microRNAs: are the answers in sight? *Nat Rev Genet,* 9**,** 102-14.

FLORES-PEREZ, A., MARCHAT, L. A., RODRIGUEZ-CUEVAS, S., BAUTISTA-PINA, V., HIDALGO-MIRANDA, A., OCAMPO, E. A., MARTINEZ, M. S., PALMA-FLORES, C., FONSECA-SANCHEZ, M. A., ASTUDILLO-DE LA VEGA, H., RUIZ-GARCIA, E., GONZALEZ-BARRIOS, J. A., PEREZ-PLASENCIA, C., STREBER, M. L. & LOPEZ-CAMARILLO, C. 2016. Dual targeting of ANGPT1 and TGFBR2 genes by miR-204 controls angiogenesis in breast cancer. *Sci Rep,* 6**,** 34504.

FRANKEL, L. B., CHRISTOFFERSEN, N. R., JACOBSEN, A., LINDOW, M., KROGH, A. & LUND, A. H. 2008. Programmed cell death 4 (PDCD4) is an important functional target of the microRNA miR-21 in breast cancer cells. *J Biol Chem,* 283**,** 1026-33.

FREDIANI, J. N. & FABBRI, M. 2016. Essential role of miRNAs in orchestrating the biology of the tumor microenvironment. *Mol Cancer,* 15**,** 42.

FULFORD, L. G., EASTON, D. F., REIS-FILHO, J. S., SOFRONIS, A., GILLETT, C. E., LAKHANI, S. R. & HANBY, A. 2006. Specific morphological features predictive for the basal phenotype in grade 3 invasive ductal carcinoma of breast. *Histopathology,* 49**,** 22-34.

FULFORD, L. G., REIS-FILHO, J. S., RYDER, K., JONES, C., GILLETT, C. E., HANBY, A., EASTON, D. & LAKHANI, S. R. 2007. Basal-like grade III invasive ductal carcinoma of the breast: patterns of metastasis and long-term survival. *Breast Cancer Res,* 9**,** R4.

GABRIELY, G., WURDINGER, T., KESARI, S., ESAU, C. C., BURCHARD, J., LINSLEY, P. S. & KRICHEVSKY, A. M. 2008. MicroRNA 21 promotes glioma invasion by targeting matrix metalloproteinase regulators. *Mol Cell Biol,* 28**,** 5369-80.

GAGGIOLI, C. 2008. Collective invasion of carcinoma cells: when the fibroblasts take the lead. *Cell Adh Migr,* 2**,** 45-7.

GAGGIOLI, C., HOOPER, S., HIDALGO-CARCEDO, C., GROSSE, R., MARSHALL, J. F., HARRINGTON, K. & SAHAI, E. 2007. Fibroblast-led collective invasion of carcinoma cells with differing roles for RhoGTPases in leading and following cells. *Nat Cell Biol,* 9**,** 1392-400.

GALIMBERTI, V., COLE, B. F., ZURRIDA, S., VIALE, G., LUINI, A., VERONESI, P., BARATELLA, P., CHIFU, C., SARGENTI, M., INTRA, M., GENTILINI, O., MASTROPASQUA, M. G., MAZZAROL, G., MASSARUT, S., GARBAY, J. R., ZGAJNAR, J., GALATIUS, H., RECALCATI, A., LITTLEJOHN, D., BAMERT, M., COLLEONI, M., PRICE, K. N., REGAN, M. M., GOLDHIRSCH, A., COATES, A. S., GELBER, R. D. & VERONESI, U. 2013. Axillary dissection versus no axillary dissection in patients with sentinel-node micrometastases (IBCSG 23-01): a phase 3 randomised controlled trial. *Lancet Oncol,* 14**,** 297-305.

GAZINSKA, P., GRIGORIADIS, A., BROWN, J. P., MILLIS, R. R., MERA, A., GILLETT, C. E., HOLMBERG, L. H., TUTT, A. N. & PINDER, S. E. 2013. Comparison of basal-like triple-negative breast cancer defined by morphology, immunohistochemistry and transcriptional profiles. *Mod Pathol,* 26**,** 955-66.

GIRALDEZ, A. J., MISHIMA, Y., RIHEL, J., GROCOCK, R. J., VAN DONGEN, S., INOUE, K., ENRIGHT, A. J. & SCHIER, A. F. 2006. Zebrafish MiR-430 promotes deadenylation and clearance of maternal mRNAs. *Science,* 312**,** 75-9.

GONG, C., NIE, Y., QU, S., LIAO, J. Y., CUI, X., YAO, H., ZENG, Y., SU, F., SONG, E. & LIU, Q. 2014. miR-21 induces myofibroblast differentiation and promotes the malignant progression of breast phyllodes tumors. *Cancer Res,* 74**,** 4341-52.

GONG, C., YAO, Y., WANG, Y., LIU, B., WU, W., CHEN, J., SU, F., YAO, H. & SONG, E. 2011. Up-regulation of miR-21 mediates resistance to trastuzumab therapy for breast cancer. *J Biol Chem,* 286**,** 19127-37.

GOURI, A., DEKAKEN, A., EL BAIRI, K., AISSAOUI, A., LAABED, N., CHEFROUR, M., CICCOLINI, J., MILANO, G. & BENHARKAT, S. 2016. Plasminogen Activator System and Breast Cancer: Potential Role in Therapy Decision Making and Precision Medicine. *Biomark Insights,* 11**,** 105-11.

GRAVES, P. & ZENG, Y. 2012. Biogenesis of mammalian microRNAs: a global view. *Genomics Proteomics Bioinformatics,* 10**,** 239-45.

GRIFFITHS-JONES, S., GROCOCK, R. J., VAN DONGEN, S., BATEMAN, A. & ENRIGHT, A. J. 2006. miRBase: microRNA sequences, targets and gene nomenclature. *Nucleic Acids Res,* 34**,** D140-4.

GRIGNOL, V., FAIRCHILD, E. T., ZIMMERER, J. M., LESINSKI, G. B., WALKER, M. J., MAGRO, C. M., KACHER, J. E., KARPA, V. I., CLARK, J., NUOVO, G., LEHMAN, A., VOLINIA, S., AGNESE, D. M., CROCE, C. M. & CARSON, W. E., 3RD 2011. miR-21 and miR-155 are associated with mitotic activity and lesion depth of borderline melanocytic lesions. *Br J Cancer,* 105**,** 1023-9.

GRIMSON, A., FARH, K. K., JOHNSTON, W. K., GARRETT-ENGELE, P., LIM, L. P. & BARTEL, D. P. 2007. MicroRNA targeting specificity in mammals: determinants beyond seed pairing. *Mol Cell,* 27**,** 91-105.

GUAN, Y., WU, Y., LIU, Y., NI, J. & NONG, S. 2016. Association of microRNA-21 expression with clinicopathological characteristics and the risk of progression in advanced prostate cancer patients receiving androgen deprivation therapy. *Prostate,* 76**,** 986-93.

GUDJONSSON, T., RONNOV-JESSEN, L., VILLADSEN, R., RANK, F., BISSELL, M. J. & PETERSEN, O. W. 2002. Normal and tumor-derived myoepithelial cells differ in their ability to interact with luminal breast epithelial cells for polarity and basement membrane deposition. *J Cell Sci,* 115**,** 39-50.

GUO, H., INGOLIA, N. T., WEISSMAN, J. S. & BARTEL, D. P. 2010. Mammalian microRNAs predominantly act to decrease target mRNA levels. *Nature,* 466**,** 835-40.

HAN, J. G., JIANG, Y. D., ZHANG, C. H., YANG, Y. M., PANG, D., SONG, Y. N. & ZHANG, G. Q. 2017. A novel panel of serum miR-21/miR-155/miR-365 as a potential diagnostic biomarker for breast cancer. *Ann Surg Treat Res,* 92**,** 55-66.

HAN, M., WANG, F., GU, Y., PEI, X., GUO, G., YU, C., LI, L., ZHU, M., XIONG, Y. & WANG, Y. 2016. MicroRNA-21 induces breast cancer cell invasion and migration by suppressing smad7 via EGF and TGF-beta pathways. *Oncol Rep,* 35**,** 73-80.

HANNA, J. A., WIMBERLY, H., KUMAR, S., SLACK, F., AGARWAL, S. & RIMM, D. L. 2012. Quantitative analysis of microRNAs in tissue microarrays by in situ hybridization. *Biotechniques,* 52**,** 235-45.

HANNAFON, B. N., TRIGOSO, Y. D., CALLOWAY, C. L., ZHAO, Y. D., LUM, D. H., WELM, A. L., ZHAO, Z. J., BLICK, K. E., DOOLEY, W. C. & DING, W. Q. 2016. Plasma exosome microRNAs are indicative of breast cancer. *Breast Cancer Res,* 18**,** 90.

HAQUE, R., AHMED, S. A., INZHAKOVA, G., SHI, J., AVILA, C., POLIKOFF, J., BERNSTEIN, L., ENGER, S. M. & PRESS, M. F. 2012. Impact of breast cancer subtypes and treatment on survival: an analysis spanning two decades. *Cancer Epidemiol Biomarkers Prev,* 21**,** 1848-55.

HELDIN, C. H., RUBIN, K., PIETRAS, K. & OSTMAN, A. 2004. High interstitial fluid pressure - an obstacle in cancer therapy. *Nat Rev Cancer,* 4**,** 806-13.

HERMANSEN, S. K., DAHLROT, R. H., NIELSEN, B. S., HANSEN, S. & KRISTENSEN, B. W. 2013. MiR-21 expression in the tumor cell compartment holds unfavorable prognostic value in gliomas. *J Neurooncol,* 111**,** 71-81.

HOSSAIN, A., KUO, M. T. & SAUNDERS, G. F. 2006. Mir-17-5p regulates breast cancer cell proliferation by inhibiting translation of AIB1 mRNA. *Mol Cell Biol,* 26**,** 8191-201.

HUANG, G. L., ZHANG, X. H., GUO, G. L., HUANG, K. T., YANG, K. Y., SHEN, X., YOU, J. & HU, X. Q. 2009a. Clinical significance of miR-21 expression in breast cancer: SYBR-Green I-based real-time RT-PCR study of invasive ductal carcinoma. *Oncol Rep,* 21**,** 673-9.

HUANG, M., LI, Y., ZHANG, H. & NAN, F. 2010. Breast cancer stromal fibroblasts promote the generation of CD44+CD24- cells through SDF-1/CXCR4 interaction. *J Exp Clin Cancer Res,* 29**,** 80.

HUANG, T. H., WU, F., LOEB, G. B., HSU, R., HEIDERSBACH, A., BRINCAT, A., HORIUCHI, D., LEBBINK, R. J., MO, Y. Y., GOGA, A. & MCMANUS, M. T. 2009b. Up-regulation of miR-21 by HER2/neu signaling promotes cell invasion. *J Biol Chem,* 284**,** 18515-24.

HUANG, Y., SIMMS, A. E., MAZUR, A., WANG, S., LEON, N. R., JONES, B., AZIZ, N. & KELLY, T. 2011. Fibroblast activation protein-alpha promotes tumor growth and invasion of breast cancer cells through non-enzymatic functions. *Clin Exp Metastasis,* 28**,** 567-79.

HUG, K. A., ANTHONY, L., ELDEIRY, D., BENSON, J., WHEELER, E., MOUSA, S. & SHI, B. 2015. Expression and Tissue Distribution of MicroRNA-21 in Malignant and Benign Breast Tissues>. *Anticancer Res,* 35**,** 3175-83.

HULEIHEL, L., HUSSEY, G. S., NARANJO, J. D., ZHANG, L., DZIKI, J. L., TURNER, N. J., STOLZ, D. B. & BADYLAK, S. F. 2016. Matrix-bound nanovesicles within ECM bioscaffolds. *Sci Adv,* 2**,** e1600502.

HUMPHREYS, D. T., WESTMAN, B. J., MARTIN, D. I. & PREISS, T. 2005. MicroRNAs control translation initiation by inhibiting eukaryotic initiation factor 4E/cap and poly(A) tail function. *Proc Natl Acad Sci U S A,* 102**,** 16961-6.

HUNTZINGER, E., BRAUN, J. E., HEIMSTADT, S., ZEKRI, L. & IZAURRALDE, E. 2010. Two PABPC1-binding sites in GW182 proteins promote miRNA-mediated gene silencing. *EMBO J,* 29**,** 4146-60.

HYNES, R. O. 2009. The extracellular matrix: not just pretty fibrils. *Science,* 326**,** 1216-9.

IORIO, M. V., FERRACIN, M., LIU, C. G., VERONESE, A., SPIZZO, R., SABBIONI, S., MAGRI, E., PEDRIALI, M., FABBRI, M., CAMPIGLIO, M., MENARD, S., PALAZZO, J. P., ROSENBERG, A., MUSIANI, P., VOLINIA, S., NENCI, I., CALIN, G. A., QUERZOLI, P., NEGRINI, M. & CROCE, C. M. 2005. MicroRNA gene expression deregulation in human breast cancer. *Cancer Res,* 65**,** 7065-70.

ISANEJAD, A., ALIZADEH, A. M., AMANI SHALAMZARI, S., KHODAYARI, H., KHODAYARI, S., KHORI, V. & KHOJASTEHNJAD, N. 2016. MicroRNA-206, let-7a and microRNA-21 pathways involved in the anti-angiogenesis effects of the interval exercise training and hormone therapy in breast cancer. *Life Sci,* 151**,** 30-40.

ITANO, N. & KIMATA, K. 2008. Altered hyaluronan biosynthesis in cancer progression. *Semin Cancer Biol,* 18**,** 268-74.

JACQUEMET, G., HAMIDI, H. & IVASKA, J. 2015. Filopodia in cell adhesion, 3D migration and cancer cell invasion. *Curr Opin Cell Biol,* 36**,** 23-31.

JANG, K., AHN, H., SIM, J., HAN, H., ABDUL, R., PAIK, S. S., CHUNG, M. S. & JANG, S. J. 2014. Loss of microRNA-200a expression correlates with tumor progression in breast cancer. *Transl Res,* 163**,** 242-51.

JONES, C., NONNI, A. V., FULFORD, L., MERRETT, S., CHAGGAR, R., EUSEBI, V. & LAKHANI, S. R. 2001. CGH analysis of ductal carcinoma of the breast with basaloid/myoepithelial cell differentiation. *Br J Cancer,* 85**,** 422-7.

JORGENSEN, S., BAKER, A., MOLLER, S. & NIELSEN, B. S. 2010. Robust one-day in situ hybridization protocol for detection of microRNAs in paraffin samples using LNA probes. *Methods,* 52**,** 375-81.

KADERA, B. E., LI, L., TOSTE, P. A., WU, N., ADAMS, C., DAWSON, D. W. & DONAHUE, T. R. 2013. MicroRNA-21 in pancreatic ductal adenocarcinoma tumor-associated fibroblasts promotes metastasis. *PLoS One,* 8**,** e71978.

KALLURI, R. & ZEISBERG, M. 2006. Fibroblasts in cancer. *Nat Rev Cancer,* 6**,** 392-401.

KAO, J., SALARI, K., BOCANEGRA, M., CHOI, Y. L., GIRARD, L., GANDHI, J., KWEI, K. A., HERNANDEZ-BOUSSARD, T., WANG, P., GAZDAR, A. F., MINNA, J. D. & POLLACK, J. R. 2009. Molecular profiling of breast cancer cell lines defines relevant tumor models and provides a resource for cancer gene discovery. *PLoS One,* 4**,** e6146.

KAPLAN, D. H., SHANKARAN, V., DIGHE, A. S., STOCKERT, E., AGUET, M., OLD, L. J. & SCHREIBER, R. D. 1998. Demonstration of an interferon gamma-dependent tumor surveillance system in immunocompetent mice. *Proc Natl Acad Sci U S A,* 95**,** 7556-61.

KAUPPILA, S., STENBACK, F., RISTELI, J., JUKKOLA, A. & RISTELI, L. 1998. Aberrant type I and type III collagen gene expression in human breast cancer in vivo. *J Pathol,* 186**,** 262-8.

KENT, O. A., MCCALL, M. N., CORNISH, T. C. & HALUSHKA, M. K. 2014. Lessons from miR-143/145: the importance of cell-type localization of miRNAs. *Nucleic Acids Res,* 42**,** 7528-38.

KETTING, R. F., FISCHER, S. E., BERNSTEIN, E., SIJEN, T., HANNON, G. J. & PLASTERK, R. H. 2001. Dicer functions in RNA interference and in synthesis of small RNA involved in developmental timing in C. elegans. *Genes Dev,* 15**,** 2654-9.

KIM, Y. K., KIM, B. & KIM, V. N. 2016. Re-evaluation of the roles of DROSHA, Export in 5, and DICER in microRNA biogenesis. *Proc Natl Acad Sci U S A,* 113**,** E1881-9.

KIRIAKIDOU, M., TAN, G. S., LAMPRINAKI, S., DE PLANELL-SAGUER, M., NELSON, P. T. & MOURELATOS, Z. 2007. An mRNA m7G cap binding-like motif within human Ago2 represses translation. *Cell,* 129**,** 1141-51.

KISS, O., TOKES, A. M., VRANIC, S., GATALICA, Z., VASS, L., UDVARHELYI, N., SZASZ, A. M. & KULKA, J. 2015. Expression of miRNAs in adenoid cystic carcinomas of the breast and salivary glands. *Virchows Arch,* 467**,** 551-62.

KJAER-FRIFELDT, S., HANSEN, T. F., NIELSEN, B. S., JOERGENSEN, S., LINDEBJERG, J., SOERENSEN, F. B., DEPONT CHRISTENSEN, R. & JAKOBSEN, A. 2012. The prognostic importance of miR-21 in stage II colon cancer: a population-based study. *Br J Cancer,* 107**,** 1169-74.

KLOOSTERMAN, W. P. & PLASTERK, R. H. 2006. The diverse functions of microRNAs in animal development and disease. *Dev Cell,* 11**,** 441-50.

KOJIMA, Y., ACAR, A., EATON, E. N., MELLODY, K. T., SCHEEL, C., BEN-PORATH, I., ONDER, T. T., WANG, Z. C., RICHARDSON, A. L., WEINBERG, R. A. & ORIMO, A. 2010. Autocrine TGF-beta and stromal cell-derived factor-1 (SDF-1) signaling drives the evolution of tumor-promoting mammary stromal myofibroblasts. *Proc Natl Acad Sci U S A,* 107**,** 20009-14.

KOZOMARA, A. & GRIFFITHS-JONES, S. 2014. miRBase: annotating high confidence microRNAs using deep sequencing data. *Nucleic Acids Res,* 42**,** D68-73.

KUANG, Y. & NIE, Y. J. 2016. Exploration of the regulatory effect of miR-21 on breast cancer cell line proliferation and invasion as well as the downstream target genes. *Asian Pac J Trop Med,* 9**,** 470-3.

KUNINTY, P. R., BOJMAR, L., TJOMSLAND, V., LARSSON, M., STORM, G., OSTMAN, A., SANDSTROM, P. & PRAKASH, J. 2016a. MicroRNA-199a and -214 as

potential therapeutic targets in pancreatic stellate cells in pancreatic tumor. *Oncotarget,* 7**,** 16396-408.

KUNINTY, P. R., SCHNITTERT, J., STORM, G. & PRAKASH, J. 2016b. MicroRNA Targeting to Modulate Tumor Microenvironment. *Front Oncol,* 6**,** 3.

KURASHIGE, J., MIMA, K., SAWADA, G., TAKAHASHI, Y., EGUCHI, H., SUGIMACHI, K., MORI, M., YANAGIHARA, K., YASHIRO, M., HIRAKAWA, K., BABA, H. & MIMORI, K. 2015. Epigenetic modulation and repression of miR-200b by cancer-associated fibroblasts contribute to cancer invasion and peritoneal dissemination in gastric cancer. *Carcinogenesis,* 36**,** 133-41.

KUZET, S. E. & GAGGIOLI, C. 2016. Fibroblast activation in cancer: when seed fertilizes soil. *Cell Tissue Res,* 365**,** 607-19.

LAKHANI, S. R., ELLIS, I. O., SCHNITT, S. J., TAN, P. H. & VAN DE VIJVER, M. J. (eds.) 2012. *WHO classification of Tumours of the Breast, Fourth Edition*.

LAN, F., YUE, X., HAN, L., SHI, Z., YANG, Y., PU, P., YAO, Z. & KANG, C. 2012. Genome-wide identification of TCF7L2/TCF4 target miRNAs reveals a role for miR-21 in Wnt-driven epithelial cancer. *Int J Oncol,* 40**,** 519-26.

LEE, K. N., JACKSON, K. W., CHRISTIANSEN, V. J., LEE, C. S., CHUN, J. G. & MCKEE, P. A. 2006. Antiplasmin-cleaving enzyme is a soluble form of fibroblast activation protein. *Blood,* 107**,** 1397-404.

LEE, K. S., NAM, S. K., KOH, J., KIM, D. W., KANG, S. B., CHOE, G., KIM, W. H. & LEE, H. S. 2016. Stromal Expression of MicroRNA-21 in Advanced Colorectal Cancer Patients with Distant Metastases. *J Pathol Transl Med,* 50**,** 270-7.

LEE, Y., AHN, C., HAN, J., CHOI, H., KIM, J., YIM, J., LEE, J., PROVOST, P., RADMARK, O., KIM, S. & KIM, V. N. 2003. The nuclear RNase III Drosha initiates microRNA processing. *Nature,* 425**,** 415-9.

LEEK, R. D., LEWIS, C. E., WHITEHOUSE, R., GREENALL, M., CLARKE, J. & HARRIS, A. L. 1996. Association of macrophage infiltration with angiogenesis and prognosis in invasive breast carcinoma. *Cancer Res,* 56**,** 4625-9.

LEHMANN, B. D., BAUER, J. A., CHEN, X., SANDERS, M. E., CHAKRAVARTHY, A. B., SHYR, Y. & PIETENPOL, J. A. 2011. Identification of human triple-negative breast cancer subtypes and preclinical models for selection of targeted therapies. *J Clin Invest,* 121**,** 2750-67.

LEIDY, J., KHAN, A. & KANDIL, D. 2014. Basal-like breast cancer: update on clinicopathologic, immunohistochemical, and molecular features. *Arch Pathol Lab Med,* 138**,** 37-43.

LEVENTAL, K. R., YU, H., KASS, L., LAKINS, J. N., EGEBLAD, M., ERLER, J. T., FONG, S. F., CSISZAR, K., GIACCIA, A., WENINGER, W., YAMAUCHI, M., GASSER, D. L. & WEAVER, V. M. 2009. Matrix crosslinking forces tumor progression by enhancing integrin signaling. *Cell,* 139**,** 891-906.

LEWIS, B. P., BURGE, C. B. & BARTEL, D. P. 2005. Conserved seed pairing, often flanked by adenosines, indicates that thousands of human genes are microRNA targets. *Cell,* 120**,** 15-20.

LI, L. Q., LI, X. L., WANG, L., DU, W. J., GUO, R., LIANG, H. H., LIU, X., LIANG, D. S., LU, Y. J., SHAN, H. L. & JIANG, H. C. 2012. Matrine inhibits breast cancer growth via miR-21/PTEN/Akt pathway in MCF-7 cells. *Cell Physiol Biochem,* 30**,** 631-41.

LI, M., LI, M., YIN, T., SHI, H., WEN, Y., ZHANG, B., CHEN, M., XU, G., REN, K. & WEI, Y. 2016. Targeting of cancerassociated fibroblasts enhances the

efficacy of cancer chemotherapy by regulating the tumor microenvironment. *Mol Med Rep,* 13**,** 2476-84.
LI, Q., ZHANG, D., WANG, Y., SUN, P., HOU, X., LARNER, J., XIONG, W. & MI, J. 2013. MiR-21/Smad 7 signaling determines TGF-beta1-induced CAF formation. *Sci Rep,* 3**,** 2038.
LIN, S. L., MILLER, J. D. & YING, S. Y. 2006. Intronic microRNA (miRNA). *J Biomed Biotechnol,* 2006**,** 26818.
LIST, M., HAUSCHILD, A. C., TAN, Q., KRUSE, T. A., MOLLENHAUER, J., BAUMBACH, J. & BATRA, R. 2014. Classification of breast cancer subtypes by combining gene expression and DNA methylation data. *J Integr Bioinform,* 11**,** 236.
LIU, J., LI, D., DANG, L., LIANG, C., GUO, B., LU, C., HE, X., CHEUNG, H. Y., HE, B., LIU, B., LI, F., LU, J., WANG, L., SHAIKH, A. B., JIANG, F., LU, C., PENG, S., ZHANG, Z., ZHANG, B. T., PAN, X., XIAO, L., LU, A. & ZHANG, G. 2017. Osteoclastic miR-214 targets TRAF3 to contribute to osteolytic bone metastasis of breast cancer. *Sci Rep,* 7**,** 40487.
LIU, J., LIU, J., LI, J., CHEN, Y., GUAN, X., WU, X., HAO, C., SUN, Y., WANG, Y. & WANG, X. 2014a. Tumor-stroma ratio is an independent predictor for survival in early cervical carcinoma. *Gynecol Oncol,* 132**,** 81-6.
LIU, J., VALENCIA-SANCHEZ, M. A., HANNON, G. J. & PARKER, R. 2005. MicroRNA-dependent localization of targeted mRNAs to mammalian P-bodies. *Nat Cell Biol,* 7**,** 719-23.
LIU, L. & QIAN, H. 2015. [Up-regulation of miR-21 promotes cell proliferation and collagen synthesis in pulmonary fibroblasts]. *Xi Bao Yu Fen Zi Mian Yi Xue Za Zhi,* 31**,** 918-22.
LIU, Y., CAI, Q., BAO, P. P., SU, Y., CAI, H., WU, J., YE, F., GUO, X., ZHENG, W., ZHENG, Y. & SHU, X. O. 2015. Tumor tissue microRNA expression in association with triple-negative breast cancer outcomes. *Breast Cancer Res Treat,* 152**,** 183-91.
LIU, Y., HU, T., SHEN, J., LI, S. F., LIN, J. W., ZHENG, X. H., GAO, Q. H. & ZHOU, H. M. 2006. Separation, cultivation and biological characteristics of oral carcinoma-associated fibroblasts. *Oral Dis,* 12**,** 375-80.
LIU, Y., WANG, X., YANG, D., XIAO, Z. & CHEN, X. 2014b. MicroRNA-21 affects proliferation and apoptosis by regulating expression of PTEN in human keloid fibroblasts. *Plast Reconstr Surg,* 134**,** 561e-73e.
LORGER, M. & FELDING-HABERMANN, B. 2010. Capturing changes in the brain microenvironment during initial steps of breast cancer brain metastasis. *Am J Pathol,* 176**,** 2958-71.
LU, M., JU, S., SHEN, X., WANG, X., JING, R., YANG, C., CHU, H. & CONG, H. 2017. Combined detection of plasma miR-127-3p and HE4 improves the diagnostic efficacy of breast cancer. *Cancer Biomark,* 18**,** 143-148.
LU, P., WEAVER, V. M. & WERB, Z. 2012. The extracellular matrix: a dynamic niche in cancer progression. *J Cell Biol,* 196**,** 395-406.
LU, Z., LIU, M., STRIBINSKIS, V., KLINGE, C. M., RAMOS, K. S., COLBURN, N. H. & LI, Y. 2008. MicroRNA-21 promotes cell transformation by targeting the programmed cell death 4 gene. *Oncogene,* 27**,** 4373-9.
MA, L. 2016. MicroRNA and Metastasis. *Adv Cancer Res,* 132**,** 165-207.
MACHESKY, L. M. 2008. Lamellipodia and filopodia in metastasis and invasion. *FEBS Lett,* 582**,** 2102-11.

MACKENZIE, T. A., SCHWARTZ, G. N., CALDERONE, H. M., GRAVEEL, C. R., WINN, M. E., HOSTETTER, G., WELLS, W. A. & SEMPERE, L. F. 2014. Stromal expression of miR-21 identifies high-risk group in triple-negative breast cancer. *Am J Pathol,* 184**,** 3217-25.

MADAR, S., GOLDSTEIN, I. & ROTTER, V. 2013. 'Cancer associated fibroblasts'--more than meets the eye. *Trends Mol Med,* 19**,** 447-53.

MADHYASTHA, R., MADHYASTHA, H., NAKAJIMA, Y., OMURA, S. & MARUYAMA, M. 2012. MicroRNA signature in diabetic wound healing: promotive role of miR-21 in fibroblast migration. *Int Wound J,* 9**,** 355-61.

MARMOT, M. G. A., D.G.; CAMERON, D. A.; DEWAR, J. A.; THOMPSON, S. G.; WILCOX, M. 2012. The benefits and harms of breast cancer screening: an independent review. *Lancet,* 380**,** 1778-86.

MAYER, I. A., ABRAMSON, V. G., LEHMANN, B. D. & PIETENPOL, J. A. 2014. New strategies for triple-negative breast cancer--deciphering the heterogeneity. *Clin Cancer Res,* 20**,** 782-90.

MELBO-JORGENSEN, C., NESS, N., ANDERSEN, S., VALKOV, A., DONNEM, T., AL-SAAD, S., KISELEV, Y., BERG, T., NORDBY, Y., BREMNES, R. M., BUSUND, L. T. & RICHARDSEN, E. 2014. Stromal expression of MiR-21 predicts biochemical failure in prostate cancer patients with Gleason score 6. *PLoS One,* 9**,** e113039.

MENG, F., HENSON, R., WEHBE-JANEK, H., GHOSHAL, K., JACOB, S. T. & PATEL, T. 2007. MicroRNA-21 regulates expression of the PTEN tumor suppressor gene in human hepatocellular cancer. *Gastroenterology,* 133**,** 647-58.

MERCIER, I., CASIMIRO, M. C., WANG, C., ROSENBERG, A. L., QUONG, J., MINKEU, A., ALLEN, K. G., DANILO, C., SOTGIA, F., BONUCCELLI, G., JASMIN, J. F., XU, H., BOSCO, E., ARONOW, B., WITKIEWICZ, A., PESTELL, R. G., KNUDSEN, E. S. & LISANTI, M. P. 2008. Human breast cancer-associated fibroblasts (CAFs) show caveolin-1 downregulation and RB tumor suppressor functional inactivation: Implications for the response to hormonal therapy. *Cancer Biol Ther,* 7**,** 1212-25.

MESKER, W. E., LIEFERS, G. J., JUNGGEBURT, J. M., VAN PELT, G. W., ALBERICI, P., KUPPEN, P. J., MIRANDA, N. F., VAN LEEUWEN, K. A., MORREAU, H., SZUHAI, K., TOLLENAAR, R. A. & TANKE, H. J. 2009. Presence of a high amount of stroma and downregulation of SMAD4 predict for worse survival for stage I-II colon cancer patients. *Cell Oncol,* 31**,** 169-78.

MESTDAGH, P., FEYS, T., BERNARD, N., GUENTHER, S., CHEN, C., SPELEMAN, F. & VANDESOMPELE, J. 2008. High-throughput stem-loop RT-qPCR miRNA expression profiling using minute amounts of input RNA. *Nucleic Acids Res,* 36**,** e143.

METZGER-FILHO, O., SUN, Z., VIALE, G., PRICE, K. N., CRIVELLARI, D., SNYDER, R. D., GELBER, R. D., CASTIGLIONE-GERTSCH, M., COATES, A. S., GOLDHIRSCH, A. & CARDOSO, F. 2013. Patterns of Recurrence and outcome according to breast cancer subtypes in lymph node-negative disease: results from international breast cancer study group trials VIII and IX. *J Clin Oncol,* 31**,** 3083-90.

MILES, D. W., CHAN, A., DIRIX, L. Y., CORTES, J., PIVOT, X., TOMCZAK, P., DELOZIER, T., SOHN, J. H., PROVENCHER, L., PUGLISI, F., HARBECK, N., STEGER, G. G., SCHNEEWEISS, A., WARDLEY, A. M., CHLISTALLA, A. &

ROMIEU, G. 2010. Phase III study of bevacizumab plus docetaxel compared with placebo plus docetaxel for the first-line treatment of human epidermal growth factor receptor 2-negative metastatic breast cancer. *J Clin Oncol,* 28**,** 3239-47.

MILLER, K., WANG, M., GRALOW, J., DICKLER, M., COBLEIGH, M., PEREZ, E. A., SHENKIER, T., CELLA, D. & DAVIDSON, N. E. 2007. Paclitaxel plus bevacizumab versus paclitaxel alone for metastatic breast cancer. *N Engl J Med,* 357**,** 2666-76.

MILLER, K. D., GRADISHAR, W., SCHUCHTER, L., SPARANO, J. A., COBLEIGH, M., ROBERT, N., RASMUSSEN, H. & SLEDGE, G. W. 2002. A randomized phase II pilot trial of adjuvant marimastat in patients with early-stage breast cancer. *Ann Oncol,* 13**,** 1220-4.

MINEMURA, H., TAKAGI, K., MIKI, Y., SHIBAHARA, Y., NAKAGAWA, S., EBATA, A., WATANABE, M., ISHIDA, T., SASANO, H. & SUZUKI, T. 2015. Abnormal expression of miR-1 in breast carcinoma as a potent prognostic factor. *Cancer Sci,* 106**,** 1642-50.

MIRBASE 2011.

MIRBASE 2016. http://www.mirbase.org/cgi-bin/mirna_summary.pl?org=hsa.

MITRA, A. K., ZILLHARDT, M., HUA, Y., TIWARI, P., MURMANN, A. E., PETER, M. E. & LENGYEL, E. 2012. MicroRNAs reprogram normal fibroblasts into cancer-associated fibroblasts in ovarian cancer. *Cancer Discov,* 2**,** 1100-8.

MOORMAN, A. M., VINK, R., HEIJMANS, H. J., VAN DER PALEN, J. & KOUWENHOVEN, E. A. 2012. The prognostic value of tumour-stroma ratio in triple-negative breast cancer. *Eur J Surg Oncol,* 38**,** 307-13.

MORINAGA, S., NAKAMURA, Y., ATSUMI, Y., MURAKAWA, M., YAMAOKU, K., AOYAMA, T., KOBAYASHI, S., UENO, M., MORIMOTO, M., YOKOSE, T. & MIYAGI, Y. 2016. Locked Nucleic Acid In Situ Hybridization Analysis of MicroRNA-21 Predicts Clinical Outcome in Patients After Resection for Pancreatic Cancer Treated with Adjuvant Gemcitabine Monotherapy. *Anticancer Res,* 36**,** 1083-8.

MOTAWI, T. M., SADIK, N. A., SHAKER, O. G., EL MASRY, M. R. & MOHAREB, F. 2016. Study of microRNAs-21/221 as potential breast cancer biomarkers in Egyptian women. *Gene,* 590**,** 210-9.

MUNAGALA, R., AQIL, F. & GUPTA, R. C. 2016. Exosomal miRNAs as biomarkers of recurrent lung cancer. *Tumour Biol,* 37**,** 10703-14.

MUNCH-PETERSEN, H. D., RALFKIAER, U., SJO, L. D., HOTHER, C., ASMAR, F., NIELSEN, B. S., BROWN, P., RALFKIAER, E. & GRONBAEK, K. 2015. Differential expression of miR-155 and miR-21 in tumor and stroma cells in diffuse large B-cell lymphoma. *Appl Immunohistochem Mol Morphol,* 23**,** 188-95.

MUSCHLER, J. & STREULI, C. H. 2010. Cell-matrix interactions in mammary gland development and breast cancer. *Cold Spring Harb Perspect Biol,* 2**,** a003202.

NEILL, D. R., WONG, S. H., BELLOSI, A., FLYNN, R. J., DALY, M., LANGFORD, T. K., BUCKS, C., KANE, C. M., FALLON, P. G., PANNELL, R., JOLIN, H. E. & MCKENZIE, A. N. 2010. Nuocytes represent a new innate effector leukocyte that mediates type-2 immunity. *Nature,* 464**,** 1367-70.

NENUTIL, R., SMARDOVA, J., PAVLOVA, S., HANZELKOVA, Z., MULLER, P., FABIAN, P., HRSTKA, R., JANOTOVA, P., RADINA, M., LANE, D. P., COATES,

P. J. & VOJTESEK, B. 2005. Discriminating functional and non-functional p53 in human tumours by p53 and MDM2 immunohistochemistry. *J Pathol,* 207**,** 251-9.

NEVE, R. M., CHIN, K., FRIDLYAND, J., YEH, J., BAEHNER, F. L., FEVR, T., CLARK, L., BAYANI, N., COPPE, J. P., TONG, F., SPEED, T., SPELLMAN, P. T., DEVRIES, S., LAPUK, A., WANG, N. J., KUO, W. L., STILWELL, J. L., PINKEL, D., ALBERTSON, D. G., WALDMAN, F. M., MCCORMICK, F., DICKSON, R. B., JOHNSON, M. D., LIPPMAN, M., ETHIER, S., GAZDAR, A. & GRAY, J. W. 2006. A collection of breast cancer cell lines for the study of functionally distinct cancer subtypes. *Cancer Cell,* 10**,** 515-27.

NIELSEN, B. S., BALSLEV, E., POULSEN, T. S., NIELSEN, D., MOLLER, T., MORTENSEN, C. E., HOLMSTROM, K. & HOGDALL, E. 2014. miR-21 Expression in Cancer Cells may Not Predict Resistance to Adjuvant Trastuzumab in Primary Breast Cancer. *Front Oncol,* 4**,** 207.

NIELSEN, C. B., SHOMRON, N., SANDBERG, R., HORNSTEIN, E., KITZMAN, J. & BURGE, C. B. 2007. Determinants of targeting by endogenous and exogenous microRNAs and siRNAs. *RNA,* 13**,** 1894-910.

NIELSEN, T. O., HSU, F. D., JENSEN, K., CHEANG, M., KARACA, G., HU, Z., HERNANDEZ-BOUSSARD, T., LIVASY, C., COWAN, D., DRESSLER, L., AKSLEN, L. A., RAGAZ, J., GOWN, A. M., GILKS, C. B., VAN DE RIJN, M. & PEROU, C. M. 2004. Immunohistochemical and clinical characterization of the basal-like subtype of invasive breast carcinoma. *Clin Cancer Res,* 10**,** 5367-74.

NIKIFOROVA, Z. N., TAIPOV, M. A., KUDRYAVCEV, I. A. & SHEVCHENKO, V. E. 2016. [The connection of miR-21 and miR-155 with regulation of 15-HPGDH mRNA in human breast cancer cells]. *Biomed Khim,* 62**,** 265-71.

NIU, J., SHI, Y., TAN, G., YANG, C. H., FAN, M., PFEFFER, L. M. & WU, Z. H. 2012. DNA damage induces NF-kappaB-dependent microRNA-21 up-regulation and promotes breast cancer cell invasion. *J Biol Chem,* 287**,** 21783-95.

NOURAEE, N., KHAZAEI, S., VASEI, M., RAZAVIPOUR, S. F., SADEGHIZADEH, M. & MOWLA, S. J. 2016. MicroRNAs contribution in tumor microenvironment of esophageal cancer. *Cancer Biomark,* 16**,** 367-76.

NOURAEE, N., VAN ROOSBROECK, K., VASEI, M., SEMNANI, S., SAMAEI, N. M., NAGHSHVAR, F., OMIDI, A. A., CALIN, G. A. & MOWLA, S. J. 2013. Expression, tissue distribution and function of miR-21 in esophageal squamous cell carcinoma. *PLoS One,* 8**,** e73009.

NOZAWA, H., CHIU, C. & HANAHAN, D. 2006. Infiltrating neutrophils mediate the initial angiogenic switch in a mouse model of multistage carcinogenesis. *Proc Natl Acad Sci U S A,* 103**,** 12493-8.

O'DONNELL, K. A., WENTZEL, E. A., ZELLER, K. I., DANG, C. V. & MENDELL, J. T. 2005. c-Myc-regulated microRNAs modulate E2F1 expression. *Nature,* 435**,** 839-43.

ONS 2014. Office for National Statistics

Cancer Registration Statistics, England: 2014.

ORIMO, A., GUPTA, P. B., SGROI, D. C., ARENZANA-SEISDEDOS, F., DELAUNAY, T., NAEEM, R., CAREY, V. J., RICHARDSON, A. L. & WEINBERG, R. A. 2005. Stromal fibroblasts present in invasive human breast carcinomas

promote tumor growth and angiogenesis through elevated SDF-1/CXCL12 secretion. *Cell,* 121**,** 335-48.
OSKARSSON, T. 2013. Extracellular matrix components in breast cancer progression and metastasis. *Breast,* 22 Suppl 2**,** S66-72.
OVERALL, C. M. & KLEIFELD, O. 2006. Tumour microenvironment - opinion: validating matrix metalloproteinases as drug targets and anti-targets for cancer therapy. *Nat Rev Cancer,* 6**,** 227-39.
PAN, Y., JIAO, G., WANG, C., YANG, J. & YANG, W. 2016. MicroRNA-421 inhibits breast cancer metastasis by targeting metastasis associated 1. *Biomed Pharmacother,* 83**,** 1398-1406.
PAQUETTE, B., THERRIAULT, H., DESMARAIS, G., WAGNER, R., ROYER, R. & BUJOLD, R. 2011. Radiation-enhancement of MDA-MB-231 breast cancer cell invasion prevented by a cyclooxygenase-2 inhibitor. *Br J Cancer,* 105**,** 534-41.
PARDOLL, D. M. 2012. The blockade of immune checkpoints in cancer immunotherapy. *Nat Rev Cancer,* 12**,** 252-64.
PARKER, J. S., MULLINS, M., CHEANG, M. C., LEUNG, S., VODUC, D., VICKERY, T., DAVIES, S., FAURON, C., HE, X., HU, Z., QUACKENBUSH, J. F., STIJLEMAN, I. J., PALAZZO, J., MARRON, J. S., NOBEL, A. B., MARDIS, E., NIELSEN, T. O., ELLIS, M. J., PEROU, C. M. & BERNARD, P. S. 2009. Supervised risk predictor of breast cancer based on intrinsic subtypes. *J Clin Oncol,* 27**,** 1160-7.
PARSONS, M. G., H. 2009. How to make tissue microarrays. *Diagnostic Histopathology,* 15**,** 142-150.
PARTRIDGE, A. H., HUGHES, M. E., WARNER, E. T., OTTESEN, R. A., WONG, Y. N., EDGE, S. B., THERIAULT, R. L., BLAYNEY, D. W., NILAND, J. C., WINER, E. P., WEEKS, J. C. & TAMIMI, R. M. 2016. Subtype-Dependent Relationship Between Young Age at Diagnosis and Breast Cancer Survival. *J Clin Oncol*.
PATEL, S. A. & GOODERHAM, N. J. 2015. IL6 Mediates Immune and Colorectal Cancer Cell Cross-talk via miR-21 and miR-29b. *Mol Cancer Res,* 13**,** 1502-8.
PEREZ-RIVAS, L. G., JEREZ, J. M., CARMONA, R., DE LUQUE, V., VICIOSO, L., CLAROS, M. G., VIGUERA, E., PAJARES, B., SANCHEZ, A., RIBELLES, N., ALBA, E. & LOZANO, J. 2014. A microRNA signature associated with early recurrence in breast cancer. *PLoS One,* 9**,** e91884.
PEROU, C. M., SORLIE, T., EISEN, M. B., VAN DE RIJN, M., JEFFREY, S. S., REES, C. A., POLLACK, J. R., ROSS, D. T., JOHNSEN, H., AKSLEN, L. A., FLUGE, O., PERGAMENSCHIKOV, A., WILLIAMS, C., ZHU, S. X., LONNING, P. E., BORRESEN-DALE, A. L., BROWN, P. O. & BOTSTEIN, D. 2000. Molecular portraits of human breast tumours. *Nature,* 406**,** 747-52.
PILLAI, R. S., ARTUS, C. G. & FILIPOWICZ, W. 2004. Tethering of human Ago proteins to mRNA mimics the miRNA-mediated repression of protein synthesis. *RNA,* 10**,** 1518-25.
PILLAI, R. S., BHATTACHARYYA, S. N., ARTUS, C. G., ZOLLER, T., COUGOT, N., BASYUK, E., BERTRAND, E. & FILIPOWICZ, W. 2005. Inhibition of translational initiation by Let-7 MicroRNA in human cells. *Science,* 309**,** 1573-6.
POLLARD, J. W. 2009. Trophic macrophages in development and disease. *Nat Rev Immunol,* 9**,** 259-70.

PORRETTI, J. C., MOHAMAD, N. A., MARTIN, G. A. & CRICCO, G. P. 2014. Fibroblasts induce epithelial to mesenchymal transition in breast tumor cells which is prevented by fibroblasts treatment with histamine in high concentration. *Int J Biochem Cell Biol,* 51**,** 29-38.

PRAT, A., PARKER, J. S., KARGINOVA, O., FAN, C., LIVASY, C., HERSCHKOWITZ, J. I., HE, X. & PEROU, C. M. 2010. Phenotypic and molecular characterization of the claudin-low intrinsic subtype of breast cancer. *Breast Cancer Res,* 12**,** R68.

PROVENZANO, P. P., INMAN, D. R., ELICEIRI, K. W., KNITTEL, J. G., YAN, L., RUEDEN, C. T., WHITE, J. G. & KEELY, P. J. 2008. Collagen density promotes mammary tumor initiation and progression. *BMC Med,* 6**,** 11.

PSAILA, B. & LYDEN, D. 2009. The metastatic niche: adapting the foreign soil. *Nat Rev Cancer,* 9**,** 285-93.

QI, L., BART, J., TAN, L. P., PLATTEEL, I., SLUIS, T., HUITEMA, S., HARMS, G., FU, L., HOLLEMA, H. & BERG, A. 2009. Expression of miR-21 and its targets (PTEN, PDCD4, TM1) in flat epithelial atypia of the breast in relation to ductal carcinoma in situ and invasive carcinoma. *BMC Cancer,* 9**,** 163.

QUESNE, J. L., JONES, J., WARREN, J., DAWSON, S. J., ALI, H. R., BARDWELL, H., BLOWS, F., PHAROAH, P. & CALDAS, C. 2012. Biological and prognostic associations of miR-205 and let-7b in breast cancer revealed by in situ hybridization analysis of micro-RNA expression in arrays of archival tumour tissue. *J Pathol,* 227**,** 306-14.

R CORE TEAM, R. 2016. *R: A language and environment for statistical computing* [Online]. Available: https://http://www.R-project.org/.

RABBANI, A., FINN, R. M. & AUSIO, J. 2005. The anthracycline antibiotics: antitumor drugs that alter chromatin structure. *Bioessays,* 27**,** 50-6.

RAKHA, E. A., REIS-FILHO, J. S. & ELLIS, I. O. 2008. Basal-like breast cancer: a critical review. *J Clin Oncol,* 26**,** 2568-81.

RASK, L., BALSLEV, E., JORGENSEN, S., ERIKSEN, J., FLYGER, H., MOLLER, S., HOGDALL, E., LITMAN, T. & NIELSEN, B. S. 2011. High expression of miR-21 in tumor stroma correlates with increased cancer cell proliferation in human breast cancer. *APMIS,* 119**,** 663-73.

REIS, R. S., EAMENS, A. L. & WATERHOUSE, P. M. 2015. Missing Pieces in the Puzzle of Plant MicroRNAs. *Trends Plant Sci,* 20**,** 721-8.

REN, Y., ZHOU, X., LIU, X., JIA, H. H., ZHAO, X. H., WANG, Q. X., HAN, L., SONG, X., ZHU, Z. Y., SUN, T., JIAO, H. X., TIAN, W. P., YANG, Y. Q., ZHAO, X. L., ZHANG, L., MEI, M. & KANG, C. S. 2016. Reprogramming carcinoma associated fibroblasts by AC1MMYR2 impedes tumor metastasis and improves chemotherapy efficacy. *Cancer Lett,* 374**,** 96-106.

RICART, A. D., TOLCHER, A. W., LIU, G., HOLEN, K., SCHWARTZ, G., ALBERTINI, M., WEISS, G., YAZJI, S., NG, C. & WILDING, G. 2008. Volociximab, a chimeric monoclonal antibody that specifically binds alpha5beta1 integrin: a phase I, pharmacokinetic, and biological correlative study. *Clin Cancer Res,* 14**,** 7924-9.

ROBERT, N. J., DIERAS, V., GLASPY, J., BRUFSKY, A. M., BONDARENKO, I., LIPATOV, O. N., PEREZ, E. A., YARDLEY, D. A., CHAN, S. Y., ZHOU, X., PHAN, S. C. & O'SHAUGHNESSY, J. 2011. RIBBON-1: randomized, double-blind, placebo-controlled, phase III trial of chemotherapy with or without bevacizumab for first-line treatment of human epidermal

growth factor receptor 2-negative, locally recurrent or metastatic breast cancer. *J Clin Oncol,* 29**,** 1252-60.

RONNOV-JESSEN, L., PETERSEN, O. W. & BISSELL, M. J. 1996. Cellular changes involved in conversion of normal to malignant breast: importance of the stromal reaction. *Physiol Rev,* 76**,** 69-125.

RUI, M., QU, Y., GAO, T., GE, Y., FENG, C. & XU, X. 2017. Simultaneous delivery of anti-miR21 with doxorubicin prodrug by mimetic lipoprotein nanoparticles for synergistic effect against drug resistance in cancer cells. *Int J Nanomedicine,* 12**,** 217-237.

SADLONOVA, A., BOWE, D. B., NOVAK, Z., MUKHERJEE, S., DUNCAN, V. E., PAGE, G. P. & FROST, A. R. 2009. Identification of molecular distinctions between normal breast-associated fibroblasts and breast cancer-associated fibroblasts. *Cancer Microenviron,* 2**,** 9-21.

SALOMON, C., KOBAYASHI, M., ASHMAN, K., SOBREVIA, L., MITCHELL, M. D. & RICE, G. E. 2013. Hypoxia-induced changes in the bioactivity of cytotrophoblast-derived exosomes. *PLoS One,* 8**,** e79636.

SALOMON, C., TORRES, M. J., KOBAYASHI, M., SCHOLZ-ROMERO, K., SOBREVIA, L., DOBIERZEWSKA, A., ILLANES, S. E., MITCHELL, M. D. & RICE, G. E. 2014. A gestational profile of placental exosomes in maternal plasma and their effects on endothelial cell migration. *PLoS One,* 9**,** e98667.

SANCHEZ, C. A., ANDAHUR, E. I., VALENZUELA, R., CASTELLON, E. A., FULLA, J. A., RAMOS, C. G. & TRIVINO, J. C. 2016. Exosomes from bulk and stem cells from human prostate cancer have a differential microRNA content that contributes cooperatively over local and pre-metastatic niche. *Oncotarget,* 7**,** 3993-4008.

SANSONE, P., BERISHAJ, M., RAJASEKHAR, V. K., CECCARELLI, C., CHANG, Q., STRILLACCI, A., SAVINI, C., SHAPIRO, L., BOWMAN, R., MASTROLEO, C., DE CAROLIS, S., DALY, L., BENITO-MARTIN, A., PERNA, F., FABBRI, N., HEALEY, J. H., SPISNI, E., CRICCA, M., LYDEN, D., BONAFE, M. & BROMBERG, J. 2017. Evolution of cancer stem-like cells in endocrine-resistant metastatic breast cancers is mediated by stromal microvesicles. *Cancer Res*.

SCHMITTER, D., FILKOWSKI, J., SEWER, A., PILLAI, R. S., OAKELEY, E. J., ZAVOLAN, M., SVOBODA, P. & FILIPOWICZ, W. 2006. Effects of Dicer and Argonaute down-regulation on mRNA levels in human HEK293 cells. *Nucleic Acids Res,* 34**,** 4801-15.

SCHMITZ, N., LAVERTY, S., KRAUS, V. B. & AIGNER, T. 2010. Basic methods in histopathology of joint tissues. *Osteoarthritis Cartilage,* 18 Suppl 3**,** S113-6.

SCHRADER, C., SCHIELKE, A., ELLERBROEK, L. & JOHNE, R. 2012. PCR inhibitors - occurrence, properties and removal. *J Appl Microbiol,* 113**,** 1014-26.

SCHREIBER, R. D., OLD, L. J. & SMYTH, M. J. 2011. Cancer immunoediting: integrating immunity's roles in cancer suppression and promotion. *Science,* 331**,** 1565-70.

SCOTT, A. M., WISEMAN, G., WELT, S., ADJEI, A., LEE, F. T., HOPKINS, W., DIVGI, C. R., HANSON, L. H., MITCHELL, P., GANSEN, D. N., LARSON, S. M., INGLE, J. N., HOFFMAN, E. W., TANSWELL, P., RITTER, G., COHEN, L. S., BETTE, P., ARVAY, L., AMELSBERG, A., VLOCK, D., RETTIG, W. J. & OLD, L. J. 2003. A Phase I dose-escalation study of sibrotuzumab in patients with

advanced or metastatic fibroblast activation protein-positive cancer. *Clin Cancer Res,* 9**,** 1639-47.

SELCUKLU, S. D., DONOGHUE, M. T., KERIN, M. J. & SPILLANE, C. 2012. Regulatory interplay between miR-21, JAG1 and 17beta-estradiol (E2) in breast cancer cells. *Biochem Biophys Res Commun,* 423**,** 234-9.

SHAH, S. H., MILLER, P., GARCIA-CONTRERAS, M., AO, Z., MACHLIN, L., ISSA, E. & EL-ASHRY, D. 2015. Hierarchical paracrine interaction of breast cancer associated fibroblasts with cancer cells via hMAPK-microRNAs to drive ER-negative breast cancer phenotype. *Cancer Biol Ther,* 16**,** 1671-81.

SHEN, S., SUN, Q., LIANG, Z., CUI, X., REN, X., CHEN, H., ZHANG, X. & ZHOU, Y. 2014. A prognostic model of triple-negative breast cancer based on miR-27b-3p and node status. *PLoS One,* 9**,** e100664.

SHIDFAR, A., COSTA, F. F., SCHOLTENS, D. M., BISCHOF, J. M., SULLIVAN, M. E., IVANCIC, D., VANIN, E. F., SOARES, M. B., WANG, J. & KHAN, S. A. 2016. Expression of miR-18a and miR-210 in normal breast tissue as candidate biomarkers of breast cancer risk. *Cancer Prev Res (Phila)*.

SHIN, V. Y., SIU, J. M., CHEUK, I., NG, E. K. & KWONG, A. 2015. Circulating cell-free miRNAs as biomarker for triple-negative breast cancer. *Br J Cancer,* 112**,** 1751-9.

SHOJAEI, F., SINGH, M., THOMPSON, J. D. & FERRARA, N. 2008. Role of Bv8 in neutrophil-dependent angiogenesis in a transgenic model of cancer progression. *Proc Natl Acad Sci U S A,* 105**,** 2640-5.

SILVA, G. & ABOUSSEKHRA, A. 2016. p16(INK4A) inhibits the pro-metastatic potentials of osteosarcoma cells through targeting the ERK pathway and TGF-beta1. *Mol Carcinog,* 55**,** 525-36.

SIMPKINS, S. A., HANBY, A. M., HOLLIDAY, D. L. & SPEIRS, V. 2012. Clinical and functional significance of loss of caveolin-1 expression in breast cancer-associated fibroblasts. *J Pathol,* 227**,** 490-8.

SINN, H. P. & KREIPE, H. 2013. A Brief Overview of the WHO Classification of Breast Tumors, 4th Edition, Focusing on Issues and Updates from the 3rd Edition. *Breast Care (Basel),* 8**,** 149-54.

SIRICA, A. E. 2011. The role of cancer-associated myofibroblasts in intrahepatic cholangiocarcinoma. *Nat Rev Gastroenterol Hepatol,* 9**,** 44-54.

SLEDGE, G. W., JR., QULALI, M., GOULET, R., BONE, E. A. & FIFE, R. 1995. Effect of matrix metalloproteinase inhibitor batimastat on breast cancer regrowth and metastasis in athymic mice. *J Natl Cancer Inst,* 87**,** 1546-50.

SOCHOR, M., BASOVA, P., PESTA, M., DUSILKOVA, N., BARTOS, J., BURDA, P., POSPISIL, V. & STOPKA, T. 2014. Oncogenic microRNAs: miR-155, miR-19a, miR-181b, and miR-24 enable monitoring of early breast cancer in serum. *BMC Cancer,* 14**,** 448.

SONG, B., WANG, C., LIU, J., WANG, X., LV, L., WEI, L., XIE, L., ZHENG, Y. & SONG, X. 2010. MicroRNA-21 regulates breast cancer invasion partly by targeting tissue inhibitor of metalloproteinase 3 expression. *J Exp Clin Cancer Res,* 29**,** 29.

SONG, C., LIU, L. Z., PEI, X. Q., LIU, X., YANG, L., YE, F., XIE, X., CHEN, J., TANG, H. & XIE, X. 2015. miR-200c inhibits breast cancer proliferation by targeting KRAS. *Oncotarget,* 6**,** 34968-78.

SONG, C., ZHANG, L., WANG, J., HUANG, Z., LI, X., WU, M., LI, S., TANG, H. & XIE, X. 2016a. High expression of microRNA-183/182/96 cluster as a prognostic biomarker for breast cancer. *Sci Rep,* 6**,** 24502.

SONG, N., LIANG, B. & WANG, D. 2016b. The function of MiR-21 expression differences and pathogenesis on familial and triple negative breast Cancer serum. *Pak J Pharm Sci,* 29**,** 679-84.

SORLIE, T., PEROU, C. M., TIBSHIRANI, R., AAS, T., GEISLER, S., JOHNSEN, H., HASTIE, T., EISEN, M. B., VAN DE RIJN, M., JEFFREY, S. S., THORSEN, T., QUIST, H., MATESE, J. C., BROWN, P. O., BOTSTEIN, D., LONNING, P. E. & BORRESEN-DALE, A. L. 2001. Gene expression patterns of breast carcinomas distinguish tumor subclasses with clinical implications. *Proc Natl Acad Sci U S A,* 98**,** 10869-74.

STANEK, L., ROZKOS, T., LACO, J., RYSKA, A., PETRUZELKA, L., DURA, M. & DUNDR, P. 2014. Comparison of immunohistochemistry, four in situ hybridization methods and quantitative polymerase chain reaction for the molecular diagnosis of HER2 status in gastric cancer: a study of 55 cases. *Mol Med Rep,* 10**,** 2669-74.

STENVOLD, H., DONNEM, T., ANDERSEN, S., AL-SAAD, S., VALKOV, A., PEDERSEN, M. I., BUSUND, L. T. & BREMNES, R. M. 2014. High tumor cell expression of microRNA-21 in node positive non-small cell lung cancer predicts a favorable clinical outcome. *BMC Clin Pathol,* 14**,** 9.

STREULI, C. H., SCHMIDHAUSER, C., BAILEY, N., YURCHENCO, P., SKUBITZ, A. P., ROSKELLEY, C. & BISSELL, M. J. 1995. Laminin mediates tissue-specific gene expression in mammary epithelia. *J Cell Biol,* 129**,** 591-603.

SUBIK, K., LEE, J. F., BAXTER, L., STRZEPEK, T., COSTELLO, D., CROWLEY, P., XING, L., HUNG, M. C., BONFIGLIO, T., HICKS, D. G. & TANG, P. 2010. The Expression Patterns of ER, PR, HER2, CK5/6, EGFR, Ki-67 and AR by Immunohistochemical Analysis in Breast Cancer Cell Lines. *Breast Cancer (Auckl),* 4**,** 35-41.

SUGIMOTO, H., MUNDEL, T. M., KIERAN, M. W. & KALLURI, R. 2006. Identification of fibroblast heterogeneity in the tumor microenvironment. *Cancer Biol Ther,* 5**,** 1640-6.

SVOBODOVA, E., KUBIKOVA, J. & SVOBODA, P. 2016. Production of small RNAs by mammalian Dicer. *Pflugers Arch,* 468**,** 1089-102.

TAGHIAN, A., MOHIUDDIN, M., JAGSI, R., GOLDBERG, S., CEILLEY, E. & POWELL, S. 2005. Current perceptions regarding surgical margin status after breast-conserving therapy: results of a survey. *Ann Surg,* 241**,** 629-39.

TAKAHASHI, R. U., MIYAZAKI, H., TAKESHITA, F., YAMAMOTO, Y., MINOURA, K., ONO, M., KODAIRA, M., TAMURA, K., MORI, M. & OCHIYA, T. 2015. Loss of microRNA-27b contributes to breast cancer stem cell generation by activating ENPP1. *Nat Commun,* 6**,** 7318.

TAKIKAWA, T., MASAMUNE, A., YOSHIDA, N., HAMADA, S., KOGURE, T. & SHIMOSEGAWA, T. 2017. Exosomes Derived From Pancreatic Stellate Cells: MicroRNA Signature and Effects on Pancreatic Cancer Cells. *Pancreas,* 46**,** 19-27.

TANG, F., HAJKOVA, P., BARTON, S. C., LAO, K. & SURANI, M. A. 2006. MicroRNA expression profiling of single whole embryonic stem cells. *Nucleic Acids Res,* 34**,** e9.

TANG, X., HOU, Y., YANG, G., WANG, X., TANG, S., DU, Y. E., YANG, L., YU, T., ZHANG, H., ZHOU, M., WEN, S., XU, L. & LIU, M. 2016. Stromal miR-200s contribute to breast cancer cell invasion through CAF activation and ECM remodeling. *Cell Death Differ,* 23**,** 132-45.

TANIC, M., YANOWSKI, K., ANDRES, E., GOMEZ-LOPEZ, G., SOCORRO, M. R., PISANO, D. G., MARTINEZ-DELGADO, B. & BENITEZ, J. 2015. miRNA expression profiling of formalin-fixed paraffin-embedded (FFPE) hereditary breast tumors. *Genom Data,* 3**,** 75-9.

THIKE, A. A., CHEOK, P. Y., JARA-LAZARO, A. R., TAN, B., TAN, P. & TAN, P. H. 2010. Triple-negative breast cancer: clinicopathological characteristics and relationship with basal-like breast cancer. *Mod Pathol,* 23**,** 123-33.

THOMSON, D. W., BRACKEN, C. P., SZUBERT, J. M. & GOODALL, G. J. 2013. On measuring miRNAs after transient transfection of mimics or antisense inhibitors. *PLoS One,* 8**,** e55214.

THUM, T., GROSS, C., FIEDLER, J., FISCHER, T., KISSLER, S., BUSSEN, M., GALUPPO, P., JUST, S., ROTTBAUER, W., FRANTZ, S., CASTOLDI, M., SOUTSCHEK, J., KOTELIANSKY, V., ROSENWALD, A., BASSON, M. A., LICHT, J. D., PENA, J. T., ROUHANIFARD, S. H., MUCKENTHALER, M. U., TUSCHL, T., MARTIN, G. R., BAUERSACHS, J. & ENGELHARDT, S. 2008. MicroRNA-21 contributes to myocardial disease by stimulating MAP kinase signalling in fibroblasts. *Nature,* 456**,** 980-4.

TIMMS, K. M., ABKEVICH, V., HUGHES, E., NEFF, C., REID, J., MORRIS, B., KALVA, S., POTTER, J., TRAN, T. V., CHEN, J., ILIEV, D., SANGALE, Z., TIKISHVILI, E., PERRY, M., ZHARKIKH, A., GUTIN, A. & LANCHBURY, J. S. 2014. Association of BRCA1/2 defects with genomic scores predictive of DNA damage repair deficiency among breast cancer subtypes. *Breast Cancer Res,* 16**,** 475.

TORRES, A., TORRES, K., WDOWIAK, P., PASZKOWSKI, T. & MACIEJEWSKI, R. 2013. Selection and validation of endogenous controls for microRNA expression studies in endometrioid endometrial cancer tissues. *Gynecol Oncol,* 130**,** 588-94.

TYAN, S. W., HSU, C. H., PENG, K. L., CHEN, C. C., KUO, W. H., LEE, E. Y., SHEW, J. Y., CHANG, K. J., JUAN, L. J. & LEE, W. H. 2012. Breast cancer cells induce stromal fibroblasts to secrete ADAMTS1 for cancer invasion through an epigenetic change. *PLoS One,* 7**,** e35128.

UOZAKI, H., MORITA, S., KUMAGAI, A., ASO, T., SOEJIMA, Y., TAKAHASHI, Y. & FUKUSATO, T. 2014. Stromal miR-21 is more important than miR-21 of tumour cells for the progression of gastric cancer. *Histopathology,* 65**,** 775-83.

VELLA, M. C., CHOI, E. Y., LIN, S. Y., REINERT, K. & SLACK, F. J. 2004. The C. elegans microRNA let-7 binds to imperfect let-7 complementary sites from the lin-41 3'UTR. *Genes Dev,* 18**,** 132-7.

VERGHESE, E. T., DRURY, R., GREEN, C. A., HOLLIDAY, D. L., LU, X., NASH, C., SPEIRS, V., THORNE, J. L., THYGESEN, H. H., ZOUGMAN, A., HULL, M. A., HANBY, A. M. & HUGHES, T. A. 2013. MiR-26b is down-regulated in carcinoma-associated fibroblasts from ER-positive breast cancers leading to enhanced cell migration and invasion. *J Pathol,* 231**,** 388-99.

VERGHESE, E. T., SHENOY, H., COOKSON, V. J., GREEN, C. A., HOWARTH, J., PARTANEN, R. H., POLLOCK, S., WATERWORTH, A., SPEIRS, V., HUGHES,

T. A. & HANBY, A. M. 2011. Epithelial-mesenchymal interactions in breast cancer: evidence for a role of nuclear localized beta-catenin in carcinoma-associated fibroblasts. *Histopathology,* 59**,** 609-18.

VODUC, K. D., CHEANG, M. C., TYLDESLEY, S., GELMON, K., NIELSEN, T. O. & KENNECKE, H. 2010. Breast cancer subtypes and the risk of local and regional relapse. *J Clin Oncol,* 28**,** 1684-91.

WAGNER, A. D., THOMSSEN, C., HAERTING, J. & UNVERZAGT, S. 2012. Vascular-endothelial-growth-factor (VEGF) targeting therapies for endocrine refractory or resistant metastatic breast cancer. *Cochrane Database of Systematic Reviews*.

WALTERS, R. W., BRADRICK, S. S. & GROMEIER, M. 2010. Poly(A)-binding protein modulates mRNA susceptibility to cap-dependent miRNA-mediated repression. *RNA,* 16**,** 239-50.

WANG, B., LOVE, T. M., CALL, M. E., DOENCH, J. G. & NOVINA, C. D. 2006. Recapitulation of short RNA-directed translational gene silencing in vitro. *Mol Cell,* 22**,** 553-60.

WANG, B., YANEZ, A. & NOVINA, C. D. 2008. MicroRNA-repressed mRNAs contain 40S but not 60S components. *Proc Natl Acad Sci U S A,* 105**,** 5343-8.

WANG, Y., RATHINAM, R., WALCH, A. & ALAHARI, S. K. 2009. ST14 (suppression of tumorigenicity 14) gene is a target for miR-27b, and the inhibitory effect of ST14 on cell growth is independent of miR-27b regulation. *J Biol Chem,* 284**,** 23094-106.

WANG, Z., LIU, H., ZHAO, R., ZHANG, H., LIU, C. & SONG, Y. 2013. [Tumor-stroma ratio is an independent prognostic factor of non-small cell lung cancer]. *Zhongguo Fei Ai Za Zhi,* 16**,** 191-6.

WARFORD, A. 2016. In situ hybridisation: Technologies and their application to understanding disease. *Prog Histochem Cytochem,* 50**,** 37-48.

WCRFI 2015. World Cancer Research Fund International

Worldwide Data 2012.

WENG, L. P., SMITH, W. M., DAHIA, P. L., ZIEBOLD, U., GIL, E., LEES, J. A. & ENG, C. 1999. PTEN suppresses breast cancer cell growth by phosphatase activity-dependent G1 arrest followed by cell death. *Cancer Res,* 59**,** 5808-14.

WHO 2016. World Health Organisation

GLOBOCAN 2012: Estimated Cancer Incidence, Mortality and Prevalence Worldwide in 2012. *Intenational Agency for Research on Cancer.*

WOLF, K., WU, Y. I., LIU, Y., GEIGER, J., TAM, E., OVERALL, C., STACK, M. S. & FRIEDL, P. 2007. Multi-step pericellular proteolysis controls the transition from individual to collective cancer cell invasion. *Nat Cell Biol,* 9**,** 893-904.

WORTHLEY, D. L., RUSZKIEWICZ, A., DAVIES, R., MOORE, S., NIVISON-SMITH, I., BIK TO, L., BROWETT, P., WESTERN, R., DURRANT, S., SO, J., YOUNG, G. P., MULLIGHAN, C. G., BARDY, P. G. & MICHAEL, M. Z. 2009. Human gastrointestinal neoplasia-associated myofibroblasts can develop from bone marrow-derived cells following allogeneic stem cell transplantation. *Stem Cells,* 27**,** 1463-8.

WU, Z. H., TAO, Z. H., ZHANG, J., LI, T., NI, C., XIE, J., ZHANG, J. F. & HU, X. C. 2016. MiRNA-21 induces epithelial to mesenchymal transition and gemcitabine resistance via the PTEN/AKT pathway in breast cancer. *Tumour Biol,* 37**,** 7245-54.

XU, J., ZHANG, W., LV, Q. & ZHU, D. 2015. Overexpression of miR-21 promotes the proliferation and migration of cervical cancer cells via the inhibition of PTEN. *Oncol Rep,* 33**,** 3108-16.

YAN, L. X., HUANG, X. F., SHAO, Q., HUANG, M. Y., DENG, L., WU, Q. L., ZENG, Y. X. & SHAO, J. Y. 2008. MicroRNA miR-21 overexpression in human breast cancer is associated with advanced clinical stage, lymph node metastasis and patient poor prognosis. *RNA,* 14**,** 2348-60.

YAN, L. X., LIU, Y. H., XIANG, J. W., WU, Q. N., XU, L. B., LUO, X. L., ZHU, X. L., LIU, C., XU, F. P., LUO, D. L., MEI, P., XU, J., ZHANG, K. P. & CHEN, J. 2016. PIK3R1 targeting by miR-21 suppresses tumor cell migration and invasion by reducing PI3K/AKT signaling and reversing EMT, and predicts clinical outcome of breast cancer. *Int J Oncol,* 48**,** 471-84.

YAN, L. X., WU, Q. N., ZHANG, Y., LI, Y. Y., LIAO, D. Z., HOU, J. H., FU, J., ZENG, M. S., YUN, J. P., WU, Q. L., ZENG, Y. X. & SHAO, J. Y. 2011. Knockdown of miR-21 in human breast cancer cell lines inhibits proliferation, in vitro migration and in vivo tumor growth. *Breast Cancer Res,* 13**,** R2.

YANG, L., FENG, Y., QI, P., XU, S. & ZHOU, Y. 2016. Mechanism of serum miR-21 in the pathogenesis of familial and triple negative breast cancer. *J Biol Regul Homeost Agents,* 30**,** 1041-1045.

YANG, Y., CHAERKADY, R., KANDASAMY, K., HUANG, T. C., SELVAN, L. D., DWIVEDI, S. B., KENT, O. A., MENDELL, J. T. & PANDEY, A. 2010. Identifying targets of miR-143 using a SILAC-based proteomic approach. *Mol Biosyst,* 6**,** 1873-82.

YANG, Y., GUO, J. X. & SHAO, Z. Q. 2017. miR-21 targets and inhibits tumor suppressor gene PTEN to promote prostate cancer cell proliferation and invasion: An experimental study. *Asian Pac J Trop Med,* 10**,** 87-91.

YAO, T. & LIN, Z. 2012. MiR-21 is involved in cervical squamous cell tumorigenesis and regulates CCL20. *Biochim Biophys Acta,* 1822**,** 248-60.

YIN, S., YU, Y. & REED, R. 2015. Primary microRNA processing is functionally coupled to RNAP II transcription in vitro. *Sci Rep,* 5**,** 11992.

YU, P., LEE, Y., LIU, W., KRAUSZ, T., CHONG, A., SCHREIBER, H. & FU, Y. X. 2005. Intratumor depletion of CD4+ cells unmasks tumor immunogenicity leading to the rejection of late-stage tumors. *J Exp Med,* 201**,** 779-91.

ZEISBERG, E. M., POTENTA, S., XIE, L., ZEISBERG, M. & KALLURI, R. 2007. Discovery of endothelial to mesenchymal transition as a source for carcinoma-associated fibroblasts. *Cancer Res,* 67**,** 10123-8.

ZENG, Y. 2006. Principles of micro-RNA production and maturation. *Oncogene,* 25**,** 6156-62.

ZHANG, C., LIU, K., LI, T., FANG, J., DING, Y., SUN, L., TU, T., JIANG, X., DU, S., HU, J., ZHU, W., CHEN, H. & SUN, X. 2016. miR-21: A gene of dual regulation in breast cancer. *Int J Oncol,* 48**,** 161-72.

ZHANG, K., WANG, Y. W., WANG, Y. Y., SONG, Y., ZHU, J., SI, P. C. & MA, R. 2017a. Identification of microRNA biomarkers in the blood of breast cancer patients based on microRNA profiling. *Gene*.

ZHANG, K., ZHAO, S., WANG, Q., YANG, H. S., ZHU, J. & MA, R. 2015. Identification of microRNAs in Nipple Discharge as Potential Diagnostic Biomarkers for Breast Cancer. *Ann Surg Oncol,* 22 Suppl 3**,** S536-44.

ZHANG, T. L., SUN, L., WANG, S. M., MENG, Y. S. & XING, X. H. 2012a. [Expression of miR-21 in multiple myeloma and its clinical significance]. *Zhongguo Shi Yan Xue Ye Xue Za Zhi,* 20**,** 616-9.

ZHANG, W. Y., LIU, W., ZHOU, Y. M., SHEN, X. M., WANG, Y. F. & TANG, G. Y. 2012b. Altered microRNA expression profile with miR-27b down-regulation correlated with disease activity of oral lichen planus. *Oral Dis,* 18**,** 265-70.

ZHANG, Z., LI, X., SUN, W., YUE, S., YANG, J., LI, J., MA, B., WANG, J., YANG, X., PU, M., RUAN, B., ZHAO, G., HUANG, Q., WANG, L., TAO, K. & DOU, K. 2017b. Loss of exosomal miR-320a from cancer-associated fibroblasts contributes to HCC proliferation and metastasis. *Cancer Lett*.

ZHAO, L., SUN, Y., HOU, Y., PENG, Q., WANG, L., LUO, H., TANG, X., ZENG, Z. & LIU, M. 2012. MiRNA expression analysis of cancer-associated fibroblasts and normal fibroblasts in breast cancer. *Int J Biochem Cell Biol,* 44**,** 2051-9.

ZHU, S., SI, M. L., WU, H. & MO, Y. Y. 2007. MicroRNA-21 targets the tumor suppressor gene tropomyosin 1 (TPM1). *J Biol Chem,* 282**,** 14328-36.

ZIYAD, S. & IRUELA-ARISPE, M. L. 2011. Molecular mechanisms of tumor angiogenesis. *Genes Cancer,* 2**,** 1085-96.

Appendix A

Ethical approval for use of FFPE tissue

Leeds (East) Research Ethics Committee
Room 5.2, Clinical Sciences Building
St James's University Hospital
Beckett Street
Leeds
LS9 7TF

Telephone: 0113 2065652
Facsimile: 0113 2066772

17 November 2006

Professor Andrew Hanby
Professor of Breast Pathology
Department of Histopathology
St James's University Hospital
Beckett Street
Leeds
LS9 7TF

Dear Professor Hanby

Full title of study: **Studies of the biological significance of breast cancer subtype, using molecular and cytogenetic profiling and in vivo models.**

REC reference number: **06/Q1206/180**

The Research Ethics Committee reviewed the above application at the meeting held on 7 November 2006.

Ethical opinion

The members of the Committee present gave a favourable ethical opinion of the above research on the basis described in the application form, protocol and supporting documentation.

Ethical review of research sites

,The Committee agreed that all sites in this study should be exempt from site-specific assessment (SSA). There is no need to complete Part C of the application form or to inform Local Research Ethics Committees (LRECs) about the research. The favourable opinion for the study applies to all sites involved in the research.

Conditions of approval

The favourable opinion is given provided that you comply with the conditions set out in the attached document. You are advised to study the conditions carefully.

Approved documents

The documents reviewed and approved at the meeting were:

Document	*Version*	*Date*
Application		03 October 2006
Investigator CV		

Protocol	1	09 October 2006
Letter from Sponsor		26 October 2006

Research governance approval

You should arrange for the R&D Department at all relevant NHS care organisations to be notified that the research will be taking place, and provide a copy of the REC application, the protocol and this letter.

All researchers and research collaborators who will be participating in the research at a NHS site must obtain final research governance approval before commencing any research procedures. Where a substantive contract is not held with the care organisation, it may be necessary for an honorary contract to be issued before approval for the research can be given.

Membership of the Committee

The members of the Ethics Committee who were present at the meeting are listed on the attached sheet.

Statement of compliance

The Committee is constituted in accordance with the Governance Arrangements for Research Ethics Committees (July 2001) and complies fully with the Standard Operating Procedures for Research Ethics Committees in the UK.

[06/Q1206/180 **Please quote this number on all correspondence**

With the Committee's best wishes for the success of this project

Yours sincerely

Ann Prothero

p/p **Dr John Holmes**
Chair

Email: ann.prothero@leedsth.nhs.uk

Enclosures: List of names and professions of members who were present at the meeting and those who submitted written comments

Standard approval conditions

Copy to: Clare Skinner
Research Office
Room 7.11, Level 7
Worsley Building
University of Leeds

R&D Department, Leeds Teaching Hospitals NHS Trust

Appendix B

Breast tissue bank ethical approval

NHS
National Research Ethics Service
Leeds (East) Research Ethics Committee
Room 5.2, Clinical Sciences Building
St James's University Hospital
Beckett Street
Leeds
LS9 7TF

Telephone: 0113 3926788
Facsimile: 0113 3926788

20 January 2010

Dr Valerie Speirs
Leeds Institute of Molecular Medicine
Wellcome Trust Brenner Building
Leeds
LS9 7TF

Dear Dr Speirs

Title of the Research Tissue Bank: **Leeds Breast Research Tissue Bank**
REC reference: **09/H1306/108**
Designated Individual: **Dr Patricia Harnden**

Thank you for your letter of 14 January 2010, responding to the Committee's request for further information on the above research tissue bank and submitting revised documentation.

The further information has been considered on behalf of the Committee by the Chair.

Confirmation of ethical opinion

On behalf of the Committee, I am pleased to confirm a favourable ethical opinion of the above research tissue bank on the basis described in the application form and supporting documentation as revised.

The Committee has also confirmed that the favourable ethical opinion applies to all research projects conducted in the UK using tissue or data supplied by the tissue bank, provided that the release of tissue or data complies with the attached conditions. It will not be necessary for these researchers to make project-based applications for ethical approval. They will be deemed to have ethical approval from this committee. You should provide the researcher with a copy of this letter as confirmation of this. The Committee should be notified of all projects receiving tissue and data from this tissue bank by means of an annual report.

Duration of ethical opinion

The favourable opinion is given for a period of five years from the date of this letter and provided that you comply with the conditions set out in the attached document. You are advised to study the conditions carefully. The opinion may be renewed for a further period of up to five years on receipt of a fresh application. It is suggested that the fresh application is made 3-6 months before the 5 years expires, to ensure continuous approval for the research tissue bank.

Approved documents

The documents reviewed and approved at the meeting were:

Document	*Version*	*Date*
Covering Letter		05 November 2009
REC application		05 November 2009
Protocol for Management of the Tissue Bank	1	16 October 2009
Annex H - SOPs		01 April 2009
Approval Letter - Study 06/Q1206/180		17 November 2006
Approval Letter - Study 06/Q1205/156		24 July 2006
Approval Letter - Study 04/Q1204/112		22 October 2004
HTA License		
SOPs (Tissue Bank) - Leeds NHST		02 November 2009
Participant Information Sheet	2	13 January 2010
Participant Consent Form	2	13 January 2011
Response to Request for Further Information		14 January 2010

Licence from the Human Tissue Authority

Thank you for providing a copy of the above licence.

Research governance

A copy of this letter is being sent to the R&D office responsible for Leeds Teaching Hospitals NHS Trust. You are advised to check their requirements for approval of the research tissue bank.

Under the Research Governance Framework (RGF), there is no requirement for NHS research permission for the establishment of research tissue banks in the NHS. Applications to NHS R&D offices through IRAS are not required as all NHS organisations are expected to have included management review in the process of establishing the research tissue bank.

Research permission is also not required by collaborators at tissue collection centres (TCCs) who provide tissue or data under the terms of a supply agreement between the organisation and the research tissue bank. TCCs are not research sites for the purposes of the RGF.

Research tissue bank managers are advised to provide R&D offices at all TCCs with a copy of the REC application for information, together with a copy of the favourable opinion letter when available. All TCCs should be listed in Part C of the REC application.

NHS researchers undertaking specific research projects using tissue or data supplied by a research tissue bank must apply for permission to R&D offices at all organisations where the research is conducted, whether or not the research tissue bank has ethical approval.

Site-specific assessment (SSA) is not a requirement for ethical review of research tissue banks. There is no need to inform Local Research Ethics Committees.

Statement of compliance

The Committee is constituted in accordance with the Governance Arrangements for Research Ethics Committees (July 2001) and complies fully with the Standard Operating Procedures for Research Ethics Committees in the UK.

After ethical review

Now that you have completed the application process please visit the National Research Ethics Service website > After Review

Here you will find links to the following:

a) Providing feedback. You are invited to give your view of the service that you have received from the National Research Ethics Service and the application procedure. If you wish to make your views known please use the feedback form available on the website.
b) Annual Reports. Please refer to the attached conditions of approval.
c) Amendments. Please refer to the attached conditions of approval.

We would also like to inform you that we consult regularly with stakeholders to improve our service. If you would like to join our Reference Group please email referencegroup@nres.npsa.nhs.uk

09/H1306/108	**Please quote this number on all correspondence**

Yours sincerely

Dr Carol Chu
Chair

E-mail: laura.milnes@leedsth.nhs.uk

Enclosures: *Standard approval conditions*

Copy to: *Patricia Harnden*

Leeds Teaching Hospitals Trust

Appendix C

Co-Path search criteria

The Leeds Teaching Hospitals Trust histopathology database (Co-path) was searched to identify potential cases for inclusion in the cohort of cases that were used for LCM qPCR and CISH. The search terms that were used are listed below.

Accession date: From 01/01/2008 To 01/10/2012

Specimen Class: individual items ‘LH’

SNOMED Code: Not used

Text Search: Include if contains any ‘basal’ in text type (ALL)

Age: Not Used

Gender: individual items ‘Female’

Part Type: individual items ‘Breast biopsy wide excision’; ‘Breast biopsy wide local excision plus lymph nodes’; ‘Breast hook wire localisation’; ‘Breast total mastectomy’; ‘Breast wide local excision’; ‘Breast Xray mastectomy’; ‘Breast Xray wide local excision’; ‘Breast radical resection and axillary tail lymph nodes’

Appendix D

Oligonucleotide insertion sequences

Technical Datasheet

SALES ORDER NO: 8021099051
CUSTOMER NO: 0078202100
SHIPMENT DATE: 19/01/2016

INSTITUTE: LEEDS UNIVERSITY
RESEARCHER: JAMES THORNE
PURCHASE ORDER NO: HGQ4600011757

Batch #	Oligo Name	Oligo #	Len	Pur	Scale	MW	Tm°	µg/OD	OD	µg	nmol	Extinction Coefficient 1/(mMcm)	Dimer	2ndry	GC %	µl for 100µM	Sequence(5'-3')
HA08706704	21 top	8021099051-000010	33	DST	0.025	10132	78.7	31.2	12.1	378.4	37.3	323.9	Yes	Weak	51.5	373	AGCGGCCGCATCAACATCAGTCTGATAAGCTAG
HA08706705	21 bottom	8021099051-000020	41	DST	0.025	12607	82.9	32.8	14.5	476.6	37.8	383.5	Yes	Moderate	51.2	378	TCGACTAGCTTATCAGACTGATGTTGATGCGGCCGCTAGCT

Appendix D PmirGLO-21 reporter plasmid oligonucleotides

Appendix D contains the technical data including the oligonucleotide sequences that were inserted to produce the pmirGLO-21 reporter plasmid

Appendix E

"Abnormal" qPCR amplification curves from the qPCR arrays that failed my manual quality control

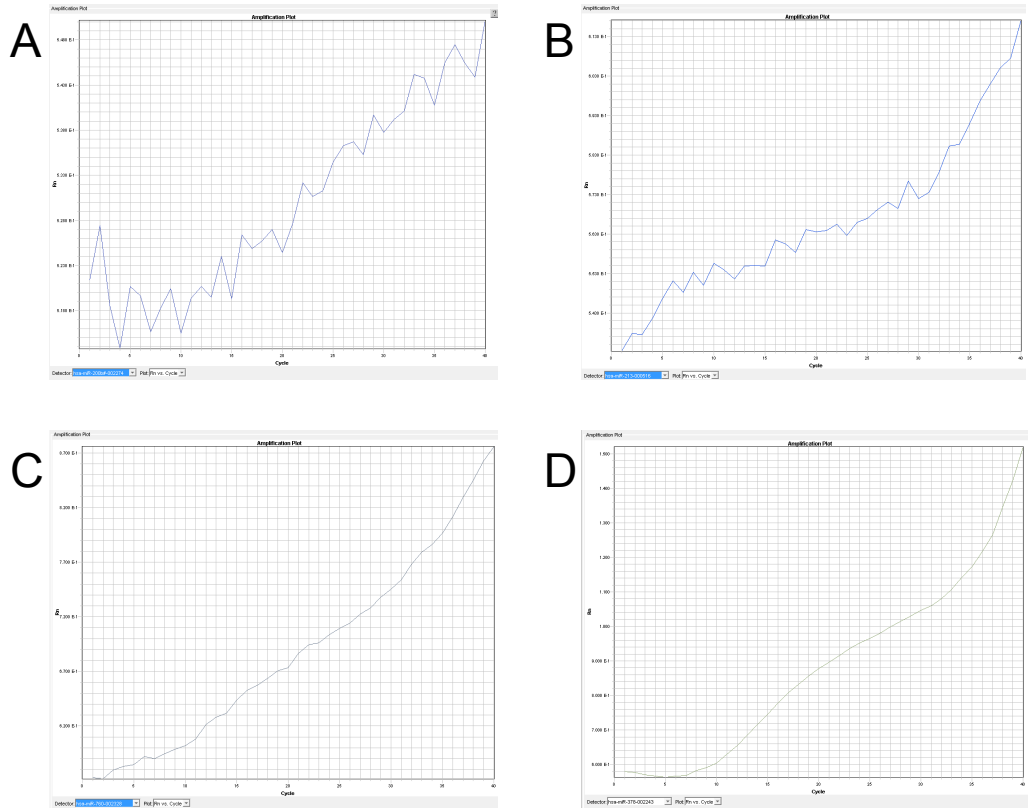

Figure E Array PCR amplification curves

Representative qPCR amplification curves that were assessed as being unreliable as they did not have a smooth sigmoidal shape. These specific amplification curves are for miR-200b# (A), miR-213 (B), miR-760 (C) and miR-378 (D).

Appendix F

Shapiro-Wilk test of normality

Tests of Normality

	Kolmogorov-Smirnov[a]			Shapiro-Wilk		
	Statistic	df	Sig.	Statistic	df	Sig.
rel_exp_B	.400	14	.000	.537	14	.000
rel_exp_C	.245	14	.022	.845	14	.019

a. Lilliefors Significance Correction

Table F MiR-21 expression levels in cells isolated from 14 clinical breast cancers do not have a normal distribution, therefore non-parametric statistical tests were appropriate

This table shows the results of the Shapiro-Wilk test comparing the distribution of the miR-21 expression level in the FFPE samples from fibroblasts of triple negative, basal-like breast cancer cases with a normal distribution. Rel_exp_B represents the data from NF samples and rel_exp_C from CAF samples. The significance is 0.000 and 0.019 for NFs and CAFs respectively, showing that the sample population is significantly different from a normal population.

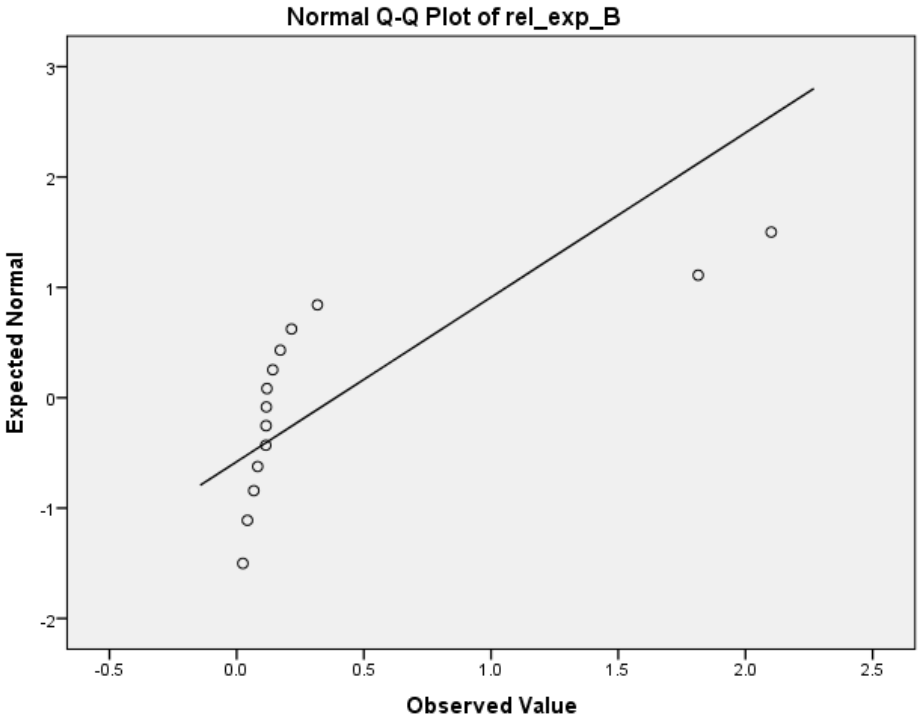

Figure F Expression levels of miR-21 in cells isolated from 14 breast cancer cases cannot be assumed to follow a normal distribution

This Q-Q plot compared the quantiles of the sample data to a normal distribution. The line represents where the points would lie if they followed a normal distribution. This clearly showed that the sample data points do not lie close to the line and therefore a statistical test that assumes normal distribution of the data should not be used.

Appendix G

"Abnormal" miR-30a-3p amplification curves

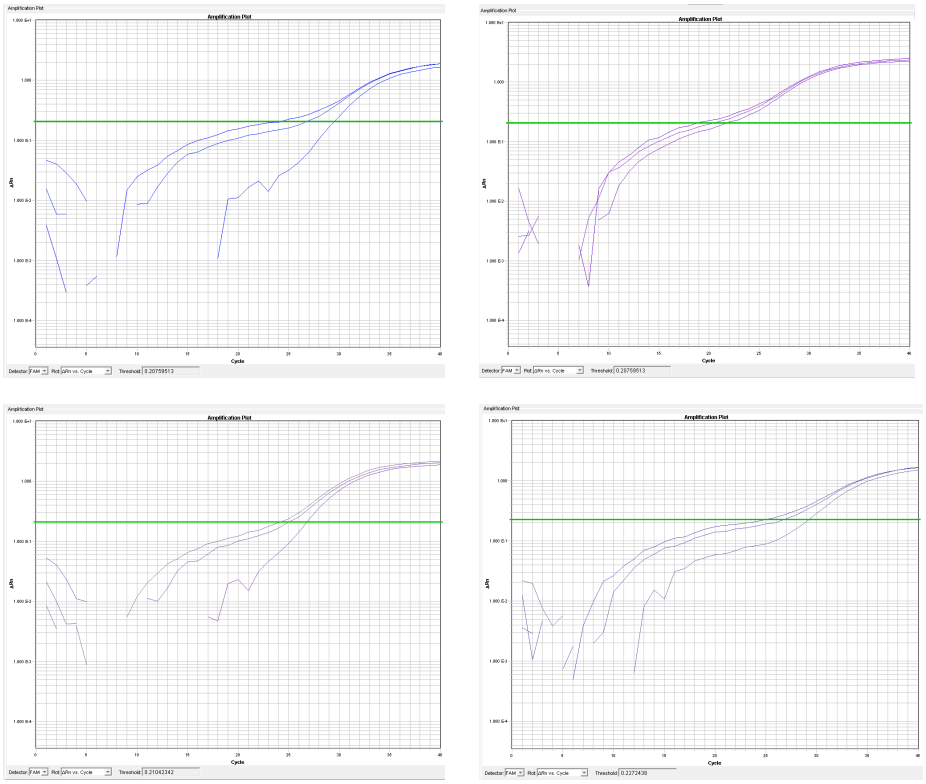

Figure G MiR-30a-3p qPCR amplification was not exponential

Some qPCR amplification curves for miR-30a-3p showed shallow slopes in the exponential phase, possibly indicating the presence of PCR inhibitors, and leading to wide variation in Ct values between technical replicates.

Appendix H

Intraclass correlation of CISH scoring by 2 independent scorers

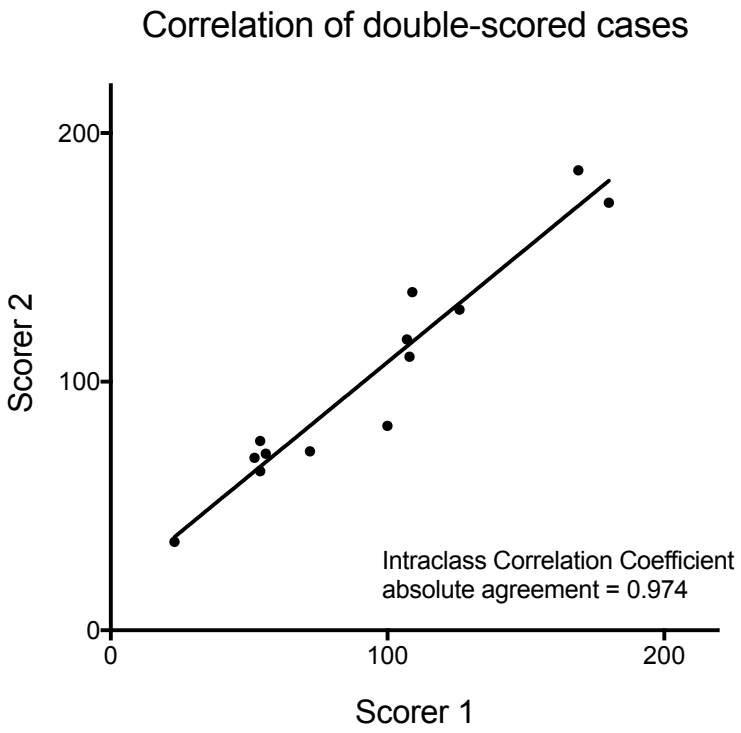

Figure H CISH miR-21 scoring shows good correlation between the two scorers

MiR-21 CISH was carried out on triple negative, basal-like breast cancer FFPE sections. Scoring of intensity and % of fibroblasts staining was carried out to give a H-score 50% of cases were scored by both scorers. Each circle represents one fibroblast sample (either NF or CAF), plotted based on the scores of the two independent scores. Linear regression of the data has also been plotted (the line). The two independent scores show good correlation, with an intraclass correlation coefficient of 0.974.

Appendix I

Correlation of CISH scores of CAFs close to and further away from tumour cells

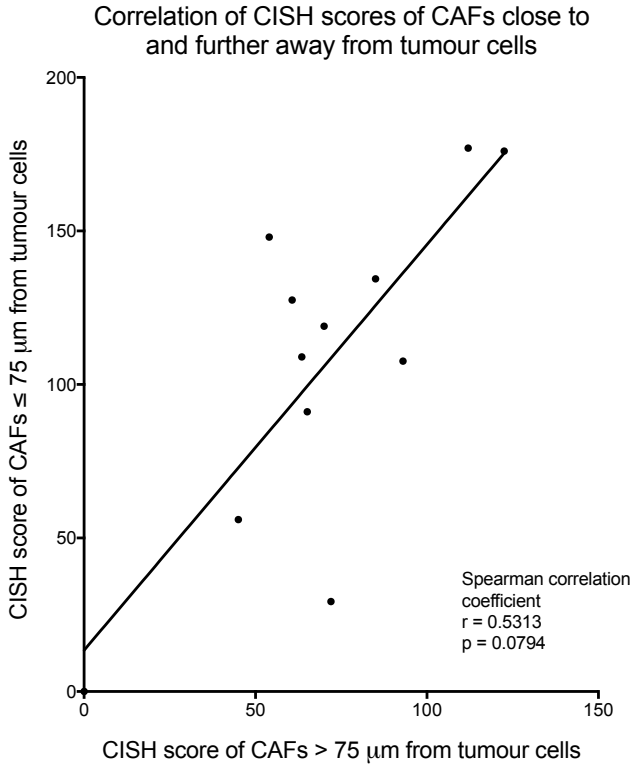

Figure I MiR-21 CISH scores of CAFs close to tumour cells and CAFs further from tumour cells did not significantly correlate with each other

MiR-21 CISH was carried out on triple negative, basal-like breast cancer FFPE sections. Scoring of intensity and % of fibroblasts staining was carried out giving an H-score. CAFs close to tumour cells (≤ 75 μm) and CAFs further away from tumour cells (> 75 μm) were scored separately for each case. Each circle represent the miR-21 CISH score for CAFs further from tumour cells (> 75 μm) plotted against the score for CAFs close to tumour cells (≤ 75 μm). The line represents the linear regression. The Spearman correlation coefficient was r = 0.5313 (p = 0.0794).

Appendix J

MiR-21 CISH score and clinical outcome analyses

J.1 Receiver operating characteristic curves for CISH score cut-offs and clinical outcomes

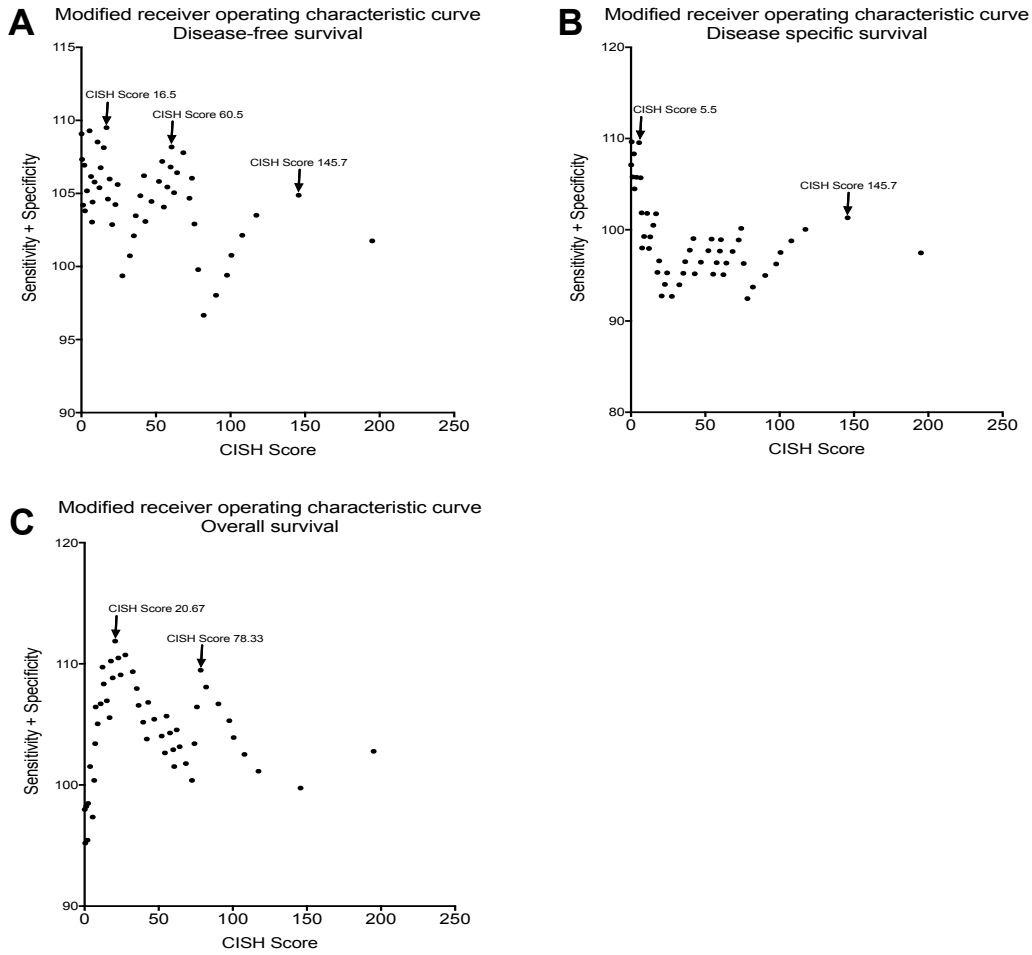

Figure J-1 Modified receiver operating characteristic curves were used to determine the optimal cut offs for CISH score low vs. CISH score high

CISH score was correlated with the clinical outcomes disease free survival, disease specific survival and overall survival. The data was dichotomised at each CISH score within the range and the sensitivity and specificity calculated. Each circle represents the CISH cut-off score plotted against the sum of sensitivity and specificity for each clinical outcome, disease-free survival (A), disease specific survival (B) and overall survival (C). The arrows highlight alternative CISH cut-off scores determined from the peaks of each curve.

J.2 Correlation of clinical outcomes with miR-21 CISH score using cut-offs determined in appendix J-1

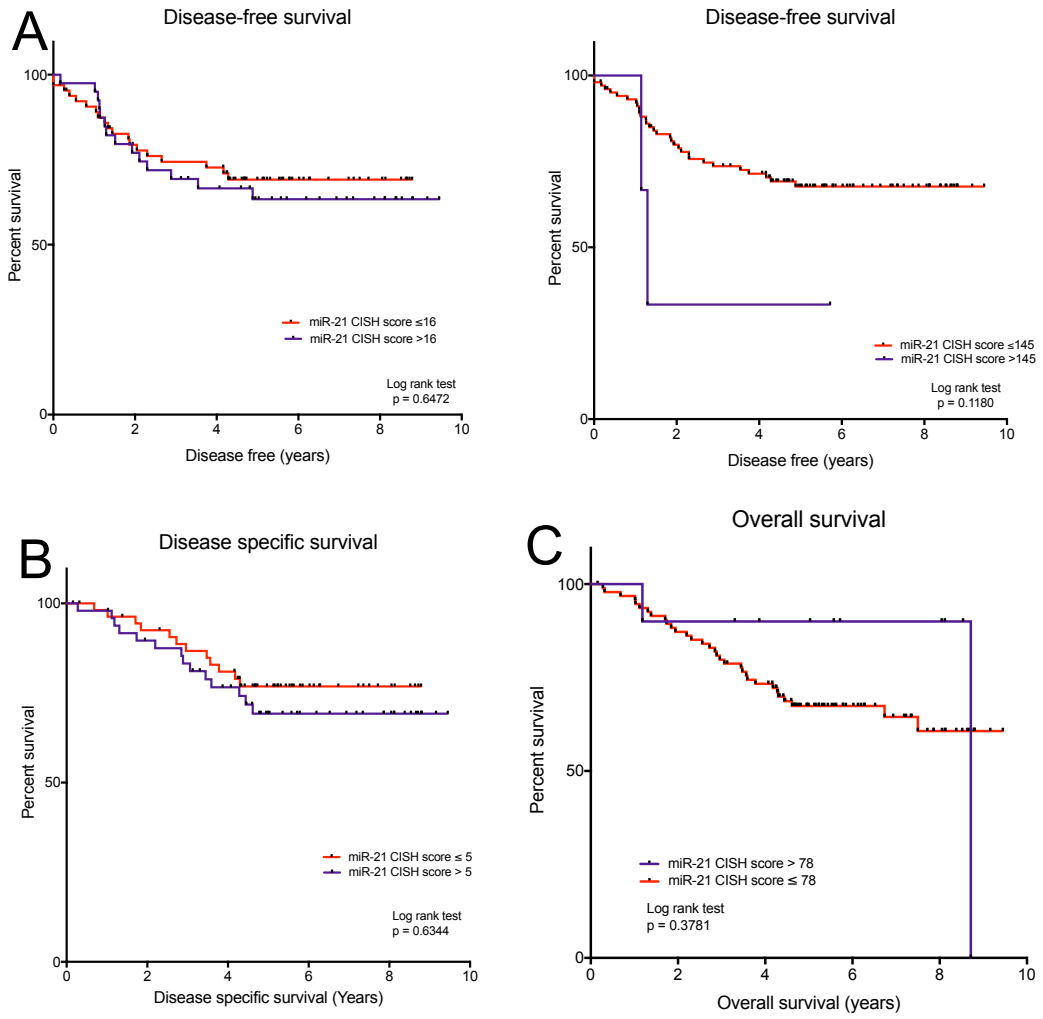

Figure J-2 Clinical outcomes did not significantly correlate with CISH staining intensity with any cut offs determined using ROC analyses

CISH scores were dichotomised into two groups, high staining (purple lines) and low or no staining (red lines) based on the cut-offs determined by modified ROC analysis (Figure J-1). Clinical outcome data was compared with CISH score and plotted on Kaplan Meier curves for disease free survival (A), disease specific survival (B) and overall survival (C). The small black squares represent where a subject was censored at length of follow up.

Appendix K

Conditioned medium transfer or transwell co-cultures with MDA-MB-231 does not alter miR-21 levels in NFs or CAFs

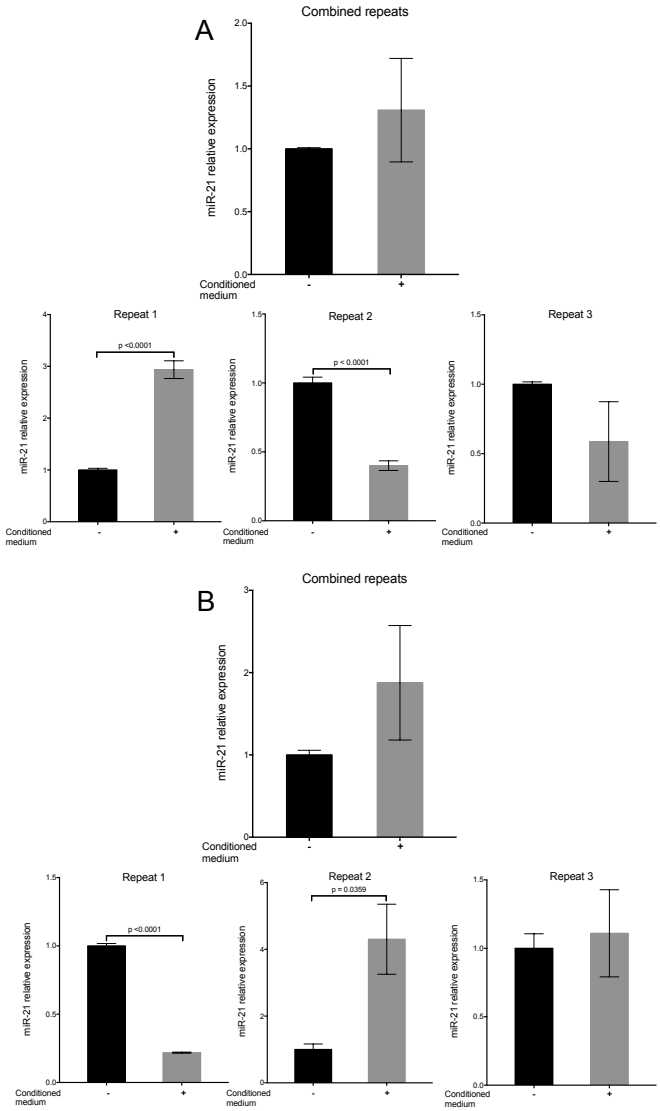

Figure K-1 Tumour cell conditioned medium does not alter miR-21 level in fibroblasts

Conditioned medium from MDA-MB-231s or the same fibroblasts was used to replace half the medium on fibroblasts (NF-1 and CAF-1) every day for 3 days. Following this RNA was extracted and miR-21 levels measured by qPCR. Data are displayed as the mean (+/- SEM) of 3 independent experiments (top panel), with each separate experiment shown below (means +/- SD of technical triplicates; bottom panel). Part A shows the data from NF-1 and part B from CAF-1.

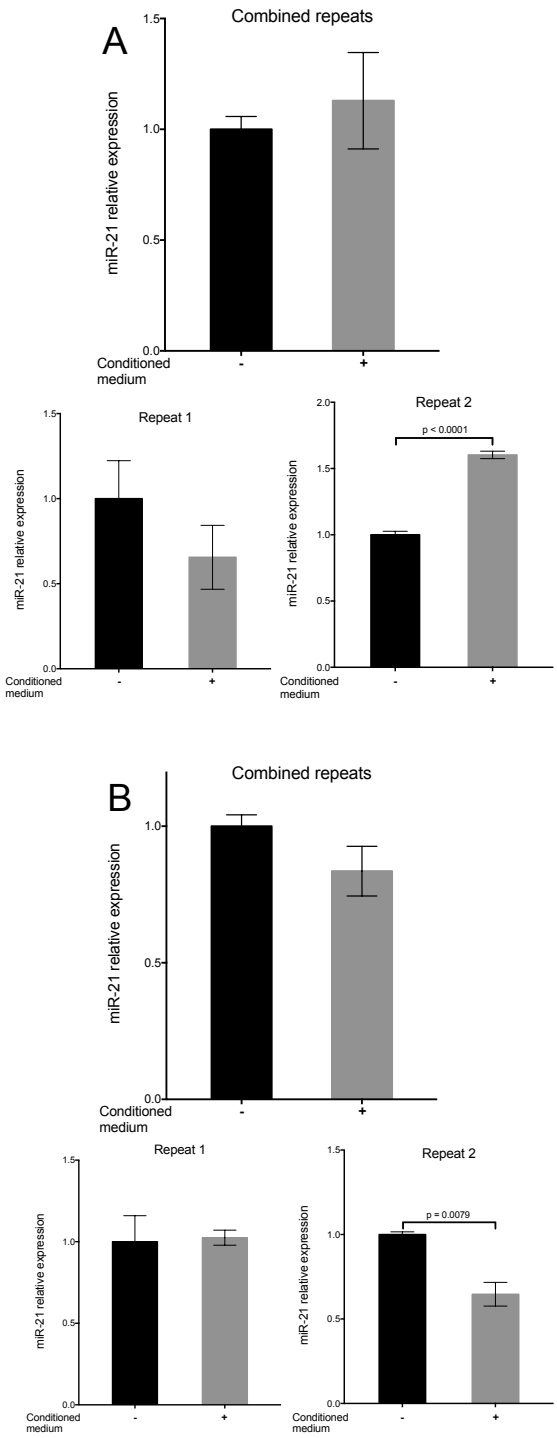

Figure K-2 Transwell co-culture with MDA-MB-231 does not significantly alter miR-21 levels in fibroblasts

Fibroblasts (NF-1 and CAF-1) were grown in the base of wells, along with either the same fibroblasts or MDA-MB-231 cells seeded into transwell inserts (membrane with 1 μm pores) for 3 days. RNA was extracted from the fibroblasts and qPCR used to measure miR-21 levels. Data are displayed as the mean (+/- SEM) of 3 independent experiments (top panel), with each separate experiment shown below (means +/- SD of technical triplicates; bottom panel). Part A shows the data from NF-1 and part B from CAF-1.